X-RAY STRUCTURAL STUDIES OF CROWN-ETHER COMPLEXES WITH DIQUAT, PARAQUAT AND BORANE-AMMONIA

by

BILLY LOUIS ALLWOOD, B.Sc.

A Thesis Presented

for the Degree of Doctor of Philosophy

of the University of London

and for the Diploma of Imperial College

Department of Chemistry,
Imperial College of Science and Technology,
University of London.

January 1985

ABSTRACT

This thesis will consist of two parts. The first part will describe and discuss the X-ray structure analyses of molecular receptors for diquat and paraquat herbicides. The second part will deal with the X-ray structure analyses of stereoisomers of 2,3,11,12 tetra-anisyl-18-crown-6 and their adducts with borane-ammonia.

Diquat has been shown to form a complex with DB30C10 in which the interactions are; charge transfer between the parallel aligned bipyridinium dications and the benzo groups of the host, pole-dipole interactions between the formally positively charged bipyridinium nitrogens and the phenolic oxygens of the host, C-H...O hydrogen bonding involving the acidic protons on the diquat and certain polyether oxygens of the host. We will describe the effects on complexation of (1) the substitution of the DB30C10 moiety, (2) the introduction of a further bridging arm into the macrocycle, (3) the use of a dinaptho based receptor c.f. dibenzo and (4) increasing the macrocycle ring size. It will be demonstrated how the study of the molecular topology, conformational flexibility, and the relative importance of different weak intermolecular forces can lead to the design of new and effective receptors for diquat and paraquat.

Borane-ammonia adducts have been shown to exhibit excellent (>90%) chemo- and diastereo-selectivites in their reduction of aldehydes and ketones. However, in most of these reagents the auxiliary is covalently bound to the boron atom and hence not easily recycled. The second part of this thesis will deal with the X-ray structure analyses of adducts

in which the boron ammine is bound non-covalently to the host and therefore can be recycled after reduction. THe structures of the stereoisomers of 2,3,11,12 tetra-anisyl-18-crown-6 and their hydrogen bonded adducts with borane-ammonia will be described. The relationship between receptor topology and host:guest stoicheiometry will also be discussed.

ACKNOWLEDGEMENTS

I would like to thank my supervisor Dr D.J. Williams for his guidance, patience and encouragement over the past three years.

I am also indebted to Dr J.F. Stoddart and his research group at Sheffield University, in particular Drs F.H. Kohnke and D. Pears, for the provision of crystals and useful and lively discussion.

My thanks are also due to the members of the Chemical Crystallography laboratory for providing a friendly and invigo rating environment in which to work. Especially Sandra Slawin for her loaning of the 'Daily Mail'.

In preparing this thesis I would like to thank Sue and Kay in the General Office for their help and time. I am also grateful to Dr B.A. King for assistance in the proof-reading of this thesis.

Finally I wish to thank the A.F.R.C. for their sponsorship of my research.

CONTENTS

	PAGE
ABSTRACT	2
ACKNOWLEDGEMENTS	4
LIST OF TABLES	10
LIST OF FIGURES	15
PART 1. THE X-RAY STRUCTURAL STUDIES OF CROWN ETHER COMPLEXES OF DIQUAT AND PARAQUAT	
CHAPTER 1. INTRODUCTION	19
1.1 The Need for Herbicides	20
1.2 Diquat and Paraquat	21
1.3 Herbicidal Activity of Diquat and Paraquat	24
1.4 Other Uses of Diquat and Paraquat	25
1.5 Diquat and Paraquat Poisoning	25
1.6 Molecular Receptors for Diquat and Paraquat	26
1.7 Crown Ethers	27
1.8 Charge Transfer Complexes involving Dibenzo Crown Ethers	29
1.9 Aim of Research	32
1.10 REFERENCES	33
CHAPTER 2. The crystal structures of the complexes of 2,20-Dimethyl-6,7,9,10,12,13,15,16,23,24,26,27,29,30,32,33-hexadecahydrodibenzo[b,q][1,4,7,10,13,16,19,22,25,28]decaoxacyclotriacontin and 2,20-bishydroxymethyl-6,7,9,10,12,13,15,16,23,24,26,27,29,30,32,33 hexadecahydrodibenzo[b,q][1,4,7,10,13,16,19,22,25,28]decaoxacyclotriacontin (disubstituted DB30C10 derivatives) with diquat.	35
2.1 INTRODUCTION	36
2.2 EXPERIMENTAL	37

2.3 DISCUSSION 42

2.4 REFERENCES 69

CHAPTER 3. The crystal structure of the complex of 1,4,7,10,13,21, 30,38,41,44,47,50-dodecaoxa[13^{15,34}][13.3.3](1,4)(1,2)(1,4)cyclophane (a macrobicyclic receptor) with diquat. 71

3.1 INTRODUCTION 72

3.2 EXPERIMENTAL 74

3.3 DISCUSSION 76

3.4 REFERENCES 92

CHAPTER 4. The crystal structures of 1,4,7,10,13,20,28,36,39,42, 45,48-dodecaoxa[13^{15,32}][13.2.2](1,4)(1,2)(1,4)cyclophane (a macro bicyclic receptor) and its complex with diquat. 94

4.1 INTRODUCTION 95

4.2 EXPERIMENTAL 96

4.3 DISCUSSION 99

4.4 REFERENCES 122

CHAPTER 5. The crystal structure of the complex of 7,8,10,11,13,14 16,17,26,27,29,30,32,33,35,36-hexadecahydrodinaptho[2,3-b:2',3'-q] [1,4,7,10,13,16,19,22,25,28]decaoxacyclotricontin (Dinaptho-30-Crown-10) with diquat. 123

5.1 INTRODUCTION 124

5.2 EXPERIMENTAL 124

5.3 DISCUSSION 126

5.4 REFERENCES 141

CHAPTER 6. The crystal structures of 1,4,7,10,13,20,23,26,29,32-decaoxa[13.13]metacyclophane (bismetaphenylene-32-crown-10) and its complex with diquat. 142

6.1 INTRODUCTION 143

6.2 EXPERIMENTAL 145

6.3 DISCUSSION 148

6.4 REFERENCES 171

CHAPTER 7. The crystal structures of 1,4,7,10,13,20,23,26,29,32-decaoxa[13.13]paracyclophane (bisparaphenylene-34-crown-10) and its complex with diquat. 173

7.1 INTRODUCTION 174

7.2 EXPERIMENTAL 175

7.3 DISCUSSION 179

7.4 REFERENCES 202

CHAPTER 8. The crystal structure of the complex of 1,4,7,10,13,20,23,26,29,32-decaoxa[13.13]paracyclophane (bisparaphenylene-34-crown-10) with paraquat. 203

8.1 INTRODUCTION 204

8.2 EXPERIMENTAL 204

8.3 DISCUSSION 206

8.4 REFERENCES 218

CHAPTER 9. CONCLUSIONS 219

9.1 Summary 220

9.2 Charge Distribution Within the Bipyridinium Dications 222

9.3 Orientation of Charge Transfer Interactions 223

9.4 Conformation of the Uncomplexed Receptors 224

9.5 Conclusion 224

9.6 REFERENCES 226

PART 2. THE X-RAY STRUCTURAL STUDIES OF CROWN ETHER COMPLEXES OF BORANE-AMMONIA

CHAPTER 10. INTRODUCTION 227

10.1 Enantioselective Reduction of Prochiral Aromatic Ketones 228

10.2 18C6 Macrocycles 230

10.3 Aim of Research 231

10.4 REFERENCES 232

CHAPTER 11. The Crystal structures of trans-syn-trans 2,3,11,12 tetra-anisyl-18-crown-6 and its complex with borane-ammonia 234

11.1 INTRODUCTION 235

11.2 EXPERIMENTAL 235

11.3 DISCUSSION 239

11.4 REFERENCES 258

CHAPTER 12. The Crystal structures of cis-anti-cis 2,3,11,12 tetra-anisyl-18-crown-6 and its complex with borane-ammonia 259

12.1 INTRODUCTION 260

12.2 EXPERIMENTAL 260

12.3 DISCUSSION 263

12.4 REFERENCES 282

CHAPTER 13. The Crystal structures of cis-syn-cis 2,3,11,12 tetra-anisyl-18-crown-6 and its complex with borane-ammonia 283

13.1 INTRODUCTION 284

13.2 EXPERIMENTAL 284

13.3 DISCUSSION 288

13.4 REFERENCES 307

CHAPTER 14. The Crystal structures of trans-syn-trans 2,3,11,12 tetra-anisyl-18-crown-6 and its complex with borane-ammonia 308

14.1 INTRODUCTION 309

14.2 EXPERIMENTAL 309

14.3 DISCUSSION 312

14.4 REFERENCES 331

CHAPTER 15. CONCLUSIONS 332

15.1 Summary 333

15.2 The Receptor C-C Bridgehead Bond length 333

15.3 The Stoicheiometry of the Borane-ammonia Complexes 333

15.4 Enantioselective Reduction of Prochiral Ketones 334

15.5 Hydrogen Bond Geometry 334

15.6 Conclusion 335

15.7 REFERENCES 336

APPENDIX 1. CRYSTALLOGRAPHIC METHODS 337

APPENDIX 2. PUBLICATIONS 345

APPENDIX 3. MOLECULAR GEOMETRY PROGRAM 347

APPENDIX 4. OBSERVED AND CALCULATED STRUCTURE FACTORS 351

LIST OF TABLES

TABLE		PAGE
2.1	Atom coordinates and temperature factors	55
2.2	Bond lengths	57
2.3	Bond angles	58
2.4	Anisotropic temperature factors	59
2.5	Hydrogen coordinates and temperature factors	61
2.6	Atom coordinates and temperature factors	62
2.7	Bond lengths	64
2.8	Bond angles	65
2.9	Anisotropic temperature factors	66
2.10	Hydrogen coordinates and temperature factors	68
2.11	Host-guest contacts for [2.diquat]	48
2.12	Host-guest contacts for [4.diquat]	48
3.1	Atom coordinates and temperature factors	83
3.2	Bond lengths	85
3.3	Bond angles	86
3.4	Anisotropic temperature factors	88
3.5	Hydrogen coordinates and temperature factors	90
3.6	Host-guest contacts for [5.diquat]	80
4.1	Atom coordinates and temperature factors	110
4.2	Bond lengths	111
4.3	Bond angles	112
4.4	Anisotropic temperature factors	113
4.5	Hydrogen coordinates and temperature factors	114
4.6	Atom coordinates and temperature factors	115
4.7	Bond lengths	117
4.8	Bond angles	118

4.9	Anisotropic temperature factors	119
4.10	Hydrogen coordinates and temperature factors	121
4.11	Host-guest contacts for [6.diquat]	106
5.1	Atom coordinates and temperature factors	136
5.2	Bond lengths	137
5.3	Bond angles	138
5.4	Anisotropic temperature factors	139
5.5	Hydrogen coordinates and temperature factors	140
5.6	Torsion angles associated with C6+ and C8+	131
5.7	Host-guest contacts for [7.diquat]	131
6.1	Atom coordinates and temperature factors	159
6.2	Bond lengths	160
6.3	Bond angles	161
6.4	Anisotropic temperature factors	162
6.5	Hydrogen coordinates and temperature factors	163
6.6	Atom coordinates and temperature factors	164
6.7	Bond lengths	166
6.8	Bond angles	167
6.9	Anisotropic temperature factors	168
6.10	Hydrogen coordinates and temperature factors	170
6.11	Host-guest contacts for [8.diquat]	154
7.1	Atom coordinates and temperature factors	190
7.2	Bond lengths	191
7.3	Bond angles	192
7.4	Anisotropic temperature factors	193
7.5	Hydrogen coordinates and temperature factors	194
7.6	Atom coordinates and temperature factors	195

7.7	Bond lengths	197
7.8	Bond angles	198
7.9	Anisotropic temperature factors	199
7.10	Hydrogen coordinates and temperature factors	201
7.11	Host-guest contacts for [9.diquat]	186
8.1	Atom coordinates and temperature factors	213
8.2	Bond lengths	214
8.3	Bond angles	215
8.4	Anisotropic temperature factors	216
8.5	Hydrogen coordinates and temperature factors	217
8.6	Host-guest contacts for [9.paraquat]	211
11.1	Atom coordinates and temperature factors	248
11.2	Bond lengths	249
11.3	Bond angles	250
11.4	Anisotropic temperature factors	251
11.5	Hydrogen coordinates and temperature factors	252
11.6	Atom coordinates and temperature factors	253
11.7	Bond lengths	254
11.8	Bond angles	255
11.9	Anisotropic temperature factors	256
11.10	Hydrogen coordinates and temperature factors	257
11.11	Nitrogen-crown ether contacts for 10a	245
11.12	Nitrogen-crown ether contacts for 10b	245
12.1	Atom coordinates and temperature factors	272
12.2	Bond lengths	273
12.3	Bond angles	274
12.4	Anisotropic temperature factors	275
12.5	Hydrogen coordinates and temperature factors	276

12.6	Atom coordinates and temperature factors	277
12.7	Bond lengths	278
12.8	Bond angles	279
12.9	Anisotropic temperature factors	280
12.10	Hydrogen coordinates and temperature factors	281
12.11	Nitrogen-crown ether contacts for 11.$(BH_3NH_3)_2$	268
13.1	Atom coordinates and temperature factors	297
13.2	Bond lengths	298
13.3	Bond angles	299
13.4	Anisotropic temperature factors	300
13.5	Hydrogen coordinates and temperature factors	301
13.6	Atom coordinates and temperature factors	302
13.7	Bond lengths	303
13.8	Bond angles	304
13.9	Anisotropic temperature factors	305
13.10	Hydrogen coordinates and temperature factors	306
13.11	Nitrogen-crown ether contacts for 13.BH_3NH_3	293
14.1	Atom coordinates and temperature factors	321
14.2	Bond lengths	322
14.3	Bond angles	323
14.4	Anisotropic temperature factors	324
14.5	Hydrogen coordinates and temperature factors	325
14.6	Atom coordinates and temperature factors	326
14.7	Bond lengths	327
14.8	Bond angles	328
14.9	Anisotropic temperature factors	329
14.10	Hydrogen coordinates and temperature factors	330

14.11 Nitrogen-crown ether contacts for $\underset{\sim\sim}{13}.BH_3NH_3$ 318

LIST OF FIGURES

FIGURE		PAGE
1.1.	Diquat and paraquat.	22
1.2.	The redox potential of diquat and paraquat.	23
1.3.	The space-filling representation of the complex formed between [Pt(bipy)$(NH_3)_2$] and DB24C8.	30
1.4.	The space-filling representation of the complex formed between [Pt(bipy)$(NH_3)_2$] and DB30C10.	30
1.5.	The similar properties of Pt(bipy)$(NH_3)_2$, diquat and paraquat.	31
1.6.	The space-filling and framework representation of [DB30C10.diquat].	30
2.1.	The skeletal representations of the structures of [2.diquat] (a) and [4.diquat] (b).	44
2.2.	The skeletal representations of the structures of the two independent complexes found in [diquat.DB30C10].	45
2.3.	The space-filling representations of the structures of [2.diquat] (a) and [4.diquat] (b).	49
2.4.	The stereo-pair representations of the structures of [2.diquat] (a) and [4.diquat] (b).	50
2.5.	Side-on views of the skeletal representations of the structures of [2.diquat] (a) and [4.diquat] (b).	51
3.1.	The structure of DB30C10.	72
3.2.	The skeletal representation of the structure of [5.diquat].	77
3.3.	Side-on view of the skeletal representation of the structure of [5.diquat].	77
3.4.	The stereo-pair representation of the structure of [5.diquat].	79
3.5.	The space-filling representation of the structure of [5.diquat].	79
4.1.	The skeletal representation of the structure of 6.	101
4.2.	The skeletal representation of the structure of [6.diquat].	101

4.3. The space-filling representation of the structure of 6. 102

4.4. The space-filling representation of the structure of [6.diquat]. 102

4.5. The stereo-pair representation of the structure of 6. 104

4.6. The stereo-pair representation of the structure of [6.diquat]. 104

4.7. Side-on view of the skeletal representation of the structure of [6.diquat]. 107

4.8. Side-on view of the skeletal representation of the structure of [5.diquat]. 107

5.1. The skeletal representation of the structure of [7.diquat]. 128

5.2. The space-filling representation of the structure of [7.diquat]. 128

5.3. The stereo-pair representation of the packing of the unit cell contents of [7.diquat][PF_6]$_2$(0.5)H_2O. 130

5.4. The stereo-pair representation of the structure of [7.diquat]. 130

5.5. Side-on view of the skeletal representation of the structure of [7.Pt(bipy)(NH_3)$_2$]. 133

5.6. Side-on view of the skeletal representation of the structure of [7.diquat]. 133

6.1. The separation between (i) the aryl oxygens in catechol, resorcinol and quinol (ii) the nitrogens in diquat and paraquat. 143

6.2. The skeletal representation of the structure of 8. 149

6.3. The skeletal representation of the structure of [8.diquat]. 149

6.4. The space-filling representation of the structure of 8. 151

6.5. The space-filling representation of the structure of [8.diquat]. 151

6.6. The stereo-pair representation of the structure of 8. 152

6.7. The stereo-pair representation of the structure of [8.diquat]. 152

6.8. Side-on view of the skeletal representation of the structure of [8.diquat]. 156

7.1. The skeletal representations of the structures of the two independent conformations found for 9. 180

7.2. The space-filling representations of the structures of the two independent conformations found for 9. 181

7.3. The stereo-pair representations of the structures of the two independent conformations found for 9. 182

7.4. The skeletal representation of the structure of [9.diquat.H_2O]. 184

7.5. The space-filling representation of the structure of [9.diquat.H_2O]. 184

7.6. The stereo-pair representation of the structure of [9.diquat.H_2O]. 187

7.7. Side-on view of the skeletal representation of the structure of [9.diquat.H_2O]. 187

8.1. The skeletal representation of the structure of [9.paraquat]. 207

8.2. The space-filling representation of the structure of [9.paraquat]. 207

8.3. The stereo-pair representation of the structure of [9.paraquat]. 209

8.4. Side-on view of the skeletal representation of the structure of [9.paraquat] 209

10.1. Trans-anti-trans 2,3,11,12 tetra-anisyl-18-crown-6 229

10.2. A graphic representation of the five stereoisomers of 2,3,11,12 tetra-anisyl-18-crown-6. 229

11.1. The skeletal representation of the structure of 10. 240

11.2. The stereo-pair representation of the structure of 10. 240

11.3. The skeletal representations of the structures of the two independent complexes found in 10.$(BH_3NH_3)_2$. 243

11.4. The stereo-pair representation of the structure of 10b. 244

11.5. The space-filling representation of 10b 244

12.1. The skeletal representation of the structure of 11. 265

12.2. The skeletal representation of the structure of $\underset{\sim\sim}{11}.(BH_3NH_3)_2$. 265

12.3. The stereo-pair representation of the structure of $\underset{\sim\sim}{11}$. 267

12.4. The stereo-pair representation of the structure of $\underset{\sim\sim}{11}.(BH_3NH_3)_2$. 267

12.5. The space-filling representation of $\underset{\sim\sim}{11}.(BH_3NH_3)_2$. 270

13.1. The skeletal representation of the structure of $\underset{\sim\sim}{12}$. 289

13.2. The stereo-pair representation of the structure of $\underset{\sim\sim}{12}$. 289

13.3. The space-filling representation of $\underset{\sim\sim}{12}$. 291

13.4. The skeletal representation of the structure of $\underset{\sim\sim}{12}.BH_3NH_3$. 291

13.5. The space-filling representations of $\underset{\sim\sim}{12}.BH_3NH_3$. 295

13.6. The stereo-pair representation of the structure of $\underset{\sim\sim}{12}.BH_3NH_3$. 296

14.1. The skeletal representation of the structure of $\underset{\sim\sim}{13}$. 314

14.2. The stereo-pair representation of the structure of $\underset{\sim\sim}{13}$. 314

14.3. The skeletal representation of the structure of $\underset{\sim\sim}{13}.BH_3NH_3$. 316

14.4. The stereo-pair representation of the structure of $\underset{\sim\sim}{13}.BH_3NH_3$. 316

14.5. The space-filling representations of $\underset{\sim\sim}{13}.BH_3NH_3$. 320

PART 1

CHAPTER 1

INTRODUCTION

1.1 The Need For Herbicides.

Losses in crop yields caused by pests, diseases and weeds (plants in the wrong place) both before and after harvest have been a problem since man started cultivating crops more than 10,000 years ago.

These losses may reach 25% in Europe, but in the less developed areas of Africa and Asia almost half the potential food yield is lost. Weeds themselves have been shown to reduce rice yields by 34% to 68% in Peru. In Latin America maize yields were reduced by 53% by allowing weeds to grow[1]. Invasion of rice paddy fields in Sri Lanka and sugar cane plantations in India by weeds which have become difficult to control has led to formerly productive land being abandoned[2].

Overall it seems that a 10% loss of agricultural production can be attributed to the effect of weeds.

Weeds are harmful to crops in many ways[3]:

1. They compete for water.
2. They compete for light.
3. They compete for nutrients.
4. They compete for space above and below ground.
5. They may reduce the quality of produce and increase the difficulty of harvesting and necessitate seed cleaning.
6. They may be poisonous to the crop.
7. They may harbour pests and diseases.

Farmers from earliest times have recognised the harmful effects of weeds and have tried to remove them. The earliest method of control was hand-pulling when labour was cheap and plentiful. This was later aided by the disturbance of the soil that accompanied cultivation and crop rotation.

With the world population rapidly increasing there will be a need for even greater yields from existing arable land. The use of Chemical Weedkillers (herbicides) is one method of controlling weeds and so increasing crop yields.

Since the discovery of the organic chemical weedkillers 2,4,-dichlorophenoxy acetic acid (2,4-D) and 4-chloro-o-tolyloxy acetic acic (MCPA), in the early 1940's, there has been a rapid increase in the use of organic chemical weedkillers. Herbicides have the advantage of enabling larger yields at a lower cost. In 1978 the world sales of herbicides were $3.7 billion and for 1984 it is estimated at $4.8 billion[3].

1.2 Diquat and Paraquat

Two commerically important herbicides are the dicationic bipyridiniums 6,7-dihydrodipyrido[1,2-a:2',1'-c]pyrazidinium (diquat) and 1,1' dialkyl-4,4'-bipyridinium (paraquat). Their herbicidal properties were first reported by I.C.I. in 1958 and 1960 respectively[4]. Diquat was a new dication, but paraquat had been known and used as a redox indicator under the name of methyl viologen since 1932.

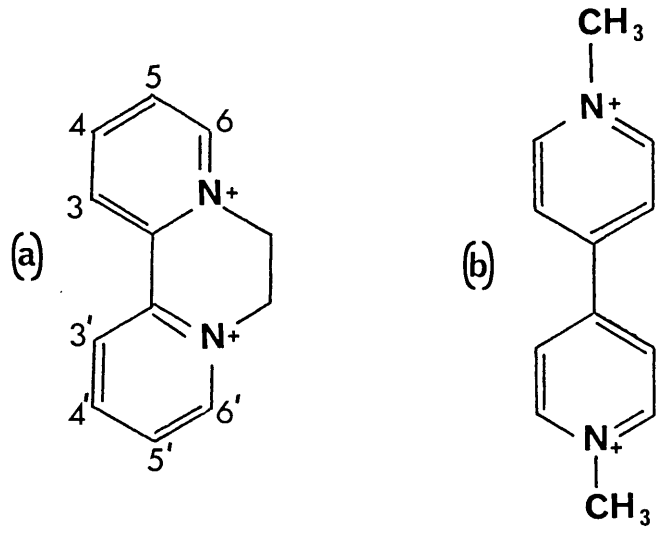


Figure 1.1. diquat (a) and paraquat (b).

Diquat and paraquat are normally marketed as the dibromide and dichloride salts respectively.

Their herbicidal properties are that they rapidly desiccate all green plant tissue in sunlight, are rendered inactive on reaching the soil, are mainly non-selective, have no residual effects, their salts are water soluble and they can be used at low concentrations, 1/8-2Lb/acre. This combination of properties has led to their world-wide use in a variety of weed control situations. New techniques such as direct-drilling have only become possible since the introduction of diquat and paraquat which can destroy existing vegetation rapidly without leaving a toxic residue in the soil.

Diquat and paraquat are normally sold to farmers in concentrated aqueous solution containing 20%-25% of active ingredients in addition to wetting agents and corrosion inhibitors, but can also be acquired in granular form.

Unfortunately, however, both diquat and paraquat show very high toxicity towards animals and man. The synthesis and applications of both diquat and paraquat and other related bipyridinium herbicides have already been extensively discussed[5].

The bipyridinium herbicides can be readily reduced to stable radical cations by a one electron transfer. The potential of the redox system between diquat and paraquat and their radical cations are -0.35V and -0.45V respectively.

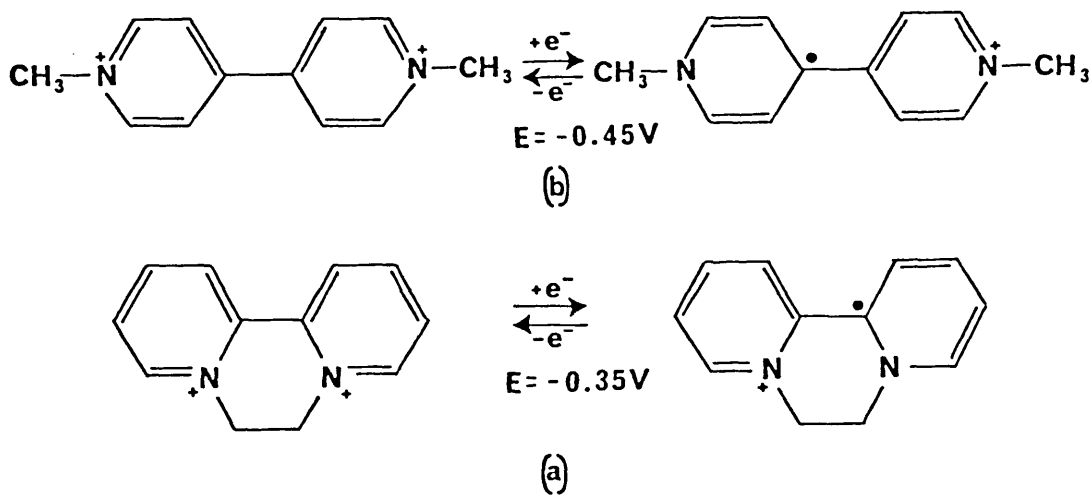


Figure 1.2. The redox potential of diquat (a) and paraquat (b).

The stability of these radical cations is due to their near planarity (diquat has a twist angle between its pyridine rings of approximately 20^{o}, whilst paraquat is planar) which enables the delocalisation of the odd electron over the whole structure.

1.3 Herbicidal Activity of Diquat and Paraquat.

The herbicidal activity of diquat and paraquat is due to their reduction in the chloroplasts by the Photosynthesis Pigment 1 in light[5] (and to a lesser extent by respiration in the dark) to their radical cations. The free radicals are then readily reoxidized by molecular oxygen to their diquaternary salts generating hydrogen peroxide and unknown intermediate radicals that destroy the plant cells. This action is thus catalytic. The energy for this reduction comes from the photolysis of water in the light and respiration in the dark. This mode of action explains why the diquat and paraquat herbicides produce rapid leaf bleaching followed by desiccation in strong sunlight. Since the bipyridinium herbicides act very rapidly in full sunlight, very little translocation occurs out of the treated areas due to the damage caused to the leaves which prevents movement of the herbicides to the conducting elements of the leaf tissue. However, in the absence of the photosynthetic electron transport system and hence rapid herbicidal action, the herbicides are translocated out of the treated leaf area. Therefore whereas in full sunlight toxicity occurs very rapidly within a few hours, in low sunlight or in the dark the herbicidal activity holds longer and the toxicity is more evenly spread over all the plant leaves as movement is possible within the xylem. Consequently the most effective conditions for maximum kill with diquat and paraquat involves spraying under dry soil conditions in the late afternoon when increased humidity and darkness can follow as soon as possible after treatment.

Diquat and paraquat can also form charge transfer complexes with electron-donor molecules including biologically important molecules[5]. Their complexes with 7,7,8,8,-tetracyanoquino-dimethane are electrically conducting[5]. So far no clear relationship has been found between charge transfer complexation and herbicidal activity, but it seems plausible that it may play some part in absorption and mobility of the herbicide in the plant. It has been suggested that complex formation may be responsible for deactivation of the herbicide on absorption in the soil and that charge transfer complexes might be involved in the transfer of one electron to diquat and paraquat in its photoreduction in plants[5].

1.4 Other Uses of Diquat and Paraquat.

Apart from their utilisation as herbicides, diquat and paraquat are used industrially in several processes such as photography and lithography due to their electrochemical properties. Currently paraquat (PQ) is attracting attention due to its ability to be reduced to its radical cation by visible light and then consequently with the aid of colloidal Platinium catalyst to reduce water via the reaction[6].

$$PQ(1+) + H_2O \text{ -------> } PQ(2+) + {}^{-}OH + (0.5)H_2$$

This photolysis of water produces energy and is attracting interest as a possible means of supplementing our dwindling natural energy resources.

1.5 Diquat and Paraquat Poisoning.

As already stated one of the problems of using diquat and paraquat herbicides is their acute toxicity to man. Numerous instances of poisoning especially from paraquat have been described in the literature, many of which have been fatal. Poisoning has often arisen from accidental ingestion of an aqueous solution. Death by diquat or paraquat poisoning is normally the result of progressive fibrosis and epilletial proliferation in the lung. Death which normally occurs after a week or two can result from consumption of as little as 0.5 - 1.5g of the herbicide.

In most cases of diquat and paraquat poisoning the herbicide is ingested and reaches the blood by absorption. The successful treatment of poisoning relies on the speed and success of removing the herbicide from the stomach and gastrointestinal tract. At present the most effective treatment for diquat and paraquat poisoning involves immediate induction of vomiting followed by administration of an aqueous suspension of Fullers earth to absorb the herbicide in the gastrointestinal tract. This treatment is then followed by an effective dose of a cathartic, such as magnesium sulphate, to promote and maintain gut clearance of the clay mineral. This treatment is then repeated every 2-4 hours for several days. Haemodialysis should be commenced immediately to remove the herbicide from the blood. This method has occasionally proved successful, but clearly an antidote to diquat and paraquat poisoning is required.

1.6 Molecular Receptors For Diquat and Paraquat.

The present interest in designing molecular receptors, to encapsulate diquat and paraquat have arisen for the following reasons:

1. To modify their biological activity as bipyridinium herbicides.
2. To gain a better understanding of the mechanism of their biological action.
3. To design an antidote to diquat/paraquat poisoning.
4. To act as chemical sensors in analysing diquat/paraquat systems.
5. To influence light-promoted water-splitting systems containing these bipyridinium dications.

1.7 Crown Ethers.

Since Pedersen first synthesised cyclic polyethers[7] (crown ethers) they have attracted considerable attention due to their ability to complex metallic and organic cations, anions and neutral molecular species. Crown ethers can also act as ionophores by forming stable lipophilic complexes with metal cations, which can then be transported into lipophilic phases, or across natural or artificial membranes. Crown ethers can be designed and synthesised which have different complexing and transport properties towards different metal cations, e.g. crown ethers can discriminate between alkali cations of different ionic radii.

In this thesis the widely adopted notation of letters and numbers will be used to identify the crown ether hosts. Thus the first number in the general description represents the size of the macrocyclic

crown ether ring, the second number represents the number of oxygen or other hetro atoms in the ring. The letters B, DB, and DN preceeding the description stand for fused benzo-, dibenzo-, and di(2,3)-naphtho rings respectively.

There is a substantial amount of structural data avaliable on crown ethers[8]. For example the minimum energy conformation of the 1,4 dioxa units $O-CH_2-CH_2-O$ is when the C-C bond torsion angle is gauche (synclinal, 60^o) and the C-O bond torsion angle is trans (antiperiplanar, 180^o), though these torsional angles can deviate significantly, if required, to achieve complex formation. The aliphatic C-C bond lengths are systematically shorter in the structures of crown ethers and their complexes than in other aliphatic ring compounds. The reason given for the shorting of the C-C bond is the slightly polarised character of the adjacent C-O bonds which causes partial positive charges on the carbon atoms.

Crown ethers can also complex positively charged or neutral organic species via hydrogen bonding interactions between N-H, O-H and polar C-H protons and the crown ether oxygens. With positively charged species, there is also the possibility of dipole-pole interactions to aid the stability of the complex.

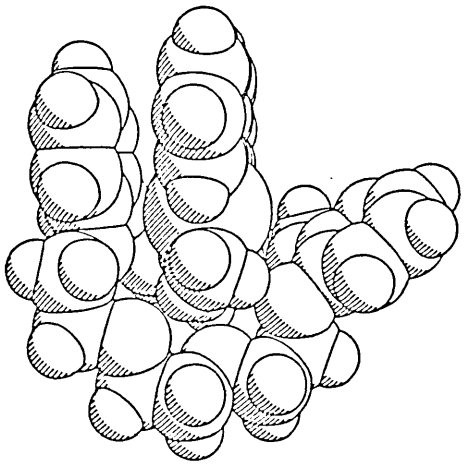
Crown ethers do not readily form complexes with transition metal cations in low oxidation states, however, by forming a transition metal complex containing ammines which are then subsequently able to interact with the crown ethers via (N-H...O) hydrogen bond formation,

adducts can be formed between transition metal complexes and crown ethers where the crown ethers act as second sphere coordination ligands for the transition metals[9]. In addition to the H-bonding interactions the stability of the adduct formed between the transition metal complex and the crown ether can be enhanced by electrostatic interactions between transition metal cation and the ether oxygen atoms.

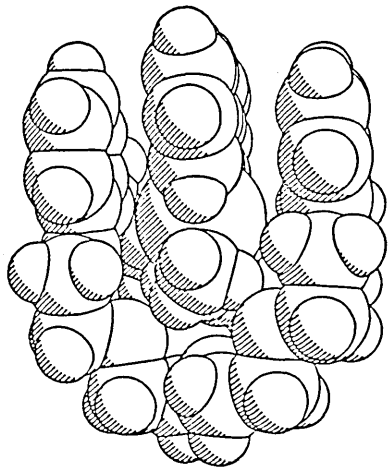
1.8 Charge Transfer Complexes Involving Dibenzo Crown Ethers.

X-ray analyses of the structures of the adducts formed between DB-crown ethers and the $Pt(bipy)(NH_3)_2$ transition metal complex revealed some unexpected results[10]. In addition to the expected H-bond and elecrostatic interactions, in the case of DB24C8 a charge transfer interaction is observed between one of the benzo groups in the crown and the π-deficient bipyridyl moiety on the Pt (figure 1.3). The DB30C10 macrocycle, however on the other hand is sufficiently large and flexible to allow both of the benzo rings to enter into stabilising interactions with the bipyridyl ligand such that the platinum complex is encapsulated by the host in a U-shaped cavity (figure 1.4). The charge transfer interactions were also evidenced by ^1H NMR and UV-visible spectra in solution. Although a broad charge transfer absorption band at 350 nm attains its maximum intensity for the DB33C11 adduct, stability constant measurements indicated optimum binding for the DB30C10 adduct. Charge transfer interactions with DB-crown ethers had never previously be reported by X-ray analysis.

As the major interaction in the Pt adduct appeared to be charge



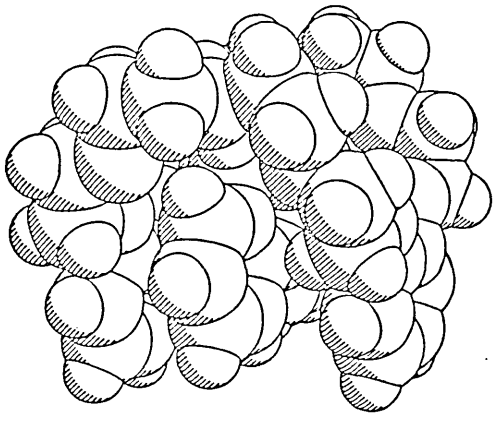
(figure 1.3)



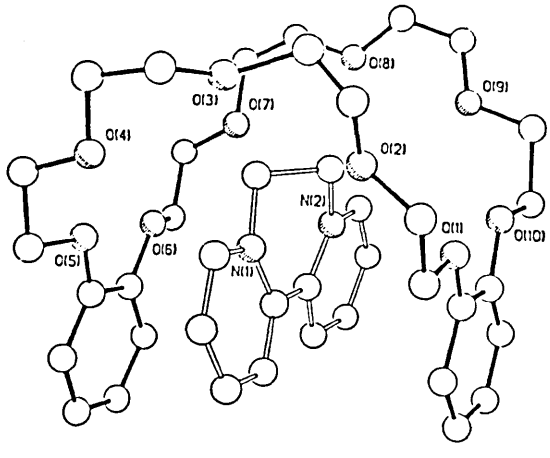
(figure 1.4)

Figure 1.3. The space-filling representation of the solid-state structure of the 1:1 complex between $[Pt(bipy)(NH_3)_2]^{2+}$ and DB24C8.

Figure 1.4. The space-filling representation of the solid-state structure of the 1:1 complex between $[Pt(bipy)(NH_3)_2]^{2+}$ and DB30C10.



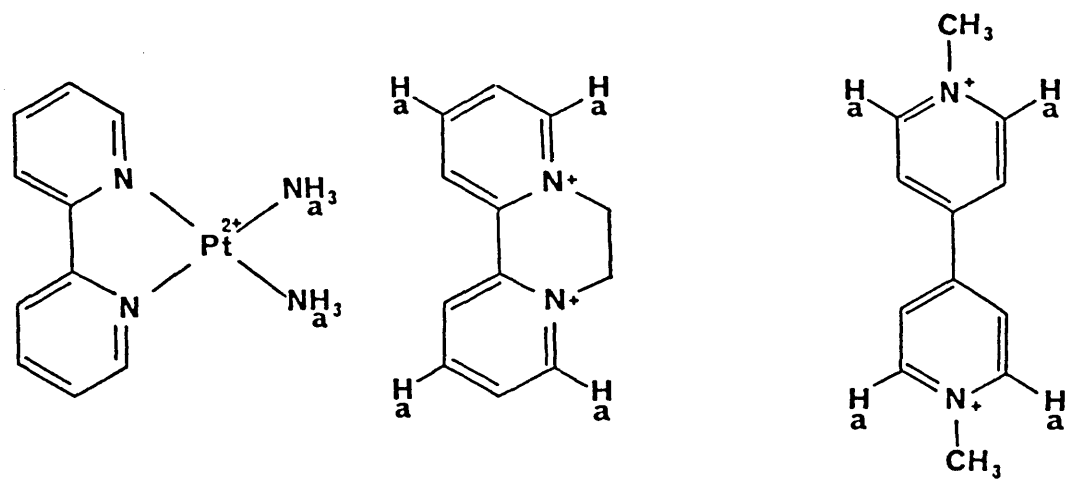
(a)



(b)

Figure 1.6. The solid-state structure in both space filling (a) and framework (b) representations of the 1:1 complex between the diquat dication and DB30C10.

transfer between the bipyridyl moiety and the benzo groups in DB30C10, the question was posed, could DB-crown ethers also form complexes with organic molecules based on the bipyridyl moiety? The first molecules considered were the bipydinium herbicides diquat and paraquat, both of which have similar properties to the $Pt(bipy)(NH_3)_2$ complex: both are dicationic species, they contain acidic hydrogens and a bipyridyl residue.



H = Acidic protons.
a

Figure 1.5. The similar properties of $Pt(bipy)(NH_3)_2$, diquat and paraquat.

Solution studies of a range of DB3nCn (n = 6 to 12) with diquat revealed the existence of charge transfer absorption bands ca. λ 400 nm[11]. The qualitative conclusion from these experiments indicated that the most stable 1:1 complex is formed between the DB30C10 macrocycle and diquat. When the crystal structure of [DB30C10][diquat, bishexaflurophosphate] was undertaken, the deep red crystal chosen had

to be sealed under solution in a Lindemann glass capillary tube due to its air sensitive nature. The structure analysis revealed (figure 1.6) that the diquat dication like the $Pt(bipy)(NH_3)_2$ complex, is encapsulated by DB30C10 in a U-shaped cavity. Again there is a parallel alignment and close contact between the π-deficient bipyridyl moiety and both benzo rings (interplanar separation of ca. 3.5 Å) enabling charge transfer to take place. The diquat complex also has stabilising H-bond interactions involving principally H-6 and H-6' on the bipyridinium ring system of the guest and certain ether oxygens in the host. There is also a linear aligment of the catechol oxygens and the formally positively charged nitrogens of diquat with two short N...O distances implying that dipole-pole interactions could be taking place. Unfortunately these DB-crown ethers were unable to form complexes with paraquat.

1.9 Aim of Research.

With the knowleage that DB-crown ethers can complex the diquat dication, this project will demonstrate how X-ray crystal structure analysis can be used to study the molecular topology and conformational flexibility of the free and complexed receptors for diquat and paraquat which are crucial in understanding how the receptors function. The project will then proceed to show how X-ray crystallography can be used as a principal design tool to aid the synthesis of new receptors which will have enhanced binding interactions and stability.

1.10 REFERENCES

1. W.W. Fletcher, 'Recent Advances In Weed Research,' Commonweath Agricultural Bureaux 1983.
2. R.J. Stephens 'Theory And Practise Of Weed Control,' MacMillan Press Ltd, 1982.
3. W.W. Fletcher, and R.C. Kirkwood, 'Herbicides And Plant Growth Regulators,' Granada Publishing Ltd, 1982.
4. R.F. Homer, R.L. Jones, and J.Stubbs, Nature, 1958, 181, 446.
   R.F. Homer, G.C. Mees, and T.E. Tomilinson, J.Sci. Food Agric., 1960, 11, 309.
5. L.A. Summers, 'The Bipyridinium Herbicides,' Academic Press, London, 1980.
6. M. Grätzel, Acc. Chem. Res., 1981, 14, 376.
7. C.J. Pedersen, J. Am. Chem., 1967, 89, 7017.
8. E. Weber, and F. Vogtle, Topics in Current Chemistry, 1981, 98, 1.
   D.J. Cram, and K.N. Trueblood, IBID, 1981, 98, 43.
   F. Vögtle, H. Seiger, and W.M. Muller, IBID, 1981, 98, 107.
   R. Hilgenfield, and W. Saenger, IBID, 1982, 101, 1.
   M. Dobler, 'Ionophores and Their Structures,' Willey-Interscience, 1981.
9. H.M. Colquhoun, and J.F. Stoddart, J. Chem. Soc., Chem. Commun., 1981, 612.
   H.M. Colquhoun, J.F. Stoddart, and D.J. Williams, J. Chem. Soc., Chem. Commun., 1981, 847, 849, 851.
   H.M. Colquhoun, D.F. Lewis, J.F. Stoddart, and D.J. Williams, J. Chem. Soc. Dalton Trans., 1983, 607.
10. H.M. Colquhoun, J.F. Stoddart, D.J. Williams, J.B. Wolstenholme,

and R. Zarzycki, Angew. Chem. Int. Ed. Engl., 1981, 20, 1051.

H.M. Colquhoun, S.M. Doughty, J.M. Maud, J.F. Stoddart, D.J. Williams, and J.B. Wolstenholme, Isr. J. Chem., 1985, 25, 15.

11. H.M. Colquhoun, E.P. Gooding, J.M. Maud, J.F. Stoddart, D.J. Williams, and J.B. Wolstenholme, J. Chem. Soc., Chem. Commun., 1983, 1140.

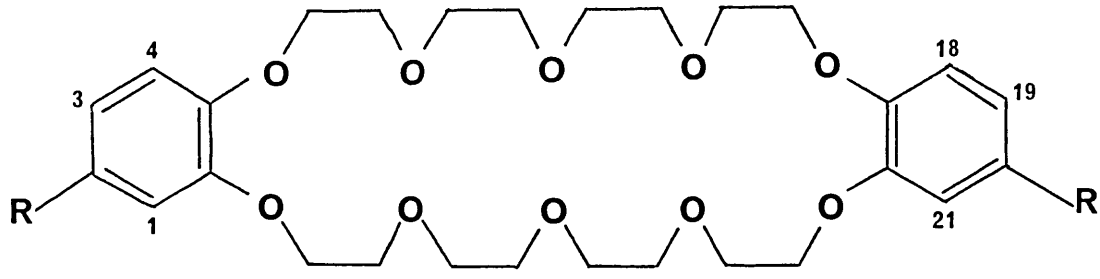
H.M. Colquhoun, E.P. Gooding, J.M. Maud, J.F. Stoddart, D.J. Williams, and J.B. Wolstenholme, J.Chem. Soc., Perkin Trans. 2, 1985, 607.

CHAPTER 2

The crystal structures of the complexes of 2,20-Dimethyl-6,7,9,10,12,13,15,16,23,24,26,27,29,30,32,33-hexadecahydrodibenzo[b,q][1,4,7,10,13,16,19,22,25,28]decaoxacyclotriacontin and 2,20-bishydroxymethyl-6,7,9,10,12,13,15,16,23,24,26,27,29,30,32,33-hexadecahydrodibenzo[b,q][1,4,7,10,13,16,19,22,25,28]decaoxacyclotriacontin (disubstituted DB30C10 derivatives) with diquat.

2.1 INTRODUCTION

Diquat has been shown to form a complex with DB30C10[1] in which the interactions are; charge transfer between the bipyridinium dication and the nearly parallel benzo groups of the host, pole-dipole interactions between the formally positively charged bipyridinium nitrogens and the phenolic oxygens of the host, and C-H...O interactions involving the acidic protons on the diquat and certain polyether oxygens of the host.



1 R = H

2 R = CH_3

3 R = CH_2OH

4 R = CHO

The following DB30C10 derivatives 2, 3, 4 were synthesised[2] and X-ray structural analyses of their complexes with [diquat][PF_6]$_2$ have been carried out[2]. The aim was to investigate the effects of the substitution of the DB30C10 moeity on complexing ability, especially how this affects the weak intermolecular binding interactions between the receptors and diquat. The stability constants for the 1:1

complexes formed in solution will also be discussed.

2.2 EXPERIMENTAL

Deep-red crystals of [2.diquat][PF_6]$_2$.H_2O were obtained from a solution of [2.diquat][PF_6]$_2$ in CH_3OH/CH_3COCH_3 by vapour diffusion with light petroleum. A crystal of dimensions 0.05 x 0.55 x 0.63 mm was used for unit cell and intensity measurements.

Crystal data: $C_{30}H_{44}O_{10}.C_{12}H_{12}N_2.P_2F_{12}.H_2O$, M = 1057, monoclinic, a = 11.698(2), b = 19.112(4), c = 22.182(5) Å, $\beta = 97.32(2)^o$, U = 4919 Å^3 space group $P2_1/n$, Z = 4, D_c = 1.43 g cm^{-3}, F(000) = 2199, μ(Cu-K_α) = 17.2 cm^{-1}.

Refined unit-cell parameters were obtained by centering 14 reflections on a Nicolet R3m diffractometer. 5043 unique reflections ($\theta < 50^o$) were measured with Cu-K_α radiation (graphite monochromator) using the omega-scan routine. Of these 3602 had $|F_o| > 3\sigma(|F_o|)$ and were considered to be observed. The net count of two reflections, the -3 -2 0 and the 0 2 4, measured as references every 50 reflections did not alter significantly during the data collection indicating that no deterioration of the crystal had occurred. The data were brought to a uniform arbitrary scale by the use of these reflections and Lorentz and polarisation corrections were applied.

The structure was solved by direct methods. A starting set comprising 3 origin defining reflections together with a further 5

automatically selected terms was used. The initial phase refinement (32 permutations) was with 200 $\underline{E}$'s > 1.8 using 1099 TPR. This was subsequently expanded to 420 probable phases with $\underline{E}$'s > 1.8 using 2197 TPR. The figures of merit for the best phase solution were NQEST = -0.252, RA(1) = 0.053, RA(2) = 0.085. An $\underline{E}$-map computed using this phase solution gave plausible positions for 43 out of the 69 non-hydrogen atoms in the structure. The remaining non-hydrogen atoms were found in a succession of $\Delta\underline{F}$-maps, which also revealed the presence of an included water molecule. The non-hydrogen atoms were refined anisotropically. The methylene and phenyl hydrogens were placed at calculated positions (C-H = 0.96 Å), assigned isotropic thermal parameters, $\underline{U}(H) = 1.2\ \underline{U}_{eq}(C)$, and allowed to ride on their parent carbon atoms. One of the methyl groups, C(39), was refined as a rigid body, (C-H = 0.96 Å, H-C-H = 109.5°), whilst the other methyl group was placed in a fixed orientation. The hydrogen atoms on the water molecule were not located. The refinement showed there to be severe disorder in one of the PF_6 anions, and consequently this anion was idealised and refined as a rigid body (P-F = 1.55 Å).

Refinement using $\underline{F}$ magnitudes was by block-cascade full-matrix least squares (607 variable parameters) and converged to $\underline{R}$ = 0.122, $\underline{R}_w$ = 0.126, a fixed weight was used [$w^{-1} = \sigma^2(\underline{F}) + 0.0005\underline{F}^2$]. The largest parameter shift/e.s.d. was 0.024, the mean shift/e.s.d. was 0.007. The residual electron density in the final difference map was within -0.43 and 0.81 $e\text{Å}^{-3}$.

Deep-red crystals of [3.diquat][PF_6]$_2$ were obtained from a solution

of [3.diquat][PF_6]$_2$ in CH_3OH/CH_3COCH_3 by vapour diffusion with heptane-light petroleum. A crystal (coated in Araldite to prevent decomposition) of dimensions 0.40 x 0.46 x 0.60 mm was used for unit cell and intensity measurements.

Crystal data: [3.diquat][PF_6]$_2$, orthorhombic, a = 11.342(4), b = 22.064(6), c = 39.40(2) Å, U = 9859 Å^3, space group $P222_1$, Z = 8

Refined unit-cell parameters were obtained by centering 25 reflections on a Nicolet R3m diffractometer. 6986 unique reflections ($\theta < 58^o$) were measured with Cu-K_α radiation (graphite monochromator) using the omega-scan routine. Of these 3820 had $|F_o| > 3\sigma(|F_o|)$ and were considered to be observed. The net count of two reflections, the -2 1 2 and the -3 -2 1, measured as references every 50 reflections did not alter significantly during the data collection indicating that no deterioration of the crystal had occurred. The data were brought to a uniform arbitrary scale by the use of these reflections and Lorentz and polarisation corrections were applied.

Unfortunately the crystal structure solution of [3.diquat][PF_6]$_2$ is proving to be particularly demanding because of the presence of two crystallographically independent molecules in a non-centrosymmetric space group and the consequent requirement to determine the positions of ~ 140 non-hydrogen atoms.

Numerous attempts using both conventional tangent refinement and random start tangent refinement, with different space groups have so

far failed to solve the phase problem. The ambiguity in the space group is due to the problem of deciding whether certain reflections are genuinely weakly observed or systematically absent. The following space groups were tried: $\underline{P}222$, $\underline{P}222_1$, $\underline{P}22_12_1$, $\underline{Pcm}2_1$ (the last due to the exceptionally weak 0kl zone).

The best phase solution obtained (in $\underline{P}222_1$) from the random start tangent refinement involved 4000 tries using 351 $\underline{E}$'s > 1.91 and 3650 TPR resulted in figures of merit of NQEST = - 0.165, R(A) = 0.071, CFOM = 0.063. Three cycles of $\Delta\underline{E}$-map recycling for this solution gave an $\underline{R}_E$ = 0.34 for 111 atomic positions using 1353 $\underline{E}$'s > 1.32. Unfortunately no recognisable structural fragments appeared.

Large starting sets incorporating $\Sigma 1$ phases, reflections which were weak links in the convergence mapping, and reflections which were principal contributors to the list of negative quartets, together with additional automatically selected terms were tried. The minimum $\underline{E}$ value for the reflections used in the intial starting set and phase expansion was also varied. As the number of negative quartets was small solutions were also ranked on R(A) instead of NQEST. The lowest $\underline{R}_E$ that was obtained was 0.35 for 112 potential atomic positions using 1352 $\underline{E}$'s > 1.32 after 3 cycles of $\Delta\underline{E}$-map recycling of one of the phase solutions. This also again failed to produce any recognisable structural fragments.

Deep-orange crystals of [4.diquat][PF_6]$_2$.0.75(CH_3CN) were obtained from a solution of [4.diquat][PF_6]$_2$ in CH_3CN by vapour diffusion with Et_2O-CH_3CN. A crystal of dimensions 0.20 x 0.35 x 0.43 mm was used

for unit cell and intensity measurements.

Crystal data: $C_{30}H_{40}O_{12}.C_{12}H_{12}N_2.P_2F_{12}.0.75(CH_3CN)$, M = 1087, orthorhombic, a = 11.445(2), b = 20.417(4), c = 21.397(5) Å, U = 5000 Å^3, space group $P2_1cn$, Z = 4, D_c = 1.45 g cm^{-3}, F(000) = 2274, μ(Cu-K_α) = 17.3 cm^{-1}.

Refined unit-cell parameters were obtained by centering 20 reflections on a Nicolet R3m diffractometer. 3578 unique reflections ($\theta \leq 58^o$) were measured with Cu-K_α radiation (graphite monochromator) using the omega-scan routine. Of these 2338 had $|F_o| > 3\sigma(|F_o|)$ and were considered to be observed. The net count of two reflections, the -3 -1 2 and the -2 -1 1, measured as references every 50 reflections did not alter significantly during the data collection indicating that no deterioration of the crystal had occurred. The data were brought to a uniform arbitrary scale by the use of these reflections and Lorentz and polarisation corrections were applied.

Several attempts at conventional multiple solution tangent refinement using a series of different, both automatically selected and hand chosen, starting sets failed to produce recognisable structural fragments. The structure was eventually solved by resorting to random start tangent refinement. 2500 tries using 229 E's > 1.85 and 2443 TPR resulted in best figures of merit of NQEST = -0.195, R(A) = 0.051, CFOM = 0.012. Three cycles of ΔE-map recycling for this solution revealed 49 potential non-hydrogen atomic positions with an R_E = 0.336 for 924 E's > 1.20. Several plausible molecular fragments

seemed to be appearing, 21 positions were retained and a further 4 cycles of $\Delta\underline{E}$-map recycling carried out. This resulted in an improved $\underline{R}_E$ = 0.292 for 64 potential non-hydrogen atomic positions. A further 3 cycles of $\Delta\underline{E}$-map recycling retaining 61 of these positions gave an $\underline{R}_E$ = 0.276 for 71 potential atoms. 63 of these positions were retained and the remaining atomic positions were obtained from subsequent $\Delta\underline{E}$-maps. A $\Delta\underline{E}$ map also revealed the presence of a partial occupancy acetonitrile molecule. The non-hydrogen atoms were refined anisotropically. The methylene and phenyl hydrogens were placed at calculated positions (C-H = 0.96 Å), assigned isotropic thermal parameters, $\underline{U}(H) = 1.2\ \underline{U}_{eq}(C)$ and allowed to ride on their parent carbon atoms. The protons on the partial occupancy acetonitrile molecule were not located. The refinement showed there to be severe disorder in both of the PF_6 anions. These anions were subsequently refined as idealised rigid bodies.

Refinement using $\underline{F}$ magnitudes was by block-cascade full-matrix least squares (622 variable parameters) and converged to $\underline{R}$ = 0.115, $\underline{R}_w$ = 0.118, a fixed weight was used [$w^{-1} = \sigma^2(\underline{F}) + 0.001\underline{F}^2$]. The largest parameter shift/e.s.d. was 0.149, the mean shift/e.s.d. was 0.034. The residual electron density in the final difference map was within -0.36 and 0.70 $e\text{Å}^{-3}$.

All computations were carried out on an Eclipse S140 computer using the SHELXTL[3] program system.

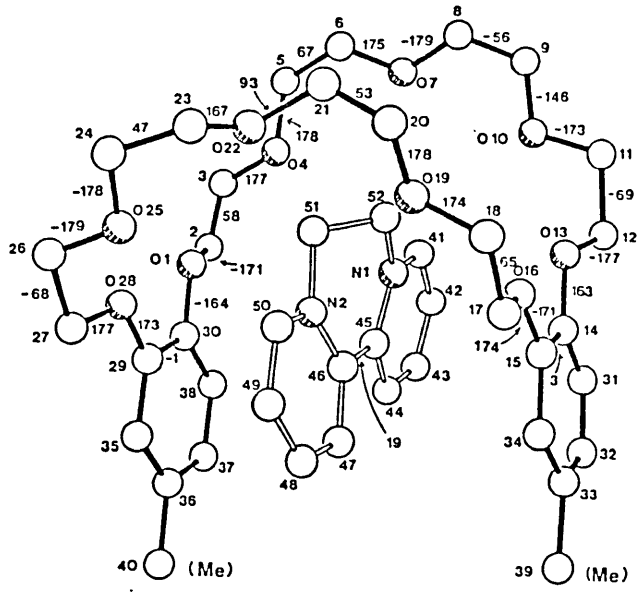
2.3 DISCUSSION

The final fractional atomic coordinates, anisotropic thermal parameters, bond lengths and bond angles for the non-hydrogen atoms in [2.diquat][PF_6]$_2$.H_2O and [4.diquat][PF_6]$_2$.0.75(CH_3CN) are shown in Tables 2.1 - 2.4 and 2.6 - 2.9 respectively. The positions and isotropic temperature factors for the hydrogen atoms in [2.diquat][PF_6]$_2$.H_2O and [4.diquat][PF_6]$_2$.0.75(CH_3CN) are shown in Tables 2.5 and 2.10 respectively.

Both receptors 2 and 4 exhibit the same mode of U-shape encapsulation of the diquat as observed for the DB30C10 receptor[1]. Their bond lengths and angles are, within the accuracy of the structure determination, in agreement with previously published work on crown ethers[4]. The torsion angles associated with the 30-membered rings in complexes [2.diquat] and [4.diquat] are shown beside the relevant C-C and C-O bonds in the skeletal structures reproduced in figure (2.1) which also provide the details of the crystallographic numbering schemes.

Inspection of the torsion angles in figure (2.1) reveals noticeable departures from the conventional 'all-gauche' polyether geometry. There are also differences in the conformation adopted by the polyether chains in [2.diquat] compared with [4.diquat]. The most noticeable torsion angle differences involve the C(21)-O(22) bond where the torsion angles are 93 and 172^o in [2.diquat] and [4.diquat] respectively, and the C(23)-C(24) bond where the signs of the torsion angles are reversed. The different conformations of the 30-membered polyether chains in [2.diquat] and [4.diquat] are very similar to the

(a)



(b)

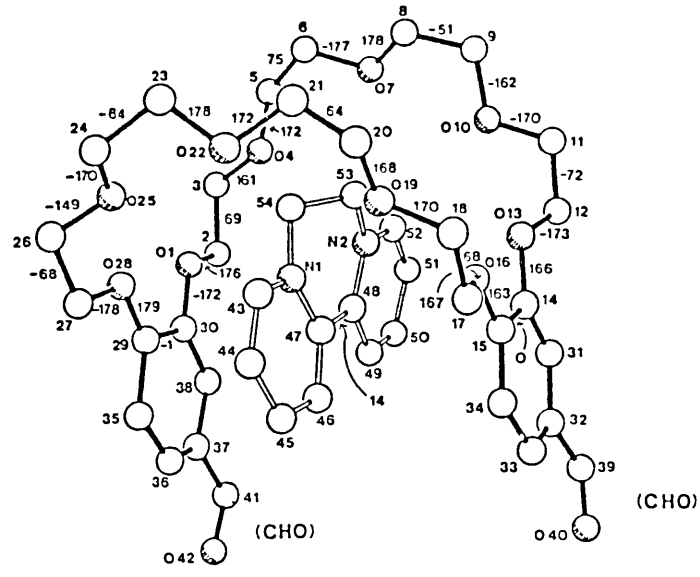
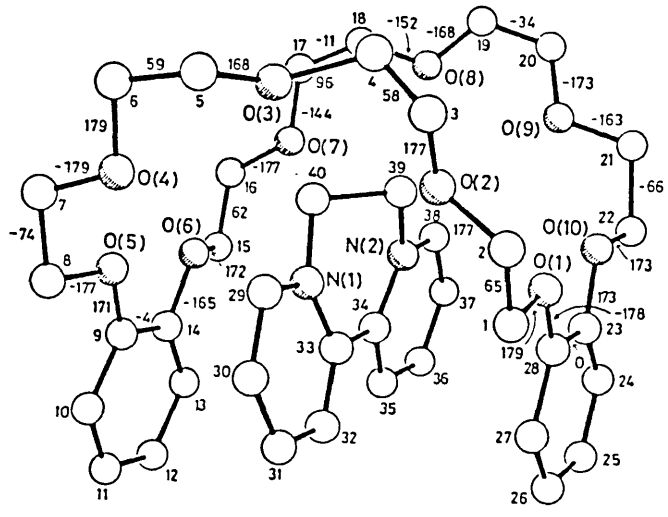


Figure 2.1. The skeletal representations of the solid-state structures of [2.diquat] (a) and [4.diquat] (b).

(a)



(b)

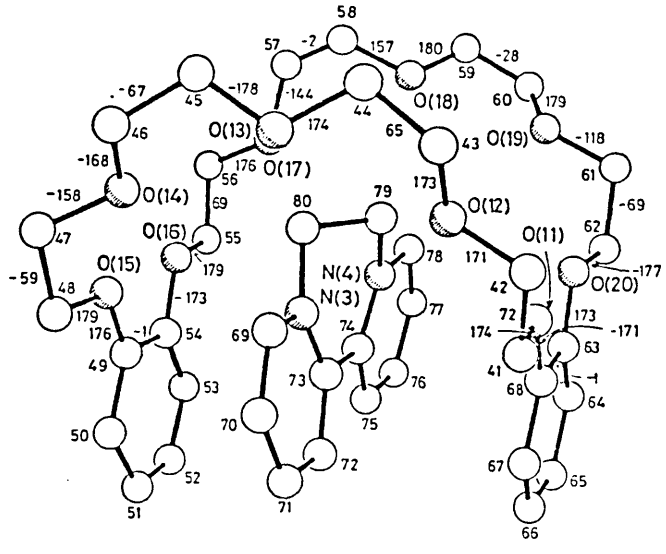


Figure 2.2. the skeletal representations of the solid-state structures of the two independent complexes I (a) and II (b), found in [diquat.DB30C10].

two independent conformations figure (2.2) observed in the [1.diquat] crystal structure.

In addition to the already mentioned disorder in the PF_6 anions, there is probable disorder in the polyether chains of both complexes as evidenced by several atoms displaying large thermal anisotropy. This is particularly pronounced in the C(3) to C(9) and C(20) to C(24) portions of the macrocycle in [2.diquat]. In no instance was it possible to identify discrete alternative sites for atoms displaying high thermal motion. A consequence of this disorder is an artificial shortening of some of the bonds and a distortion of the associated angles [see tables 2.2,2.3,2.7 and 2.8]. This disorder coupled with that of the PF_6 anions is a principle cause of the somewhat high R-factors obtained. A contributary factor to the disorder may be the absence of strong stabilising hydrogen bonding interactions between the guest and the ether oxygens. Disorder was also present in both the crystallographically independent conformations observed for [1.diquat]. However in the [1.Pt(bipy)$(NH_3)_2$] adduct[5] where three of the ten ether oxygens are involved in relatively strong N-H...O hydrogen bonds, to three of the six hydrogen atoms in the two ammine ligands, disorder was not nearly so pronounced.

In view of the very limited established data and uncertainty in this area[6], we have chosen to define the criteria for consideration of possible [C-H...O] interactions as [C...O] < 3.4, [H...O] < 2.5 Å and C-H...O > 140^{o}. These criteria will also be adopted for possible C-H...F interactions. The geometric parameters for possible [C...O] and [C-H...O] contacts (selected on the basis of the above criteria)

which could enhance host-guest interactions are listed in tables [2.11 and 2.12]. In [2.diquat] only the methylene protons [H(51b) and H(52b)] are probably involved in C-H...O interactions. In [4.diquat] only the the most acidic[7] protons, those on C(43) and C(52), are possibly involved in C-H...O interactions.

The space-filling and stereo-pair representations of the structures figures (2.3 and 2.4) help to provide a better overall appreciation of the interactions involved between the diquat dication and DB30C10 derivatives.

The side-on views, of [2.diquat] and [4.diquat] figure (2.5) show that the polyether chains form hydrophilic loops around the aromatic protons (C(41) and C(50)in [2.diquat], C(43) and C(52) in [4.diquat]). The geometry of the overlap between the bipyridyl units and the benzo rings can clearly be seen. The near parallel alignment of the benzo rings with respect to the bipyridinium moiety should be advantageous for charge transfer[8]. For maximum charge transfer interaction to occur between the two parallel phenyl rings the two groups should not be eclipsed, but slighty displaced with respect to each other[8]. The separations between the benzo rings in the hosts are ~ 7.0 and 6.9 Å with 4.7 and 3.8° departures from parallel alignment for [2.diquat] and [4.diquat] respectively. The distance of 3.4 Å in both structures between one of the mean planes of the benzo rings of the host and the nearest overlapping atom of the diquat [C(45) in [2.diquat] and C(47) in [4.diquat]] is ideal for charge transfer between the π-electron rich catechol units in the host[8] and the π-deficient bipyridinium ring

TABLE 2.11. Selected host-guest contact distances, and relevant hydrogen contact distances and angles where appropriate, in order of increasing $X^a...O$ distance for [2.diquat].

$X^a...O$	$R(X^a...O)$ (Å)	$R(H...O)$ (Å)	$\psi(^o)^b$	$\theta(^o)^c$
C(41)-O(10)	3.12			
C(50)-O(25)	3.14			
N -O(13)	3.21			
C(41)-O(13)	3.28			
C(50)-O(19)	3.28			
C(50)-O(28)	3.29			
C(52)-O(13)	3.30			
C(51)-O(1)	3.32	2.42[d]	49[d]	156[d]
C(52)-O(16)	3.33	2.45[e]	39[e]	153[e]
C(51)-O(19)	3.35			
C(41)-O(4)	3.38			

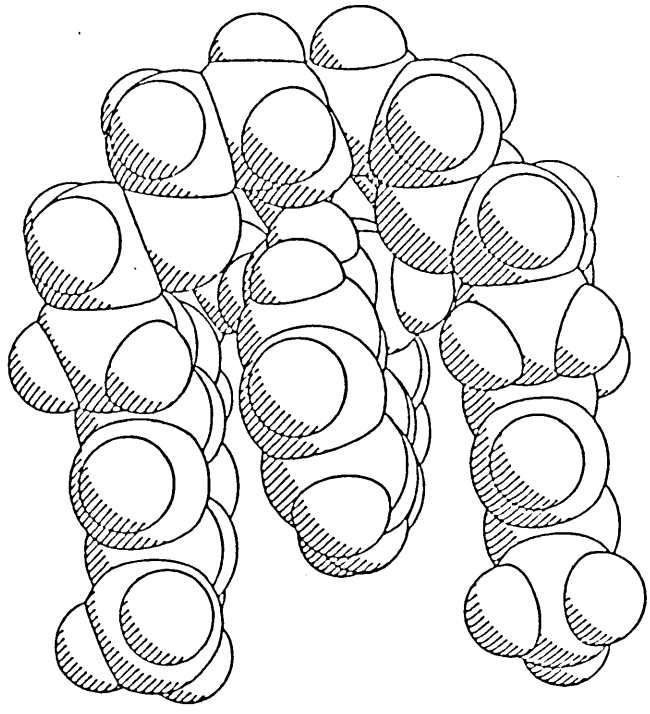
[a] Carbon or Nitrogen atom of the diquat dication.
[b] Angles between COC planes and HO vectors.
[c] C-H...O angles.
[d] H(51b)
[e] H(52b)

TABLE 2.12. Selected host-guest contact distances, and relevant hydrogen contact distances and angles where appropriate, in order of increasing $X^a...O$ distance for [4.diquat].

$X^a...O$	$R(X^a...O)$ (Å)	$R(H...O)$ (Å)	$\psi(^o)^b$	$\theta(^o)^c$
C(52)-O(10)	2.99			
C(43)-O(19)	3.09			
N(2) -O(13)	3.19			
C(43)-O(22)	3.20	2.26	41	165
C(43)-O(25)	3.20			
C(52)-O(4)	3.23			
C(52)-O(13)	3.25			
N(2) -O(4)	3.32			
C(52)-O(7)	3.37	2.48	42	153
C(53)-O(13)	3.38			
N(1) -O(19)	3.39			

[a] Carbon or Nitrogen atom of diquat dication.
[b] Angles between COC planes and HO vectors.
[c] C-H...O angles.

(a)



(b)

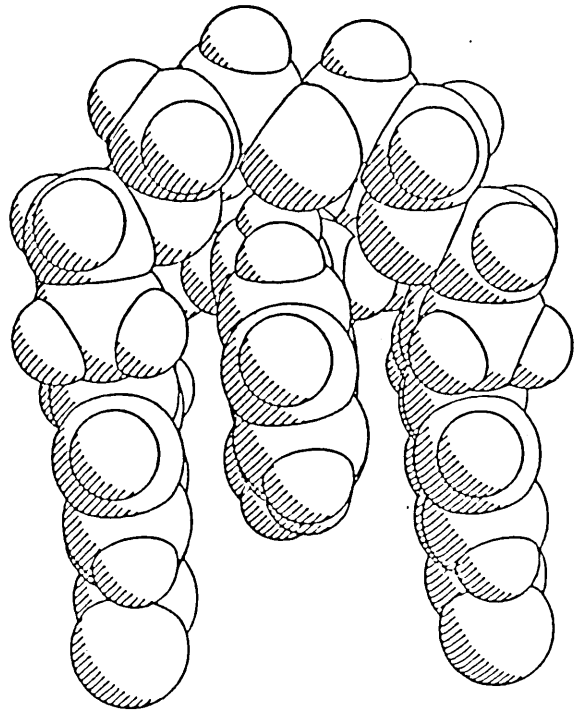
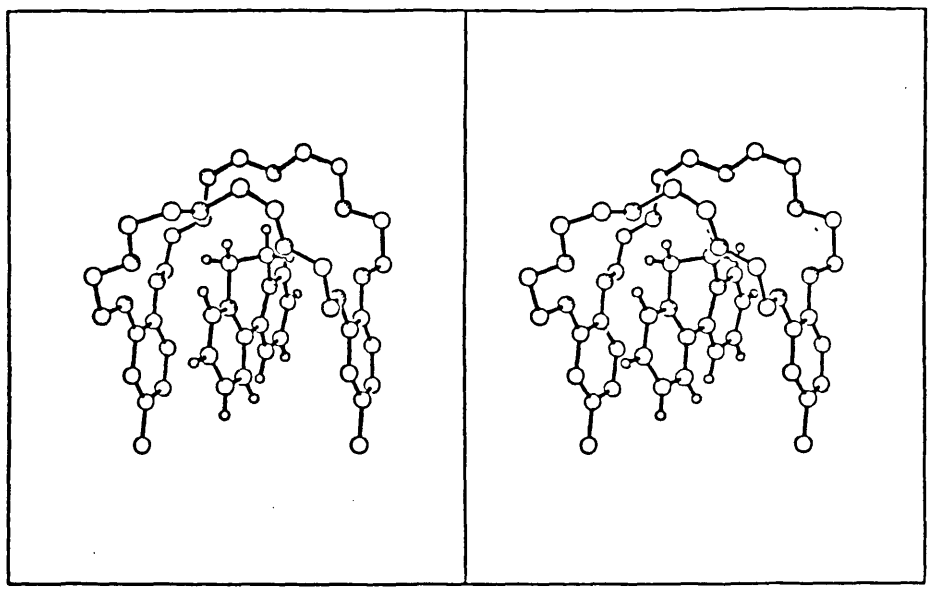


Figure 2.3. The space-filling representations of the solid-state structures of [2.diquat] (a) and [4.diquat] (b).

(a)



(B)

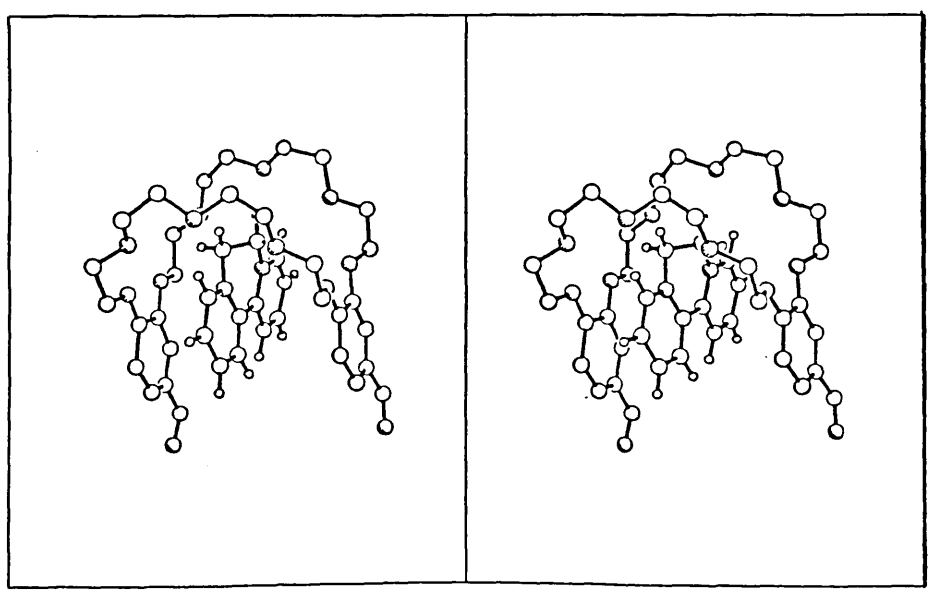
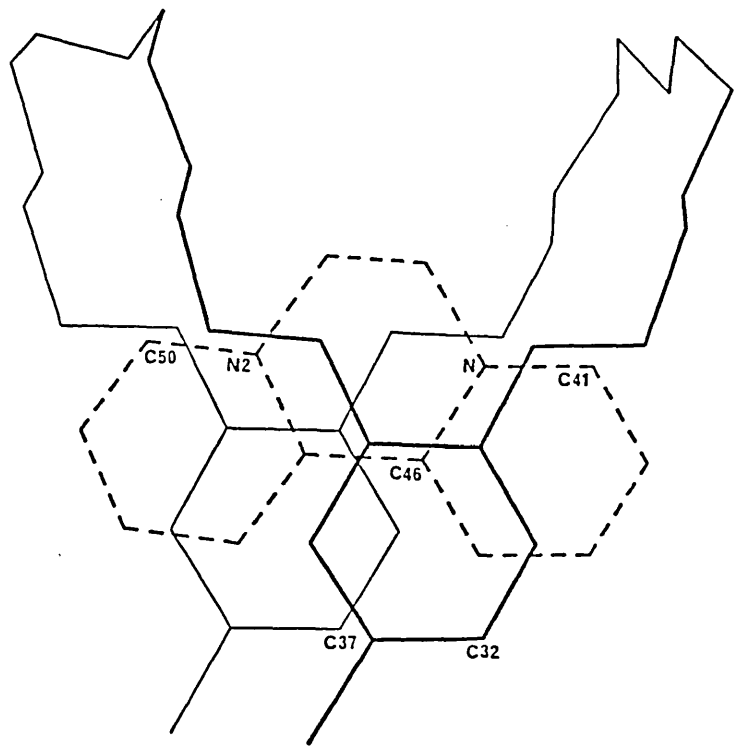


Figure 2.4. The stereo-pair representations of the solid-state structures of [2.diquat] (a) and [4.diquat] (b).

(a)



(b)

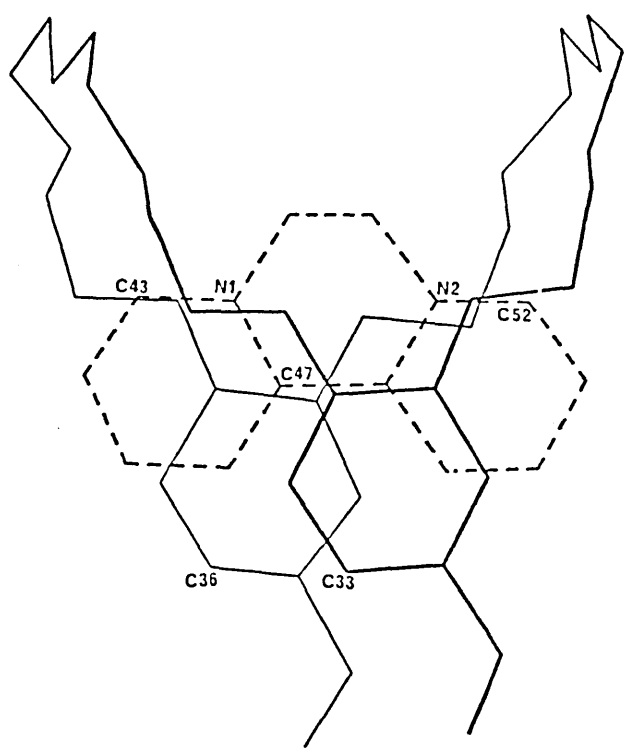


Figure 2.5. Side-on views (view normal to mean plane of diquat dication) of the skeletal representations of the solid-state structures of [2.diquat] (a) and [4.diquat] (b).

in the guest.

The dihedral angles between the mean planes of the pyridinium rings are 19(1) and 14(2)^{o} for complexes [2.diquat] and [4.diquat] respectively. These are consistent with the previously observed dihedral angles for the diquat molecule[1,9].

The ortho-related oxymethylene units in the hosts adopt a co-planar geometry with respect to their phenyl rings. This conformational feature allows delocalisation of the non-bonding electrons on the phenolic oxygens into the aromatic rings by means of good overlap between the lone pair orbitals of the catechol oxygens and the π^{*}-orbital of the benzo rings[10]. This stereoelectronic interaction probably enhances charge transfer between the catechol rings and the bipyridinium dication.

As observed for the two crystallographically independent structures of [1.diquat], in both [2.diquat] and [4.diquat] there is also a near alignment and close juxtaposition of the phenolic oxygens atoms in the hosts with the formally positively charged nitrogen atoms in the guest. This arrangement may impart some electrostatic stabilisation upon the complexes. The N...O distances are; N...O(13) 3.21, N(2)...O(28) 3.41 Å in [2.diquat]; N(1)...O(28) 3.41, N(2)...O(13) 3.19 Å in [4.diquat], and the O...N...O angles are; O(1)...N...O(13) 168, O(16)...N(2)...O(28) 171^{o} in [2.diquat]; O(16)...N(1)...O(28) 168, O(13)...N(2)...O(1) 172^{o} in [4.diquat].

The water molecule in [2.diquat] is involved in three fairly short

contacts to crown ether oxygens of the host; O(h)...O(1) 3.27, O(h)...O(25) 3.31, O(h)...O(28) 3.18 Å, however it lies outside the crown ether cavity. There is also a fairly short contact in [4.diquat] between one of the methylene carbons on the diquat and a symmetry related acetonitrile nitrogen atom, N(55)...C(49) 3.37, N(55)...H(49) 2.44 Å, with a N...H-C angle of 163°. In both structures there are no significant contacts between the PF_6 anions and the complexes.

Although in [4.diquat] the benzo rings pack parallel to each other in the crystal lattice there is no overlap between them. The closest non-hydrogen intermolecular crown-crown contact is 3.39 Å between C(36) and C(39) in adjacent benzo rings. In [2.diquat] the closest non-hydrogen intermolecular complex-complex contact is 3.53 Å between O(28) and C(39). The lack of significant intermolecular complex-complex contacts (less than normal van der Waals distances) seems to reinforce the discrete nature of the 1:1 complexes as evidenced by solution studies[2].

A major difference between the complexes is the observed intensities of the absorption bands in solution[2]. Evidence for the stoicheiometry of the complexes in solution and measurements of their stability constants and derived free energies for the equilibrium,

$$[\text{diquat}][PF_6]_2 + \underset{\sim}{2},\ \underset{\sim}{3} \text{ or } \underset{\sim}{4} \rightleftharpoons [\text{diquat}.\underset{\sim}{2},\ \underset{\sim}{3} \text{ or } \underset{\sim}{4}][PF_6]_2$$

have been obtained from a treatment of the dependence on concentration of the absorption bands at 400 nm in acetone for 1:1

mixtures of [diquat][PF_6]$_2$ with 2, 3 or 4. For 2, 3 and 4, Ka = 48000, 50000, and 2100 dm^3 mol^{-1} respectively corresponding to ΔG^0 = -6.4, -6.4, and -4.5 kcal mol^{-1}. The values for [1.diquat][PF_6]$_2$ in acetone are 17500 dm^3 mol^{-1} and -5.8 kcal mol^{-1}. The order (3 ≈ 2 > 1 > 4) of the stabilities of the 1:1 complexes involving the receptor molecules 1 - 4 is in accord with expectation.

The presence of electron-withdrawing CHO groups at the 2 and 20 positions of the catechol rings should decrease their π-donor capabilities, so the presence of electron-donating CH_3 groups in these positions should enhance the ability of the catechol rings to act as π-donors towards the π-electron deficient bipyridinium dication. It is unlikely, however, that the explanation of the relative stabilities of the 1:1 complexes is as straightforward as this: the stabilising pole-dipole intermolecular interactions are probably also influenced by the nature of the substituents at C(2) and C(20).

Although X-ray structure analyses are not available for the uncomplexed hosts in [2.diquat] and [4.diquat], it is expected that they would have a fairly flat extended conformation similar to that observed for the free DB30C10 receptor[11]. The next objective is to introduce rigidity into the receptor to reduce its conformational flexibility and energy of complexation and hence increase complex stability.

TABLE 2.1. Coordinates ($\times 10^4$) and temperature factors ($Å^2 \times 10^3$)

atom	x	y	z	U
O(1)	-3290(6)	4944(4)	6838(3)	98(3)*
C(2)	-3436(14)	4999(9)	6205(6)	155(9)*
C(3)	-2866(13)	5519(13)	6019(7)	213(13)*
O(4)	-1698(7)	5570(5)	6164(4)	143(4)*
C(5)	-1228(12)	6159(7)	5883(7)	174(9)*
C(6)	-25(11)	6216(6)	6056(7)	164(8)*
O(7)	587(7)	5706(4)	5855(5)	153(5)*
C(8)	1728(11)	5799(7)	5977(8)	193(10)*
C(9)	2400(10)	5271(6)	5760(6)	147(7)*
O(10)	2113(7)	4607(5)	5980(4)	139(4)*
C(11)	3032(10)	4144(7)	6092(5)	101(6)*
C(12)	2588(10)	3437(6)	6242(5)	96(5)*
O(13)	2194(6)	3488(3)	6816(3)	87(3)*
C(14)	1796(8)	2874(5)	7046(4)	78(4)*
C(15)	1700(8)	2871(6)	7651(4)	78(4)*
O(16)	1954(6)	3488(3)	7957(3)	88(3)*
C(17)	2031(9)	3484(6)	8590(4)	106(5)*
C(18)	2422(9)	4165(6)	8822(5)	114(6)*
O(19)	1628(6)	4718(4)	8644(3)	116(4)*
C(20)	1985(10)	5352(7)	8931(7)	188(9)*
C(21)	1282(11)	5885(7)	8757(10)	250(12)*
O(22)	82(9)	5848(6)	8777(7)	201(7)*
C(23)	-293(14)	6062(10)	9242(8)	187(11)*
C(24)	-1511(10)	6168(6)	9218(6)	127(6)*
O(25)	-2106(6)	5580(4)	9951(4)	129(4)*
C(26)	-3284(9)	5640(6)	8891(5)	115(6)*
C(27)	-3791(9)	4967(5)	8604(4)	94(5)*
O(28)	-3534(5)	4933(3)	7997(3)	77(3)*
C(29)	-3874(8)	4350(5)	7670(4)	81(4)*
C(30)	-3736(7)	4351(5)	7063(4)	72(4)*
C(31)	1538(8)	2296(5)	6696(5)	95(5)*
C(32)	1160(10)	1709(7)	6932(4)	119(6)*
C(33)	1075(10)	1675(5)	7529(5)	105(5)*
C(34)	1296(9)	2257(6)	7913(5)	94(5)*
C(35)	-4363(8)	3756(5)	7909(4)	75(4)*
C(36)	-4656(9)	3178(5)	7527(5)	104(5)*
C(37)	-4484(11)	3176(9)	6941(5)	124(7)*
C(38)	-4024(10)	3761(7)	6685(7)	114(7)*
C(39)	598(15)	1042(9)	7819(7)	182(9)*
C(40)	-5130(11)	2547(7)	7796(6)	130(6)*
N	-430(6)	4010(4)	6719(4)	72(3)*
C(41)	-308(9)	4021(6)	6138(5)	92(5)*
C(42)	-732(10)	3489(8)	5758(6)	107(6)*
C(43)	-1289(11)	2975(8)	6006(7)	112(7)*
C(44)	-1464(8)	2968(6)	6595(6)	93(5)*
C(45)	-1027(7)	3492(4)	6975(4)	64(4)*
C(46)	-1143(7)	3504(4)	7611(4)	70(4)*
C(47)	-1469(8)	2940(5)	7935(6)	93(5)*
C(48)	-1591(9)	3024(6)	8549(6)	106(6)*
C(49)	-1426(9)	3643(7)	8819(6)	106(6)*
C(50)	-1059(8)	4190(6)	8503(4)	85(5)*
N(2)	-968(6)	4119(4)	7918(3)	67(3)*
C(51)	-652(8)	4759(4)	7569(4)	82(4)*
C(52)	134(8)	4558(5)	7132(4)	82(4)*
F(1)	458(3)	1937(2)	9863(1)	83(1)*
F(11)	873(8)	2189(4)	10518(3)	163(4)*

F(12)	165(9)	1698(4)	9223(3)	188(5)*
F(13)	-763(8)	2030(6)	9962(6)	275(8)*
F(14)	497(9)	2703(4)	9657(3)	176(5)*
F(15)	350(10)	1180(4)	10075(4)	207(5)*
F(16)	1690(7)	1840(7)	9790(6)	297(8)*
F(2)	5582(3)	3287(2)	9864(1)	97(1)*
F(21)	5784(3)	3031(2)	9223(1)	262(8)*
F(22)	5157(3)	4001(2)	9592(1)	208(6)*
F(23)	5380(3)	3542(2)	10504(1)	220(6)*
F(24)	6007(3)	2572(2)	10135(1)	212(6)*
F(25)	6831(3)	3571(2)	9971(1)	309(9)*
F(26)	4333(3)	3002(2)	9757(1)	340(10)*
Oh	-2397(8)	6347(4)	7602(4)	154(5)*

* Equivalent isotropic U defined as one third of the trace of the orthogonalised U_{ij} tensor

TABLE 2.2. Bond lengths (Å)

O(1)-C(2)	1.396(14)	O(1)-C(30)	1.368(12)
C(2)-C(3)	1.294(27)	C(3)-O(4)	1.366(17)
O(4)-C(5)	1.430(17)	C(5)-C(6)	1.415(19)
C(6)-O(7)	1.320(16)	O(7)-C(8)	1.339(15)
C(8)-C(9)	1.401(19)	C(9)-O(10)	1.416(16)
O(10)-C(11)	1.390(15)	C(11)-C(12)	1.501(18)
C(12)-O(13)	1.412(14)	O(13)-C(14)	1.383(12)
C(14)-C(15)	1.361(14)	C(14)-C(31)	1.362(14)
C(15)-O(16)	1.373(12)	C(15)-C(34)	1.417(16)
O(16)-C(17)	1.395(11)	C(17)-C(18)	1.452(16)
C(18)-O(19)	1.429(13)	O(19)-C(20)	1.406(15)
C(20)-C(21)	1.336(19)	C(21)-O(22)	1.412(18)
O(22)-C(23)	1.240(23)	C(23)-C(24)	1.433(20)
C(24)-O(25)	1.413(14)	O(25)-C(26)	1.372(13)
C(26)-C(27)	1.523(15)	C(27)-O(28)	1.419(11)
O(29)-C(29)	1.360(11)	C(29)-C(30)	1.378(13)
C(29)-C(35)	1.406(13)	C(30)-C(38)	1.419(17)
C(31)-C(32)	1.337(16)	C(32)-C(33)	1.343(16)
C(33)-C(34)	1.404(16)	C(33)-C(39)	1.510(20)
C(35)-C(36)	1.408(14)	C(36)-C(37)	1.339(17)
C(36)-C(40)	1.475(17)	C(37)-C(38)	1.392(21)
N-C(41)	1.312(14)	N-C(45)	1.377(12)
N-C(52)	1.489(12)	C(41)-C(42)	1.373(17)
C(42)-C(43)	1.336(20)	C(43)-C(44)	1.348(22)
C(44)-C(45)	1.365(14)	C(45)-C(46)	1.434(13)
C(46)-C(47)	1.377(14)	C(46)-N(2)	1.360(11)
C(47)-C(48)	1.396(19)	C(48)-C(49)	1.329(18)
C(49)-C(50)	1.357(17)	C(50)-N(2)	1.324(12)
N(2)-C(51)	1.519(11)	C(51)-C(52)	1.469(14)
P(1)-F(11)	1.547(7)	P(1)-F(12)	1.489(7)
P(1)-F(13)	1.483(11)	P(1)-F(14)	1.537(9)
P(1)-F(15)	1.530(9)	P(1)-F(16)	1.481(10)
P(2)-F(21)	1.549	P(2)-F(22)	1.549
P(2)-F(23)	1.548	P(2)-F(24)	1.549
P(2)-F(25)	1.549	P(2)-F(26)	1.549

TABLE 2.3. Bond Angles (deg.)

C(2)-O(1)-C(30)	115.2(9)	O(1)-C(2)-C(3)	112.2(13)
C(2)-C(3)-O(4)	121.3(17)	C(3)-O(4)-C(5)	112.4(12)
O(4)-C(5)-C(6)	111.5(11)	C(5)-C(6)-O(7)	114.6(11)
C(6)-O(7)-C(8)	113.8(10)	O(7)-C(8)-C(9)	115.0(12)
C(8)-C(9)-O(10)	111.1(12)	C(9)-O(10)-C(11)	114.8(9)
O(10)-C(11)-C(12)	109.3(9)	C(11)-C(12)-O(13)	107.5(9)
C(12)-O(13)-C(14)	116.0(8)	O(13)-C(14)-C(15)	116.2(8)
O(13)-C(14)-C(31)	122.6(9)	C(15)-C(14)-C(31)	121.2(10)
C(14)-C(15)-O(16)	116.4(9)	C(14)-C(15)-C(34)	118.8(9)
O(16)-C(15)-C(34)	124.8(9)	C(15)-O(16)-C(17)	118.4(8)
O(16)-C(17)-C(18)	109.2(9)	C(17)-C(18)-O(19)	113.7(8)
C(18)-O(19)-C(20)	111.6(8)	O(19)-C(20)-C(21)	113.0(12)
C(20)-C(21)-O(22)	122.1(13)	C(21)-O(22)-C(23)	117.9(14)
O(22)-C(23)-C(24)	118.1(14)	C(23)-C(24)-O(25)	109.7(11)
C(24)-O(25)-C(26)	114.1(9)	O(25)-C(26)-C(27)	107.5(9)
C(26)-C(27)-O(28)	108.5(8)	C(27)-O(28)-C(29)	117.3(7)
O(28)-C(29)-C(30)	117.2(8)	O(28)-C(29)-C(35)	124.6(9)
C(30)-C(29)-C(35)	118.2(9)	O(1)-C(30)-C(29)	117.1(8)
O(1)-C(30)-C(38)	121.0(9)	C(29)-C(30)-C(38)	121.9(10)
C(14)-C(31)-C(32)	121.3(10)	C(31)-C(32)-C(33)	119.8(11)
C(32)-C(33)-C(34)	121.8(11)	C(32)-C(33)-C(39)	122.4(11)
C(34)-C(33)-C(39)	115.3(11)	C(15)-C(34)-C(33)	117.0(10)
C(29)-C(35)-C(36)	119.1(9)	C(35)-C(36)-C(37)	122.1(11)
C(35)-C(36)-C(40)	118.7(11)	C(37)-C(36)-C(40)	119.1(11)
C(36)-C(37)-C(38)	120.5(13)	C(30)-C(38)-C(37)	118.1(12)
C(41)-N-C(45)	122.9(8)	C(41)-N-C(52)	119.8(8)
C(45)-N-C(52)	117.3(8)	N-C(41)-C(42)	121.0(10)
C(41)-C(42)-C(43)	116.7(12)	C(42)-C(43)-C(44)	123.3(13)
C(43)-C(44)-C(45)	120.0(11)	N-C(45)-C(44)	116.2(9)
N-C(45)-C(46)	120.8(7)	C(44)-C(45)-C(46)	123.0(9)
C(45)-C(46)-C(47)	124.6(9)	C(45)-C(46)-N(2)	118.7(8)
C(47)-C(46)-N(2)	116.7(9)	C(46)-C(47)-C(48)	119.2(10)
C(47)-C(48)-C(49)	121.0(12)	C(48)-C(49)-C(50)	119.3(12)
C(49)-C(50)-N(2)	119.8(10)	C(46)-N(2)-C(50)	123.7(8)
C(46)-N(2)-C(51)	119.1(7)	C(50)-N(2)-C(51)	118.3(8)
N(2)-C(51)-C(52)	109.8(7)	N-C(52)-C(51)	109.0(7)
F(11)-P(1)-F(12)	175.1(6)	F(11)-P(1)-F(13)	91.0(6)
F(12)-P(1)-F(13)	93.9(7)	F(11)-P(1)-F(14)	88.0(4)
F(12)-P(1)-F(14)	91.1(4)	F(13)-P(1)-F(14)	89.7(6)
F(11)-P(1)-F(15)	92.0(4)	F(12)-P(1)-F(15)	89.1(5)
F(13)-P(1)-F(15)	87.1(6)	F(14)-P(1)-F(15)	176.8(6)
F(11)-P(1)-F(16)	87.1(6)	F(12)-P(1)-F(16)	88.1(7)
F(13)-P(1)-F(16)	177.8(8)	F(14)-P(1)-F(16)	91.2(6)
F(15)-P(1)-F(16)	92.0(7)	F(21)-P(2)-F(22)	90.0
F(21)-P(2)-F(23)	180.0	F(22)-P(2)-F(23)	90.0
F(21)-P(2)-F(24)	90.0	F(22)-P(2)-F(24)	180.0
F(23)-P(2)-F(24)	90.0	F(21)-P(2)-F(25)	90.0
F(22)-P(2)-F(25)	90.0	F(23)-P(2)-F(25)	90.0
F(24)-P(2)-F(25)	90.0	F(21)-P(2)-F(26)	90.0
F(22)-P(2)-F(26)	90.0	F(23)-P(2)-F(26)	90.0
F(24)-P(2)-F(26)	90.0	F(25)-P(2)-F(26)	180.0

TABLE 2.4. Anisotropic temperature factors ($Å^2 \times 10^3$)

atom	U_{11}	U_{22}	U_{33}	U_{23}	U_{13}	U_{12}
O(1)	87(5)	126(6)	79(5)	17(4)	1(4)	-1(4)
C(2)	159(15)	229(18)	68(9)	44(10)	-26(9)	-51(13)
C(3)	116(13)	414(34)	107(12)	108(16)	5(10)	70(17)
O(4)	102(6)	182(9)	151(8)	68(7)	34(5)	29(6)
C(5)	173(15)	137(12)	233(17)	63(12)	106(13)	56(11)
C(6)	159(14)	95(10)	252(18)	37(11)	78(13)	6(9)
O(7)	119(7)	90(6)	272(11)	5(6)	65(7)	4(5)
C(8)	100(11)	130(12)	359(23)	54(14)	64(13)	-6(10)
C(9)	85(9)	163(13)	197(14)	73(11)	38(9)	-25(9)
O(10)	72(6)	137(7)	209(9)	80(7)	21(6)	7(5)
C(11)	72(9)	137(12)	94(9)	21(8)	14(7)	-2(9)
C(12)	100(9)	103(10)	98(9)	-10(8)	17(7)	27(8)
O(13)	103(5)	84(5)	76(5)	3(4)	19(4)	11(4)
C(14)	56(6)	93(8)	80(7)	-7(6)	-4(5)	16(6)
C(15)	77(7)	84(8)	67(7)	-7(6)	-10(6)	10(6)
O(16)	106(5)	100(5)	53(4)	4(4)	-2(4)	19(4)
C(17)	85(8)	126(10)	101(9)	-7(8)	-12(7)	18(7)
C(18)	81(8)	167(12)	91(8)	-17(8)	4(7)	6(8)
O(19)	81(5)	126(6)	139(7)	-53(5)	5(5)	-4(5)
C(20)	90(10)	168(14)	308(20)	-154(14)	32(11)	-35(9)
C(21)	107(12)	119(12)	526(32)	-172(17)	51(15)	-32(10)
O(22)	121(8)	163(10)	330(17)	-152(11)	71(10)	-54(7)
C(23)	138(15)	170(17)	246(22)	-113(15)	-5(14)	-36(12)
C(24)	112(10)	97(9)	167(12)	-60(9)	-5(9)	-4(8)
O(25)	84(5)	129(7)	170(8)	-53(6)	-0(5)	2(5)
C(26)	105(9)	128(10)	105(9)	-42(8)	-4(7)	21(8)
C(27)	90(8)	113(9)	78(7)	7(7)	10(6)	6(7)
O(28)	87(5)	73(4)	71(4)	3(3)	10(3)	-7(4)
C(29)	69(7)	72(7)	101(8)	-1(6)	3(6)	7(6)
C(30)	50(6)	89(7)	74(7)	-8(6)	-5(5)	13(5)
C(31)	88(9)	93(8)	107(9)	11(7)	25(7)	-7(7)
C(32)	130(11)	165(12)	61(7)	-7(8)	12(7)	23(9)
C(33)	98(9)	55(7)	151(11)	11(7)	-21(8)	-29(7)
C(34)	58(7)	125(10)	98(9)	24(8)	11(6)	10(7)
C(35)	66(7)	76(7)	92(7)	2(6)	-1(5)	4(5)
C(36)	60(7)	56(7)	138(12)	10(7)	-16(7)	-5(6)
C(37)	108(11)	172(15)	83(10)	-16(9)	-24(8)	56(11)
C(38)	80(9)	139(12)	119(11)	-17(10)	-7(8)	38(9)
C(39)	208(17)	146(14)	177(15)	-14(12)	-37(13)	-23(13)
C(40)	129(11)	109(10)	147(12)	5(9)	-1(9)	-15(8)
N	74(6)	53(5)	85(6)	-11(5)	0(5)	2(4)
C(41)	56(7)	118(10)	103(9)	9(8)	15(7)	9(6)
C(42)	73(9)	162(13)	87(9)	-37(9)	10(7)	23(9)
C(43)	64(9)	135(13)	134(13)	-45(11)	-2(9)	8(8)
C(44)	50(7)	92(8)	146(12)	-37(8)	13(8)	1(6)
C(45)	51(6)	49(6)	87(7)	-17(5)	-10(5)	11(5)
C(46)	58(6)	49(6)	97(7)	-3(5)	-12(5)	6(5)
C(47)	72(8)	57(7)	150(11)	12(8)	17(8)	-4(6)
C(48)	65(8)	119(10)	134(11)	45(9)	5(8)	17(7)
C(49)	79(8)	133(11)	109(10)	-1(9)	25(7)	1(8)
C(50)	81(8)	102(9)	71(7)	-5(7)	3(6)	-9(7)
N(2)	51(5)	65(5)	83(5)	-4(4)	-0(4)	7(4)
C(51)	85(9)	54(6)	99(9)	-5(6)	-13(6)	2(6)
C(52)	64(7)	58(6)	123(9)	-3(6)	7(6)	-1(5)
F(1)	96(2)	86(2)	66(2)	-6(2)	2(2)	1(2)
F(11)	263(9)	127(6)	84(5)	5(4)	-37(5)	2(6)

TABLE 2.4. cont/d.

F(12)	315(11)	170(7)	75(5)	-29(5)	8(6)	-92(7)
F(13)	135(8)	251(12)	474(18)	1(12)	169(10)	24(8)
F(14)	307(11)	99(6)	119(6)	14(5)	10(6)	-24(6)
F(15)	374(14)	91(5)	142(7)	29(5)	-22(7)	-27(7)
F(16)	98(6)	384(16)	410(16)	-187(14)	40(8)	37(8)
F(2)	125(3)	94(2)	71(2)	9(2)	9(2)	-1(2)
F(21)	558(22)	143(8)	98(6)	16(5)	93(9)	-41(10)
F(22)	249(11)	179(9)	201(9)	83(7)	45(8)	64(8)
F(23)	355(14)	217(10)	100(6)	12(6)	74(7)	135(10)
F(24)	377(15)	141(7)	131(7)	37(6)	86(8)	102(9)
F(25)	141(9)	306(15)	474(20)	-191(14)	21(11)	-65(10)
F(26)	145(9)	314(16)	538(24)	183(16)	-49(11)	-114(10)
Oh	160(8)	97(6)	206(9)	8(6)	26(7)	-0(6)

The anisotropic temperature factor exponent takes the form:

$$-2\pi^2(h^2a^{*2}U_{11} + \ldots + 2\,hka^*b^*U_{12}\cos\gamma^* + \ldots)$$

TABLE 2.5. Coordinates ($\times 10^4$) and temperature factors ($\AA^2 \times 10^3$)

atom	x	y	z	U
H(2a)	-4239	5062	6062	149
H(2b)	-3166	4576	6039	149
H(3a)	-3011	5522	5582	231
H(3b)	-3183	5934	6175	231
H(5a)	-1598	6576	6003	209
H(5b)	-1376	6107	5450	209
H(6a)	117	6219	6491	163
H(6b)	229	6650	5900	163
H(8a)	1917	6237	5801	220
H(8b)	1915	5821	6410	220
H(9a)	2266	5268	5324	176
H(9b)	3199	5367	5892	176
H(11a)	3419	4109	5736	122
H(11b)	3562	4310	6427	122
H(12a)	3196	3097	6258	104
H(12b)	1966	3300	5940	104
H(17a)	1286	3386	8709	114
H(17b)	2567	3129	8751	114
H(18a)	3141	4269	8675	150
H(18b)	2539	4140	9257	150
H(20a)	2748	5460	8844	182
H(20b)	1994	5291	9361	182
H(21a)	1554	6277	9006	267
H(21b)	1382	5979	8342	267
H(23a)	-71	5724	9556	210
H(23b)	79	6500	9350	210
H(24a)	-1729	6577	8980	165
H(24b)	-1702	6232	9623	165
H(26a)	-3534	5705	9283	117
H(26b)	-3527	6032	8635	117
H(27a)	-4611	4963	8607	96
H(27b)	-3455	4572	8928	96
H(31)	1631	2307	6273	117
H(32)	948	1313	6676	140
H(34)	1183	2242	9333	108
H(35)	-4491	3743	8328	106
H(37)	-4674	2768	6697	118
H(38)	-3906	3766	6265	128
H(39a)	445	647	7546	200
H(39b)	-147	1136	7982	200
H(39c)	1108	861	8178	200
H(40a)	-4919	2141	7572	161
H(40b)	-5964	2583	7736	161
H(40c)	-4849	2512	8205	161
H(41)	86	4407	5979	116
H(42)	-635	3490	5335	139
H(43)	-1575	2591	5751	130
H(44)	-1996	2594	6745	118
H(47)	-1613	2494	7741	111
H(48)	-1795	2629	8790	133
H(49)	-1568	3705	9232	135
H(50)	-861	4626	8703	114
H(51a)	-281	5097	7848	92
H(51b)	-1339	4959	7354	92
H(52a)	303	4959	6899	93
H(52b)	836	4377	7347	93

TABLE 2.6. Coordinates ($\times 10^4$) and temperature factors ($Å^2 \times 10^3$)

atom	x	y	z	U
O(1)	-5442(7)	8544(4)	3366(3)	78(3)*
C(2)	-5041(15)	8629(7)	4028(5)	98(6)*
C(3)	-5038(16)	7959(9)	4317(7)	125(8)*
O(4)	-4156(10)	7555(5)	4058(5)	106(4)*
C(5)	-3983(16)	7035(9)	4505(8)	147(9)*
C(6)	-3258(14)	6564(6)	4257(8)	121(7)*
O(7)	-2104(12)	6805(5)	4258(6)	135(6)*
C(8)	-1455(18)	6397(8)	4010(9)	154(10)*
C(9)	-221(25)	6591(7)	3962(7)	186(13)*
O(10)	-31(11)	7248(5)	3676(5)	117(5)*
C(11)	1069(16)	7434(7)	3435(7)	111(7)*
C(12)	1121(13)	8105(6)	3280(5)	84(5)*
O(13)	414(7)	8139(4)	2728(3)	72(3)*
C(14)	427(11)	8784(7)	2450(6)	79(5)*
C(15)	-38(11)	9820(6)	1858(6)	73(5)*
O(16)	-462(8)	8259(3)	1619(4)	76(3)*
C(17)	-631(11)	9240(5)	990(6)	81(5)*
C(18)	-836(14)	7585(7)	763(7)	99(6)*
O(19)	-1938(9)	7342(4)	984(4)	89(4)*
C(20)	-2236(17)	6742(7)	675(9)	125(8)*
C(21)	-3158(15)	6427(7)	949(9)	120(8)*
O(22)	-4209(10)	6800(4)	906(5)	110(4)*
C(23)	-5197(15)	6404(7)	1128(9)	136(8)*
C(24)	-6245(14)	6817(7)	1094(7)	116(7)*
O(25)	-6170(9)	7335(5)	1491(5)	116(5)*
C(26)	-7226(13)	7704(8)	1570(7)	129(8)*
C(27)	-6924(13)	8387(7)	1690(5)	103(6)*
O(28)	-6377(8)	8418(4)	2282(4)	85(3)*
C(29)	-6082(12)	9021(8)	2476(5)	89(6)*
C(30)	-5558(11)	9112(7)	3063(6)	84(5)*
C(31)	864(11)	9371(6)	2715(7)	90(6)*
C(32)	822(11)	9956(6)	2399(7)	78(5)*
C(33)	425(13)	10000(7)	1815(6)	87(6)*
C(34)	-72(12)	9410(7)	1540(7)	93(6)*
C(35)	-6204(16)	9640(10)	2099(9)	133(9)*
C(36)	-5803(22)	10210(10)	2359(8)	149(11)*
C(37)	-5442(15)	10284(7)	2891(7)	107(6)*
C(38)	-5239(13)	9751(6)	3277(6)	93(6)*
C(39)	1364(14)	10549(7)	2683(7)	105(6)*
O(40)	1377(12)	11077(4)	2434(5)	131(5)*
C(41)	-5025(19)	10927(7)	3154(10)	156(10)*
O(42)	-5272(20)	11416(6)	2880(10)	274(12)*
N(1)	-3453(8)	8305(4)	1986(4)	57(3)*
C(43)	-3925(10)	8263(6)	1414(6)	80(5)*
C(44)	-4069(11)	8789(5)	1057(5)	70(5)*
C(45)	-3647(12)	9380(7)	1242(5)	87(5)*
C(46)	-3121(12)	9422(6)	1847(5)	74(5)*
C(47)	-3038(9)	8881(5)	2203(4)	51(4)*
C(48)	-2541(9)	8877(5)	2823(5)	60(4)*
C(49)	-2296(10)	9464(5)	3190(5)	61(4)*
C(50)	-1852(11)	9451(6)	3729(5)	77(5)*
C(51)	-1565(12)	8863(7)	4007(6)	87(6)*
C(52)	-1800(11)	8325(6)	3669(5)	72(5)*
N(2)	-2268(7)	8311(4)	3124(4)	51(3)*
C(53)	-2412(14)	7714(5)	2702(7)	108(7)*
C(54)	-3451(13)	7735(5)	2379(6)	86(5)*

N(55)	2673(13)	5934(6)	2539(6)	108(8)*
C(56)	3198(15)	6276(6)	2776(7)	67(6)*
C(57)	3982(17)	6738(10)	3063(8)	98(8)*
F(1)	1543	5526	-92	102(2)*
F(11)	1050	4868	212	228(9)*
F(12)	2699	5148	-299	325(13)*
F(13)	942	5338	-740	196(7)*
F(14)	2035	6183	-396	278(11)*
F(15)	386	5903	116	310(12)*
F(16)	2144	5713	556	299(11)*
F(2)	3026	5608	4896	104(2)*
F(21)	2731	5786	4187	227(9)*
F(22)	4386	5613	4735	254(10)*
F(23)	1665	5602	5056	284(11)*
F(24)	3320	5430	5604	276(12)*
F(25)	2966	4947	4729	161(6)*
F(26)	3085	6368	5063	240(9)*

* Equivalent isotropic U defined as one third of the trace of the orthogonalised U_{ij} tensor

TABLE 2.7. Bond lengths (Å)

O(1)-C(2)	1.497(13)	O(1)-C(30)	1.335(16)
C(2)-C(3)	1.500(23)	C(3)-O(4)	1.417(21)
O(4)-C(5)	1.442(21)	C(5)-C(6)	1.376(23)
C(6)-O(7)	1.409(21)	O(7)-C(8)	1.236(22)
C(8)-C(9)	1.470(35)	C(9)-O(10)	1.491(17)
O(10)-C(11)	1.412(22)	C(11)-C(12)	1.411(20)
C(12)-O(13)	1.443(15)	O(13)-C(14)	1.353(16)
C(14)-C(15)	1.375(19)	C(14)-C(31)	1.416(19)
C(15)-O(16)	1.344(14)	C(15)-C(34)	1.393(18)
O(16)-C(17)	1.360(14)	C(17)-C(18)	1.442(18)
C(18)-O(19)	1.436(19)	C(19)-C(20)	1.432(18)
C(20)-C(21)	1.368(25)	C(21)-O(22)	1.428(20)
O(22)-C(23)	1.469(20)	C(23)-C(24)	1.468(23)
C(24)-O(25)	1.359(18)	O(25)-C(26)	1.435(18)
C(26)-C(27)	1.459(22)	C(27)-O(28)	1.414(14)
O(28)-C(29)	1.342(18)	C(29)-C(30)	1.404(18)
C(29)-C(35)	1.505(26)	C(30)-C(38)	1.431(19)
C(31)-C(32)	1.373(18)	C(32)-C(33)	1.333(20)
C(32)-C(39)	1.490(19)	C(33)-C(34)	1.457(20)
C(35)-C(36)	1.369(29)	C(36)-C(37)	1.222(23)
C(37)-C(38)	1.385(19)	C(37)-C(41)	1.507(21)
C(39)-O(40)	1.201(17)	C(41)-O(42)	1.192(23)
N(1)-C(43)	1.340(15)	N(1)-C(47)	1.351(13)
N(1)-C(54)	1.435(14)	C(43)-C(44)	1.329(17)
C(44)-C(45)	1.359(17)	C(45)-C(46)	1.430(16)
C(46)-C(47)	1.344(15)	C(47)-C(48)	1.444(15)
C(48)-C(49)	1.448(15)	C(48)-N(2)	1.359(13)
C(49)-C(50)	1.282(15)	C(50)-C(51)	1.380(19)
C(51)-C(52)	1.344(19)	C(52)-N(2)	1.284(14)
N(2)-C(53)	1.525(15)	C(53)-C(54)	1.377(21)
N(55)-C(56)	1.051(22)	C(56)-C(57)	1.372(24)
P(1)-F(11)	1.595	P(1)-F(12)	1.595
P(1)-F(13)	1.595	P(1)-F(14)	1.595
P(1)-F(15)	1.595	P(1)-F(16)	1.595
P(2)-F(21)	1.595	P(2)-F(22)	1.595
P(2)-F(23)	1.595	P(2)-F(24)	1.595
P(2)-F(25)	1.595	P(2)-F(26)	1.595

TABLE 2.8. Bond Angles (deg.)

C(2)-O(1)-C(30)	113.0(9)	O(1)-C(2)-C(3)	106.7(11)
C(2)-C(3)-O(4)	111.8(13)	C(3)-O(4)-C(5)	105.5(12)
O(4)-C(5)-C(6)	110.0(15)	C(5)-C(6)-O(7)	108.7(12)
C(6)-O(7)-C(8)	109.1(13)	O(7)-C(8)-C(9)	115.2(15)
C(8)-C(9)-O(10)	114.3(17)	C(9)-O(10)-C(11)	121.5(15)
O(10)-C(11)-C(12)	112.6(14)	C(11)-C(12)-O(13)	106.6(11)
C(12)-O(13)-C(14)	117.4(9)	O(13)-C(14)-C(15)	116.6(12)
O(13)-C(14)-C(31)	126.0(11)	C(15)-C(14)-C(31)	117.4(12)
C(14)-C(15)-O(16)	116.4(11)	C(14)-C(15)-C(34)	120.6(12)
O(16)-C(15)-C(34)	122.9(11)	C(15)-O(16)-C(17)	116.9(9)
O(16)-C(17)-C(18)	112.5(10)	C(17)-C(18)-O(19)	110.7(12)
C(18)-O(19)-C(20)	110.7(11)	O(19)-C(20)-C(21)	112.9(15)
C(20)-C(21)-O(22)	111.7(13)	C(21)-O(22)-C(23)	109.5(11)
O(22)-C(23)-C(24)	107.3(12)	C(23)-C(24)-O(25)	111.4(13)
C(24)-O(25)-C(26)	115.4(11)	O(25)-C(26)-C(27)	108.8(12)
C(26)-C(27)-O(28)	107.7(11)	C(27)-O(28)-C(29)	115.4(10)
O(28)-C(29)-C(30)	120.4(13)	O(28)-C(29)-C(35)	125.5(12)
C(30)-C(29)-C(35)	114.1(14)	O(1)-C(30)-C(29)	111.3(12)
O(1)-C(30)-C(38)	127.6(11)	C(29)-C(30)-C(38)	121.1(13)
C(14)-C(31)-C(32)	121.8(13)	C(31)-C(32)-C(33)	122.1(13)
C(31)-C(32)-C(39)	119.4(13)	C(33)-C(32)-C(39)	118.0(12)
C(32)-C(33)-C(34)	117.1(13)	C(15)-C(34)-C(33)	120.7(13)
C(29)-C(35)-C(36)	117.7(16)	C(35)-C(36)-C(37)	126.6(18)
C(36)-C(37)-C(38)	121.1(15)	C(36)-C(37)-C(41)	124.3(16)
C(38)-C(37)-C(41)	114.1(14)	C(30)-C(38)-C(37)	118.8(13)
C(32)-C(39)-O(40)	123.6(14)	C(37)-C(41)-O(42)	118.1(19)
C(43)-N(1)-C(47)	120.6(9)	C(43)-N(1)-C(54)	118.9(9)
C(47)-N(1)-C(54)	120.3(9)	N(1)-C(43)-C(44)	121.7(11)
C(43)-C(44)-C(45)	120.3(11)	C(44)-C(45)-C(46)	117.9(11)
C(45)-C(46)-C(47)	119.5(11)	N(1)-C(47)-C(46)	119.8(9)
N(1)-C(47)-C(48)	116.7(9)	C(46)-C(47)-C(48)	123.5(10)
C(47)-C(48)-C(49)	123.8(9)	C(47)-C(48)-N(2)	122.0(9)
C(49)-C(48)-N(2)	114.2(9)	C(48)-C(49)-C(50)	122.9(10)
C(49)-C(50)-C(51)	120.5(11)	C(50)-C(51)-C(52)	115.6(12)
C(51)-C(52)-N(2)	126.2(12)	C(48)-N(2)-C(52)	120.5(9)
C(48)-N(2)-C(53)	112.0(9)	C(52)-N(2)-C(53)	126.9(10)
N(2)-C(53)-C(54)	111.5(10)	N(1)-C(54)-C(53)	108.7(11)
N(55)-C(56)-C(57)	177.6(17)	F(11)-P(1)-F(12)	90.0
F(11)-P(1)-F(13)	90.0	F(12)-P(1)-F(13)	90.0
F(11)-P(1)-F(14)	180.0	F(12)-P(1)-F(14)	90.0
F(13)-P(1)-F(14)	90.0	F(11)-P(1)-F(15)	90.0
F(12)-P(1)-F(15)	180.0	F(13)-P(1)-F(15)	90.0
F(14)-P(1)-F(15)	90.0	F(11)-P(1)-F(16)	90.0
F(12)-P(1)-F(16)	90.0	F(13)-P(1)-F(16)	180.0
F(14)-P(1)-F(16)	90.0	F(15)-P(1)-F(16)	90.0
F(21)-P(2)-F(22)	90.0	F(21)-P(2)-F(23)	90.0
F(22)-P(2)-F(23)	180.0	F(21)-P(2)-F(24)	180.0
F(22)-P(2)-F(24)	90.0	F(23)-P(2)-F(24)	90.0
F(21)-P(2)-F(25)	90.0	F(22)-P(2)-F(25)	90.0
F(23)-P(2)-F(25)	90.0	F(24)-P(2)-F(25)	90.0
F(21)-P(2)-F(26)	90.0	F(22)-P(2)-F(26)	90.0
F(23)-P(2)-F(26)	90.0	F(24)-P(2)-F(26)	90.0
F(25)-P(2)-F(26)	180.0		

TABLE 2.9. Anisotropic temperature factors ($Å^2 \times 10^3$)

atom	U_{11}	U_{22}	U_{33}	U_{23}	U_{13}	U_{12}
O(1)	67(5)	106(6)	61(5)	2(4)	-9(4)	28(5)
C(2)	127(13)	134(12)	33(6)	-0(7)	12(8)	16(11)
C(3)	75(11)	217(19)	82(11)	19(11)	-10(9)	-36(13)
O(4)	83(6)	109(8)	126(8)	63(6)	-26(7)	-17(6)
C(5)	108(14)	153(16)	191(18)	85(14)	-53(14)	-21(12)
C(6)	125(14)	51(7)	137(16)	26(9)	71(13)	-15(9)
O(7)	141(10)	89(7)	174(11)	34(7)	7(9)	41(8)
C(8)	178(19)	90(11)	195(19)	-37(12)	147(17)	-48(13)
C(9)	387(37)	91(11)	90(10)	25(8)	-11(16)	135(18)
O(10)	129(10)	100(7)	121(8)	14(6)	36(7)	25(7)
C(11)	109(14)	126(13)	97(11)	26(10)	6(10)	26(12)
C(12)	87(10)	101(10)	62(8)	12(7)	22(7)	-2(8)
O(13)	83(6)	73(5)	59(5)	13(4)	-3(5)	7(4)
C(14)	50(7)	116(11)	72(9)	-16(8)	25(7)	-21(7)
C(15)	62(8)	79(8)	77(9)	19(7)	9(7)	10(7)
O(16)	85(6)	64(5)	79(5)	-9(4)	3(5)	-36(5)
C(17)	58(8)	77(8)	108(10)	13(7)	24(8)	7(7)
C(18)	87(11)	102(11)	106(11)	-25(9)	1(9)	-3(9)
O(19)	79(6)	73(6)	116(7)	-15(5)	5(6)	-16(5)
C(20)	98(13)	88(11)	190(18)	-56(11)	4(13)	-4(11)
C(21)	97(13)	76(10)	188(18)	-23(11)	7(13)	5(10)
O(22)	99(7)	81(6)	151(8)	-58(6)	12(7)	-21(6)
C(23)	111(13)	103(12)	194(17)	-69(12)	42(13)	-39(11)
C(24)	88(11)	158(14)	103(11)	-34(10)	-12(9)	-44(11)
O(25)	79(7)	135(8)	133(8)	-34(7)	-6(6)	-5(6)
C(26)	84(11)	205(17)	98(11)	-71(11)	-32(9)	43(12)
C(27)	80(9)	200(15)	28(6)	-21(7)	-4(7)	44(11)
O(28)	76(6)	108(7)	71(5)	-3(5)	6(5)	9(5)
C(29)	71(9)	140(13)	57(8)	4(8)	-2(7)	43(9)
C(30)	45(7)	118(11)	89(9)	2(8)	8(7)	37(8)
C(31)	49(7)	88(9)	135(12)	-18(9)	8(8)	22(7)
C(32)	55(8)	72(8)	107(11)	-19(8)	11(8)	-0(7)
C(33)	88(10)	96(10)	77(9)	16(8)	-19(8)	-4(8)
C(34)	69(9)	98(10)	112(11)	5(9)	-14(9)	2(9)
C(35)	111(14)	154(16)	135(15)	40(14)	34(13)	66(14)
C(36)	228(26)	117(14)	102(13)	14(11)	62(14)	79(17)
C(37)	106(12)	86(9)	130(12)	1(9)	72(11)	32(9)
C(38)	100(11)	76(9)	101(10)	-28(8)	28(9)	25(9)
C(39)	102(12)	101(11)	112(11)	-49(9)	-13(9)	13(10)
O(40)	155(11)	57(5)	181(10)	-14(6)	-18(9)	6(7)
C(41)	155(18)	88(11)	226(20)	18(12)	91(17)	10(12)
O(42)	297(24)	109(10)	415(25)	59(14)	102(23)	61(14)
N(1)	66(6)	55(5)	51(5)	-11(4)	-1(5)	-12(5)
C(43)	59(8)	78(8)	102(10)	-13(7)	9(7)	-9(7)
C(44)	76(8)	76(8)	57(7)	-14(6)	11(7)	2(7)
C(45)	101(11)	119(10)	42(7)	32(7)	19(7)	44(9)
C(46)	91(10)	61(7)	71(8)	25(6)	20(7)	0(7)
C(47)	39(6)	62(7)	51(6)	8(5)	9(5)	4(5)
C(48)	37(6)	53(6)	91(8)	1(6)	12(6)	5(5)
C(49)	74(8)	43(6)	66(7)	-14(5)	-6(6)	2(6)
C(50)	67(8)	88(8)	75(8)	-28(7)	21(7)	-0(7)
C(51)	65(9)	128(12)	69(9)	-16(8)	-25(7)	3(8)
C(52)	54(7)	84(9)	79(8)	28(7)	-8(7)	1(7)
N(2)	53(5)	51(5)	51(5)	6(4)	-11(4)	6(4)
C(53)	109(13)	40(7)	176(15)	19(8)	-10(11)	5(7)
C(54)	94(10)	59(7)	105(10)	-3(7)	-2(9)	-20(8)

N(55)	187(19)	45(7)	92(10)	-3(7)	-16(13)	18(10)
C(56)	72(11)	37(8)	85(10)	-10(7)	15(10)	15(8)
C(57)	92(14)	134(16)	68(11)	-13(11)	8(10)	36(13)
P(1)	102(3)	86(3)	117(3)	28(2)	-47(3)	-16(3)
F(11)	349(22)	154(10)	181(12)	65(9)	-105(13)	-118(13)
F(12)	119(12)	365(23)	492(31)	148(23)	104(17)	85(15)
F(13)	279(17)	167(10)	144(9)	7(7)	-85(10)	22(11)
F(14)	295(22)	245(16)	293(18)	135(14)	-18(17)	-37(17)
F(15)	274(22)	347(22)	309(19)	-101(17)	-119(19)	206(19)
F(16)	427(25)	107(8)	364(19)	-19(10)	-317(20)	13(11)
F(2)	112(3)	98(3)	102(3)	-5(2)	-19(3)	-29(3)
F(21)	316(21)	199(11)	166(10)	48(8)	-114(13)	-59(14)
F(22)	127(11)	227(15)	408(24)	-16(15)	-27(14)	-67(12)
F(23)	162(14)	252(18)	440(26)	67(19)	113(18)	21(14)
F(24)	507(33)	223(13)	97(8)	-1(8)	-122(14)	-5(18)
F(25)	241(13)	97(6)	145(8)	-4(6)	-106(9)	-12(8)
F(26)	369(22)	111(8)	238(13)	-55(9)	-3(15)	3(12)

The anisotropic temperature factor exponent takes the form:

$$-2\pi^2(h^2a^{*2}U_{11} + \ldots + 2\,hka^*b^*U_{12}\cos\gamma^* + \ldots)$$

TABLE 2.10. Coordinates ($\times 10^4$) and temperature factors ($Å^2 \times 10^3$)

atom	x	y	z	U
H(2a)	-4271	8813	4037	123
H(2b)	-5570	8910	4249	123
H(3a)	-5784	7756	4251	143
H(3b)	-4999	8003	4758	143
H(5a)	-4724	6841	4606	194
H(5b)	-3635	7210	4877	194
H(6a)	-3301	6172	4504	163
H(6b)	-3493	6469	3836	163
H(8a)	-1494	6002	4252	179
H(8b)	-1738	6314	3595	179
H(9a)	102	6597	4376	198
H(9b)	103	6271	3714	198
H(11a)	1218	7183	3064	147
H(11b)	1660	7341	3741	147
H(12a)	812	8362	3617	100
H(12b)	1913	8235	3198	100
H(17a)	-1294	8507	887	101
H(17b)	52	8411	787	101
H(18a)	-222	7304	909	134
H(18b)	-841	7589	314	134
H(20a)	-1570	6456	684	144
H(20b)	-2434	6840	249	144
H(21a)	-3274	6014	742	147
H(21b)	-2981	6351	1382	147
H(23a)	-5063	6273	1552	147
H(23b)	-5291	6023	871	147
H(24a)	-6918	6559	1201	135
H(24b)	-6326	6979	675	135
H(26a)	-7686	7676	1196	145
H(26b)	-7666	7533	1916	145
H(27a)	-7618	8651	1691	119
H(27b)	-6398	8543	1374	119
H(31)	1198	9359	3126	118
H(33)	457	10405	1586	113
H(34)	-421	9430	1133	108
H(35)	-6546	9634	1690	164
H(36)	-5809	10593	2099	145
H(38)	-4890	9810	3681	118
H(39)	1719	10507	3087	139
H(41)	-4576	10943	3533	216
H(43)	-4160	7843	1258	93
H(44)	-4473	8752	665	90
H(45)	-3705	9758	977	104
H(46)	-2826	9833	1997	77
H(49)	-2475	9882	2997	89
H(50)	-1718	9854	3950	93
H(51)	-1217	8840	4415	103
H(52)	-1604	7910	3853	101
H(53a)	-2396	7326	2956	120
H(53b)	-1778	7701	2409	120
H(54a)	-3527	7348	2127	103
H(54b)	-4090	7758	2668	103

2.4 REFERENCES

1. H.M. Colquhoun, E.P. Gooding, J.M. Maud, J.F. Stoddart, D.J. Williams and J.B. Wolstenholme, J. Chem. Soc., Chem. Commun., 1983, 1140.

   H.M. Colquhoun, E.P. Gooding, J.M. Maud, J.F. Stoddart, D.J. Williams, and J.B. Wolstenholme, J.Chem. Soc. Perkin Trans. 2, 1985, 607.

2. B.L. Allwood, F.H. Kohnke, J.F. Stoddart, and D.J. Williams, Tetrahedron Lett., 1985, 26, 1681.

3. G.M. Sheldrick, SHELXTL, An integrated system for solving, refining, and displaying crystal structures from diffraction data, University of Göttingen, Federal Republic of Germany, 1981.

4. I. Goldberg, The Chemistry of Functional Groups. Supplement E: The Chemistry of Ethers, Crown Ethers, Hydroxyl Groups and their Sulphur Analogues. 1980, Part 1, 175. Editor S. Patel, Chichester: John Wiley.

5. H.M. Colquhoun, J.F. Stoddart, D.J. Williams, J.B. Wolstenholme and R. Zarzycki, Angew. Chem. Int. Ed. Engl., 1981, 20, 1051.

   H.M. Colquhoun, S.M. Doughty, J.M. Maud, J.F. Stoddart, D.J. Williams and J.B. Wolstenholme, Isr. J. Chem., 1985, 25, 15.

6. R. Taylor, and O. Kennard, J. Amer. Chem. Soc., 1982, 104, 5063.

7. K.W. Ratts, R.K. Howe, and W.G. Phillips, J. Am. Chem. Soc., 1969, 91, 6115.

8. R. Foster, 'Organic Charge-Transfer Complexes,' Academic Press, London, 1969

9. J. E. Derry, and T. A. Hamor, Nature, 1969, 221, 464.

   P.D. Sullivan, and M.L. Williams, J. Am. Chem. Soc., 1972, 98, 1711

T. Sundaresan, and S.C. Wallwork, Acta. Cryst., 1972, B28, 3065.

10. O. Hofer, Monatsh. Chem., 1978, 109, 405.

11. M.A. Bush, and M.R. Truter, J.Chem. Soc., Perkin Trans. 2, 1972, 345.

CHAPTER 3

The crystal structure of the complex of 1,4,7,10,13,21,30,38,41,44,47, 50-dodecaoxa[13^{15,34}][13.3.3](1,4)(1,2)(1,4)cyclophane (a macrobicyclic receptor) with diquat.

3.1 INTRODUCTION

The ability of DB30C10 to change from an essentially extended conformation in its 'free' form[1a] (figure 3.1) to a range of differently folded geometries on complexation[1] demonstates the high degree of conformational flexibility of this molecule. However, if major conformational changes are necessary to bring about or improve binding interactions, the energy and likely entropy changes involved will destabilize the complex relative to one where the optimal arrangement of the receptor binding sites initially exists in a conformational energy minimum[2].

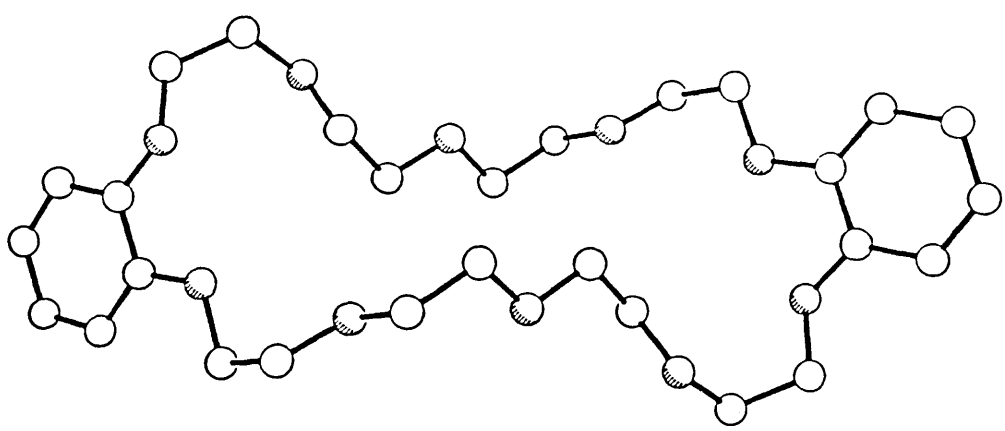
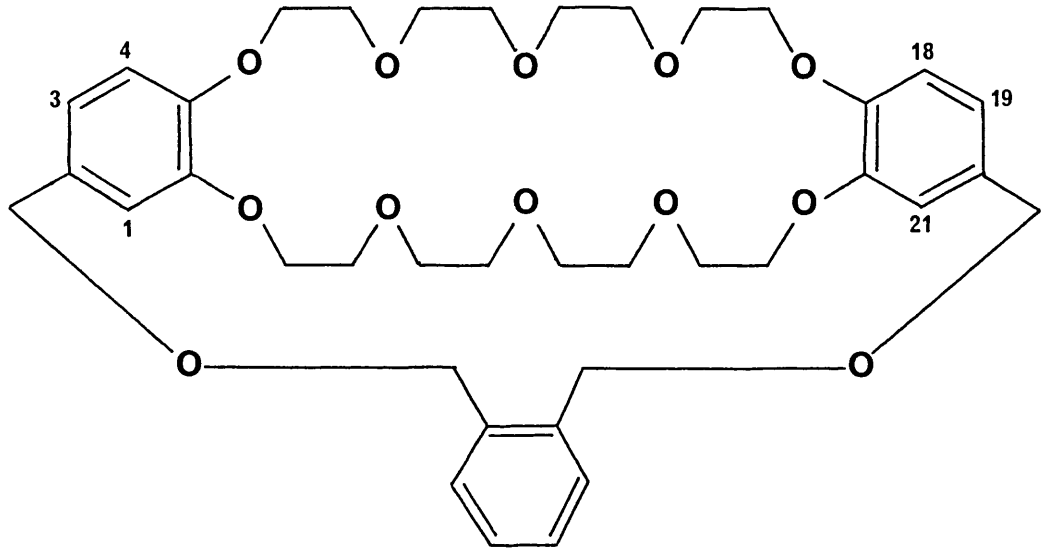


Figure 3.1. The solid-state structure of DB30C10.

In designing receptors for specific organic guests the aim is to synthesise receptors which in their free form have a preorganised cavity and conformation suitable for the guest. Thus the amount of

reorganisation of the host needed for complexation is minimised and complexation is enhanced. It has been suggested[3] that one way to overcome this problem is to design hosts in which the polar binding subunits are connected by rigid apolar shaping components.



5

It was therefore decided to synthesise a macrobicyclic host 5 based on the optimum DB30C10 constitution and containing a rigid apolar bridge at the 2,20 positions. The X-ray structure analysis of $[5.diquat][PF_6]_2(C_2H_3N)_{1.5}$ has been carried out to examine the complexing ability of 5 towards the diquat dication. The stability constant for the 1:1 complex formed in solution will also be discussed. The use of a macrobicyclic host could also lead to a macrocyclic cryptate effect on complexation of the diquat dication

cf. DB30C10 and its derivatives[1e,4].

3.2 EXPERIMENTAL

Deep-red crystals of [5.diquat][PF_6]$_2$(C_2H_3N)$_{1.5}$ were obtained from a solution of [5.diquat][PF_6]$_2$ in MeCN by vapour diffusion with Et_2O. A crystal (coated in Araldite to prevent decomposition) of dimensions 0.50 x 0.50 x 0.58 mm was used for unit cell and intensity measurements.

Crystal Data: $C_{38}H_{50}O_{12}.C_{12}H_{12}N_2.P_2F_{12}.(C_2H_3N)_{1.5}$, *M* = 1235, triclinic, *a* = 11.471(1), *b* = 12.279(2), *c* = 23.062(4) Å, α = 76.71(1) β = 89.38(1), γ = 70.91(1)°, *U* = 2980 Å^3, space group $P\bar{1}$, *Z* = 2, D_c = 1.38 g cm^{-3}, *F*(000) = 1276, μ(Cu-K_α) = 15.13 cm^{-1}.

Refined unit-cell parameters were obtained by centering 18 reflections on a Nicolet R3m diffractometer. 5859 unique reflections ($\theta < 50°$) were measured with Cu-K_α radiation (graphite monochromator) using the omega-scan routine. Of these 4708 had $|F_o| > 3\sigma(|F_o|)$ and were considered to be observed. The net count of two reflections, the 2 3 -1 and the 2 2 4, measured as references every 50 reflections did not alter significantly during the data collection indicating that no deterioration of the crystal had occurred. The data were brought to a uniform arbitrary scale by the use of these reflections and Lorentz and polarisation corrections were applied.

Several attempts at conventional mutiple solution tangent refinement using a series of different, both automaticially selected

and hand chosen, starting sets failed to produce recognisable structural fragments. The structure was eventually solved by resorting to random start tangent refinement. 2000 tries using 489 $\underline{E}$'s > 1.80 with 4653 TPR resulted in best figures of merit of NQEST = -0.650, R(A) = 0.035, CFOM = -0.063. This solution revealed 60 of the 83 potential non-hydrogen atomic positions. The remaining non-hydrogen atoms were obtained from subsequent $\Delta\underline{F}$-maps. A $\Delta\underline{F}$-map also revealed the presence of both a full and partial occupancy acetonitrile molecule. The non-hydrogen atoms of [5.diquat] and the acetonitrile molecules were refined anisotropically. Both PF_6^- groups displayed severe disorder. Each group was seperated into two discrete orientations with site occupancies of 65 and 35% respectively and the groups were refined as rigid bodies. The major occupancy PF_6^- groups were refined anisotropically whilst the minor occupancy PF_6^- groups were refined isotropically. Two discrete positions were observed for C9 and each was refined with 50% occupancy. The methylene and phenyl hydrogens were placed at calculated positions (C-H = 0.96 Å), assigned isotropic thermal parameters, $\underline{U}(H) = 1.2\ \underline{U}_{eq}(C)$ and allowed to ride on their parent carbon atoms. The protons on the full and partial occupancy acetonitrile molecule were not located.

Refinement using $\underline{F}$ magnitudes was by block-cascade full-matrix least squares (808 variable parameters) and converged to $\underline{R}$ = 0.106, $\underline{R}_w$ = 0.113, a fixed weight was used [$w^{-1} = \sigma^2(\underline{F}) + 0.001\underline{F}^2$]. The largest parameter shift/e.s.d. was 0.374, the mean shift/e.s.d. was 0.079. The residual electron density in the final difference map was within -0.47 and 0.64 $eÅ^{-3}$.

All computations were carried out on an Eclipse S140 computer using the SHELXTL[5] program system.

3.3 DISCUSSION

The final fractional atomic coordinates, anisotropic thermal parameters, bond lengths and bond angles for the non-hydrogen atoms are shown in Tables 3.1 - 3.4. The positions and isotropic temperature factors for the hydrogen atoms are listed in Table 3.5.

The torsion angles associated with the polyether chains and the diether bridge in [5.diquat] are shown beside the relevant C-C and C-O bonds in the skeletal drawing of the structure in figure 3.2. The figure also provides the details of the crystallographic numbering scheme.

The X-ray analysis of [5.diquat] reveals how the host achieves again the classic mode of complexation of diquat that has been observed previously by DB30C10 and its derivatives[1e,4]. The gross conformation of the DB30C10 moiety of the host is similar to that in the [4.diquat.] complex. The only significant change compared to the equivalent torsional angles in [4.diquat] is a reversal of the sign about the C(5)-C(6) bond. The torsional angles about the bonds between C(8) and O(10) also vary in sign and magnitude. However, there is probably disorder in this region as evidenced by several other atoms displaying large thermal anisotropy and two discrete orientations being observed for C(9).

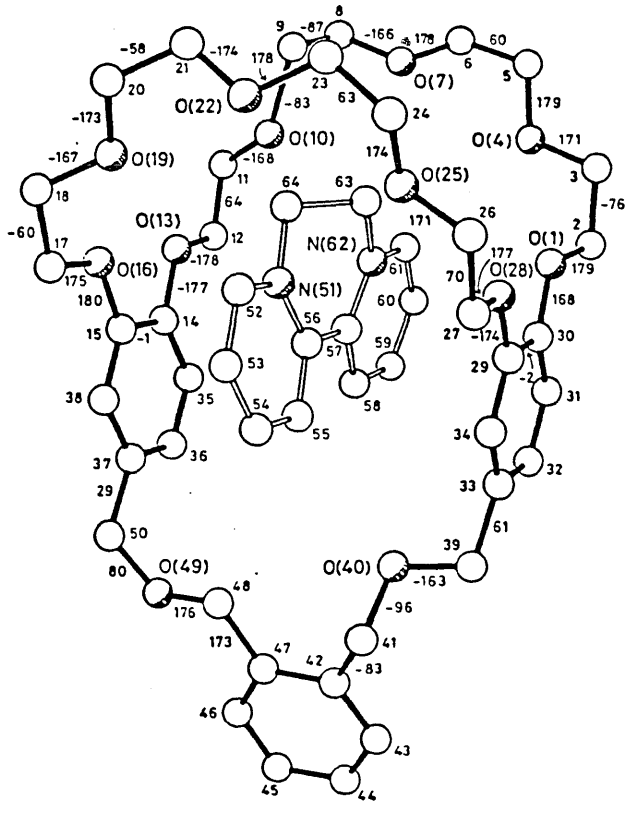


Figure 3.2. The skeletal representation of the solid-state structure of [5.diquat]. The torsional angles taking into account the alternative positions for C(9), are 154, -15, -136 and 177°, respectively for the region O(7) to C(11).

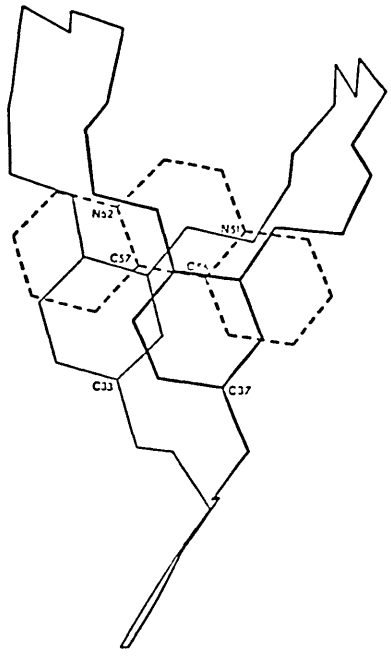


Figure 3.3. Side-on view (view normal to mean plane of diquat dication) of the skeletal representation of the solid-state structure of [5.diquat].

There is also very high thermal motion for C(43) and C(44) in the benzene ring of the diether bridge, however it was not possible to identify discrete alternative sites for these atoms. The combination of high thermal motion and disorder in the complex is the principal cause of the somewhat high final value of R.

The side-on and stereo views (figures 3.3 and 3.4) of [5.diquat] show that the polyether chains again form hydrophilic loops over the the $CHN^{+}CH_2CH_2N^{+}CH$ regions of the diquat. These views also illustrate the degree of overlap between the nearly parallel π-electron-rich catechol units and the π-electron-deficient bipyridinium ring system. The separation between the catechol units is ~ 6.5 Å with a 9.8° departure from parallel alignment. The two pyridine rings [C(57) to N(62) and N(51) to C(56)] depart 4 and 5° from parallel alignment with respect to the mean plane of the catechol rings which they overlap. The distance of 3.3 Å between the mean planes of one of the benzo rings of the host and the nearest overlapping atom of the diquat [C(57)] is ideal for charge transfer[6].

There are two probable C-H...O interactions between the polyether chain oxygens and the acidic protons on the diquat [see table 3.6]. In addition there is a further stabilising C-H...O interaction between the diether bridge and the dication [see table 3.6].

As observed for the previous diquat complexes with DB30C10 and its derivatives[1e,4] there is a horizontal alignment of the aryl oxygen

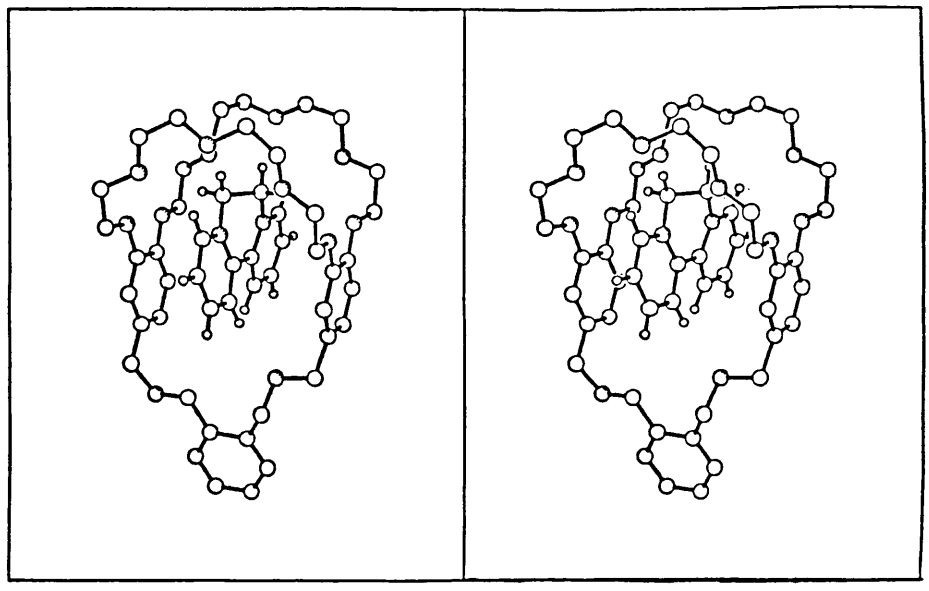


Figure 3.4. The stereo-pair representation of the solid-state structure of [5.diquat].

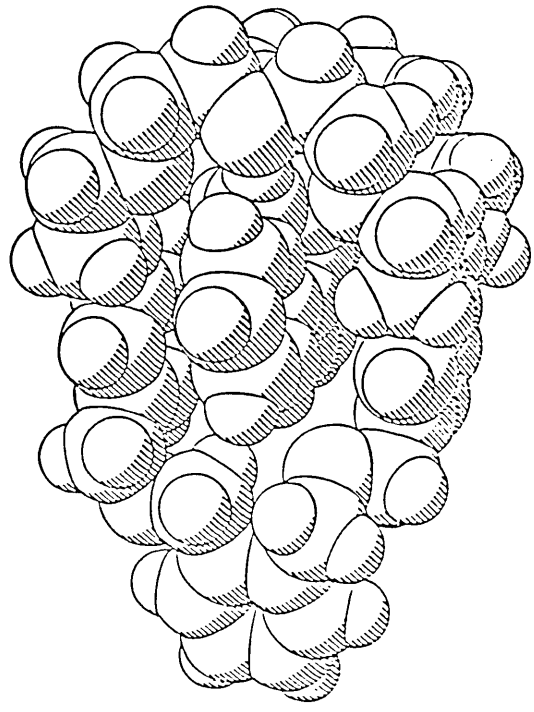


Figure 3.5. The space-filling representation of the solid-state structure of [5.diquat].

TABLE 3.6. Selected host-guest contact distances, and relevant hydrogen contact distances and angles where appropriate, in order of increasing $X^a...O$ distance for [5.diquat].

$X^a...O$	$R(X^a...O)$ (Å)	$R(H...O)$ (Å)	$\psi(^o)^b$	$\theta(^o)^c$
C(52)-O(19)	3.11			
C(61)-O(1)	3.11			
C(61)-O(4)	3.12			
C(55)-O(40)	3.17	2.31	16	149
N(62)-O(1)	3.24			
C(63)-O(10)	3.27			
C(52)-O(25)	3.27			
C(63)-O(28)	3.32	2.48[d]	52[d]	146[d]
C(64)-O(25)	3.32			
C(52)-O(22)	3.31	2.46	26	147
N(51)-O(25)	3.33			
C(64)-O(22)	3.38			
N(51)-O(16)	3.38			
N(62)-O(10)	3.38			
C(64)-O(19)	3.40			

[a] [b] Carbon or Nitrogen of the diquat dication.
[c] Angles between COC planes and HO vectors.
[d] C-H...O angles.
H(63a)

atoms with the formally positively charged nitrogen atoms of the diquat, consistent with electrostatic bonding between them. The N...O distances and the O...N...O angles are; O(1)...N(62) 3.24, O(13)...N(62) 3.78 Å, O(1)...N(62)...O(13) 174°, O(16)...N(51) 3.38, N(51)...O(28) 3.76 Å, O(16)...N(51)...O(28) 171°.

The dihedral angle between the pyridine rings is 17.6(9)°. This is in accord with the previously observed dihedral angles[1e,4,7] for the diquat molecule.

The space-filling representation (figure 3.5) of [5.diquat] shows that the diquat dication, despite the opportunity for, and existence of, additional hydrogen bonding interactions from the diquat to the diether bridge, is drawn into the DB30C10 portion of the host to the same extent, relative to the catechol units, as in the previous complexes[1e,4]. This results in an unneccesarily large gap between the diquat and the diether bridge. It can also be seen that of the two diether bridge oxygens only O(40) is directed towards the diquat and hence is able to interact via C-H...O or electrostatic interactions with the diquat dication.

There are two potential hydrogen bonds between the PF_6 anion and the [5.diquat] complex: C(44)...F(24) 3.31, H(44)...F(24) 2.39 Å C-H...F angle 160°; C(53)...F(25) 3.32, H(53)...F(53) 2.48 Å, C-H...F angle 146°. The closest contact of the acetonitrile to the complex is 3.35 Å between N(71) and C(8). The shortest contact between the acetonitrile and the anions is 3.11 Å between C(83) and F(11).

Solution studies[8] demonstrate that the gross supramolecular structure of the 1:1 complex is similar in solution to that obtained in the solid state. The host has been shown by ^{1}H n.m.r. and UV spectrophotometric methods to form a more stable complex (ΔG^{o} = -7.4 Kcal mol^{-1}) with diquat than the previous hosts 1 - 4[1e,9]. This enhanced complexation of diquat by 5 relative to receptors 1 - 4 implies that it does exhibit a macrobicyclic cryptate effect. Solution studies of the kinetic stability of [5.diquat] indicate that an energy demanding conformational change occurs in 5 prior to complexation.

The macrobicyclic host 5 has so far proved to be the most successful receptor for diquat. This is possibily due mainly to a macrobicyclic cryptate effect rather than the introduction of a rigid apolar group into the host. The X-ray analysis indicates that reduction in the size of the diether bridge could produce a tighter fit between the host and guest. This should again improve complex stability and guest binding capability. The reduction in the diether bridge could also reduce the conformational flexibility of the free host.

TABLE 3.1. Coordinates ($\times 10^4$) and temperature factors ($\AA^2 \times 10^3$).

atom	x	y	z	U
O(1)	8531(4)	4476(4)	7252(2)	62(1)*
C(2)	7688(6)	5313(6)	6784(3)	68(2)*
C(3)	7395(6)	4704(7)	6374(3)	76(2)*
O(4)	8394(4)	4381(4)	6009(2)	78(2)*
C(5)	8265(7)	3626(8)	5656(4)	94(2)*
C(6)	9311(9)	3354(10)	5289(4)	134(2)*
O(7)	10411(5)	2804(6)	5600(3)	126(2)*
C(8)	11382(12)	2526(13)	5211(6)	209(2)*
C(9)	12220(18)	1816(14)	5579(7)	144(2)*
C(9')	12510(12)	2402(17)	5352(7)	115(2)*
O(10)	12839(5)	2775(6)	5814(3)	112(2)*
C(11)	13732(8)	3353(8)	5590(4)	116(2)*
C(12)	14089(8)	3843(8)	6028(4)	110(2)*
O(13)	14710(5)	2935(4)	6531(2)	97(2)*
C(14)	15093(7)	3251(8)	7020(4)	82(2)*
C(15)	15752(6)	2265(7)	7480(4)	74(2)*
O(16)	15899(5)	1156(4)	7373(2)	92(2)*
C(17)	16560(7)	128(6)	7829(4)	87(2)*
C(18)	16527(7)	-913(7)	7666(4)	93(2)*
O(19)	15275(5)	-853(4)	7596(2)	94(2)*
C(20)	15101(8)	-1914(7)	7557(4)	106(2)*
C(21)	13829(9)	-1750(8)	7411(5)	126(2)*
O(22)	13081(6)	-1282(5)	7842(3)	108(2)*
C(23)	11829(9)	-1207(9)	7750(5)	135(2)*
C(24)	11060(9)	-753(7)	8219(4)	112(2)*
O(25)	10993(5)	401(4)	8220(2)	77(1)*
C(26)	10151(7)	818(6)	8637(3)	80(2)*
C(27)	10198(7)	1957(6)	8721(3)	73(2)*
O(28)	9667(4)	2869(4)	8190(2)	63(1)*
C(29)	9588(6)	4006(6)	8202(3)	55(2)*
C(30)	8944(6)	4881(6)	7687(3)	56(2)*
C(31)	8828(6)	6055(6)	7663(3)	67(2)*
C(32)	9333(6)	6349(6)	8106(3)	74(2)*
C(33)	9975(6)	5505(7)	8592(3)	73(2)*
C(34)	10064(6)	4328(6)	8645(3)	62(2)*
C(35)	14856(7)	4408(7)	7075(4)	94(2)*
C(36)	15299(7)	4554(8)	7596(4)	98(2)*
C(37)	15940(7)	3605(7)	8049(4)	90(2)*
C(38)	16175(7)	2457(7)	7989(4)	81(2)*
C(39)	10617(7)	5822(7)	9077(4)	96(2)*
O(40)	11864(5)	5224(6)	9103(3)	109(2)*
C(41)	12546(9)	5156(8)	9651(4)	112(2)*
C(42)	13078(8)	6100(7)	9561(4)	96(2)*
C(43)	12546(9)	7100(8)	9763(4)	126(2)*
C(44)	13159(13)	7965(8)	9711(5)	219(2)*
C(45)	14294(14)	7785(10)	9487(6)	225(2)*
C(46)	14812(11)	6814(8)	9267(4)	134(2)*
C(47)	14225(8)	5970(7)	9295(4)	96(2)*
C(48)	14779(8)	4795(8)	9087(4)	117(2)*
O(49)	15806(7)	4874(7)	8782(4)	158(2)*
C(50)	16449(8)	3793(8)	8596(5)	122(2)*
N(51)	13021(4)	1824(4)	7868(2)	50(1)*
C(52)	13625(6)	877(6)	8305(3)	63(2)*
C(53)	13978(6)	1044(6)	8834(3)	67(2)*
C(54)	13680(6)	2162(6)	8920(3)	64(2)*
C(55)	13029(6)	3120(6)	8469(3)	57(2)*

C(56)	12716(5)	2941(5)	7933(3)	47(2)*
C(57)	12035(5)	3929(5)	7439(3)	50(2)*
C(58)	12016(6)	5085(6)	7404(3)	64(2)*
C(59)	11333(6)	5991(6)	6919(3)	74(2)*
C(60)	10744(7)	5726(6)	6484(3)	81(2)*
C(61)	10803(6)	4577(6)	6520(3)	69(2)*
N(62)	11438(5)	3717(4)	6993(2)	54(2)*
C(63)	11436(6)	2493(6)	7056(3)	66(2)*
C(64)	12719(6)	1618(6)	7299(3)	64(2)*
N(71)	2343(10)	1825(8)	3923(4)	168(2)*
C(72)	3252(11)	1010(9)	3962(4)	130(2)*
C(73)	4376(11)	-25(9)	4000(5)	149(2)*
N(81)	634(12)	967(14)	3055(8)	138(2)*
C(82)	601(15)	335(17)	3500(10)	153(2)*
C(83)	445(15)	-5(13)	4114(8)	105(2)*
F(1)	6626(2)	2229(2)	4354(1)	95(1)*
F(11)	7349(8)	1570(8)	4966(2)	242(2)*
F(12)	5869(10)	2870(8)	3739(3)	192(2)*
F(13)	7313(7)	1155(5)	4088(4)	241(2)*
F(14)	7629(7)	2801(5)	4158(3)	218(2)*
F(15)	5850(9)	3340(6)	4580(5)	174(2)*
F(16)	5598(9)	1717(11)	4618(5)	191(2)*
F(11')	6932(7)	2546(6)	3683(2)	182(3)
F(12')	8042(4)	1712(6)	4540(3)	173(3)
F(13')	5231(6)	2691(17)	4141(10)	213(3)
F(14')	6654(14)	2039(13)	5049(2)	135(3)
F(15')	6623(7)	3478(4)	4409(3)	154(3)
F(16')	6749(14)	1077(8)	4140(7)	145(3)
P(2)	12083(2)	1176(2)	10425(1)	81(1)*
F(21)	12372(4)	-126(3)	10799(2)	139(2)*
F(22)	11811(6)	2461(3)	10035(2)	151(2)*
F(23)	10666(3)	1409(5)	10447(3)	168(2)*
F(24)	12061(5)	741(5)	9838(2)	110(2)*
F(25)	13503(3)	859(8)	10353(4)	139(2)*
F(26)	12013(10)	1652(8)	10995(3)	174(2)*
F(23')	13175(4)	1281(6)	10789(3)	120(2)
F(24')	11073(10)	822(12)	10146(6)	137(3)
F(25')	11195(5)	1617(7)	10905(3)	127(3)
F(26')	12949(14)	701(15)	9951(6)	166(3)

* Equivalent isotropic U defined as one third of the trace of the orthogonalised U_{ij} tensor

TABLE 3.2. Bond lengths (Å)

O(1)-C(2)	1.422(7)	O(1)-C(30)	1.367(9)
C(2)-C(3)	1.436(12)	C(3)-O(4)	1.420(9)
O(4)-C(5)	1.409(12)	C(5)-C(6)	1.452(13)
C(6)-O(7)	1.343(11)	O(7)-C(8)	1.426(15)
C(8)-C(9)	1.238(19)	C(8)-C(9′)	1.289(21)
C(9)-O(10)	1.743(23)	C(9′)-O(10)	1.355(21)
O(10)-C(11)	1.455(13)	C(11)-C(12)	1.415(15)
C(12)-O(13)	1.413(8)	O(13)-C(14)	1.394(11)
C(14)-C(15)	1.411(9)	C(14)-C(35)	1.392(13)
C(15)-O(16)	1.395(11)	C(15)-C(38)	1.371(13)
O(16)-C(17)	1.433(8)	C(17)-C(18)	1.426(13)
C(18)-O(19)	1.422(10)	O(19)-C(20)	1.405(11)
C(20)-C(21)	1.438(14)	C(21)-O(22)	1.405(12)
O(22)-C(23)	1.424(13)	C(23)-C(24)	1.482(15)
C(24)-O(25)	1.393(11)	O(25)-C(26)	1.415(9)
C(26)-C(27)	1.473(12)	C(27)-O(28)	1.436(7)
O(28)-C(29)	1.375(9)	C(29)-C(30)	1.424(8)
C(29)-C(34)	1.355(11)	C(30)-C(31)	1.392(10)
C(31)-C(32)	1.354(12)	C(32)-C(33)	1.362(9)
C(33)-C(34)	1.391(11)	C(33)-C(39)	1.534(13)
C(35)-C(36)	1.379(14)	C(36)-C(37)	1.373(10)
C(37)-C(38)	1.385(13)	C(37)-C(50)	1.492(15)
C(39)-O(40)	1.373(9)	O(40)-C(41)	1.464(12)
C(41)-C(42)	1.452(15)	C(42)-C(43)	1.365(13)
C(42)-C(47)	1.422(13)	C(43)-C(44)	1.437(18)
C(44)-C(45)	1.363(22)	C(45)-C(46)	1.358(17)
C(46)-C(47)	1.398(17)	C(47)-C(48)	1.558(14)
C(48)-O(49)	1.384(13)	O(49)-C(50)	1.451(13)
N(51)-C(52)	1.341(7)	N(51)-C(56)	1.343(8)
N(51)-C(64)	1.457(9)	C(52)-C(53)	1.369(11)
C(53)-C(54)	1.363(10)	C(54)-C(55)	1.379(8)
C(55)-C(56)	1.375(10)	C(56)-C(57)	1.464(7)
C(57)-C(58)	1.396(10)	C(57)-N(62)	1.360(9)
C(58)-C(59)	1.406(8)	C(59)-C(60)	1.371(12)
C(60)-C(61)	1.374(11)	C(61)-N(62)	1.350(7)
N(62)-C(63)	1.476(10)	C(63)-C(64)	1.530(8)
N(71)-C(72)	1.173(13)	C(72)-C(73)	1.471(14)
N(81)-C(82)	1.143(26)	C(82)-C(83)	1.409(28)
P(1)-F(11)	1.549(6)	P(1)-F(12)	1.565(7)
P(1)-F(13)	1.554(8)	P(1)-F(14)	1.547(8)
P(1)-F(15)	1.565(9)	P(1)-F(16)	1.566(12)
P(1)-F(11′)	1.571(5)	P(1)-F(12′)	1.562(5)
P(1)-F(13′)	1.555(9)	P(1)-F(14′)	1.567(5)
P(1)-F(15′)	1.567(6)	P(1)-F(16′)	1.566(13)
P(2)-F(21)	1.561(3)	P(2)-F(22)	1.557(4)
P(2)-F(23)	1.558(4)	P(2)-F(24)	1.568(5)
P(2)-F(25)	1.563(4)	P(2)-F(26)	1.548(8)
P(2)-F(23′)	1.571(7)	P(2)-F(24′)	1.556(15)
P(2)-F(25′)	1.564(7)	P(2)-F(26′)	1.552(15)

TABLE 3.3. Bond Angles (deg.)

C(2)-O(1)-C(30)	118.6(5)	O(1)-C(2)-C(3)	109.4(6)
C(2)-C(3)-O(4)	109.9(7)	C(3)-O(4)-C(5)	113.6(7)
O(4)-C(5)-C(6)	110.2(9)	C(5)-C(6)-O(7)	114.4(8)
C(6)-O(7)-C(8)	111.0(8)	O(7)-C(8)-C(9)	99.6(12)
O(7)-C(8)-C(9′)	122.9(14)	C(8)-C(9)-O(10)	101.1(13)
C(8)-C(9′)-O(10)	123.1(14)	C(9)-O(10)-C(11)	135.0(8)
C(9′)-O(10)-C(11)	105.6(9)	O(10)-C(11)-C(12)	110.6(7)
C(11)-C(12)-O(13)	110.4(8)	C(12)-O(13)-C(14)	118.7(7)
O(13)-C(14)-C(15)	113.3(8)	O(13)-C(14)-C(35)	125.3(6)
C(15)-C(14)-C(35)	121.4(8)	C(14)-C(15)-O(16)	115.5(7)
C(14)-C(15)-C(38)	119.0(8)	O(16)-C(15)-C(38)	125.6(6)
C(15)-O(16)-C(17)	117.4(6)	O(16)-C(17)-C(18)	109.6(7)
C(17)-C(18)-O(19)	109.1(6)	C(18)-O(19)-C(20)	115.5(6)
O(19)-C(20)-C(21)	112.3(6)	C(20)-C(21)-O(22)	110.0(9)
C(21)-O(22)-C(23)	112.3(8)	O(22)-C(23)-C(24)	111.7(10)
C(23)-C(24)-O(25)	112.5(8)	C(24)-O(25)-C(26)	109.4(6)
O(25)-C(26)-C(27)	111.0(7)	C(26)-C(27)-O(28)	109.1(6)
C(27)-O(28)-C(29)	116.7(5)	O(28)-C(29)-C(30)	113.8(6)
O(28)-C(29)-C(34)	126.2(5)	C(30)-C(29)-C(34)	120.1(6)
O(1)-C(30)-C(29)	116.3(6)	O(1)-C(30)-C(31)	126.2(5)
C(29)-C(30)-C(31)	117.4(7)	C(30)-C(31)-C(32)	121.2(6)
C(31)-C(32)-C(33)	121.1(7)	C(32)-C(33)-C(34)	119.4(8)
C(32)-C(33)-C(39)	121.3(7)	C(34)-C(33)-C(39)	119.3(6)
C(29)-C(34)-C(33)	120.7(6)	C(14)-C(35)-C(36)	117.4(7)
C(35)-C(36)-C(37)	122.1(9)	C(36)-C(37)-C(38)	120.1(9)
C(36)-C(37)-C(50)	120.7(9)	C(38)-C(37)-C(50)	119.1(7)
C(15)-C(38)-C(37)	120.1(7)	C(33)-C(39)-O(40)	108.7(7)
C(39)-O(40)-C(41)	114.6(7)	O(40)-C(41)-C(42)	110.6(7)
C(41)-C(42)-C(43)	121.6(9)	C(41)-C(42)-C(47)	120.5(8)
C(43)-C(42)-C(47)	117.7(9)	C(42)-C(43)-C(44)	119.8(10)
C(43)-C(44)-C(45)	121.3(10)	C(44)-C(45)-C(46)	119.3(14)
C(45)-C(46)-C(47)	120.8(12)	C(42)-C(47)-C(46)	121.0(8)
C(42)-C(47)-C(48)	114.4(9)	C(46)-C(47)-C(48)	124.5(8)
C(47)-C(48)-O(49)	106.8(9)	C(48)-O(49)-C(50)	111.9(9)
C(37)-C(50)-O(49)	117.9(7)	C(52)-N(51)-C(56)	122.4(6)
C(52)-N(51)-C(64)	117.9(5)	C(56)-N(51)-C(64)	119.6(4)
N(51)-C(52)-C(53)	119.4(7)	C(52)-C(53)-C(54)	120.0(6)
C(53)-C(54)-C(55)	119.4(7)	C(54)-C(55)-C(56)	119.8(6)
N(51)-C(56)-C(55)	118.8(5)	N(51)-C(56)-C(57)	119.3(6)
C(55)-C(56)-C(57)	121.8(6)	C(56)-C(57)-C(58)	121.5(6)
C(56)-C(57)-N(62)	119.5(6)	C(58)-C(57)-N(62)	118.9(5)
C(57)-C(58)-C(59)	118.3(7)	C(58)-C(59)-C(60)	120.3(7)
C(59)-C(60)-C(61)	120.4(6)	C(60)-C(61)-N(62)	119.0(7)
C(57)-N(62)-C(61)	123.1(6)	C(57)-N(62)-C(63)	117.5(5)
C(61)-N(62)-C(63)	119.3(6)	N(62)-C(63)-C(64)	109.2(6)
N(51)-C(64)-C(63)	108.4(5)	N(71)-C(72)-C(73)	178.6(12)
N(81)-C(82)-C(83)	156.8(23)	F(11)-P(1)-F(12)	178.2(6)
F(11)-P(1)-F(13)	90.4(5)	F(12)-P(1)-F(13)	89.2(5)
F(11)-P(1)-F(14)	90.9(4)	F(12)-P(1)-F(14)	90.8(5)
F(13)-P(1)-F(14)	90.8(4)	F(11)-P(1)-F(15)	93.8(5)
F(12)-P(1)-F(15)	86.5(5)	F(13)-P(1)-F(15)	175.4(5)
F(14)-P(1)-F(15)	90.9(5)	F(11)-P(1)-F(16)	85.2(5)
F(12)-P(1)-F(16)	93.1(6)	F(13)-P(1)-F(16)	94.9(6)
F(14)-P(1)-F(16)	173.1(5)	F(15)-P(1)-F(16)	83.7(6)
F(11′)-P(1)-F(12′)	89.3(4)	F(11′)-P(1)-F(13′)	88.6(8)
F(12′)-P(1)-F(13′)	176.4(10)	F(11′)-P(1)-F(14′)	162.9(7)
F(12′)-P(1)-F(14′)	77.5(6)	F(13′)-P(1)-F(14′)	105.1(10)
F(11′)-P(1)-F(15′)	89.1(4)	F(12′)-P(1)-F(15′)	89.3(4)

F(13')-P(1)-F(15')	93.5(9)	F(14')-P(1)-F(15')	80.1(7)
F(11')-P(1)-F(16')	76.6(6)	F(12')-P(1)-F(16')	88.7(6)
F(13')-P(1)-F(16')	88.1(10)	F(14')-P(1)-F(16')	113.4(8)
F(15')-P(1)-F(16')	165.6(6)	F(21)-P(2)-F(22)	178.3(3)
F(21)-P(2)-F(23)	91.1(3)	F(22)-P(2)-F(23)	89.5(3)
F(21)-P(2)-F(24)	89.5(3)	F(22)-P(2)-F(24)	88.9(3)
F(23)-P(2)-F(24)	89.3(3)	F(21)-P(2)-F(25)	87.1(4)
F(22)-P(2)-F(25)	92.1(4)	F(23)-P(2)-F(25)	173.8(5)
F(24)-P(2)-F(25)	84.7(5)	F(21)-P(2)-F(26)	92.0(3)
F(22)-P(2)-F(26)	89.6(4)	F(23)-P(2)-F(26)	87.2(5)
F(24)-P(2)-F(26)	176.2(4)	F(25)-P(2)-F(26)	98.8(6)
F(21)-P(2)-F(23')	89.4(3)	F(22)-P(2)-F(23')	91.1(4)
F(21)-P(2)-F(24')	79.3(5)	F(22)-P(2)-F(24')	100.2(5)
F(23')-P(2)-F(24')	168.7(5)	F(21)-P(2)-F(25')	89.1(3)
F(22)-P(2)-F(25')	92.5(3)	F(23')-P(2)-F(25')	88.9(4)
F(24')-P(2)-F(25')	90.6(6)	F(21)-P(2)-F(26')	89.3(6)
F(22)-P(2)-F(26')	89.0(6)	F(23')-P(2)-F(26')	92.3(7)
F(24')-P(2)-F(26')	87.9(9)	F(25')-P(2)-F(26')	178.0(8)

TABLE 3.4. Anisotropic temperature factors ($Å^2 \times 10^3$)

atom	U_{11}	U_{22}	U_{33}	U_{23}	U_{13}	U_{12}
O(1)	53(2)	58(2)	65(2)	-14(2)	-5(2)	-6(2)
C(2)	45(2)	75(2)	69(2)	-13(2)	-6(2)	-3(2)
C(3)	53(2)	91(2)	75(2)	-15(2)	-6(2)	-17(2)
O(4)	66(2)	107(2)	71(2)	-32(2)	2(2)	-34(2)
C(5)	85(3)	116(3)	88(3)	-30(2)	-17(2)	-38(2)
C(6)	174(3)	178(3)	114(3)	-91(2)	49(3)	-106(3)
O(7)	80(2)	182(3)	147(2)	-109(2)	19(2)	-37(2)
C(8)	164(3)	307(3)	211(3)	-197(3)	97(3)	-60(3)
C(9)	208(3)	81(3)	73(3)	-34(3)	-7(3)	53(3)
C(9')	24(3)	227(3)	99(3)	-97(3)	1(3)	-6(3)
O(10)	75(2)	168(3)	88(2)	-54(2)	12(2)	-17(2)
C(11)	94(3)	136(3)	60(2)	10(3)	15(2)	13(3)
C(12)	73(3)	116(3)	102(3)	22(3)	22(2)	-12(2)
O(13)	68(2)	79(2)	112(2)	25(2)	-15(2)	-13(2)
C(14)	40(2)	110(3)	90(3)	-6(2)	4(2)	-27(2)
C(15)	33(2)	76(2)	96(3)	-3(2)	2(2)	-7(2)
O(16)	83(2)	76(2)	92(2)	-11(2)	-14(2)	-1(2)
C(17)	62(3)	80(2)	87(3)	-16(2)	-13(2)	15(2)
C(18)	79(3)	78(2)	89(3)	-23(2)	-8(2)	19(2)
O(19)	99(2)	59(2)	106(2)	-34(2)	-13(2)	9(2)
C(20)	121(3)	68(2)	102(3)	-31(2)	14(3)	13(2)
C(21)	138(3)	83(2)	157(3)	-76(2)	-1(3)	-6(3)
O(22)	123(2)	82(2)	128(2)	-49(2)	21(2)	-29(2)
C(23)	131(3)	102(3)	190(3)	-76(2)	-23(3)	-35(2)
C(24)	117(3)	88(3)	141(3)	-28(3)	11(3)	-45(2)
O(25)	80(2)	55(2)	96(2)	-15(2)	15(2)	-28(2)
C(26)	70(3)	73(2)	83(3)	6(2)	4(2)	-21(2)
C(27)	55(2)	88(3)	63(2)	-3(2)	7(2)	-16(2)
O(28)	61(2)	64(2)	55(2)	-4(2)	-3(2)	-16(2)
C(29)	41(2)	64(2)	58(2)	-18(2)	14(2)	-14(2)
C(30)	33(2)	62(2)	64(2)	-9(2)	11(2)	-7(2)
C(31)	46(2)	60(2)	80(2)	-16(2)	7(2)	1(2)
C(32)	58(2)	67(2)	81(2)	-23(2)	-10(2)	4(2)
C(33)	46(2)	87(2)	87(2)	-51(2)	17(2)	-4(2)
C(34)	42(2)	77(2)	60(2)	-19(2)	12(2)	-8(2)
C(35)	58(2)	64(2)	140(3)	10(2)	24(2)	-18(2)
C(36)	71(3)	101(3)	135(3)	-41(2)	45(2)	-38(2)
C(37)	61(2)	103(3)	115(3)	-35(2)	40(2)	-35(2)
C(38)	52(2)	96(2)	107(3)	-43(2)	24(2)	-29(2)
C(39)	82(3)	93(3)	99(3)	-47(2)	-4(2)	4(2)
O(40)	70(2)	152(2)	124(2)	-84(2)	-6(2)	-26(2)
C(41)	132(3)	117(3)	113(3)	-46(2)	4(3)	-63(2)
C(42)	102(3)	89(3)	80(3)	-33(2)	-12(2)	3(2)
C(43)	119(3)	113(3)	109(3)	-49(2)	-28(3)	28(3)
C(44)	402(3)	51(3)	154(3)	-21(2)	-156(3)	-6(3)
C(45)	393(3)	129(3)	196(3)	-9(3)	-109(3)	-161(3)
C(46)	175(3)	119(3)	100(3)	14(3)	-46(3)	-67(3)
C(47)	129(3)	84(2)	72(2)	-14(2)	-26(2)	-33(2)
C(48)	83(3)	134(3)	147(3)	-54(3)	39(3)	-38(2)
O(49)	158(3)	151(3)	179(3)	-26(2)	35(2)	-82(2)
C(50)	96(3)	123(3)	183(3)	-101(2)	53(3)	-43(2)
N(51)	49(2)	50(2)	49(2)	-19(2)	8(2)	-9(2)
C(52)	57(2)	62(2)	64(2)	-22(2)	8(2)	-7(2)
C(53)	63(2)	57(2)	70(2)	-11(2)	-2(2)	-9(2)
C(54)	52(2)	81(2)	53(2)	-11(2)	-5(2)	-17(2)
C(55)	50(2)	55(2)	74(2)	-25(2)	15(2)	-21(2)

TABLE 3.4. cont/d.

C(56)	39(2)	50(2)	56(2)	-19(2)	14(2)	-13(2)
C(57)	36(2)	53(2)	57(2)	-14(2)	10(2)	-9(2)
C(58)	56(2)	54(2)	77(2)	-13(2)	14(2)	-13(2)
C(59)	64(2)	56(2)	92(3)	-7(2)	12(2)	-13(2)
C(60)	64(2)	71(2)	80(3)	5(2)	13(2)	-4(2)
C(61)	51(2)	88(2)	53(2)	-2(2)	1(2)	-15(2)
N(62)	45(2)	64(2)	53(2)	-15(2)	15(2)	-16(2)
C(63)	69(2)	83(2)	59(2)	-26(2)	15(2)	-37(2)
C(64)	75(2)	54(2)	65(2)	-23(2)	16(2)	-19(2)
N(71)	245(3)	109(3)	115(3)	-15(3)	15(3)	-20(3)
C(72)	207(3)	119(3)	69(3)	-14(2)	12(3)	-66(3)
C(73)	155(3)	103(3)	144(3)	-12(3)	17(3)	4(3)
N(81)	67(3)	155(3)	198(3)	-57(3)	-20(3)	-36(3)
C(82)	80(3)	161(3)	184(3)	48(3)	-70(3)	-53(3)
C(83)	103(3)	81(3)	109(3)	18(3)	2(3)	-31(3)
P(1)	121(2)	82(1)	80(1)	-9(1)	5(1)	-37(1)
F(11)	245(3)	295(3)	115(3)	65(3)	-50(3)	-71(3)
F(12)	265(3)	146(3)	78(2)	-14(3)	-41(3)	39(3)
F(13)	182(3)	144(3)	374(3)	-144(3)	-74(3)	37(3)
F(14)	237(3)	298(3)	219(3)	-54(3)	113(3)	-229(2)
F(15)	197(3)	154(3)	193(3)	-93(3)	100(3)	-55(3)
F(16)	209(3)	271(3)	164(3)	-42(3)	53(3)	-182(2)
P(2)	84(1)	80(1)	61(1)	-11(1)	12(1)	-10(1)
F(21)	187(3)	95(2)	112(2)	-1(2)	22(2)	-32(2)
F(22)	192(3)	91(2)	130(2)	14(2)	-13(2)	-22(2)
F(23)	81(3)	168(3)	235(3)	-53(3)	75(3)	-15(3)
F(24)	113(3)	120(3)	74(2)	-28(2)	-25(2)	-1(2)
F(25)	53(2)	164(3)	166(3)	-13(3)	-17(2)	-10(2)
F(26)	236(3)	149(3)	70(2)	-59(2)	-43(3)	49(3)

The anisotropic temperature factor exponent takes the form:

$$-2\pi^2(h^2a^{*2}U_{11} + \ldots + 2\,hka^*b^*U_{12}\cos\gamma^* + \ldots)$$

TABLE 3.5. Coordinates ($\times 10^4$) and temperature factors ($Å^2 \times 10^3$).

atom	x	y	z	U
H(2a)	6946	5727	6947	87
H(2b)	8062	5871	6576	87
H(3a)	6664	5216	6128	91
H(3b)	7250	4001	6595	91
H(5a)	8246	2896	5911	115
H(5b)	7510	4002	5406	115
H(6a)	9323	4090	5037	158
H(6b)	9188	2857	5046	158
H(8a)	11650	3163	5010	230
H(8b)	11264	2100	4916	230
H(8a')	11186	3045	4832	230
H(8b')	11509	1706	5159	230
H(9a)	11933	1368	5895	140
H(9b)	12865	1257	5395	140
H(9'a)	13065	1602	5388	130
H(9'b)	12796	2886	4986	130
H(11a)	13374	3972	5239	124
H(11b)	14452	2777	5492	124
H(12a)	14624	4277	5862	124
H(12b)	13362	4372	6150	124
H(17a)	16182	179	8199	106
H(17b)	17404	92	7873	106
H(18a)	16962	-1602	7973	115
H(18b)	16913	-966	7297	115
H(20a)	15599	-2224	7256	125
H(20b)	15355	-2473	7936	125
H(21a)	13749	-2499	7400	150
H(21b)	13569	-1209	7026	150
H(23a)	11497	-676	7369	157
H(23b)	11804	-1982	7751	157
H(24a)	11415	-1261	8602	128
H(24b)	10240	-765	8154	128
H(26a)	9329	921	8496	97
H(26b)	10364	245	9014	97
H(27a)	11041	1894	8796	79
H(27b)	9733	2156	9052	79
H(31)	8380	6667	7325	79
H(32)	9232	7167	8081	87
H(34)	10469	3738	8999	78
H(35)	14389	5081	6768	111
H(36)	15168	5342	7641	112
H(38)	16638	1796	8303	154
H(39a)	10300	5595	9456	117
H(39b)	10469	6661	8980	117
H(41a)	13194	4401	9763	138
H(41b)	11989	5239	9964	138
H(43)	11768	7214	9941	163
H(44)	12760	8685	9835	224
H(45)	14715	8345	9484	247
H(46)	15591	6703	9090	160
H(48a)	14184	4718	8824	151
H(48b)	15003	4128	9426	151
H(50a)	17290	3755	8537	143
H(50b)	16434	3146	8919	143
H(52)	13801	88	8251	76
H(53)	14433	377	9148	82

H(54)	13929	2283	9290	72
H(55)	12796	3910	8528	68
H(58)	12459	5259	7701	76
H(59)	11278	6798	6893	87
H(60)	10281	6351	6154	93
H(61)	10400	4389	6212	81
H(63a)	10830	2349	7325	79
H(63b)	11243	2389	6673	79
H(64a)	13321	1739	7022	77
H(64b)	12718	818	7359	77

3.4 REFERENCES

1a. M.A. Bush, and M.R. Truter, J. Chem. Soc., Perkin 2, 1972, 345.

b. J.D. Owen, and M.R. Truter, J. Chem. Soc., Dalton, 1979, 1831.

c. J. Hasek, D. Hlavata, and K.Huml, Acta. Cryst., 1980, B36, 1782.

d. H.M. Colquhoun, J.F. Stoddart, D.J. Williams, J.B. Wolstenholme and R. Zarzycki, Angew. Chem. Int. Ed. Engl., 1981, 20, 1051.

H.M. Colquhoun, S.M. Doughty, J.M. Maud, J.F. Stoddart, D.J. Williams, and J.B. Wolstenholme, Isr. J. Chem., 1985, 25, 15.

e. H.M. Colquhoun, E.P. Gooding, J.M. Maud, J.F. Stoddart, D.J. Williams and J.B. Wolstenholme, J. Chem. Soc., Chem. Commun., 1983, 1140.

H.M. Colquhoun, E.P. Gooding, J.M. Maud, J.F. Stoddart, D.J. Williams, J.B. Wolstenholme, J.Chem. Soc., Perkin Trans. 2, 1985, 607.

f. J. Hasek, D. Hlavata, and K.Huml, Acta. Cryst., 1979, B35, 330.

g. J.D. Owen, M.R. Truter, and J.N. Wingfield, Acta. Cryst., 1984, C40, 1515.

h. H.M. Colquohoun, S.M Doughty, J.F. Stoddart, and D.J. Williams Angew. Chem. Int. Ed. Engl., 1984, 25, 235.

2. R.C. Hayward, Chem. Soc. Reviews, 1983, 285.

3. J.M. Lehn, 'Biomimetic Chemistry,' eds. Z.I. Yoshida and N. Ise, Kodansha, Tokyo, Elsevier, Amsterdam, 1983, p. 163 and referencse therein.

4. See chapter 2.

5. G.M. Sheldrick, SHELXTL, An integrated system for solving, refining, and displaying crystal structures from diffraction

data, University of Göttingen, Federal Republic of Germany, 1981.

6. R.Foster, 'Organic Charge-Transfer Complexes,' Academic Press, London, 1969.

7. J. E. Derry, and T. A. Hamor, Nature, 1969, 221, 464.

P.D. Sullivan, and M.L. Williams, J. Am. Chem. Soc., 1972, 98, 1711.

T. Sundaresan, and S.C. Wallwork, Acta. Cryst., 1972, B28, 3065.

8. F.H. Kohnke, and J.F. Stoddart, J. Chem. Soc., Chem. Commun., 1985, 314.

9. B.L. Allwood, F.H. Kohnke, J.F. Stoddart, and D.J. Williams, Tetrahedron Lett., 1985, 26, 1681.

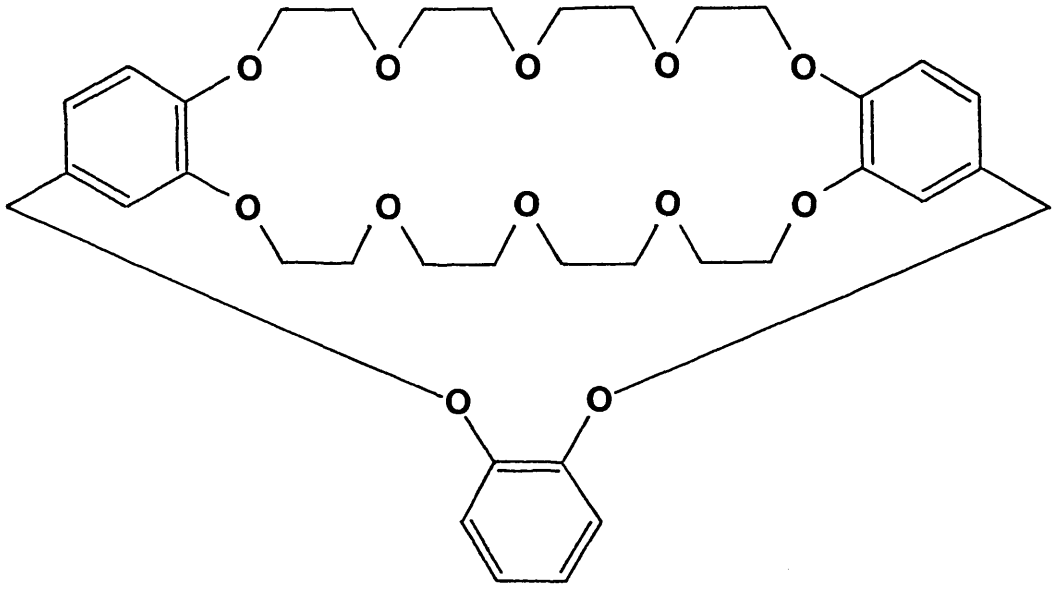
CHAPTER 4

The crystal structures of 1,4,7,10,13,20,28,36,39,42,45,48-dodecaoxa-[13^{15,32}][13.2.2](1,4)(1,2)(1,4)cyclophane (a macrobicyclic receptor) and its complex with diquat.

4.1 INTRODUCTION

The crystal structure of [5.diquat][1] revealed that the separation between the diether bridge and the diquat dication is larger than is necessary for an ideal supramolecular match. It was therefore decided to synthesise receptor 6 which contained a reduced apolar bridge.

In this case we were fortunate in being able to obtain crystals of both 6 and [6.diquat] and were thus able to study both the complexed and uncomplexed forms of the host molecule.



6

The X-ray crystal structure analysis has been carried out of the uncomplexed receptor 6 to determine whether it contained a preorganised cavity for encapsulation of the diquat dication. The structure analysis of [6.diquat][PF_6]$_2$ has been carried out to ascertain if the supermolecular match had been improved. The stability

constant of the 1:1 complex in solution will also be discussed.

4.2 EXPERIMENTAL

Clear colourless crystals of $[\underset{\sim}{6}](X_3^{\dagger})(H_2O)$ were obtained from a a solution of $\underset{\sim}{6}$ in $CHCl_3$ by vapour diffusion with pentane. A crystal (coated in Araldite to prevent decomposition) of dimensions 0.23 x 0.30 x 0.63 mm was used for unit cell and intensity measurements.

Crystal data: $C_{36}H_{46}O_{12}.X_3.(H_2O)_2$, M = 743‡, orthorhombic, a = 9.034(2), b = 28.871(6), c = 31.402(9) Å, U = 8190 Å^3, space group Pcab, Z = 8, D_c = 1.21‡ g cm^{-3}, $F(000)$ = 3168‡, μ(Cu-K_α) = 7.24‡ cm^{-1}.

† X represents atoms of unidentified solvent fragment assigned atomic mass of carbon.

‡ includes contribution from unidentified solvent fragment.

Refined unit-cell parameters were obtained by centering 18 reflections on a Nicolet R3m diffractometer. 4190 unique reflections ($\theta \leq 50^{\circ}$) were measured with Cu-K_α radiation (graphite monochromator) using the omega-scan routine. Of these 2693 had $|F_o| > 3\sigma(|F_o|)$ and were considered to be observed. The net count of two reflections, the 1 7 1 and the -1 5 3, measured as references every 50 reflections did not alter significantly during the data collection indicating that no deterioration of the crystal had occurred. The data were brought to a uniform arbitrary scale by the use of these reflections and Lorentz and polarisation corrections were applied.

The structure was solved by direct methods. A starting set

comprising 3 origin defining reflections together with a further 8 automatically selected terms was used. The initial phase refinement (256 permutations) was with 200 $\underline{E}$'s > 2.0 using 1677 TPR. This was subsequently expanded to 416 probable phases with $\underline{E}$'s > 1.72 using 4244 TPR. The figures of merit for the best phase solution were NQEST = -0.199, RA(1) = 0.039, RA(2) = 0.114. Three cycles of automatic $\Delta\underline{E}$-map recycling for this solution revealed 49 potential non-hydrogen atomic positions with an $\underline{R}_E$ = 0.33 for 1004 $\underline{E}$'s > 1.20. The remaining non-hydrogen atoms were found in subsequent $\Delta\underline{F}$-maps. A $\Delta\underline{F}$-map also revealed the the presence of two water molecules and an unidentified solvent fragment. The atoms of the solvent fragment were refined anisotropically as carbon atoms. The remaining non-hydrogen atoms were also refined anisotropically. The methylene and phenyl hydrogens were placed at calculated positions (C-H = 0.96 Å), assigned isotropic thermal parameters, $\underline{U}$(H) = 1.2 $\underline{U}_{eq}$(C), and allowed to ride on their parent carbon atoms. The protons on the water molecules were not located.

Damped refinement (due to poor convergence in normal refinement and oscillating parameter shifts) using $\underline{F}$ magnitudes was by block-cascade full-matrix least squares (478 variable parameters) and converged to $\underline{R}$ = 0.166, $\underline{R}_w$ = 0.166, unit weight were used (as refined or fixed values led to divergence in refinement) largest parameter shift/e.s.d. was 0.157, the mean shift/e.s.d. was 0.034. The residual electron density in the final difference map was within -0.33 and 0.68 $e\text{Å}^{-3}$.

Orange crystals of $[\underset{\sim}{6}.\text{diquat}][PF_6]_2[X_2^{\dagger}]$ were obtained from a solution of $[\underset{\sim}{6}.\text{diquat}][PF_6]_2$ in acetone by vapour diffusion from light petroleum. A crystal of dimensions 0.05 x 0.20 x0.35 mm was used for unit cell and intensity measurements.

Crystal data: $C_{36}H_{46}O_{12}.C_{12}H_{12}N_2.P_2F_{12}.X_2$, M = 1169‡, triclinic, a = 12.762(2), b = 13.176(2), c = 19.196(5) Å, α = 106.32(2), β = 95.13(2), γ = 111.74(1)°, U = 2809 Å^3, space group $P\bar{1}$, Z = 2, D_c = 1.39‡ g cm^{-3}, $F(000)$ = 1212‡, μ(Cu-K_α) = 15.72‡ cm^{-1}.

Refined unit-cell parameters were obtained by centering 18 reflections on a Nicolet R3m diffractometer. 5770 unique reflections ($\theta < 50°$) were measured with Cu-K_α radiation (graphite monochromator) using the omega-scan routine. Of these 4225 had $|F_o| > 3\sigma(|F_o|)$ and were considered to be observed. The net count of two reflections, the 1 2 2 and the -1 2 -1, measured as references every 50 reflections did not alter significantly during the data collection indicating that no deterioration of the crystal had occurred. The data were brought to a uniform arbitrary scale by the use of these reflections and Lorentz and polarisation corrections were applied.

The structure was solved by direct methods. A starting set comprising 3 origin defining reflections together with a further 5 automatically selected terms was used. The initial phase refinement (32 permutations) was with 200 E's > 1.86 using 619 TPR. This was subsequently expanded to 414 probable phases with E's > 1.86 using 922 TPR. The figures of merit for the best phase solution were NQEST = -

0.386, RA(1) = 0.011, RA(2) = 0.082. This solution gave potential atomic positions for 49 of the 76 non-hydrogen atoms. The remaining non-hydrogen atoms were located in a succession of $\Delta\underline{F}$-maps. A $\Delta\underline{F}$-map also revealed the presence of an unidentified disordered solvent fragment. The atoms in the disordered solvent fragment were refined isotropically as carbons with 50% site occupancies. The remaining non-hydrogen atoms were refined anisotropically. The methylene and phenyl hydrogens were placed at calculated positions (C-H = 0.96 Å) assigned isotropic thermal parameters, $\underline{U}(H) = 1.2\ \underline{U}_{eq}(C)$, and allowed to ride on their parent carbon atoms.

Refinement using $\underline{F}$ magnitudes was by block-cascade full-matrix least squares (701 variable parameters) and converged to $\underline{R}$ = 0.081, $\underline{R}_w$ = 0.083, a fixed weight was used [$w^{-1} = \sigma^2(\underline{F}) + 0.001\underline{F}^2$]. The largest parameter shift/e.s.d. was 0.041, the mean shift/e.s.d. was 0.012. The residual electron density in the final difference map was within -0.30 and 0.75 $e\text{Å}^{-3}$.

Computations were carried out on an Eclipse S140 computer using the SHELXTL[2] program system.

4.3 DISCUSSION

The final fractional atomic coordinates, anisotropic thermal parameters, bond lengths and bond angles for the non-hydrogen atoms in $[\underset{\sim}{6}](X_3)(H_2O)_2$ and $[\underset{\sim}{6}.\text{diquat}][PF_2]_2(X_2)$ are shown in Tables 4.1 - 4.4 and 4.6 - 4.9 respectively. The positions and isotropic temperature factors of the hydrogen atoms are listed in Tables 4.5 and

4.10 respectively.

The torsion angles associated with the polyether chains and the diether bridge in 6 and [6.diquat] are shown beside the relevant C-C and C-O bonds in the skeletal drawings of the structures in figures 4.1 and 4.2. These figures also provide the details of the crystallographic numbering schemes.

The crystal structure of the uncomplexed receptor 6 reveals that it has a more preorganised shape for complexation of diquat than uncomplexed DB30C10[3] (see figure 4.3), even though there is some self-filling of its cavity. The principal conformational changes that take place in 6 to enable the complexation of the diquat dication involve rotation about the C(26)-C(27), C(2)-C(3) and C(8)-C(9) bonds, the signs of their torsional angles are reversed, and changes in the magnitude of the torsional angle about the C(25)-C(26), O(4)-C(5), C(28)-C(29) and C(48)-C(37) bonds. The gross effect of these changes are to produce a rotation of one of the catechol rings by ~ 60^{o} to achieve a near parallel alignment of the two catechol units allowing complexation of diquat to occur.

One of the water molecules O(53) is probably hydrogen bonded to the periphery of one of the polyether chains of 6; O(53)...O(13) 3.07, O(53)...O(19) 3.19, O(53)...O(10) 3.25 Å. The other water molecule O(52) has a short contact 2.13 Å to C(50) of the disordered solvent fragment. This indicates that it could also be part of the disordered solvent fragment. The shortest contact between O(53) and the

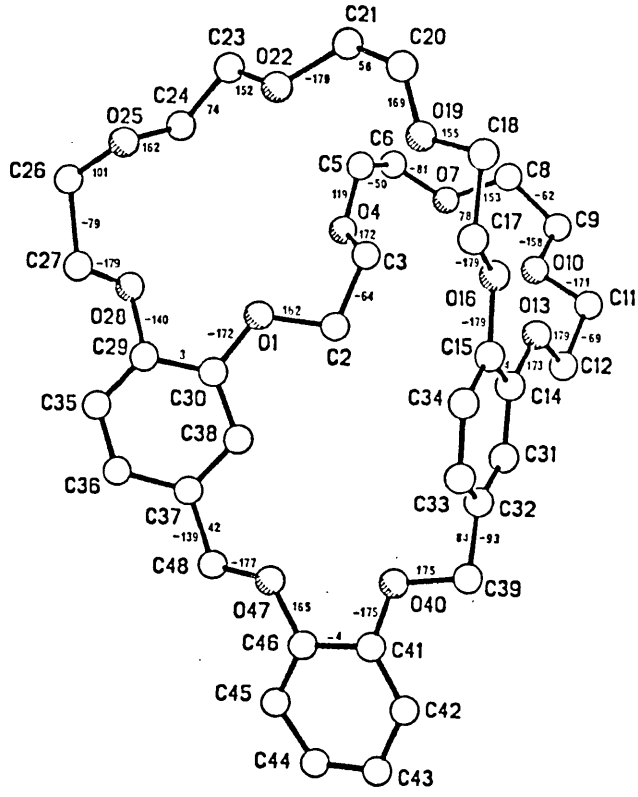


Figure 4.1. The skeletal representation of the solid-state structure of 6.

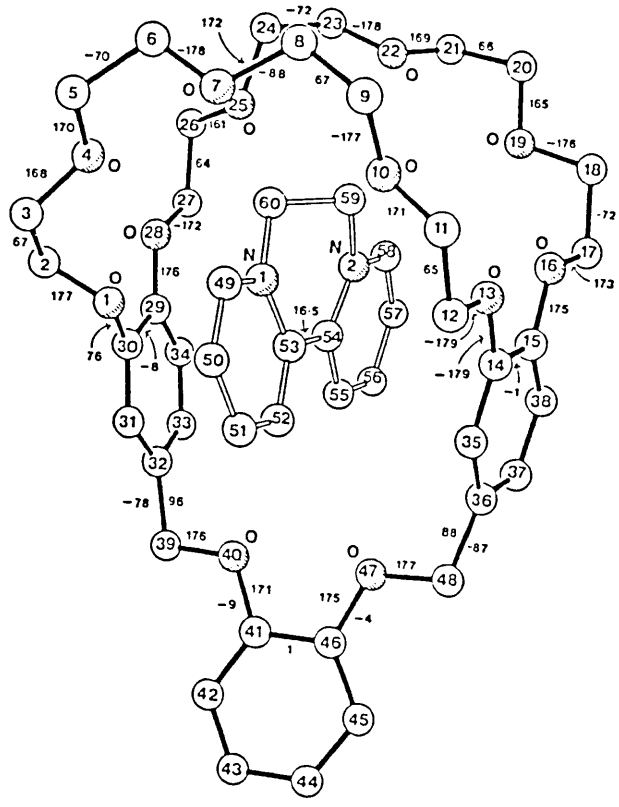


Figure 4.2. The skeletal representation of the solid-state structure of [6.diquat]

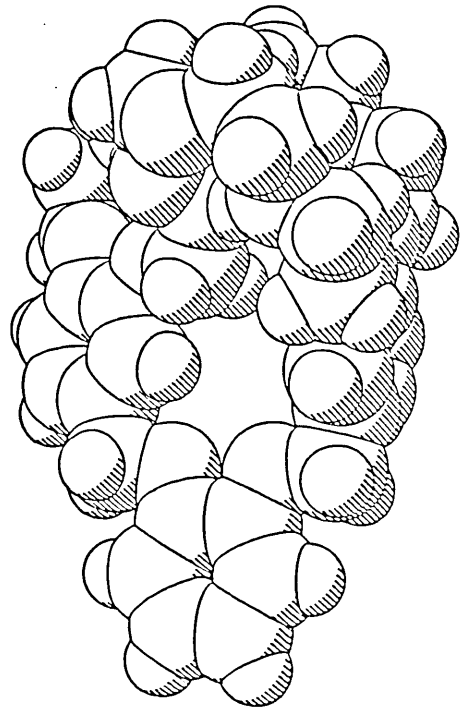


Figure 4.3. The space-filling representation of the solid-state structure of 6.

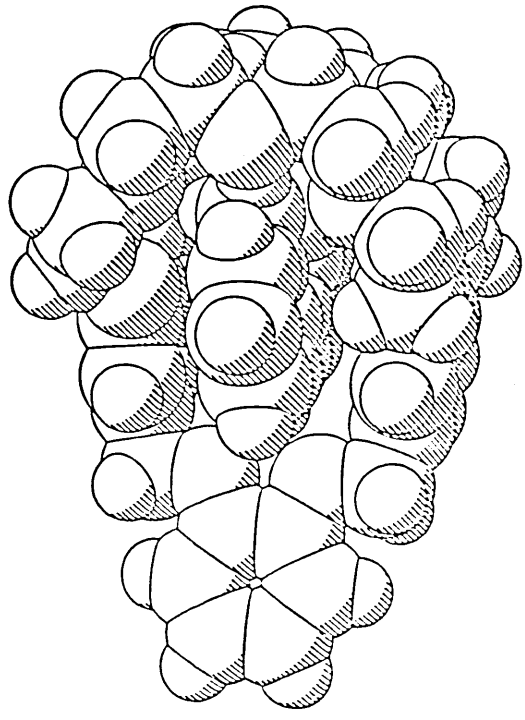


Figure 4.4. The space-filling representation of the solid-state structure of [6.diquat].

disordered solvent fragment or O(52) is 3.25 Å to C(50). The shortest contact between 6 and the solvent fragment or O(52) is 3.7 Å. There are no other significiant contacts of less than normal van der Waals distances between symmetry related receptors.

Thermal motion in the structure as a whole is very high. Although there is almost certainly disorder in portions of the polyether chains no discrete alternative atomic positions could be identified for any of the atoms. These factors coupled with the poor crystal quality, limited number of observed reflections and the high final R-factor, preclude any detailed discussion of the structure.

The conformation of the 30-membered ring of the complexed receptor 6 is similar to that of the complexed bicyclic receptor 5[1]. The major differences; (i) a change in the torsional angle about the O(1)-C(30) bond in [6.diquat] which rather surprisingly changes from an anti geometry in [5.diquat] to a nearly orthogonal geometry with a consequent loss of planarity of the methoxy group with respect to benzo ring and (ii) a reversal of the sign of the C(2)-C(3) bond torsional angle.

The dihedral angle between the mean planes of the pyridinium rings is 16.5(7)° which is in accord with the previously observed values[1,4].

The space-filling and stereo-pair representations of [6.diquat] (see figures 4.4 and 4.6) show that a consequence of the shorter apolar bridge of receptor 6 is an improved supramolecular match

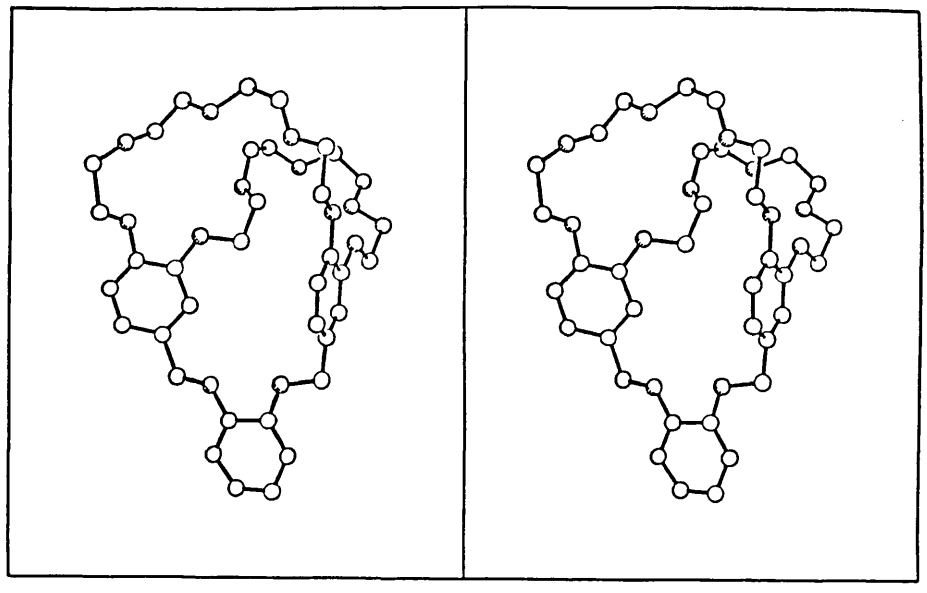


Figure 4.5. The stereo-pair representation of the solid-state structure of 6.

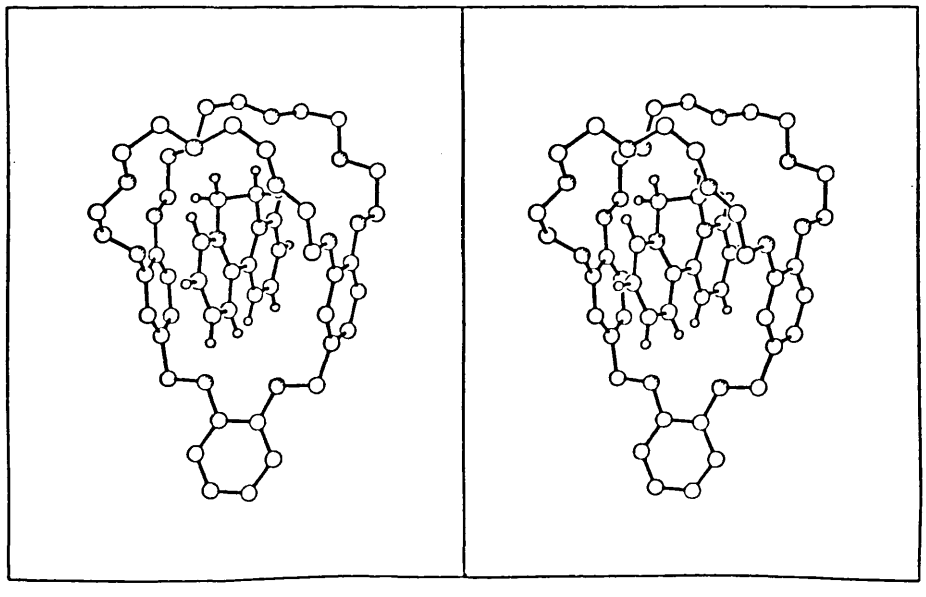


Figure 4.6. The stereo-pair representation of the solid-state structure of [6.diquat].

between the host and the diquat. This is also reflected in a loss of structural disorder in the two polyether chains. It can be seen (figure 4.4) that both the diether bridge oxygens are now directed towards the diquat dication, whereas in [5.diquat] only one is, thus enhancing electostatic interactions between the receptor and the guest. As in [5.diquat] there is a hydrogen bond contact between the diether bridge and the diquat dication [see table 4.11].

There are three potential C-H...O interactions [see table 4.11] between the polyether chains and the diquat dication, as well as seven other O(host)...C(guest) contacts of less 3.4 Å. These could also enhance the complex electrostatic binding interactions.

The side-on view (figure 4.7) reveals that only one of the pyridine rings of the diquat dication has any appreciable overlap with the two catechol units. The separation between the overlapping regions of the catechol units is ~ 6.2 Å. This is the closest distance yet observed between the catechol groups of the DB30C10 derivatives receptors complexed with diquat. Instead of the catechol units being nearly parallel there is now a 17° splay angle between them. This is almost certainly due to the reduced length of diether bridge which draws C(32) and C(36) closer together causing a slight V alignment of the catechol units. Where previously the two catechol units of the host have had a lateral displacement (shearing) producing very little plane-plane overlap (see figure 4.8), in [6.diquat] the catechol units are significantly overlapped. Previously the units had been in nearly in register[4a,b,c] (the only symmetry operations

TABLE 4.11. Selected host-guest contact distances, and relevant hydrogen contact distances and angles where appropriate, in order of increasing $X^a...O$ distance for [6.diquat].

$X^a...O$	$R(X^a...O)$ (Å)	$R(H...O)$ (Å)	$\psi(^o)^b$	$\theta(^o)^c$
N(1) -O(1)	2.89			
C(49)-O(10)	3.07			
C(49)-O(7)	3.12	2.25	44	150
C(49)-O(1)	3.14			
C(58)-O(19)	3.15			
N(1) -O(10)	3.18			
C(60)-O(4)	3.20			
C(49)-O(4)	3.20			
C(60)-O(1)	3.23			
C(60)-O(7)	3.24	2.35[d]	72[d]	154[d]
C(60)-O(10)	3.24			
C(59)-O(25)	3.27			
C(60)-O(25)	3.29			
C(52)-O(47)	3.36	2.43	47	163

[a] Carbon or Nitrogen atom of the diquat dication.
[b] Angles between COC planes and HO vectors.
[c] C-H...O angles.
[d] H(60b)

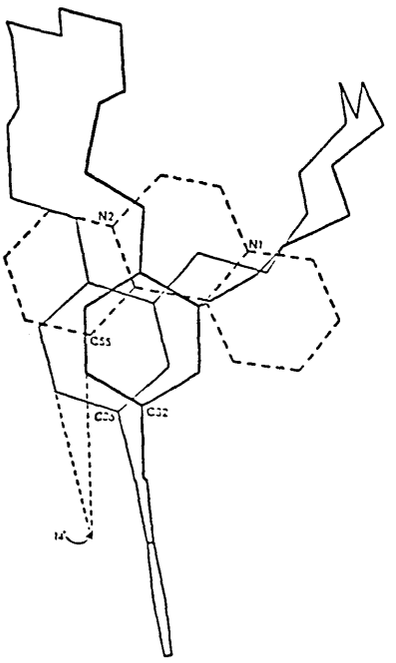


Figure 4.7. Side-on view (view normal to mean plane of diquat dication) of the skeletal representations of the solid-state structures of [6.diquat].

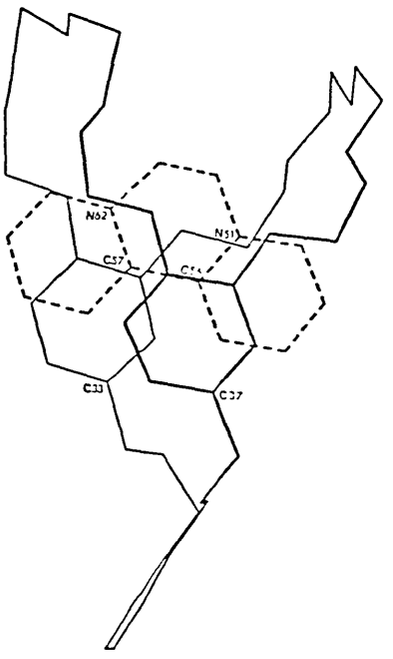


Figure 4.8. Side-on view (view normal to mean plane of diquat dication) of the skeletal representations of the solid-state structures of [5.diquat].

needed to bring about superimposition were translations), but they are now rotated in plane with respect to each other by ~ 14°. The distance of 3.3 Å between the mean planes of one of the benzo rings and the nearest overlapping atom of the diquat, C(55), is ideal for the charge transfer interactions[5].

Characteristically the complex retains the linear alignments between the catechol oxygens of the host and the formally positively charged nitrogens of the guest. The N...O distances and O...N...O angles are: O(1)...N(1) 2.89, O(13)...N(1) 3.70 Å, O(1)...N(1)...O(13) 163°; O(16)...N(2) 3.45, O(28)...N(2) 3.76 Å, O(16)...N(2)...O(28) 171°. The distance between N(1) and O(1) of 2.89 Å is very much shorter than previously observed in complexes between DB30C10 derivatives and diquat. This length is comparable with that normally associated with a N^+-H...O hydrogen bond[6] and the angle between the O(1)...N(1) vector and the C(30)-O(1)-C(2) plane is 21°.

In the crystal lattice the closest contact between the disordered solvent fragment and [6.diquat] is 3.56 Å between X(1) and C(12). The closest contact between this fragment and the PF_6 anion is 3.47 Å between X(2) and F(13). There are no significant contacts less than normal van der Waals distances between [6.diquat] and the PF_6 anion or symmetry related complexes.

From a comparison of the complexation strength in solution of [5.diquat][7], (K_a = 2 x 10^5 mol^{-1}), with that of [6.diquat][8] (K_a > 9 x 10^5 mol^{-1}, ΔG^o > 8.1 Kcal mol^{-1}) it is clear that the shortening of the diether bridge has increased the thermodynamic and kinetic

stabilities of the diquat complex. These studies indicate that the host still undergoes an energy demanding conformation change prior to complexation.

The two macrobicycle host 5 and 6 have both shown increased complexing ability towards the diquat dication relative to hosts 1 - 4. However, though a substantial portion of the host 6 is correctly arranged for binding diquat, complexation still requires an energy demanding conformation change of the host. Therefore our results demonstate the need to introduce one further bridging unit between the two catechol rings of DB30C10 in order to provide a more rigidly defined receptor for the diquat dication.

TABLE 4.1. Coordinates ($\times 10^4$) and temperature factors ($\AA^2 \times 10^3$)

atom	x	y	z	U
O(1)	4618(13)	1553(4)	4199(3)	109(3)*
C(2)	5300(20)	1153(6)	4406(6)	131(3)*
C(3)	5547(22)	782(7)	4057(6)	170(3)*
O(4)	4349(16)	619(5)	3880(5)	176(3)*
C(5)	4493(29)	343(7)	3527(7)	216(3)*
C(6)	3941(30)	-83(8)	3585(8)	226(3)*
O(7)	4227(19)	-384(5)	3918(5)	182(3)*
C(8)	5570(22)	-648(8)	3892(8)	219(3)*
C(9)	6175(26)	-785(7)	4293(7)	188(3)*
O(10)	6487(15)	-377(4)	4493(5)	167(3)*
C(11)	7501(21)	-469(6)	4789(7)	156(3)*
C(12)	7694(21)	-29(6)	5073(6)	135(3)*
O(13)	8379(13)	308(4)	4802(4)	128(3)*
C(14)	8653(16)	724(6)	5011(6)	114(3)*
C(15)	9475(17)	1035(6)	4768(6)	113(3)*
O(16)	9819(12)	892(4)	4341(4)	121(3)*
C(17)	10709(20)	1213(7)	4084(6)	164(3)*
C(18)	10860(23)	983(11)	3656(8)	268(3)*
O(19)	9522(19)	1063(6)	3457(4)	200(3)*
C(20)	9560(28)	1057(13)	3051(9)	281(3)*
C(21)	8151(30)	1058(10)	2831(9)	245(3)*
O(22)	7174(20)	1453(6)	2943(5)	204(3)*
C(23)	5854(28)	1454(14)	2745(9)	353(3)*
C(24)	4637(33)	1686(10)	2975(10)	302(3)*
O(25)	4759(22)	2174(6)	2973(6)	242(3)*
C(26)	3269(30)	2366(11)	3075(8)	283(3)*
C(27)	3323(33)	2512(9)	3583(6)	247(3)*
O(28)	3159(15)	2151(4)	3800(4)	133(3)*
C(29)	3140(18)	2204(5)	4226(4)	90(3)*
C(30)	3890(16)	1875(5)	4441(4)	79(3)*
C(31)	8243(19)	840(6)	5413(5)	113(3)*
C(32)	8667(20)	1253(7)	5567(5)	112(3)*
C(33)	9494(20)	1550(7)	5342(6)	126(3)*
C(34)	9910(17)	1458(5)	4937(6)	117(3)*
C(35)	2397(20)	2533(5)	4421(4)	107(3)*
C(36)	2384(18)	2535(6)	4841(5)	104(3)*
C(37)	3131(16)	2196(5)	5090(4)	82(3)*
C(38)	3899(15)	1856(5)	4880(4)	80(3)*
C(39)	8174(19)	1394(6)	5983(5)	131(3)*
O(40)	6832(13)	1661(4)	5911(3)	118(3)*
C(41)	6054(20)	1812(5)	6257(5)	109(3)*
C(42)	6334(25)	1771(6)	6682(5)	151(3)*
C(43)	5461(32)	1942(8)	7020(7)	241(3)*
C(44)	4247(30)	2141(7)	6901(5)	215(3)*
C(45)	3793(26)	2196(6)	6480(6)	168(3)*
C(46)	4696(22)	2034(6)	6160(5)	116(3)*
O(47)	4494(12)	2080(4)	5726(3)	113(3)*
C(48)	3106(18)	2188(6)	5573(5)	115(3)*
C(49)	5545(20)	390(9)	2086(8)	215(3)*
C(50)	3825(34)	403(11)	2075(12)	394(3)*
C(51)	2717(20)	396(8)	2316(4)	127(3)*
O(52)	3662(17)	1080(5)	1814(4)	179(3)*
O(53)	8967(24)	67(7)	3866(7)	294(3)*

* Equivalent isotropic U defined as one third of the trace of the orthogonolised U_{ij} tensor

TABLE 4.2. Bond lengths (Å)

O(1)-C(2)	1.463(20)	O(1)-C(30)	1.369(17)
C(2)-C(3)	1.547(26)	C(3)-O(4)	1.306(25)
O(4)-C(5)	1.369(25)	C(5)-C(6)	1.340(31)
C(6)-O(7)	1.383(29)	O(7)-C(8)	1.435(27)
C(8)-C(9)	1.430(33)	C(9)-O(10)	1.364(25)
O(10)-C(11)	1.332(24)	C(11)-C(12)	1.564(26)
C(12)-O(13)	1.432(22)	O(13)-C(14)	1.389(21)
C(14)-C(15)	1.392(24)	C(14)-C(31)	1.358(25)
C(15)-O(16)	1.438(21)	C(15)-C(34)	1.390(23)
O(16)-C(17)	1.466(23)	C(17)-C(18)	1.504(34)
C(18)-O(19)	1.380(27)	O(19)-C(20)	1.276(31)
C(20)-C(21)	1.448(38)	C(21)-O(22)	1.485(33)
O(22)-C(23)	1.346(32)	C(23)-C(24)	1.476(42)
C(24)-O(25)	1.413(33)	O(25)-C(26)	1.491(34)
C(26)-C(27)	1.653(32)	C(27)-O(28)	1.253(27)
O(28)-C(29)	1.345(17)	C(29)-C(30)	1.349(20)
C(29)-C(35)	1.314(21)	C(30)-C(38)	1.380(19)
C(31)-C(32)	1.342(26)	C(32)-C(33)	1.340(26)
C(32)-C(39)	1.439(24)	C(33)-C(34)	1.351(26)
C(35)-C(36)	1.321(20)	C(36)-C(37)	1.422(21)
C(37)-C(38)	1.369(20)	C(37)-C(48)	1.518(21)
C(39)-O(40)	1.455(21)	O(40)-C(41)	1.364(19)
C(41)-C(42)	1.364(22)	C(41)-C(46)	1.417(26)
C(42)-C(43)	1.413(30)	C(43)-C(44)	1.294(37)
C(44)-C(45)	1.392(26)	C(45)-C(46)	1.376(26)
C(46)-O(47)	1.382(18)	O(47)-C(48)	1.379(19)
C(49)-C(50)	1.555(36)	C(50)-C(51)	1.255(38)

TABLE 4.3. Bond Angles (deg.)

C(2)-O(1)-C(30)	119.5(11)	O(1)-C(2)-C(3)	107.0(14)
C(2)-C(3)-O(4)	115.6(17)	C(3)-O(4)-C(5)	118.4(18)
O(4)-C(5)-C(6)	112.9(20)	C(5)-C(6)-O(7)	127.6(23)
C(6)-O(7)-C(8)	116.5(18)	O(7)-C(8)-C(9)	114.8(20)
C(8)-C(9)-O(10)	104.2(17)	C(9)-O(10)-C(11)	106.8(15)
O(10)-C(11)-C(12)	108.1(14)	C(11)-C(12)-O(13)	105.2(15)
C(12)-O(13)-C(14)	112.6(14)	O(13)-C(14)-C(15)	113.2(16)
O(13)-C(14)-C(31)	127.1(16)	C(15)-C(14)-C(31)	119.6(16)
C(14)-C(15)-O(16)	116.2(15)	C(14)-C(15)-C(34)	120.7(17)
O(16)-C(15)-C(34)	123.1(15)	C(15)-O(16)-C(17)	116.8(13)
O(16)-C(17)-C(18)	105.2(17)	C(17)-C(18)-O(19)	104.6(19)
C(18)-O(19)-C(20)	115.3(20)	O(19)-C(20)-C(21)	117.0(23)
C(20)-C(21)-O(22)	114.2(24)	C(21)-O(22)-C(23)	114.7(22)
O(22)-C(23)-C(24)	115.7(26)	C(23)-C(24)-O(25)	113.0(26)
C(24)-O(25)-C(26)	107.4(21)	O(25)-C(26)-C(27)	106.0(20)
C(26)-C(27)-O(28)	108.1(20)	C(27)-O(28)-C(29)	116.6(15)
O(28)-C(29)-C(30)	114.3(13)	O(28)-C(29)-C(35)	123.4(14)
C(30)-C(29)-C(35)	122.2(13)	O(1)-C(30)-C(29)	116.2(12)
O(1)-C(30)-C(38)	121.7(12)	C(29)-C(30)-C(38)	122.1(13)
C(14)-C(31)-C(32)	118.5(16)	C(31)-C(32)-C(33)	122.4(17)
C(31)-C(32)-C(39)	119.4(16)	C(33)-C(32)-C(39)	118.1(17)
C(32)-C(33)-C(34)	121.8(17)	C(15)-C(34)-C(33)	116.8(16)
C(29)-C(35)-C(36)	118.2(15)	C(35)-C(36)-C(37)	122.8(15)
C(36)-C(37)-C(38)	118.1(13)	C(36)-C(37)-C(48)	123.4(13)
C(38)-C(37)-C(48)	118.5(13)	C(30)-C(38)-C(37)	116.6(13)
C(32)-C(39)-O(40)	105.5(14)	C(39)-O(40)-C(41)	118.4(12)
O(40)-C(41)-C(42)	130.9(16)	O(40)-C(41)-C(46)	114.9(13)
C(42)-C(41)-C(46)	114.2(16)	C(41)-C(42)-C(43)	127.1(20)
C(42)-C(43)-C(44)	114.2(19)	C(43)-C(44)-C(45)	125.2(21)
C(44)-C(45)-C(46)	118.6(20)	C(41)-C(46)-C(45)	120.8(15)
C(41)-C(46)-O(47)	111.6(14)	C(45)-C(46)-O(47)	127.5(17)
C(46)-O(47)-C(48)	119.1(13)	C(37)-C(48)-O(47)	109.8(12)
C(49)-C(50)-C(51)	141.7(31)		

TABLE 4.4. Anisotropic temperature factors ($Å^2 \times 10^3$)

atom	U_{11}	U_{22}	U_{33}	U_{23}	U_{13}	U_{12}
O(1)	129(5)	107(5)	93(5)	-3(4)	-14(5)	24(5)
C(2)	117(5)	125(5)	151(6)	-10(5)	-27(5)	55(5)
C(3)	199(6)	151(6)	158(6)	-44(5)	-16(6)	106(5)
O(4)	173(5)	144(5)	211(5)	-68(5)	-38(5)	0(5)
C(5)	345(6)	129(6)	175(6)	-61(6)	9(6)	-62(6)
C(6)	335(6)	151(6)	192(6)	2(6)	-40(6)	-98(6)
O(7)	194(6)	169(5)	183(5)	37(5)	-5(5)	-44(5)
C(8)	119(6)	226(6)	313(6)	-163(6)	75(6)	-18(6)
C(9)	238(6)	120(6)	206(6)	16(6)	-79(6)	-22(6)
O(10)	132(5)	117(5)	252(6)	-13(5)	-50(5)	-14(5)
C(11)	112(6)	115(5)	240(6)	73(5)	-8(6)	-9(5)
C(12)	118(6)	103(5)	185(6)	36(5)	-3(6)	-34(5)
O(13)	103(5)	103(5)	178(5)	45(5)	-31(5)	-34(5)
C(14)	56(5)	109(5)	178(6)	86(5)	-31(5)	-24(5)
C(15)	74(5)	124(5)	140(6)	10(5)	-21(5)	29(5)
O(16)	78(5)	131(5)	154(5)	36(5)	-12(5)	-12(5)
C(17)	110(6)	209(6)	174(6)	57(6)	-19(6)	-70(5)
C(18)	99(6)	471(6)	235(6)	124(6)	-17(6)	-20(6)
O(19)	216(6)	258(6)	127(5)	39(5)	48(5)	-20(6)
C(20)	163(6)	430(6)	249(6)	71(6)	-45(6)	-27(6)
C(21)	272(6)	212(6)	251(6)	-36(6)	82(6)	-0(6)
O(22)	214(6)	187(5)	213(6)	-32(5)	-35(6)	-35(5)
C(23)	198(6)	581(6)	280(6)	-267(6)	92(6)	-109(6)
C(24)	358(6)	226(6)	321(6)	-14(6)	16(6)	-145(6)
O(25)	264(6)	252(6)	212(6)	21(6)	18(6)	-76(6)
C(26)	338(6)	314(6)	198(6)	96(6)	14(6)	183(6)
C(27)	453(6)	169(6)	119(6)	10(6)	31(6)	91(6)
O(28)	179(5)	106(5)	115(5)	30(5)	-23(5)	15(5)
C(29)	125(5)	88(5)	57(5)	8(5)	-35(5)	8(5)
C(30)	93(5)	71(5)	72(5)	-24(5)	-5(5)	11(5)
C(31)	109(5)	127(5)	105(5)	25(5)	-18(5)	-6(5)
C(32)	110(6)	128(5)	97(5)	35(5)	-16(5)	-16(5)
C(33)	116(5)	120(5)	141(6)	-16(5)	-40(5)	25(5)
C(34)	79(5)	92(5)	179(6)	2(5)	-19(5)	-15(5)
C(35)	150(6)	84(5)	85(5)	-3(5)	-12(5)	40(5)
C(36)	103(5)	87(5)	122(5)	2(5)	4(5)	18(5)
C(37)	84(5)	71(5)	91(5)	-1(5)	-1(5)	-8(5)
C(38)	78(5)	71(5)	89(5)	-15(5)	-2(5)	3(5)
C(39)	142(6)	124(5)	128(5)	38(5)	-46(5)	12(5)
O(40)	120(5)	129(5)	103(5)	14(5)	-10(5)	-1(5)
C(41)	144(6)	100(5)	84(5)	16(5)	-32(5)	-18(5)
C(42)	248(6)	119(5)	87(5)	13(5)	-48(6)	-27(6)
C(43)	437(6)	159(6)	128(6)	12(6)	-97(6)	-18(6)
C(44)	406(6)	200(6)	38(5)	-8(5)	14(6)	-3(6)
C(45)	247(6)	127(6)	129(5)	-27(5)	77(6)	25(6)
C(46)	183(6)	96(5)	68(5)	22(5)	-18(5)	-28(5)
O(47)	92(5)	151(5)	95(5)	12(5)	3(5)	4(5)
C(48)	104(5)	115(5)	126(5)	1(5)	9(5)	-3(5)
C(49)	90(5)	267(6)	288(6)	-241(5)	-104(5)	72(5)
C(50)	373(6)	315(6)	494(6)	-316(6)	-223(6)	24(6)
C(51)	119(6)	214(6)	46(5)	-8(5)	40(5)	-43(6)
O(52)	221(5)	152(5)	163(5)	-34(5)	-95(5)	-45(5)
O(53)	303(6)	273(6)	305(6)	-11(6)	38(6)	-102(6)

The anisotropic temperature factor exponent takes the form:

$$-2\pi^2(h^2a^{*2}U_{11} + \ldots + 2\,hka^*b^*U_{12}\cos\gamma^* + \ldots)$$

TABLE 4.5. Coordinates ($\times 10^4$) and temperature factors ($Å^2 \times 10^3$)

atom	x	y	z	U
H(2a)	6228	1239	4532	157
H(2b)	4655	1033	4623	157
H(3a)	6075	528	4183	203
H(3b)	6141	919	3837	203
H(5a)	5524	319	3456	261
H(5b)	3970	486	3296	261
H(6a)	2886	-44	3586	265
H(6b)	4232	-252	3335	265
H(8a)	6296	-463	3747	261
H(8b)	5372	-922	3729	261
H(9a)	7056	-966	4255	217
H(9b)	5465	-960	4454	217
H(11a)	7180	-725	4961	182
H(11b)	8425	-546	4655	182
H(12a)	8315	-95	5313	170
H(12b)	6750	81	5171	170
H(17a)	10213	1506	4056	197
H(17b)	11663	1259	4212	197
H(18a)	11032	657	3689	320
H(18b)	11658	1119	3497	320
H(20a)	10086	1330	2962	333
H(20b)	10098	787	2964	333
H(21a)	8341	1069	2530	297
H(21b)	7646	775	2899	297
H(23a)	5980	1615	2479	421
H(23b)	5566	1140	2690	421
H(24a)	4653	1581	3265	357
H(24b)	3713	1601	2846	357
H(26a)	3071	2633	2902	335
H(26b)	2517	2137	3027	335
H(27a)	2539	2725	3645	293
H(27b)	4258	2653	3649	293
H(31)	7662	632	5583	140
H(33)	9802	1835	5471	156
H(34)	10475	1677	4773	140
H(35)	1876	2766	4262	127
H(36)	1845	2774	4986	132
H(38)	4419	1617	5031	95
H(39a)	7966	1127	6156	158
H(39b)	8912	1581	6120	158
H(42)	7225	1607	6755	186
H(43)	5741	1912	7314	289
H(44)	3604	2262	7117	257
H(45)	2864	2343	6419	211
H(48a)	2409	1960	5668	138
H(48b)	2818	2488	5677	138

TABLE 4.6. Coordinates ($\times 10^4$) and temperature factors ($Å^2 \times 10^3$)

atom	x	y	z	U
O(1)	10192(4)	13760(5)	8064(3)	87(3)*
C(2)	10669(7)	14861(7)	8119(5)	90(5)*
C(3)	10661(7)	14973(7)	7306(4)	78(4)*
O(4)	9497(4)	14588(4)	6969(3)	85(3)*
C(5)	9357(7)	14848(7)	6312(4)	77(5)*
C(6)	8106(7)	14220(7)	5921(5)	77(5)*
O(7)	7815(4)	13037(4)	5636(3)	64(3)*
C(8)	6672(7)	12351(7)	5238(4)	72(5)*
C(9)	6505(6)	11132(6)	4851(4)	63(4)*
O(10)	6629(4)	10602(4)	5394(2)	53(2)*
C(11)	6542(6)	9473(6)	5036(4)	58(4)*
C(12)	6858(6)	8942(6)	5584(4)	53(4)*
O(13)	6030(4)	8787(4)	6045(2)	53(2)*
C(14)	6219(5)	8318(5)	6588(4)	47(3)*
C(15)	5379(6)	8155(6)	7013(4)	51(3)*
O(16)	4500(4)	8473(4)	6859(3)	61(3)*
C(17)	3602(6)	8220(7)	7257(4)	69(4)*
C(18)	2818(6)	8766(7)	7074(4)	70(4)*
O(19)	3408(4)	9974(5)	7425(3)	90(3)*
C(20)	2692(7)	10550(8)	7319(6)	94(6)*
C(21)	3259(8)	11796(10)	7868(7)	123(8)*
O(22)	4247(4)	12414(5)	7724(4)	99(3)*
C(23)	4630(7)	13608(7)	8142(6)	105(6)*
C(24)	5706(8)	14233(8)	7940(5)	102(6)*
O(25)	6647(4)	14034(4)	8243(3)	83(3)*
C(26)	7231(7)	14815(7)	8959(4)	76(4)*
C(27)	7915(6)	14340(6)	9329(4)	64(4)*
O(28)	8771(4)	14238(4)	8927(2)	61(2)*
C(29)	9397(6)	13690(6)	9131(4)	53(3)*
C(30)	10178(6)	13518(6)	8699(4)	61(4)*
C(31)	10823(7)	12931(7)	8846(4)	70(4)*
C(32)	10695(6)	12496(6)	9411(4)	66(4)*
C(33)	9948(7)	12673(6)	9840(4)	73(4)*
C(34)	9313(6)	13278(6)	9707(4)	63(4)*
C(35)	7148(5)	8060(5)	6731(4)	48(3)*
C(36)	7270(6)	7644(6)	7317(4)	52(4)*
C(37)	6429(6)	7460(6)	7723(4)	62(4)*
C(38)	5471(6)	7695(6)	7573(4)	60(4)*
C(39)	11303(7)	11730(7)	9497(5)	91(5)*
O(40)	10605(4)	10623(4)	8946(3)	81(3)*
C(41)	10990(7)	9749(7)	8860(4)	69(4)*
C(42)	12078(7)	9934(7)	9206(4)	72(4)*
C(43)	12401(7)	9035(7)	9083(4)	78(5)*
C(44)	11632(7)	7955(7)	8640(4)	80(5)*
C(45)	10526(7)	7725(7)	8269(4)	70(4)*
C(46)	10213(6)	8655(6)	8395(4)	59(4)*
O(47)	9162(4)	8580(4)	8072(3)	64(3)*
C(48)	8356(6)	7501(6)	7538(4)	63(4)*
N(1)	8350(4)	11737(4)	6978(3)	43(3)*
C(49)	8998(5)	11891(6)	6472(4)	49(3)*
C(50)	9784(6)	11413(6)	6376(4)	56(4)*
C(51)	9904(6)	10778(6)	6809(4)	57(4)*
C(52)	9236(5)	10615(5)	7318(4)	48(3)*
C(53)	8426(5)	11081(5)	7403(3)	43(3)*
C(54)	7668(5)	10911(5)	7923(3)	42(3)*
C(55)	7857(6)	10489(6)	8481(4)	57(4)*

C(56)	7105(6)	10317(6)	8947(4)	68(4)*
C(57)	6172(7)	10603(7)	8878(4)	71(4)*
C(58)	5985(6)	11011(6)	8315(4)	61(4)*
N(2)	6715(4)	11142(4)	7854(3)	48(3)*
C(59)	6449(5)	11503(6)	7217(4)	53(4)*
C(60)	7559(5)	12316(6)	7114(4)	52(4)*
F(1)	9718(2)	7663(2)	5479(1)	64(1)*
F(11)	10457(5)	6988(5)	5636(3)	112(3)*
F(12)	8999(4)	8372(4)	5337(3)	106(3)*
F(13)	9479(5)	7027(4)	4610(3)	102(3)*
F(14)	10834(4)	8661(4)	5429(3)	105(3)*
F(15)	9947(4)	8305(4)	6345(3)	104(3)*
F(16)	8595(4)	6687(4)	5541(3)	111(3)*
F(2)	4575(2)	7048(2)	9501(1)	83(1)*
F(21)	4129(7)	6462(6)	8646(3)	188(5)*
F(22)	4970(6)	8271(5)	9425(4)	165(5)*
F(23)	5002(6)	7626(6)	10358(3)	148(4)*
F(24)	4100(8)	5833(6)	9575(4)	188(6)*
F(25)	3380(5)	7090(6)	9609(4)	149(5)*
F(26)	5757(6)	7076(8)	9400(5)	206(6)*
X(1)	5363(19)	6347(19)	4029(12)	107(7)
X(2)	6711(26)	6098(25)	3582(17)	169(10)
X(3)	6088(33)	5082(35)	4009(21)	230(15)
X(4)	5883(22)	5984(23)	3961(13)	124(8)

* Equivalent isotropic U defined as one third of the trace of the orthogonalised U_{ij} tensor

TABLE 4.7. Bond lengths (Å)

O(1)-C(2)	1.317(11)	O(1)-C(30)	1.344(10)
C(2)-C(3)	1.608(13)	C(3)-O(4)	1.403(9)
O(4)-C(5)	1.410(11)	C(5)-C(6)	1.501(10)
C(6)-O(7)	1.386(10)	O(7)-C(8)	1.401(8)
C(8)-C(9)	1.491(12)	C(9)-O(10)	1.435(10)
O(10)-C(11)	1.409(9)	C(11)-C(12)	1.518(12)
C(12)-O(13)	1.431(9)	O(13)-C(14)	1.399(10)
C(14)-C(15)	1.396(10)	C(14)-C(35)	1.374(11)
C(15)-O(16)	1.371(10)	C(15)-C(38)	1.389(12)
O(16)-C(17)	1.424(10)	C(17)-C(18)	1.502(14)
C(18)-O(19)	1.404(9)	O(19)-C(20)	1.422(14)
C(20)-C(21)	1.531(13)	C(21)-O(22)	1.327(12)
O(22)-C(23)	1.417(10)	C(23)-C(24)	1.467(13)
C(24)-O(25)	1.429(13)	O(25)-C(26)	1.399(8)
C(26)-C(27)	1.483(14)	C(27)-O(28)	1.417(10)
O(28)-C(29)	1.357(11)	C(29)-C(30)	1.394(11)
C(29)-C(34)	1.360(11)	C(30)-C(31)	1.380(14)
C(31)-C(32)	1.359(13)	C(32)-C(33)	1.355(12)
C(32)-C(39)	1.516(15)	C(33)-C(34)	1.384(14)
C(35)-C(36)	1.404(11)	C(36)-C(37)	1.372(11)
C(36)-C(48)	1.507(12)	C(37)-C(38)	1.393(12)
C(39)-O(40)	1.430(8)	O(40)-C(41)	1.386(12)
C(41)-C(42)	1.387(12)	C(41)-C(46)	1.385(9)
C(42)-C(43)	1.360(15)	C(43)-C(44)	1.359(10)
C(44)-C(45)	1.405(12)	C(45)-C(46)	1.390(14)
C(46)-O(47)	1.382(10)	O(47)-C(48)	1.428(7)
N(1)-C(49)	1.341(9)	N(1)-C(53)	1.366(10)
N(1)-C(60)	1.475(10)	C(49)-C(50)	1.369(12)
C(50)-C(51)	1.368(12)	C(51)-C(52)	1.365(10)
C(52)-C(53)	1.383(11)	C(53)-C(54)	1.456(9)
C(54)-C(55)	1.379(11)	C(54)-N(2)	1.362(10)
C(55)-C(56)	1.370(11)	C(56)-C(57)	1.383(13)
C(57)-C(58)	1.376(12)	C(58)-N(2)	1.340(10)
N(2)-C(59)	1.485(10)	C(59)-C(60)	1.497(9)
P(1)-F(11)	1.579(8)	P(1)-F(12)	1.588(7)
P(1)-F(13)	1.584(5)	P(1)-F(14)	1.572(5)
P(1)-F(15)	1.584(5)	P(1)-F(16)	1.573(5)
P(2)-F(21)	1.551(6)	P(2)-F(22)	1.554(8)
P(2)-F(23)	1.553(6)	P(2)-F(24)	1.542(8)
P(2)-F(25)	1.576(8)	P(2)-F(26)	1.526(9)
X(1)-X(4)	0.949(43)	X(2)-X(4)	1.324(44)
X(3)-X(4)	1.333(62)		

TABLE 4.8. Bond Angles (deg.)

C(2)-O(1)-C(30)	117.6(6)	O(1)-C(2)-C(3)	110.3(6)
C(2)-C(3)-O(4)	106.1(6)	C(3)-O(4)-C(5)	112.8(6)
O(4)-C(5)-C(6)	108.8(7)	C(5)-C(6)-O(7)	109.6(8)
C(6)-O(7)-C(8)	115.4(7)	O(7)-C(8)-C(9)	110.9(8)
C(8)-C(9)-O(10)	109.3(6)	C(9)-O(10)-C(11)	109.8(5)
O(10)-C(11)-C(12)	112.1(5)	C(11)-C(12)-O(13)	109.0(7)
C(12)-O(13)-C(14)	115.6(6)	O(13)-C(14)-C(15)	113.8(7)
O(13)-C(14)-C(35)	125.4(6)	C(15)-C(14)-C(35)	120.8(7)
C(14)-C(15)-O(16)	117.6(7)	C(14)-C(15)-C(38)	119.3(8)
O(16)-C(15)-C(38)	123.1(7)	C(15)-O(16)-C(17)	117.0(6)
O(16)-C(17)-C(18)	108.1(7)	C(17)-C(18)-O(19)	107.9(6)
C(18)-O(19)-C(20)	111.3(6)	O(19)-C(20)-C(21)	108.5(8)
C(20)-C(21)-O(22)	111.9(9)	C(21)-O(22)-C(23)	110.3(8)
O(22)-C(23)-C(24)	107.1(8)	C(23)-C(24)-O(25)	111.9(9)
C(24)-O(25)-C(26)	113.2(7)	O(25)-C(26)-C(27)	109.9(7)
C(26)-C(27)-O(28)	108.5(7)	C(27)-O(28)-C(29)	117.1(6)
O(28)-C(29)-C(30)	116.8(7)	O(28)-C(29)-C(34)	125.8(7)
C(30)-C(29)-C(34)	117.3(8)	O(1)-C(30)-C(29)	120.3(8)
O(1)-C(30)-C(31)	117.9(7)	C(29)-C(30)-C(31)	121.1(8)
C(30)-C(31)-C(32)	120.3(8)	C(31)-C(32)-C(33)	119.0(9)
C(31)-C(32)-C(39)	118.9(8)	C(33)-C(32)-C(39)	121.8(9)
C(32)-C(33)-C(34)	121.1(9)	C(29)-C(34)-C(33)	121.0(8)
C(14)-C(35)-C(36)	120.1(7)	C(35)-C(36)-C(37)	118.9(8)
C(35)-C(36)-C(48)	120.4(7)	C(37)-C(36)-C(48)	120.5(7)
C(36)-C(37)-C(38)	121.5(8)	C(15)-C(38)-C(37)	119.4(7)
C(32)-C(39)-O(40)	104.6(7)	C(39)-O(40)-C(41)	117.8(6)
O(40)-C(41)-C(42)	123.4(6)	O(40)-C(41)-C(46)	115.6(7)
C(42)-C(41)-C(46)	121.0(9)	C(41)-C(42)-C(43)	120.0(7)
C(42)-C(43)-C(44)	119.2(9)	C(43)-C(44)-C(45)	123.0(10)
C(44)-C(45)-C(46)	117.0(6)	C(41)-C(46)-C(45)	119.8(8)
C(41)-C(46)-O(47)	115.8(8)	C(45)-C(46)-O(47)	124.4(5)
C(46)-O(47)-C(48)	118.9(6)	C(36)-C(48)-O(47)	107.6(6)
C(49)-N(1)-C(53)	121.8(7)	C(49)-N(1)-C(60)	120.4(6)
C(53)-N(1)-C(60)	117.7(6)	N(1)-C(49)-C(50)	120.7(7)
C(49)-C(50)-C(51)	118.9(7)	C(50)-C(51)-C(52)	120.2(8)
C(51)-C(52)-C(53)	120.7(8)	N(1)-C(53)-C(52)	117.6(6)
N(1)-C(53)-C(54)	119.1(7)	C(52)-C(53)-C(54)	123.2(7)
C(53)-C(54)-C(55)	122.4(7)	C(53)-C(54)-N(2)	119.8(7)
C(55)-C(54)-N(2)	117.8(6)	C(54)-C(55)-C(56)	120.3(8)
C(55)-C(56)-C(57)	120.3(8)	C(56)-C(57)-C(58)	118.8(8)
C(57)-C(58)-N(2)	119.7(8)	C(54)-N(2)-C(58)	123.0(7)
C(54)-N(2)-C(59)	118.2(6)	C(58)-N(2)-C(59)	118.7(6)
N(2)-C(59)-C(60)	108.4(5)	N(1)-C(60)-C(59)	109.8(6)
F(11)-P(1)-F(12)	178.5(2)	F(11)-P(1)-F(13)	91.1(3)
F(12)-P(1)-F(13)	90.0(3)	F(11)-P(1)-F(14)	90.3(3)
F(12)-P(1)-F(14)	88.7(3)	F(13)-P(1)-F(14)	89.7(3)
F(11)-P(1)-F(15)	89.5(3)	F(12)-P(1)-F(15)	89.4(3)
F(13)-P(1)-F(15)	179.4(4)	F(14)-P(1)-F(15)	90.5(3)
F(11)-P(1)-F(16)	90.6(3)	F(12)-P(1)-F(16)	90.4(3)
F(13)-P(1)-F(16)	91.4(3)	F(14)-P(1)-F(16)	178.6(3)
F(15)-P(1)-F(16)	88.5(3)	F(21)-P(2)-F(22)	90.7(4)
F(21)-P(2)-F(23)	179.0(4)	F(22)-P(2)-F(23)	89.7(4)
F(21)-P(2)-F(24)	88.8(4)	F(22)-P(2)-F(24)	176.1(5)
F(23)-P(2)-F(24)	90.7(4)	F(21)-P(2)-F(25)	91.9(4)
F(22)-P(2)-F(25)	88.4(5)	F(23)-P(2)-F(25)	87.2(4)
F(24)-P(2)-F(25)	87.7(5)	F(21)-P(2)-F(26)	88.7(5)
F(22)-P(2)-F(26)	88.6(5)	F(23)-P(2)-F(26)	92.1(4)
F(24)-P(2)-F(26)	95.3(6)	F(25)-P(2)-F(26)	177.0(5)
X(1)-X(4)-X(2)	131.8(37)	X(1)-X(4)-X(3)	144.9(34)
X(2)-X(4)-X(3)	82.0(30)		

TABLE 4.9. Anisotropic temperature factors ($Å^2 \times 10^3$)

atom	U_{11}	U_{22}	U_{33}	U_{23}	U_{13}	U_{12}
O(1)	75(4)	107(4)	77(4)	39(3)	14(3)	31(3)
C(2)	80(6)	74(6)	90(7)	20(5)	-22(5)	19(5)
C(3)	78(6)	60(5)	74(6)	14(4)	-1(5)	16(5)
O(4)	84(4)	79(4)	88(4)	53(3)	-0(3)	14(3)
C(5)	101(7)	63(5)	74(6)	40(5)	13(5)	30(5)
C(6)	80(6)	76(6)	90(6)	49(5)	8(5)	36(5)
O(7)	65(4)	56(3)	74(4)	32(3)	3(3)	25(3)
C(8)	69(6)	91(6)	76(6)	47(5)	12(5)	41(5)
C(9)	62(5)	86(6)	56(5)	39(4)	13(4)	36(4)
O(10)	57(3)	60(3)	44(3)	18(2)	9(2)	26(2)
C(11)	52(5)	70(5)	49(4)	23(4)	13(4)	19(4)
C(12)	51(4)	62(5)	46(4)	15(4)	13(4)	25(4)
O(13)	45(3)	70(3)	53(3)	29(3)	16(2)	27(2)
C(14)	47(4)	50(4)	48(4)	21(4)	13(4)	20(4)
C(15)	54(5)	54(5)	46(4)	16(4)	7(4)	24(4)
O(16)	53(3)	83(4)	63(3)	37(3)	21(2)	33(3)
C(17)	46(5)	78(6)	84(6)	35(5)	25(4)	21(4)
C(18)	49(5)	86(6)	75(6)	39(5)	18(4)	20(4)
O(19)	52(3)	100(4)	130(5)	46(4)	13(3)	40(3)
C(20)	61(6)	101(8)	126(8)	37(7)	14(6)	42(6)
C(21)	105(8)	145(10)	157(10)	49(9)	34(8)	93(8)
O(22)	71(4)	95(4)	135(5)	31(4)	24(4)	44(3)
C(23)	87(7)	95(7)	131(9)	19(6)	-3(6)	56(6)
C(24)	109(7)	82(7)	113(8)	27(6)	-1(6)	49(6)
O(25)	79(4)	84(4)	81(4)	13(3)	2(3)	44(3)
C(26)	83(6)	69(6)	72(6)	4(4)	13(5)	42(5)
C(27)	64(5)	55(5)	66(5)	13(4)	13(4)	23(4)
O(28)	59(3)	72(3)	59(3)	23(3)	18(2)	32(3)
C(29)	55(4)	54(4)	44(4)	6(4)	6(3)	23(4)
C(30)	69(5)	73(5)	29(4)	13(4)	-4(4)	21(5)
C(31)	61(5)	82(6)	57(5)	3(5)	1(4)	38(5)
C(32)	68(5)	57(5)	58(5)	7(4)	-6(4)	26(4)
C(33)	76(6)	65(5)	69(5)	21(4)	-1(4)	24(4)
C(34)	73(5)	53(5)	60(5)	16(4)	12(4)	25(4)
C(35)	47(4)	46(4)	54(5)	16(4)	10(3)	22(4)
C(36)	54(5)	46(4)	56(5)	14(4)	5(4)	24(4)
C(37)	74(5)	54(5)	69(5)	36(4)	19(4)	28(4)
C(38)	58(5)	66(5)	63(5)	31(4)	24(4)	24(4)
C(39)	93(7)	76(6)	88(7)	-1(5)	-16(5)	46(5)
O(40)	82(4)	65(4)	87(4)	8(3)	-15(3)	41(3)
C(41)	75(5)	83(6)	68(5)	27(5)	12(4)	52(5)
C(42)	75(6)	85(6)	62(5)	24(5)	-8(4)	43(5)
C(43)	76(6)	105(7)	62(5)	24(5)	1(4)	53(6)
C(44)	98(6)	112(7)	82(6)	52(5)	24(5)	83(6)
C(45)	80(6)	81(6)	66(5)	26(5)	12(4)	53(5)
C(46)	64(5)	75(5)	56(5)	29(4)	10(4)	44(4)
O(47)	66(3)	61(3)	72(3)	20(3)	2(3)	38(3)
C(48)	72(5)	57(5)	69(5)	24(4)	8(4)	36(4)
N(1)	39(3)	45(3)	46(3)	14(3)	9(3)	19(3)
C(49)	49(4)	52(4)	46(4)	20(4)	8(3)	20(4)
C(50)	48(4)	69(5)	56(5)	24(4)	11(4)	27(4)
C(51)	49(4)	67(5)	68(5)	24(4)	13(4)	35(4)
C(52)	43(4)	47(4)	53(4)	17(4)	0(3)	21(3)
C(53)	46(4)	40(4)	41(4)	14(3)	-1(3)	16(3)
C(54)	42(4)	42(4)	35(4)	9(3)	2(3)	14(3)
C(55)	65(5)	54(5)	45(4)	12(4)	4(4)	24(4)

C(56)	84(6)	66(5)	48(5)	15(4)	9(4)	28(5)
C(57)	77(6)	78(6)	52(5)	25(4)	28(4)	20(5)
C(58)	55(5)	69(5)	56(5)	20(4)	21(4)	22(4)
N(2)	48(3)	49(3)	43(3)	13(3)	5(3)	19(3)
C(59)	51(4)	63(5)	48(4)	13(4)	4(3)	34(4)
C(60)	61(5)	55(5)	48(4)	19(4)	10(4)	33(4)
P(1)	68(1)	69(1)	71(1)	32(1)	27(1)	35(1)
F(11)	146(5)	134(4)	122(4)	74(3)	49(4)	102(4)
F(12)	93(4)	110(4)	143(5)	48(3)	27(3)	70(3)
F(13)	141(4)	112(4)	69(3)	32(3)	34(3)	65(4)
F(14)	66(3)	118(4)	144(5)	75(4)	38(3)	26(3)
F(15)	125(4)	106(4)	73(3)	21(3)	25(3)	45(3)
F(16)	102(4)	93(4)	120(4)	43(3)	37(3)	12(3)
P(2)	87(2)	101(2)	73(2)	41(1)	30(1)	42(1)
F(21)	205(7)	181(7)	76(4)	37(4)	24(4)	-24(5)
F(22)	195(7)	116(5)	199(7)	86(5)	78(6)	48(5)
F(23)	169(6)	210(7)	77(4)	37(4)	22(4)	100(5)
F(24)	314(10)	130(5)	182(7)	92(5)	134(7)	112(6)
F(25)	106(4)	221(7)	169(6)	112(6)	52(4)	81(5)
F(26)	127(6)	302(10)	201(8)	44(7)	66(5)	124(6)

The anisotropic temperature factor exponent takes the form:

$$-2\pi^2(h^2a^{*2}U_{11} + \ldots + 2\,hka^*b^*U_{12}\cos\gamma^* + \ldots)$$

TABLE 4.10. Coordinates ($\times 10^4$) and temperature factors ($Å^2 \times 10^3$)

atom	x	y	z	U
H(2a)	10234	15251	8369	103
H(2b)	11450	15212	8400	103
H(3a)	10996	14498	7021	94
H(3b)	11087	15767	7346	94
H(5a)	9588	15670	6436	87
H(5b)	9826	14608	5997	87
H(6a)	7981	14489	5518	93
H(6b)	7631	14367	6262	93
H(8a)	6164	12348	5578	83
H(8b)	6491	12674	4878	83
H(9a)	7074	11133	4557	75
H(9b)	5746	10706	4535	75
H(11a)	5760	8991	4766	68
H(11b)	7051	9508	4696	68
H(12a)	7615	9450	5886	63
H(12b)	6850	8204	5317	63
H(17a)	3180	7395	7119	82
H(17b)	3931	8547	7782	82
H(18a)	2119	8473	7244	83
H(18b)	2636	8587	6545	83
H(20a)	2613	10562	6819	109
H(20b)	1942	10153	7405	109
H(21a)	3411	11774	8361	137
H(21b)	2742	12167	7842	137
H(23a)	4058	13875	8018	128
H(23b)	4758	13721	8664	128
H(24a)	5889	15049	8130	120
H(24b)	5596	13983	7408	120
H(26a)	7743	15541	8927	94
H(26b)	6680	14937	9243	94
H(27a)	7415	13590	9332	71
H(27b)	8277	14853	9831	71
H(31)	11363	12831	8545	82
H(33)	9859	12371	10243	84
H(34)	8800	13404	10025	75
H(35)	7717	8167	6432	57
H(37)	6503	7164	8119	72
H(38)	4878	7537	7852	69
H(39a)	11350	11681	9988	119
H(39b)	12067	12028	9405	119
H(42)	12600	10695	9534	89
H(43)	13167	9164	9299	95
H(44)	11848	7316	8583	92
H(45)	10007	6961	7943	90
H(48a)	8671	7306	7109	71
H(48b)	8189	6897	7753	71
H(49)	8910	12344	6176	59
H(50)	10248	11521	6014	66
H(51)	10452	10438	6750	69
H(52)	9332	10176	7623	58
H(55)	8521	10317	8542	69
H(56)	7232	10001	9323	81
H(57)	5660	10511	9216	82
H(58)	5334	11203	8251	73
H(59a)	6076	10834	6774	58
H(59b)	5949	11893	7324	58
H(60a)	7913	12996	7551	60
H(60b)	7402	12537	6693	60

4.4 REFERENCES

1. See chapter 3.
2. G.M. Sheldrick, SHELXTL, An integrated system for solving, refining, and displaying crystal structures from diffraction data, University of Göttingen, Federal Republic of Germany, 1981.
3. M.A. Bush, and M.R. Truter, J. Chem. Soc., Perkin 2, 1972, 345.

4a. H.M. Colquhoun, E.P. Gooding, J.M. Maud, J.F. Stoddart, D.J. Williams and J.B. Wolstenholme, J. Chem. Soc., Chem. Commun., 1983, 1140.

H.M. Colquhoun, E.P. Gooding, J.M. Maud, J.F. Stoddart, D.J. Williams, J.B. Wolstenholme, J.Chem. Soc. Perkin Trans. 2, 1985, 607.

b. See chapter 2.

c. J. E. Derry, and T. A. Hamor, Nature, 1969, 221, 464.

d. P.D. Sullivan, and M.L. Williams, J. Am. Chem. Soc., 1972, 98, 1711.

e. T. Sundaresan, and S.C. Wallwork, Acta. Cryst., 1972, B28, 3065.

5. R.Foster, 'Organic Charge-Transfer Complexes,' Academic Press, London, 1969.
6. R. Taylor, and O. Kennard, Acc. Chem. Res., 1984, 17, 326.
7. F.H. Kohnke, and J.F. Stoddart, J. Chem. Soc., Chem. Commun., 1985, 314.
8. B.L. Allwood, F.H. Kohnke, J.F. Stoddart, and D.J. Williams, Angew. Chem. Int. Ed. Engl., 1985, 24, 581.

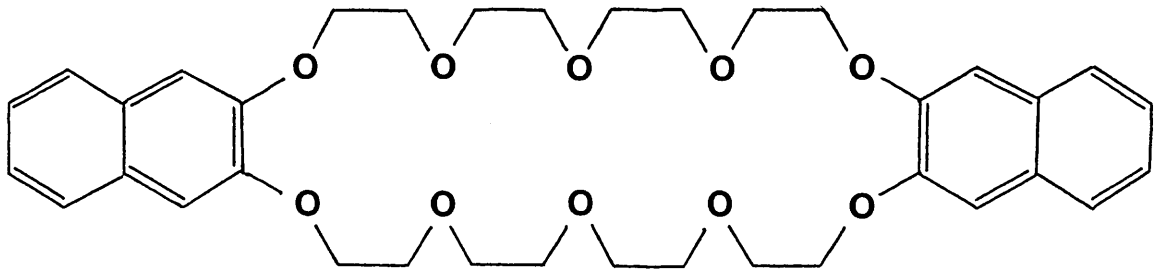
CHAPTER 5

The crystal structure of the complex of 7,8,10,11,13,14,16,17,26,27, 29,30,32,33,35,36-hexadecahydrodinaptho[2,3-b:2',3'-q][1,4,7,10,13,16, 19,22,25,28]decaoxacyclotricontin (Dinaptho-30-Crown-10) with diquat.

5.1 INTRODUCTION

So far[1] with the aid of X-ray structure analysis we have been able to design molecular receptors for diquat which have been successful in showing enhanced complex stability in solution. However, the relative importance of the various weak intermolecular forces within the complexes e.g. charge transfer, dipole-pole and C-H...O interactions has still to be addressed.

In order to try to investigate the relative importance of charge transfer versus the other forms of interactions, we complexed diquat with DN30C10 (7). This molecule contains two 2,3 naptho-rings and thus a more extended π-electron rich system than its dibenzo counterpart. The crystal structure analysis of [7.diquat] has been carried out to ascertain whether the mode of binding of the diquat dication would be affected by the extended π-system. The stability constant of the 1:1 complex formed in solution will also be discused.



7

5.2 EXPERIMENTAL

Orange crystals of [7.diquat][PF_6]$_2$[H_2O]$_{0.5}$ were obtained from a

solution of [7.diquat][PF_6]$_2$ in CH_2Cl_2 by vapour diffusion with n-pentane/n-heptane. A crystal of dimensions 0.30 x 0.43 x 0.73 mm was used for unit cell and intensity measurements.

Crystal data: $C_{36}H_{44}O_{10}.C_{12}H_{12}N_2.P_2F_{12}.(0.5)H_2O$, M = 1120, monoclinic, a = 22.353(5), b = 11.005(4), c = 22.423(6) Å, β = 104.00(2)°, U = 5352 Å^3, space group $I2/c$ (body-centred cell chosen because C-face-centred cell gave β = 128.1°), Z = 4 (complex possesses a crystallographic 2-fold axis), D_c = 1.39 g cm^{-3}, $F(000)$ = 2324, μ(Cu-K_α) = 16.05 cm^{-1}.

Refined unit-cell parameters were obtained by centering 20 reflections on a Nicolet R3m diffractometer. 3594 unique reflections ($\theta < 58°$) were measured with Cu-K_α radiation (graphite monochromator) using the omega-scan routine. Of these 2996 had $|F_o| > 3\sigma(|F_o|)$ and were considered to be observed. The net count of two reflections, the 6 -1 -3 and the -1 1 -6, measured as references every 50 reflections did not alter significantly during the data collection indicating that no deterioration of the crystal had occurred. The data were brought to a uniform arbitrary scale by the use of these reflections and Lorentz and polarisation corrections were applied.

The structure was solved by direct methods. A starting set consisting of 2 origin defining reflections together with a further 8 automatically selected terms was used. The initial phase refinement (256 permutations) was with 200 E's > 1.64 using 1765 TPR. This was expanded to 414 probable phases with E's > 1.64 using 2484 TPR. The

figures of merit for the best phase solution were NQEST = -0.228, RA(1) = 0.013, RA(2) = 0.173. Three cycles of ΔE-map recycling of this solution gave an R_E = 0.33 for 36 non-hydrogen atoms with 886 E's > 1.20. The remaining non-hydrogen atoms were found in subsequent ΔF-maps. A ΔF-map also revealed the presence of a 25% occupancy water molecule. Two discrete positions were located for both C(6) and C(8) and they were refined with occupancies of 40 and 60%. The non-hydrogen atoms were refined anisotropically. The carbon hydrogens were placed at calculated positions (C-H = 0.96 Å), assigned isotropic thermal parameters, $U(H) = 1.2\ U_{eq}(C)$, and allowed to ride on their parent carbon atoms. The protons on the partial occupancy water molecule were not located. Thermal motion was high in the PF_6 anion and the group was refined as a rigid body.

A damped refinement (due to instability in refinement of parameters of C6 and C6+) using F magnitudes was by block-cascade full-matrix least squares (346 variable parameters) and converged to R = 0.116, R_w = 0.146, $[w^{-1} = \sigma^2(F) + 0.0022F^2]$. The largest parameter shift/e.s.d. was 0.221, the mean shift/e.s.d. was 0.029. The residual electron density in the final difference map was within -0.54 and 0.70 $e Å^{-3}$.

Computations were carried out on an Eclipse S140 computer using the SHELXTL[2] program system.

5.3 DISCUSSION

The final fractional atomic coordinates, anisotropic thermal parameters, bond lengths and bond angles for the non-hydrogen atoms are shown in Tables 5.1 -5.4. The positions and isotropic temperature factors of the hydrogen atoms are listed in Table 5.5.

The torsion angles associated with the 30-membered rings in [7.diquat] are shown beside the relevant C-C and C-O bonds in the skeletal drawing of the structure reproduced in figure 5.1 which also provides the details of the crystallographic numbering scheme. The torsional angles taking into account the minor occupancy positions for C(6) and C(8) are shown in table 5.6.

The 1:1 [7.diquat] complex possesses a crystallographic 2-fold axis coincident with the C_2 axis of the diquat dication.

The receptor DN30C10 adopts a sugar-tong conformation in order to encapsulate the diquat dication. The torsion angles for the 30 membered ring, with the exception of the torsion angle about the C(9)-C(10) bond which changes significantly in magnitude, are similar to those in [6.diquat][1c].

The dihedral angle between the two pyridinium rings in the diquat dication is 16^{o}, which is in agreement with previously observed values[1,3].

Interestingly the diquat dication is inserted deeply into the receptor cleft. The complex retains the characterictic[1] alignment

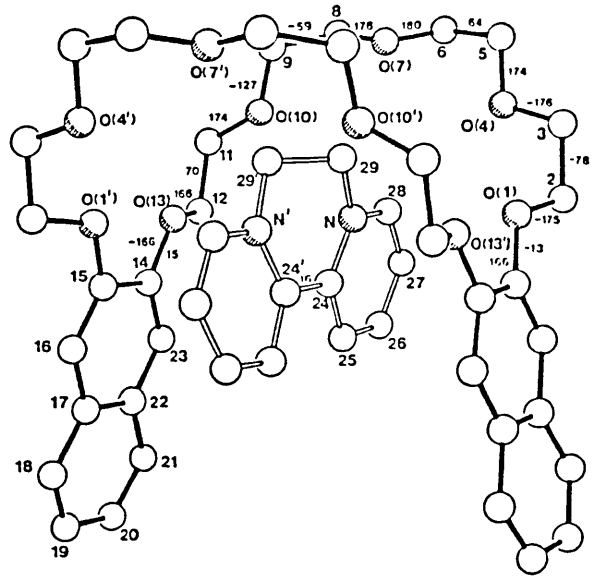


Figure 5.1. The skeletal representation of the solid-state structure of [7.diquat].

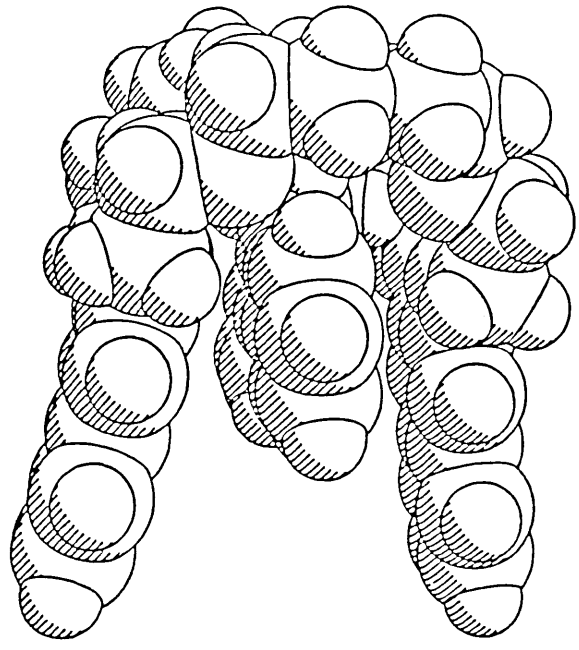


Figure 5.2. The space-filling representation of the solid-state structure of [7.diquat].

between the aryl oxygens [O(1) and O(13), and O(1') and O(13') atoms] and the bipyridinium nitrogens [N and N', respectively] O(1)...N 3.20, O(13)...N 3.62 Å, O(1)...N...O(16) 178°.

The distance of 3.4 Å between one the mean planes of the naptho-rings and nearest overlapping atom of the bipyridinium dication, C(24), is ideal for charge transfer[4]. It should be noted that the two naptho-groups are not parallel but have a 22° splay angle between them. The closest interatomic contact between atoms of the naptho rings is 7.0 Å between C(14) and C(14').

The complex has two potential C-H...O interaction [see table 5.7] between an acidic proton on the diquat, H(29), and a polyether oxygen, O(13'), of the host. There are 12 contacts of less than 3.4 Å between the diquat and the polyether chains oxygens of the host which could enhance electrostatic stabilisation of the complex.

There are no significant contacts of less than normal van der Waals distances between symmetry related DN30C10 receptors. From observation of the stereo-pair packing diagram (figure 5.3) it can clearly been seen that there are no charge transfer interactions between adjacent DN30C10 receptors. The closest contact of the partial occupancy water molecule O(30) to the complex is 3.15 Å to a symmetry related C(8+). This water molecule is probably disordered around the two-fold axis as there is only 1.76 Å between water molecules across this axis. There is the possibility of a very weak hydrogen bond

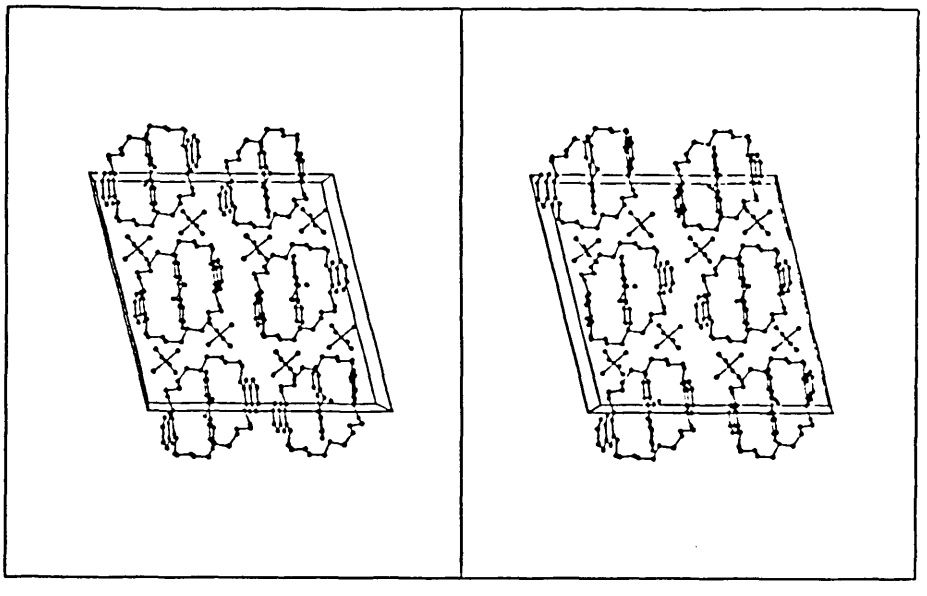


Figure 5.3. The stereo-pair representation of the packing of the unit cell contents of [7.diquat][PF_6]$_2$(0.5)H_2O.

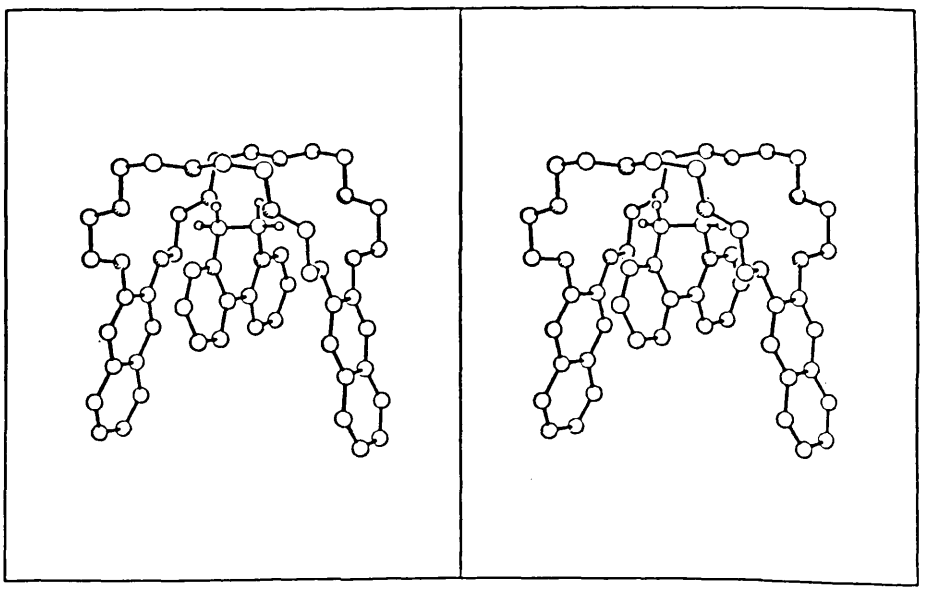


Figure 5.4. The stereo-pair representation of the solid-state structure of [7.diquat].

TABLE 5.6. The torsion angles (°) associated with the partial occupany atoms C6+ and C8+ in [7.diquat].

C3 O4 C5 C6+	-135
O4 C5 C6+ O7	-41
C5 C6+ O7 C8+	180
C6+ O7 C8+ C9	170
O7 C8+ C9 O10	58
C8+ C9 O10 C11	175

TABLE 5.7. Selected host-guest contact distances, and relevant hydrogen contact distances and angles where appropriate, in order of increasing $X^a...O$ distance for [7.diquat].

$X^a...O$	$R(X^a...O)$ (Å)	$R(H...O)$ (Å)	$\psi(°)^b$	$\theta(°)^c$
C(28)-O(4)	3.08			
C(28)-O(1)	3.12			
N -O(10)	3.20			
C(29)-O(13')	3.29	2.45	33	145
C(28)-O(10)	3.33			
C(29)-O(10)	3.38			
N -O(1)	3.40			

[a] Carbon or Nitrogen atom of the diquat dication.
[b] Angles between COC planes and HO vectors.
[c] C-H...O angles.

between F(1) and another symmetry related C(8+); C(8+)...F(1) 3.15, H(8b+)...F(1) 2.27 Å, C(8+)-H(8b+)...F(1) 151°, though this short interaction should be treated with caution as it is between a fluorine atom undergoing considerable anisotropic thermal motion and a partial occupancy carbon atom of the host.

It appears that an optimising of the dipole-pole N...O interactions is preferred by the diquat dication to an increase in charge transfer interactions which could be obtained by increasing its overlap with the extended π-electron rich naptho groups of the host.

The alignment of the diquat nitrogens and the catechol oxygens though consistent with that observed in previous diquat complexes is in striking contrast to the geometry observed for DN30C10 complex with $[Pt(bipy)(NH_3)_2]^{5}$. In this latter complex the bipyridyl moiety is slewed dramatically with respect to the two naptho groups (see figure 5.5) thus achieving increased overlap with the extended π-electron rich systems c.f. its complex with DB30C10[6]. Interestingly there is an almost linear alignment between one aryl oxygen on each of the two naptho groups [O(1) and O(13)] with the Pt dication; Pt...O(1) 3.58, Pt...O(13) 3.55 Å, O(1)...Pt...O(13) 156°. The two ammine ligands as observed previously straddle one of the polyether chains of the 30 membered ring with both nitrogens within hydrogen bond distances of O(4) and O(10).

Clearly, in both [7.$Pt(bipy)(NH_3)_2$] and [7.diquat] coulombic forces, including hydrogen bonding, dipole-pole and charge transfer

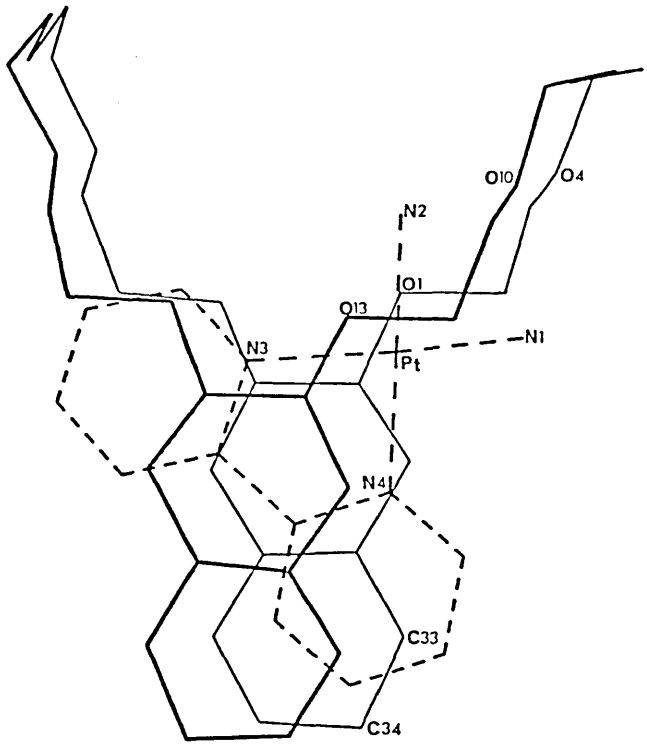


Figure 5.5. Side-on view (view normal to mean plane of bipyridine ligand) of the skeletal representation of the solid-state structure of [7.Pt(bipy)$(NH_3)_2$].

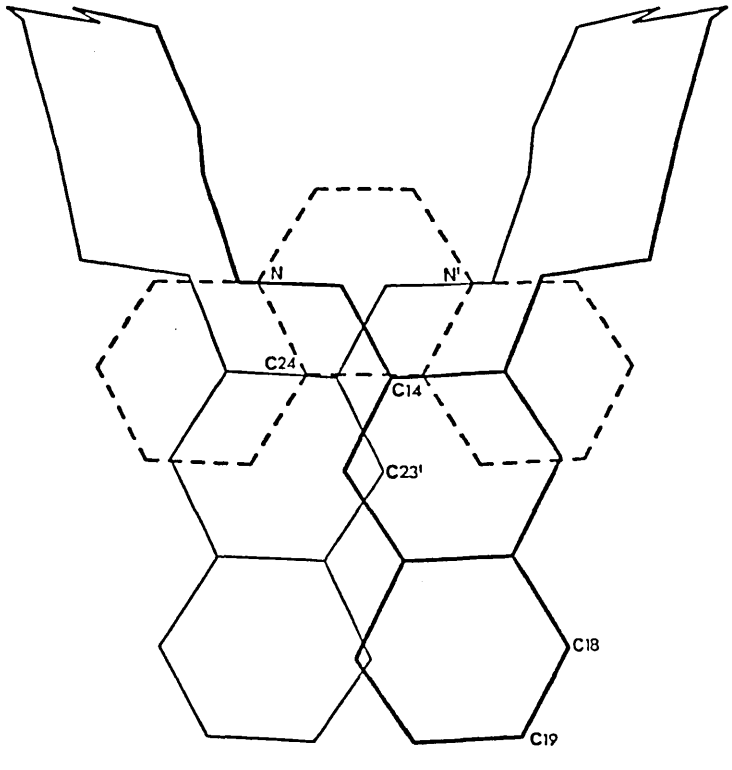


Figure 5.6. Side-on view (view normal to mean plane of diquat dication) of the skeletal representation of the solid-state structure of [7.diquat].

interactions, play significant roles in the binding of the dications. In [7.Pt(bipy)$(NH_3)_2$], these interactions are optimised by overlap of the π-electron rich naptho rings with the π-electron deficient bipyridinium ring system. The net result is the observed slewing of the [Pt(bipy)$(NH_3)_2$] dication within the cavity of the DN30C10 receptor. By contrast, in [7.diquat], the formal positive charges reside mainly in the region of the two nitrogen atoms in the dication and so the geometrical requirement for optimising the electrostatic interactions is an alignment of the N and N' with O(1) and O(13), and O(1') and O(13'), respectively. The near coincidence in the separation between N and N'(2.8 Å) in the dication with the distance between the two pairs of aryl oxygens (2.6 Å) in the DN30C10 results in the near colinear alignment and planarity of O(1)-N-O(13) and O(1')-N'-O(13'). However, this constraint produces a shearing (see figure 5.6) of the naptho rings with respect to each other, whilst in the [7.Pt(bipy)$(NH_3)_2$] adduct the two napho rings are nearly eclipsed. It is possible this shearing increasing charge transfer by allowing a greater portion of the dication to overlap with the naptho ring systems whilst still retaining the dipole-pole interactions.

Derived ΔG^o's from the observation[1d] of charge transfer absorption bands in solution indicate that the diquat complex with DB30C10 has enhanced charge transfer interactions and complex stability compared to the corresponding DN30C10 complex (ΔG^o = -4.92 and -4.29 Kcal mol^{-1} respectively). There is also strong evidence from ^{1}H.n.m.r spectroscopy that the distinctly different binding geometries for [7.diquat] and [7.Pt(bipy)$(NH_3)_2$] are also retained in solution. In particular the the ^{1}H resonaces due to C(18)H and C(19)H of the

naphtho-groups are virtually unaffected ($\Delta\delta$ = -0.12 and 0.00 ppm respectively) by adduct formation with diquat, in keeping with the observed solid-state structure. Interactions with $[Pt(bipy)(NH_3)_2]$ however leads to substantial upfield shifts of these resonances ($\Delta\delta$ = 0.60 and 0.27 ppm) as a consequence of ring-current shielding by the bipyridine ligand which is in close proximity to C(33)H and C(34)H.

The crystal structure of [7.diquat] has clearly indicated that the the dipole-pole interactions predominate over charge transfer interactions. This will have a marked influence on the future design and subsequent synthesis of hosts for diquat and paraquat.

TABLE 5.1. Coordinates ($\times 10^4$) and temperature factors ($Å^2 \times 10^3$)

atom	x	y	z	U
O(1)	8807(2)	10861(3)	5883(2)	72(1)*
C(2)	8154(3)	11047(5)	5670(3)	80(1)*
C(3)	8026(3)	12335(6)	5725(3)	90(2)*
O(4)	8041(3)	12658(4)	6321(2)	109(1)*
C(5)	7880(4)	13862(7)	6408(3)	113(2)*
C(6)	7850(9)	14011(13)	7031(7)	156(2)*
C(6')	8223(12)	14457(15)	6868(9)	138(2)*
O(7)	8429(4)	13831(5)	7428(3)	172(2)*
C(8)	8336(7)	14005(11)	8006(6)	127(2)*
C(8')	8802(12)	14507(15)	7922(9)	134(2)*
C(9)	8864(4)	13778(7)	8473(4)	127(2)*
O(10)	9117(2)	12600(4)	8487(2)	102(1)*
C(11)	9198(3)	12049(6)	9051(3)	94(2)*
C(12)	9404(3)	10777(6)	9043(3)	83(1)*
O(13)	10012(2)	10744(4)	8982(2)	85(1)*
C(14)	10316(2)	9647(5)	9099(2)	67(1)*
C(15)	10977(2)	9722(5)	9180(2)	60(1)*
C(16)	11320(2)	8704(5)	9318(2)	65(1)*
C(17)	11047(3)	7548(5)	9381(3)	69(1)*
C(18)	11398(3)	6486(6)	9554(3)	87(2)*
C(19)	11127(3)	5420(6)	9624(4)	106(2)*
C(20)	10487(4)	5341(6)	9518(4)	107(2)*
C(21)	10135(3)	6332(6)	9447(3)	96(2)*
C(22)	10406(3)	7491(5)	9283(3)	71(1)*
C(23)	10043(2)	8548(5)	9140(3)	71(1)*
N	9357(2)	10776(4)	7340(2)	67(1)*
C(24)	9659(3)	9687(5)	7456(2)	67(1)*
C(25)	9325(3)	8627(6)	7481(3)	86(1)*
C(26)	8702(3)	8690(7)	7384(3)	104(2)*
C(27)	8408(3)	9791(7)	7266(3)	104(2)*
C(28)	8741(3)	10801(7)	7259(3)	93(2)*
C(29)	9696(3)	11881(5)	7273(3)	74(1)*
P(1)	6912(1)	7516(1)	6180(1)	81(1)*
F(1)	6413(1)	7996(1)	6477(1)	189(2)*
F(2)	6450(1)	7507(1)	5556(1)	232(2)*
F(3)	6731(1)	6217(1)	6295(1)	204(2)*
F(4)	7092(1)	8815(1)	6065(1)	232(2)*
F(5)	7372(1)	7528(1)	6805(1)	286(2)*
F(6)	7409(1)	7035(1)	5881(1)	254(2)*
O(30)	5314(13)	9291(20)	7815(13)	185(2)*

* Equivalent isotropic U defined as one third of the trace of the orthogonalised U_{ij} tensor

TABLE 5.2. Bond lengths (Å)

O(1)-C(2)	1.437(6)	O(1)-C(15a)	1.362(6)
C(2)-C(3)	1.457(9)	C(3)-O(4)	1.376(8)
O(4)-C(5)	1.399(9)	C(5)-C(6)	1.422(18)
C(5)-C(6')	1.303(20)	C(6)-O(7)	1.396(18)
C(6')-O(7)	1.409(20)	O(7)-C(8)	1.373(16)
O(7)-C(8')	1.423(19)	C(8)-C(9)	1.397(15)
C(8')-C(9)	1.451(21)	C(9)-O(10)	1.412(9)
O(10)-C(11)	1.376(8)	C(11)-C(12)	1.475(10)
C(12)-O(13)	1.398(7)	O(13)-C(14)	1.379(7)
C(14)-C(15)	1.448(7)	C(14)-C(23)	1.368(8)
C(15)-C(16)	1.350(7)	C(15)-O(1a)	1.362(6)
C(16)-C(17)	1.432(8)	C(17)-C(18)	1.409(8)
C(17)-C(22)	1.397(8)	C(18)-C(19)	1.348(10)
C(19)-C(20)	1.394(11)	C(20)-C(21)	1.345(10)
C(21)-C(22)	1.434(9)	C(22)-C(23)	1.410(8)
N-C(24)	1.370(7)	N-C(28)	1.345(8)
N-C(29)	1.460(7)	C(24)-C(25)	1.393(8)
C(24)-C(24a)	1.491(11)	C(25)-C(26)	1.359(10)
C(26)-C(27)	1.372(11)	C(27)-C(28)	1.340(11)
C(29)-C(29a)	1.486(10)	P(1)-F(1)	1.525
P(1)-F(2)	1.525	P(1)-F(3)	1.524
P(1)-F(4)	1.524	P(1)-F(5)	1.525
P(1)-F(6)	1.524		

TABLE 5.3. Bond Angles (deg.)

C(2)-O(1)-C(15a)	116.9(4)	O(1)-C(2)-C(3)	108.4(5)
C(2)-C(3)-O(4)	112.0(5)	C(3)-O(4)-C(5)	115.8(5)
O(4)-C(5)-C(6)	108.7(8)	O(4)-C(5)-C(6')	117.7(10)
C(5)-C(6)-O(7)	110.8(14)	C(5)-C(6')-O(7)	117.6(13)
C(6)-O(7)-C(8)	104.8(11)	C(6')-O(7)-C(8')	116.2(11)
O(7)-C(8)-C(9)	112.9(12)	O(7)-C(8')-C(9)	106.9(13)
C(8)-C(9)-O(10)	116.3(8)	C(8')-C(9)-O(10)	118.8(11)
C(9)-O(10)-C(11)	112.8(6)	O(10)-C(11)-C(12)	112.2(6)
C(11)-C(12)-O(13)	109.8(5)	C(12)-O(13)-C(14)	116.7(5)
O(13)-C(14)-C(15)	114.5(5)	O(13)-C(14)-C(23)	125.4(5)
C(15)-C(14)-C(23)	120.0(5)	C(14)-C(15)-C(16)	119.1(5)
C(14)-C(15)-O(1a)	114.5(4)	C(16)-C(15)-O(1a)	126.3(5)
C(15)-C(16)-C(17)	121.9(5)	C(16)-C(17)-C(18)	122.8(5)
C(16)-C(17)-C(22)	118.0(5)	C(18)-C(17)-C(22)	119.2(5)
C(17)-C(18)-C(19)	121.2(6)	C(18)-C(19)-C(20)	120.4(6)
C(19)-C(20)-C(21)	120.2(7)	C(20)-C(21)-C(22)	121.2(6)
C(17)-C(22)-C(21)	117.8(5)	C(17)-C(22)-C(23)	120.7(5)
C(21)-C(22)-C(23)	121.5(5)	C(14)-C(23)-C(22)	120.2(5)
C(24)-N-C(28)	119.0(5)	C(24)-N-C(29)	120.3(5)
C(28)-N-C(29)	120.6(5)	N-C(24)-C(25)	119.8(5)
N-C(24)-C(24a)	117.8(3)	C(25)-C(24)-C(24a)	122.4(3)
C(24)-C(25)-C(26)	119.2(6)	C(25)-C(26)-C(27)	120.0(7)
C(26)-C(27)-C(28)	119.5(7)	N-C(28)-C(27)	122.4(7)
N-C(29)-C(29a)	110.0(4)	F(1)-P(1)-F(2)	89.9
F(1)-P(1)-F(3)	90.0	F(2)-P(1)-F(3)	90.0
F(1)-P(1)-F(4)	90.0	F(2)-P(1)-F(4)	90.0
F(3)-P(1)-F(4)	180.0	F(1)-P(1)-F(5)	89.9
F(2)-P(1)-F(5)	179.8	F(3)-P(1)-F(5)	90.1
F(4)-P(1)-F(5)	90.0	F(1)-P(1)-F(6)	179.8
F(2)-P(1)-F(6)	89.9	F(3)-P(1)-F(6)	90.0
F(4)-P(1)-F(6)	90.0	F(5)-P(1)-F(6)	90.3

TABLE 5.4. Anisotropic temperature factors ($Å^2 \times 10^3$)

atom	U_{11}	U_{22}	U_{33}	U_{23}	U_{13}	U_{12}
O(1)	55(2)	73(2)	84(2)	-9(2)	11(2)	6(2)
C(2)	73(2)	89(2)	73(2)	3(2)	6(2)	17(2)
C(3)	98(3)	92(2)	75(2)	4(2)	9(2)	28(2)
O(4)	151(2)	93(2)	81(2)	7(2)	23(2)	52(2)
C(5)	152(3)	90(2)	93(3)	9(2)	22(2)	60(2)
C(6)	263(3)	124(3)	98(3)	23(3)	80(3)	107(3)
C(6')	238(3)	85(3)	97(3)	26(3)	51(3)	82(3)
O(7)	273(3)	121(2)	96(2)	-20(2)	-8(2)	95(2)
C(8)	174(3)	86(3)	114(3)	-17(3)	20(3)	59(3)
C(8')	237(3)	71(3)	101(3)	14(3)	59(3)	24(3)
C(9)	168(3)	101(3)	97(3)	-31(2)	4(3)	25(3)
O(10)	130(2)	99(2)	71(2)	-5(2)	16(2)	36(2)
C(11)	86(2)	121(3)	76(2)	-10(2)	24(2)	21(2)
C(12)	67(2)	105(3)	76(2)	10(2)	18(2)	12(2)
O(13)	53(2)	92(2)	110(2)	29(2)	23(2)	7(2)
C(14)	61(2)	80(2)	58(2)	13(2)	11(2)	7(2)
C(15)	51(2)	83(2)	47(2)	6(2)	12(2)	-3(2)
C(16)	42(2)	90(2)	63(2)	2(2)	14(2)	2(2)
C(17)	67(2)	79(2)	63(2)	6(2)	22(2)	2(2)
C(18)	69(2)	92(2)	105(2)	3(2)	32(2)	10(2)
C(19)	111(3)	80(2)	142(3)	19(2)	56(2)	20(2)
C(20)	112(3)	69(2)	151(3)	4(2)	51(2)	-11(2)
C(21)	83(2)	100(3)	106(3)	15(2)	24(2)	-19(2)
C(22)	60(2)	86(2)	67(2)	5(2)	16(2)	-11(2)
C(23)	46(2)	90(2)	77(2)	15(2)	13(2)	-3(2)
N	70(2)	79(2)	54(2)	6(2)	17(2)	6(2)
C(24)	79(2)	71(2)	50(2)	1(2)	12(2)	-9(2)
C(25)	89(2)	75(2)	88(2)	6(2)	12(2)	-9(2)
C(26)	94(3)	116(3)	97(3)	6(2)	34(2)	-40(2)
C(27)	80(2)	153(3)	75(2)	19(2)	11(2)	-21(3)
C(28)	78(2)	124(3)	75(2)	7(2)	16(2)	25(2)
C(29)	92(2)	63(2)	69(2)	2(2)	23(2)	8(2)
P(1)	72(1)	88(1)	88(1)	0(1)	29(1)	-3(1)
F(1)	142(2)	225(3)	227(3)	-21(3)	98(2)	28(2)
F(2)	171(3)	394(3)	114(2)	25(3)	-0(2)	-34(3)
F(3)	171(3)	106(2)	329(3)	25(3)	50(3)	-29(2)
F(4)	216(3)	135(2)	343(3)	80(3)	63(3)	-40(2)
F(5)	191(3)	420(3)	178(3)	63(3)	-90(2)	-136(3)
F(6)	196(3)	310(3)	320(3)	-51(3)	186(2)	16(3)
O(30)	211(3)	157(3)	193(3)	1(3)	59(3)	41(3)

The anisotropic temperature factor exponent takes the form:

$$-2\pi^2(h^2a^{*2}U_{11} + \ldots + 2\,hka^*b^*U_{12}\cos\gamma^* + \ldots)$$

TABLE 5.5. Coordinates ($\times 10^4$) and temperature factors ($Å^2 \times 10^3$)

atom	x	y	z	U
H(2a)	8020	10800	5248	92
H(2b)	7941	10580	5916	92
H(3a)	7625	12513	5471	101
H(3b)	8330	12800	5586	101
H(5a)	7486	14042	6140	138
H(5b)	8185	14402	6317	138
H(5a')	7889	14301	6039	138
H(5b')	7468	13856	6462	138
H(6a)	7713	14818	7084	188
H(6b)	7567	13431	7122	188
H(6a')	7985	15146	6944	168
H(6b')	8579	14738	6741	168
H(8a)	8217	14836	8035	160
H(8b)	8016	13476	8055	160
H(8a')	9207	14648	7856	168
H(8b')	8616	15269	7977	168
H(9a)	8755	13911	8856	152
H(9b)	9175	14349	8430	152
H(9a')	8455	13689	8566	152
H(9b')	9115	14224	8808	152
H(11a)	9503	12494	9345	106
H(11b)	8814	12064	9171	106
H(12a)	9141	10357	8703	99
H(12b)	9382	10388	9420	99
H(16)	11759	8757	9378	72
H(18)	11839	6525	9624	96
H(19)	11376	4710	9747	116
H(20)	10296	4578	9567	120
H(21)	9695	6262	9266	105
H(23)	9602	8494	9070	79
H(25)	9533	7860	7566	102
H(26)	8466	7966	7396	115
H(27)	7967	9836	7190	121
H(28)	8533	11570	7195	103
H(29a)	9759	11918	6865	92
H(29b)	9463	12576	7344	92

5.4 REFERENCES

1a. See chapter 2.

b. See chapter 3.

c. See chapter 4.

d. H.M. Colquhoun, E.P. Gooding, J.M. Maud, J.F. Stoddart, D.J. Williams and J.B. Wolstenholme, J. Chem. Soc., Chem. Commun., 1983, 1140.

H.M. Colquhoun, E.P. Gooding, J.M. Maud, J.F. Stoddart, D.J. Williams, J.B. Wolstenholme, J.Chem. Soc. Perkin Trans. 2, 1985, 607.

2. G.M. Sheldrick, SHELXTL, An integrated system for solving, refining, and displaying crystal structures from diffraction data, University of Göttingen, Federal Republic of Germany, 1981.

3. J. E. Derry, and T. A. Hamor, Nature, 1969, 221, 464.

P.D. Sullivan, and M.L. Williams, J. Am. Chem. Soc., 1972, 98, 1711.

T. Sundaresan, and S.C. Wallwork, Acta. Cryst., 1972, B28, 3065.

4. R. Foster, 'Organic Charge-Transfer Complexes,' Academic press, London, 1969.

5. A.M.Z. Slawin, and D.J. Williams, unpublished results.

6. H.M. Colquhoun, J.F. Stoddart, D.J. Williams, J.B. Wolstenholme and R. Zarzycki, Angew. Chem. Int. Ed. Engl., 1981, 20, 1051.

H.M. Colquhoun, S.M. Doughty, J.M. Maud, J.F. Stoddart, D.J. Williams and J.B. Wolstenholme, Isr. J. Chem., 1985, 25, 15.

CHAPTER 6

The crystal structures of 1,4,7,10,13,20,23,26,29,32-decaoxa[13.13]metacyclophane (bismetaphenylene-32-crown-10) and its complex with diquat.

6.1 INTRODUCTION

The X-ray crystal structure[1] of the complex formed between DN30C10 and diquat has indicated that the electrostatic dipole-pole interactions probably play a more important role in complex binding than those due to charge transfer. In both DB30C10 and DN30C10 the separation of the catechol oxygens is *ca.* 2.6 Å. This is close to the N...N separation in diquat *ca.* 2.8 Å and so is ideally suited to enable both nitrogens of the diquat dication to achieve two simultaneous linear O...N...O dipole-pole interactions.

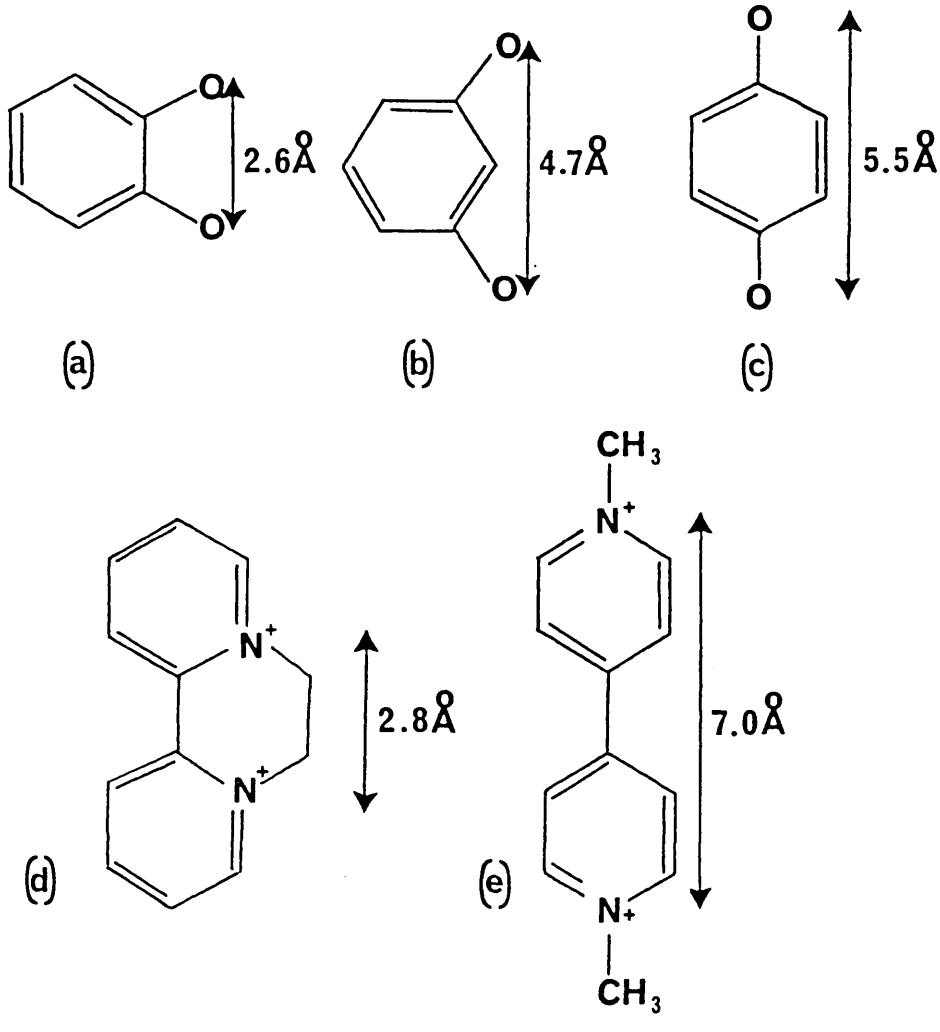
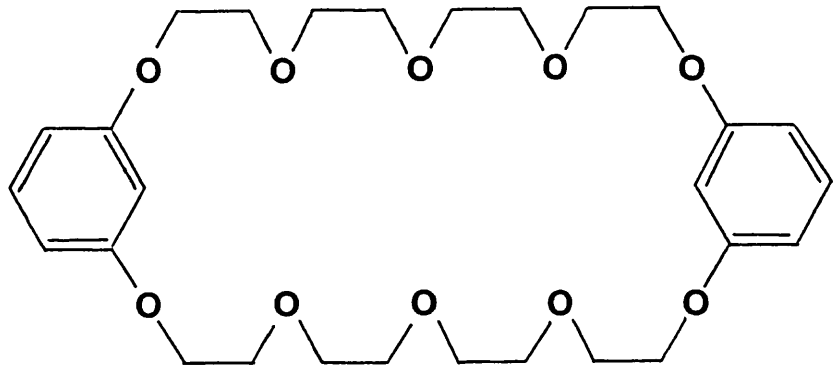


Figure 6.1. The separation between (i) the aryl oxygens in (a) catechol, (b) resorcinol and (c) quinol; (ii) the nitrogens atoms in (d) diquat and (e) paraquat.

To date we have been unsuccessful in complexing paraquat with either DB30C10 or any of the subsequently synthesised diquat receptors[1,2]. This could be due to the inability of paraquat to form two linear O...N...O interactions with the hosts to enable complexation.



8

It was therefore decided to attempt to complex diquat and paraquat with 8, a receptor containing resorcinol units instead of catechol units. The separation of the oxygens in the resorcinol unit is ca. 4.7 Å. This distance is almost half-way between the N...N separation in diquat (ca. 2.8 Å) and paraquat (ca. 7.0 Å). The opportunity for both nitrogens of either diquat or paraquat to form two linear dipole-pole interactions is thus diminished though the potential for charge transfer is retained. Solution studies indicated that for the first time separate complexation of both diquat and paraquat had been achieved using 8 as a receptor. Unfortunately the quality of the crystals purporting to be of [8.paraquat] was so poor that a single crystal X-ray study was not possible.

The X-ray crystal structure analyses of the uncomplexed receptor 8 and of [8.diquat][PF_6]$_2$ have been carried out. The aim was to discover the conformation of the 32 membered macrocycle and to investigate its binding of the diquat dication. The stability constant of the 1:1 complex formed in solution will also be discussed.

6.2 EXPERIMENTAL

Clear colourless crystals of 8 were obtained from a solution of 8 in acetone by vapour diffusion with n-pentane. A crystal of dimensions 0.50 x 0.50 x 0.50 mm was used for unit cell and intensity measurements.

Crystal data: $C_{28}H_{40}O_{10}$, M = 537, monoclinic, a = 7.026(2), b = 22.766(5), c = 8.977(3) Å, β = 96.04(3)°, U = 1428 Å^3, space group $P2_1/a$, Z = 2 (the receptor possesses a crystallographic centre of symmetry), D_c = 1.25 g cm^{-3}, F(000) = 576, μ(Cu-K_α) = 7.44 cm^{-1}.

Refined unit-cell parameters were obtained by centering 18 reflections on a Nicolet R3m diffractometer. 1463 unique reflections ($\theta < 50°$) were measured with Cu-K_α radiation (graphite monochromator) using the omega-scan routine. Of these 1425 had $|F_o| > 3\sigma(|F_o|)$ and were considered to be observed. The net count of two reflections, the -1 1 -1 and the 2 0 3, measured as references every 50 reflections did not alter significantly during the data collection indicating that no deterioration of the crystal had occurred. The data were brought to a uniform arbitrary scale by the use of these reflections and Lorentz and polarisation corrections were applied.

The structure was solved by direct methods. An initial starting set comprising three origin defining reflections together with a further 5 automatically selected terms was used. The initial phase expansion (32 permutations) was with 192 $\underline{E}$'s > 1.2 using 1986 TPR. This was subsequently expanded to 359 probable phases with $\underline{E}$'s > 1.2 using 3942 TPR. The figures of merit for the best phase solution were NQEST = -0.563, RA(1) = 0.031, RA(2) = 0.073. This solution revealed plausible positions for all the non-hydrogen atoms in the structure. The non-hydrogen atoms were refined anisotropically. The methylene and phenyl hydrogens were placed at calculated positions (C-H = 0.96 Å), assigned isotropic thermal parameters, $\underline{U}(H) = 1.2\ \underline{U}_{eq}(C)$, and allowed to ride on their parent carbon atoms.

Refinement using $\underline{F}$ magnitudes was by block-cascade full-matrix least squares (172 variable parameters) and converged to $\underline{R}$ = 0.050, $\underline{R}_w$ = 0.068, $[w^{-1} = \sigma^2(\underline{F}) + 0.0097\underline{F}^2]$. The largest parameter shift/e.s.d. was 0.046, the mean shift/e.s.d. was 0.011. The residual electron density in the final difference map was within -0.28 and 0.17 $eÅ^{-3}$.

Yellow crystals of [8.diquat][PF_6]$_2$.$(CH_3)_2O$ were obtained by recrystallisation from acetone. A crystal of dimensions 0.13 x 0.23 x 0.45 mm was used for unit cell and intensity measurements.

Crystal data: $C_{28}H_{40}O_{10}.C_{12}H_{12}N_2.P_2F_{12}.C_3H_6O$, triclinic, $\underline{a}$ = 10.431(3), $\underline{b}$ = 11.261(4), $\underline{c}$ = 22.279(7) Å, α = 82.05(3), β = 82.09(2), γ = 74.96(3)°. $\underline{U}$ = 2489 $Å^3$, space group $P\bar{1}$, $\underline{Z}$ = 2, $\underline{D}_c$ = 1.43 g cm^{-3},

$\underline{F}(000) = 1112$, $\mu(Cu\text{-}\underline{K}_\alpha) = 17.04$ cm^{-1}.

Refined unit-cell parameters were obtained by centering 18 reflections on a Nicolet R3m diffractometer. 5117 unique reflections ($\theta < 50^o$) were measured with Cu-$\underline{K}_\alpha$ radiation (graphite monochromator) using the omega-scan routine. Of these 4378 had $|\underline{F}_o| > 3\sigma(|\underline{F}_o|)$ and were considered to be observed. The net count of two reflections, the 2 3 3 and the 2 2 4, measured as references every 50 reflections did not alter significantly during the data collection indicating that no deterioration of the crystal had occurred. The data were brought to a uniform arbitrary scale by the use of these reflections and Lorentz and polarisation corrections were applied.

The structure was solved by direct methods. An initial starting set comprising three origin defining reflections together with a further 8 automatically selected terms was used. The initial phase expansion (256 permutations) was with 200 $\underline{E}$'s > 2.1 using 556 TPR. This was subsequently expanded to 407 probable phases with $\underline{E}$'s > 1.84 using 993 TPR. The figures of merit for the best phase solution were NQEST = -0.581, RA(1) = 0.009, RA(2) = 0.044. This solution gave plausible positions for 68 of the non-hydrogen atom positions in the structure. The remaining non-hydrogen atoms were located from subsequent $\Delta\underline{F}$-maps, which also revealed the presence of an acetone molecule. The non-hydrogen atoms were refined anisotropically. The protons on the acetone molecule were not located. The methylene and phenyl hydrogens were placed at calculated positions (C-H = 0.96 Å), assigned isotropic thermal parameters, $\underline{U}(H) = 1.2\ \underline{U}_{eq}(C)$ and allowed to ride on their parent carbon atoms.

Refinement using $\underline{F}$ magnitudes was by block-cascade full-matrix least squares (632 variable parameters) and converged to $\underline{R}$ = 0.094, $\underline{R}_w$ = 0.116, $[w^{-1} = \sigma^2(\underline{F}) + 0.0014\underline{F}^2]$. The largest parameter shift/e.s.d. was 0.058, the mean shift/e.s.d. was 0.011. The residual electron density in the final difference map was within -0.46 and 0.67 $e\text{Å}^{-3}$.

All computations were carried out on an Eclipse S140 computer using the SHELXTL[3] program system.

6.3 DISCUSSION

The final fractional atomic coordinates, anisotropic thermal parameters, bond lengths and bond angles for the non-hydrogen atoms of $\underset{\sim}{8}$ and $[\underset{\sim}{8}.\text{diquat}][PF_6]_2(CH_3)_2O$ are shown in Tables 6.1 - 6.4 and 6.6 - 6.9 respectively. The positions and isotropic temperature factors for the hydrogen atoms are listed in Tables 6.5 and 6.10 respectively.

The torsion angles associated with the 32-membered rings in $\underset{\sim}{8}$ and $[\underset{\sim}{8}.\text{diquat}]$ and are shown beside the relevant C-C and C-O bonds in the skeletal drawings of the structures reproduced in figures 6.2 and 6.3 which also provides the details of the crystallographic numbering schemes.

The $\underline{X}$-ray structure of the free receptor $\underset{\sim}{8}$ reveals an unusually open conformation for the macrocyclic ring. Normally large

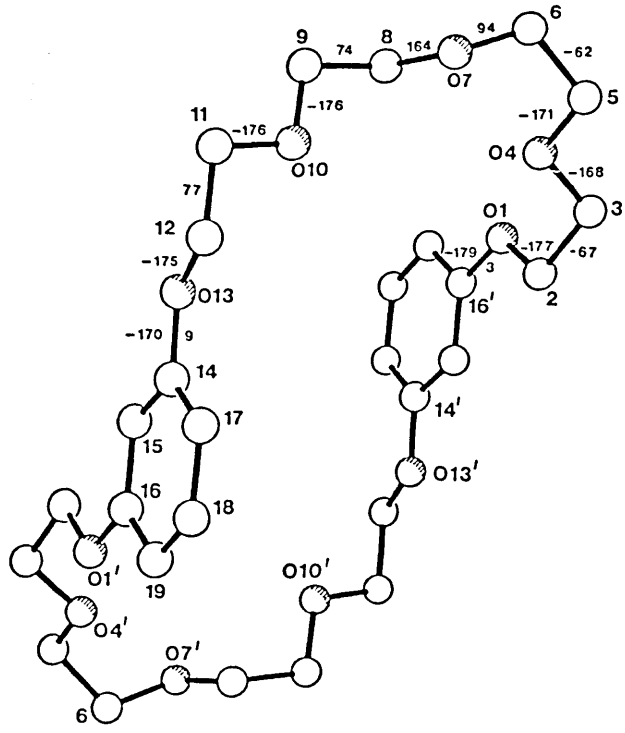


Figure 6.2. The skeletal representation of the solid-state structure of 8.

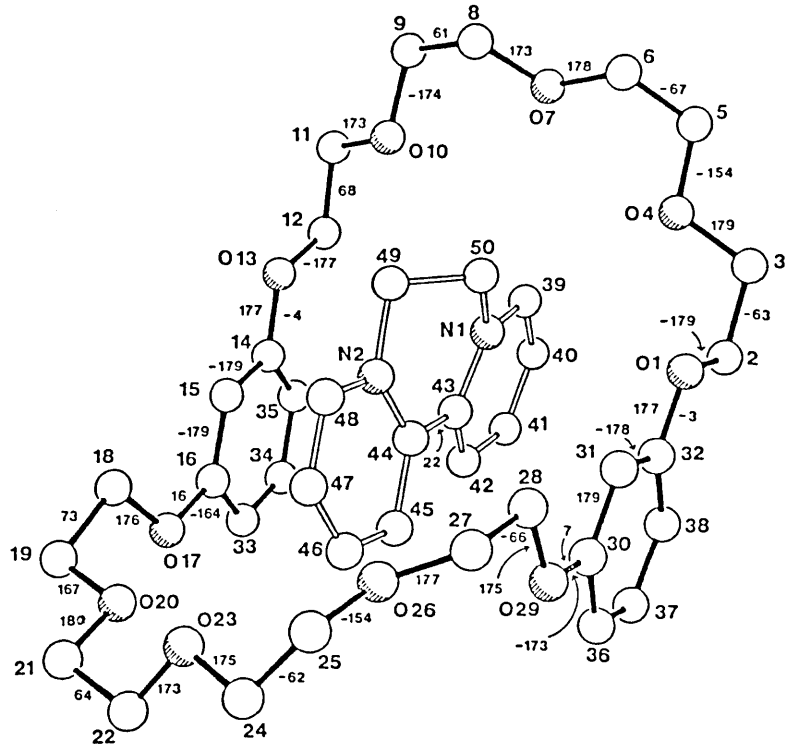


Figure 6.3. The skeletal representation of the solid-state structure of [8.diquat].

uncomplexed macrocycles[4] and uncomplexed natural neutral ionophore[5] rings have a tendency to collapse on themselves, i.e. they are self-filling. However, 8 possesses a large clear passage (figure 6.4) through the centre of the ring (approximate free pathway 4.9 x 7.8 Å).

The uncomplexed macrocycle 8 retains an 'all gauche' arrangement of its torsional angles, except for the C(6)-O(7) bond torsional angle which deviates significantly from an expected trans disposition.

The bond lengths and angles of the 32-membered ring are in agreement with previously published values for crown ethers[6].

Inspection of the crystal packing of 8 reveals that there are no contacts of other than normal van der Waals distances between symmetry related macrocycles.

The X-ray analysis of [8.diquat] reveals the diquat dication to be cradled between the approximately parallel resorcinol units in the receptor (3° between their mean planes and ~ 7 Å interplanar separation). The complexed receptor has an approximate mirror plane passing through O(7) and O(23) and parallel to the resorcinol rings, compared to a centre of symmetry in its uncomplexed form.

The dihedral angle between the pyridinium rings is 21.8(9)° which is in agreement with previously observed values[1,2,7].

There are some striking similarities in the mode of binding of diquat by 8, compared with that observed for DB30C10 and its

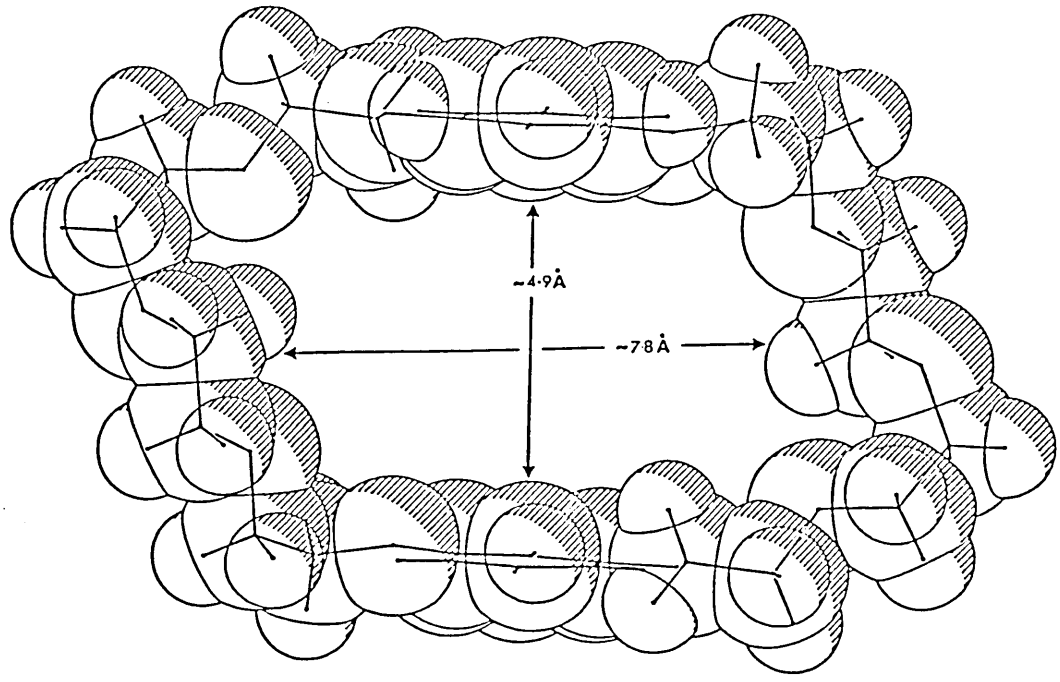


Figure 6.4. The space-filling representation of the solid-state structure of 8.

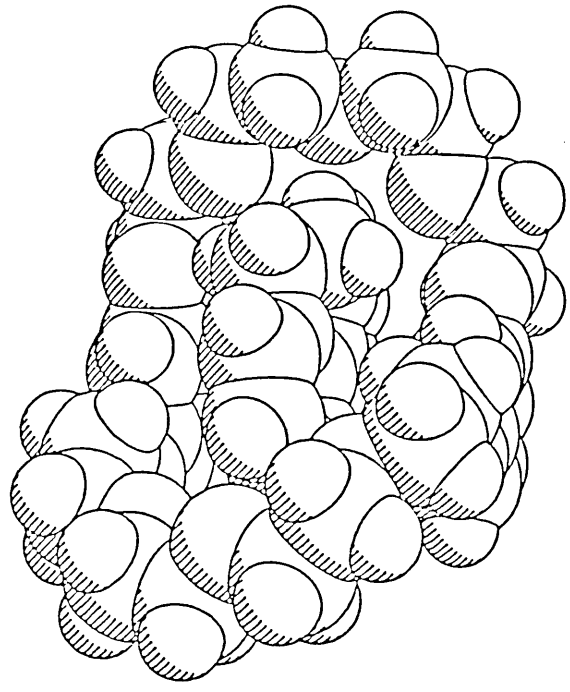


Figure 6.5. The space-filling representation of the solid-state structure of [8.diquat].

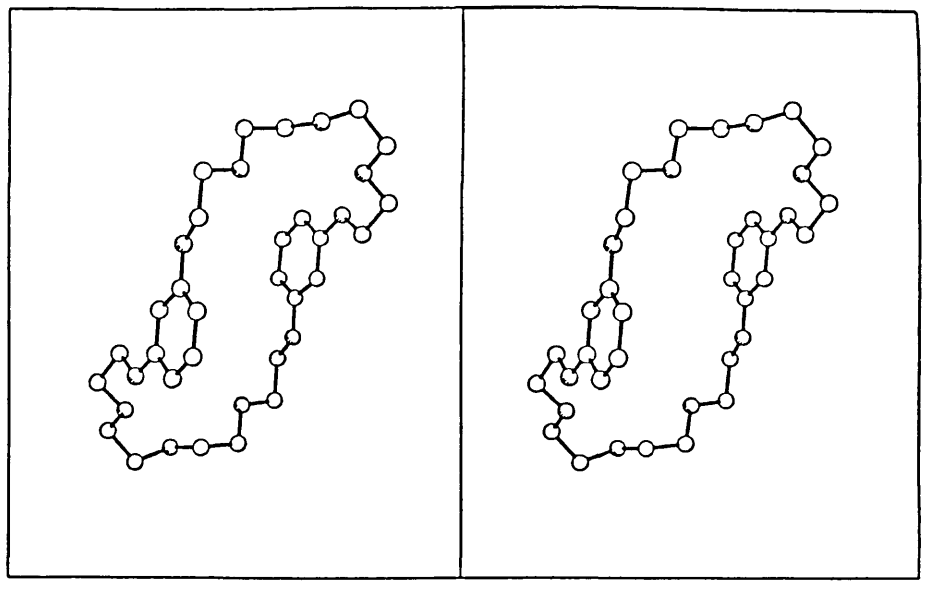


Figure 6.6. The stereo-pair representation of the solid-state structure of 8.

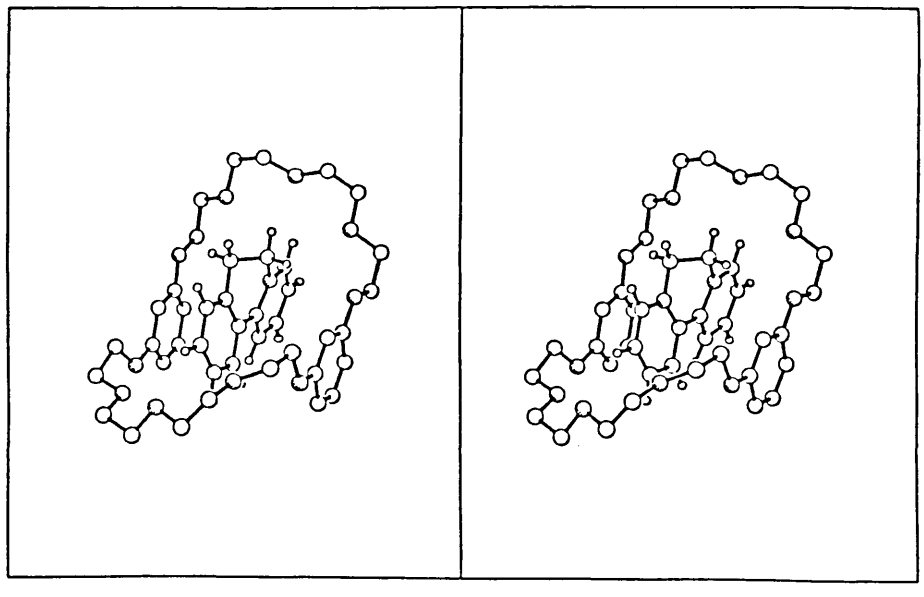


Figure 6.7. The stereo-pair representation of the solid-state structure of [8.diquat].

derivatives[1,2]. Again binding of the dication is by a combination of: C-H...O interactions [see table 6.11]; electrostatic interactions between one of the nitrogen atoms and two of the resorcinol oxygen atoms; charge transfer interactions between the π-electron-rich rescorcinol rings and the π-deficient bipyridinium dication. The distance of 3.3 Å between the mean planes of one of the resorcinol units and the nearest overlapping atom of the diquat, C(42), is ideal for charge transfer[8]. As in the case of the catechol derived receptors, the phenoxymethylene units in 8 are all nearly coplanar[9] with the resorcinol rings, thus enhancing their π-donating character.

However there are some important differences:

(I) Although both linking polyether chains adopt an 'all gauche ' conformation, only one chain is looped over the region of the $CHNCH_2$ groups of the dication while the other encircles the edge of one of the pyridinium rings.

(II) Despite several short C...O contacts between diquat and the polyether oxygens [see table 6.11], there appears to be only one C-H...O hydrogen bonding interaction: C(50)...O(7) 3.32, H(50b)...O(7) 2.38 Å, C-H...O angle at H(50b), 167°.

(III) Because of the distance separating the oxygens in the resorcinol units (4.7 Å), it is not possible to achieve simultaneous alignment of both oxygen atoms on each resorcinol unit with both nitrogens of the dication. However one of the nitrogens atoms, N(1) is positioned almost colinearly with respect to two of the

TABLE 6.11. Selected host-guest contact distances, and relevant hydrogen contact distances and angles where appropriate, in order of increasing $X^a...O$ distance for [8.diquat].

$X^a...O$	$R(X^a...O)$ (Å)	$R(H...O)$ (Å)	$\psi(^o)^b$	$\theta(^o)^c$
C(39)-O(4)	3.10			
C(47)-O(26)	3.17			
C(47)-O(20)	3.27			
C(50)-O(10)	3.29			
C(50)-O(4)	3.29			
C(50)-O(7)	3.32	2.38[d]	80[d]	167[d]
C(46)-O(20)	3.38			
C(49)-O(10)	3.39			

[a] Carbon or Nitrogen atom of the diquat dication.
[b] Angles between COC planes and HO vectors.
[c] C-H...O angles.
[d] H(50b)

resorcinol oxygen atoms, O(1) and O(13) [O(1)...N(2)...O(13) angle of 168° compared with 106° for [O(17)...N(2)...O(29)]. The distances [O(1)...N(2) 3.47, O(13)...N(2) 3.71 Å] involved in this alignment are longer that in previous complexes and are not significantly less than normal van der Waals contact distances indicating perhaps that this alignment maybe a consequence of a combination of charge transfer and packing requirements rather than specific dipole-pole electrostatic binding interaction between the host and diquat.

(IV) There is a 22° in plane rotation of one of the resorcinol units with respect to the other, whereas previously, except for [6.diquat], the catechol units have been almost in register. The view looking on to the mean plane of the diquat dication (figure 6.8) shows that there is an appreciable overlap of the two resorcinol rings, whilst previously, with the exception of [6.diquat], the catechol rings have had a more staggered relationship.

Comparison of the torsional angles of the free and complexed host illustrates very elegantly the conformation changes required to achieve complexation. Essentially rotation about only four bonds in the uncomplexed host occurs, O(1)-C(16'), C(13')-C(14'), C(6)-O(7), C(6')-O(7'), the torsion angles about all the other bonds undergoing only very minor changes.

The closest contact between the acetone molecule and the complex is 3.15 Å between O(51) on the acetone and C(48) on the diquat dication. It is noteworthy that the acetone molecule approaches the $CHNCH_2$ portion of the diquat which does not have a polyether loop over

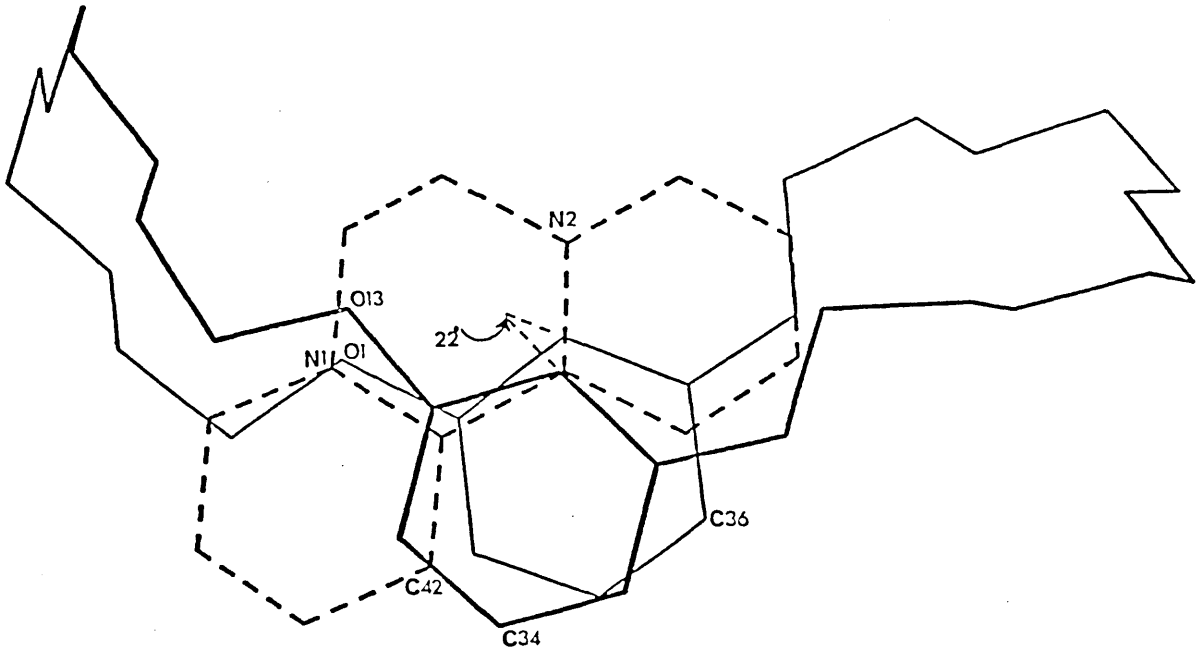


Figure 6.8. Side-on view (view normal to mean plane of diquat dication) of the skeletal representation of the solid-state structure of [8.diquat].

it. There are two potential hydrogen bonds between the PF_6 anions and the complex [C(35)...F(11) 3.28, H(35)...F(11) 2.35 Å, C-H...F angle at H(35) 162°; C(45)...F(21) 3.10, H(45)...F(21) 2.19 Å, C-H...F angle at H(45) 157°]. However, as the fluorines are undergoing considerable anisotropic thermal motion these contacts may not be significant. There are no contacts of less than normal van der Waals distances between symmetry related 1:1 complexes.

Thermal motion in [8.diquat] is high, it is particulary pronounced in the PF_6 anions and in portions of the polyether chains, and also unsually, in regions of the diquat dication. These factors contribute to the high R-factor obtained.

Solution studies[10] of the charge transfer absorption bands give evidence for 1:1 complexation of the host with both diquat and paraquat from which derived ΔG^o's for the equilibrium

$$[\text{bipyridinium}][PF_6]_2 + 8 \underset{<--}{\overset{-->}{}} [\text{bipyridinium}.8][PF_6]_2$$

are -3.9 and -3.5 Kcal mol^{-1} for paraquat and diquat respectively. Thus host 8 binds both the bipyridinium dications almost equally as well. This is in contrast to DB30C10 which only encapsulates diquat. The value of ΔG^o = -5.8 Kcal mol^{-1} for [1.diquat]^2 indicates that diquat forms a more stable complex in solution with DB30C10 than with 8.

These results demonstate that designing a receptor with a

preorganised cavity for complexation of the diquat dication is not by itself a guarantee of increasing complex stability.

TABLE 6.1. Coordinates ($\times 10^4$) and temperature factors ($\AA^2 \times 10^3$)

atom	x	y	z	U
O(1)	5336(2)	4109(1)	1953(2)	65(1)*
O(2)	4350(3)	5004(1)	729(3)	65(1)*
O(3)	2561(3)	5548(1)	1215(3)	73(1)*
O(4)	3013(2)	5111(1)	2293(2)	60(1)*
O(5)	1400(3)	4772(1)	2565(3)	60(1)*
O(6)	1007(3)	4279(1)	3973(3)	69(1)*
O(7)	3331(2)	3970(1)	3684(2)	58(1)*
O(8)	5108(3)	4160(1)	4252(2)	56(1)*
O(9)	4501(3)	3651(1)	4392(2)	58(1)*
O(10)	4052(2)	3474(1)	2902(1)	62(1)*
O(11)	9097(3)	2966(1)	3030(2)	56(1)*
O(12)	9610(3)	2939(1)	1486(2)	57(1)*
O(13)	10907(2)	3236(1)	1190(1)	58(1)*
O(14)	10686(3)	3237(1)	-209(2)	46(1)*
O(15)	12325(3)	3560(1)	-344(2)	48(1)*
O(16)	13038(3)	3579(1)	-1714(2)	50(1)*
O(17)	9704(3)	2934(1)	-1414(2)	51(1)*
O(18)	10517(3)	2980(1)	-2775(2)	56(1)*
O(19)	12114(3)	3312(1)	-2957(2)	55(1)*

* Equivalent isotropic U defined as one third of the trace of the orthogonalised U_{ij} tensor

TABLE 6.2. Bond lengths (Å)

O(1)–O(2)	1.416(3)	O(1)–C(16a)	1.352(2)
C(2)–C(3)	1.407(3)	C(3)–O(4)	1.400(3)
O(4)–C(5)	1.411(2)	C(5)–C(6)	1.402(3)
C(6)–C(7)	1.389(2)	O(7)–C(8)	1.418(2)
C(8)–C(9)	1.470(3)	C(9)–C(10)	1.402(2)
C(10)–C(11)	1.406(3)	C(11)–C(12)	1.407(3)
C(12)–C(13)	1.425(2)	C(13)–C(14)	1.365(2)
C(14)–C(15)	1.393(3)	C(14)–C(17)	1.391(3)
C(15)–C(16)	1.377(3)	C(16)–C(19)	1.393(3)
C(16)–C(16a)	1.359(2)	C(17)–C(18)	1.379(3)
C(18)–C(19)	1.370(3)		

TABLE 6.3. Bond Angles (deg.)

C(2)-O(1)-C(16a)	117.7(2)	O(1)-C(2)-C(3)	108.6(2)
C(2)-C(3)-O(4)	110.0(2)	C(3)-O(4)-C(5)	112.3(1)
O(4)-C(5)-C(6)	110.1(2)	C(5)-C(6)-O(7)	114.5(2)
C(6)-O(7)-C(8)	113.9(2)	O(7)-C(8)-C(9)	109.6(2)
C(8)-C(9)-O(10)	110.1(2)	C(9)-O(10)-C(11)	113.1(2)
O(10)-C(11)-C(12)	109.0(2)	C(11)-C(12)-O(13)	107.5(2)
C(12)-O(13)-C(14)	118.3(1)	O(13)-C(14)-C(15)	114.9(2)
O(13)-C(14)-C(17)	124.0(2)	C(15)-C(14)-C(17)	121.0(2)
C(14)-C(15)-C(16)	119.7(2)	C(15)-C(16)-C(19)	120.3(2)
C(15)-C(16)-O(1a)	124.2(2)	C(19)-C(16)-O(1a)	115.5(2)
C(14)-C(17)-C(18)	118.2(2)	C(17)-C(18)-C(19)	122.2(2)
C(16)-C(19)-C(18)	118.5(2)		

TABLE 6.4. Anisotropic temperature factors ($\AA^2 \times 10^3$)

atom	U_{11}	U_{22}	U_{33}	U_{23}	U_{13}	U_{12}
O(1)	74(1)	65(1)	57(1)	0(1)	12(1)	-10(1)
O(2)	67(1)	64(1)	62(1)	10(1)	-4(1)	-12(1)
O(3)	56(1)	81(2)	80(2)	24(1)	-11(1)	-4(1)
O(4)	45(1)	60(1)	73(1)	19(1)	-5(1)	-9(1)
O(5)	43(1)	57(1)	82(2)	3(1)	7(1)	-3(1)
O(6)	48(1)	67(1)	91(2)	7(1)	21(1)	-2(1)
O(7)	51(1)	54(1)	70(1)	-4(1)	4(1)	-3(1)
O(8)	55(1)	67(1)	47(1)	-5(1)	6(1)	-5(1)
O(9)	55(1)	75(1)	45(1)	2(1)	9(1)	-2(1)
O(10)	63(1)	82(1)	42(1)	7(1)	10(1)	19(1)
O(11)	54(1)	62(1)	54(1)	4(1)	10(1)	-0(1)
O(12)	49(1)	62(1)	62(1)	-5(1)	0(1)	-8(1)
O(13)	59(1)	69(1)	49(1)	-17(1)	14(1)	-16(1)
O(14)	52(1)	43(1)	42(1)	-2(1)	2(1)	3(1)
O(15)	55(1)	43(1)	44(1)	-4(1)	1(1)	-2(1)
O(16)	54(1)	38(1)	57(1)	6(1)	4(1)	-2(1)
O(17)	50(1)	52(1)	47(1)	-3(1)	-0(1)	-5(1)
O(18)	67(1)	56(1)	41(1)	-2(1)	-7(1)	-2(1)
O(19)	75(1)	51(1)	39(1)	4(1)	3(1)	3(1)

The anisotropic temperature factor exponent takes the form:

$$-2\pi^2(h^2a^{*2}U_{11} + \ldots + 2\,hka^*b^*U_{12}\cos\gamma^* + \ldots)$$

TABLE 6.5. Coordinates ($\times 10^4$) and temperature factors ($Å^2 \times 10^3$)

atom	x	y	z	U
Ir(2a)	4045	4071	-90	44
Ir(2b)	5155	5405	411	66
Ir(3a)	1812	5379	366	76
Ir(3b)	1030	5052	1436	79
Ir(5a)	377	5029	2770	63
Ir(5b)	1093	4539	1696	63
Ir(6a)	753	4165	4055	60
Ir(6b)	2294	4617	4729	59
Ir(8a)	5644	4442	35?0	57
Ir(8b)	5137	4330	5214	57
Ir(9a)	5894	3332	4966	59
Ir(9b)	7655	3760	5005	59
Ir(11a)	9240	3029	3695	59
Ir(11b)	7378	2641	3381	59
Ir(12a)	7513	2091	764	60
Ir(12b)	9061	2441	1436	60
Ir(15)	12963	3758	513	42
Ir(17)	8672	2698	-1310	45
Ir(18)	9909	2771	-3621	55
Ir(19)	12578	3347	-3922	52

TABLE 6.6. Coordinates ($\times 10^4$) and temperature factors ($Å^2 \times 10^3$)

atom	x	y	z	U
O(1)	7269(4)	-1418(4)	7685(2)	91(2)*
C(2)	7779(7)	-2009(6)	8233(3)	96(3)*
C(3)	6622(7)	-2201(5)	8668(3)	88(3)*
O(4)	5746(4)	-1079(4)	8792(2)	85(2)*
C(5)	4605(7)	-1181(6)	9190(3)	95(3)*
C(6)	3499(7)	-61(6)	9074(4)	93(3)*
O(7)	3832(4)	996(4)	9242(2)	75(2)*
C(8)	2937(6)	2120(7)	9119(3)	86(3)*
C(9)	3165(7)	3107(6)	9375(3)	85(3)*
O(10)	4437(4)	3279(4)	9102(2)	79(2)*
C(11)	4864(8)	4152(6)	9386(3)	94(3)*
C(12)	6250(7)	4176(5)	9145(3)	76(3)*
O(13)	6261(4)	4679(4)	8520(2)	75(2)*
C(14)	7430(6)	4712(5)	8206(3)	66(2)*
C(15)	7422(6)	5149(5)	7602(3)	65(2)*
C(16)	8570(6)	5214(5)	7239(3)	71(3)*
O(17)	8625(5)	5659(4)	6632(2)	94(2)*
C(18)	7420(8)	6236(6)	6413(3)	90(3)*
C(19)	7724(10)	6803(7)	5748(3)	112(4)*
O(20)	7996(6)	5921(4)	5404(2)	110(3)*
C(21)	7970(10)	6266(7)	4784(3)	117(4)*
C(22)	8261(11)	5231(9)	4419(3)	137(5)*
O(23)	7282(6)	4556(4)	4550(2)	103(2)*
C(24)	7477(11)	3647(8)	4152(3)	129(5)*
C(25)	6577(9)	2884(8)	4310(3)	114(4)*
O(26)	6697(6)	2215(4)	4879(2)	117(3)*
C(27)	6287(8)	1124(6)	4963(3)	95(3)*
C(28)	6567(7)	510(6)	5593(3)	91(3)*
O(29)	7948(5)	138(4)	5616(2)	93(2)*
C(30)	8381(6)	-344(6)	6156(4)	77(3)*
C(31)	7589(6)	-631(5)	6681(3)	63(2)*
C(32)	8153(6)	-1149(5)	7206(3)	74(3)*
C(33)	9788(7)	4828(7)	7478(3)	97(3)*
C(34)	9817(7)	4415(7)	8064(3)	102(4)*
C(35)	8677(7)	4360(6)	8454(3)	93(3)*
C(36)	9764(7)	-583(7)	6197(4)	109(4)*
C(37)	10279(7)	-1063(7)	6722(4)	106(4)*
C(38)	9525(6)	-1372(6)	7241(3)	88(3)*
N(1)	7081(5)	1423(4)	9172(2)	65(2)*
C(39)	7271(8)	951(5)	9763(3)	98(3)*
C(40)	8545(9)	739(7)	9930(5)	142(5)*
C(41)	9534(10)	1038(8)	9524(7)	200(7)*
C(42)	9284(9)	1581(7)	7916(5)	135(5)*
C(43)	8037(6)	1757(5)	7746(3)	76(3)*
C(44)	7677(7)	2290(6)	7152(3)	84(3)*
C(45)	8616(10)	2345(8)	6630(4)	144(5)*
C(46)	8138(13)	2911(9)	6069(4)	188(7)*
C(47)	6899(13)	3435(8)	6053(3)	160(6)*
C(48)	5994(10)	3384(6)	6540(3)	105(4)*
N(2)	6389(5)	2920(4)	7079(2)	73(2)*
C(49)	5397(6)	2802(5)	7613(2)	63(2)*
C(50)	5755(5)	1587(5)	7979(2)	62(2)*
O(51)	4320(5)	5788(5)	7123(2)	107(2)*
C(52)	3659(7)	6351(7)	7514(3)	93(3)*
C(53)	2645(10)	5780(11)	7913(5)	160(6)*
C(54)	3772(12)	7553(9)	7654(6)	166(6)*

TABLE 6.6. cont/d.

P(1)	768(2)	7434(2)	9540(1)	81(1)*
F(11)	488(6)	6779(7)	10179(2)	192(4)*
F(12)	1009(6)	8169(5)	9913(2)	166(3)*
F(13)	2279(5)	6992(7)	9590(4)	224(4)*
F(14)	-760(5)	7896(6)	9503(2)	160(3)*
F(15)	838(9)	6273(6)	9229(3)	225(5)*
F(16)	675(8)	8614(6)	9812(3)	210(4)*
P(2)	2999(2)	1296(2)	6817(1)	101(1)*
F(21)	1677(5)	1984(7)	6545(3)	204(4)*
F(22)	3353(8)	351(11)	6386(4)	292(7)*
F(23)	2168(6)	524(6)	7249(3)	192(3)*
F(24)	4262(5)	710(7)	7091(3)	201(4)*
F(25)	2634(7)	2175(9)	7324(4)	256(5)*
F(26)	3776(7)	2161(8)	6462(4)	238(5)*

* Equivalent isotropic U defined as one third of the trace of the orthogonalised U_{ij} tensor

TABLE 6.7. Bond lengths (Å)

O(1)-C(2)	1.410(9)	O(1)-C(32)	1.367(7)
C(2)-C(3)	1.482(10)	C(3)-O(4)	1.391(7)
O(4)-C(5)	1.403(8)	C(5)-C(6)	1.492(9)
C(6)-O(7)	1.432(9)	O(7)-C(8)	1.433(7)
C(8)-C(9)	1.449(11)	C(9)-O(10)	1.431(8)
O(10)-C(11)	1.431(9)	C(11)-C(12)	1.477(11)
C(12)-O(13)	1.429(7)	O(13)-C(14)	1.371(7)
C(14)-C(15)	1.372(8)	C(14)-C(35)	1.376(9)
C(15)-C(16)	1.379(9)	C(16)-O(17)	1.372(7)
C(16)-C(32)	1.370(10)	O(17)-C(18)	1.396(9)
C(18)-C(19)	1.519(9)	C(19)-O(20)	1.379(9)
O(20)-C(21)	1.403(8)	C(21)-C(22)	1.456(13)
C(22)-O(23)	1.402(14)	O(23)-C(24)	1.403(11)
C(24)-C(25)	1.408(15)	C(25)-O(26)	1.386(8)
O(26)-C(27)	1.384(10)	C(27)-C(28)	1.497(9)
C(28)-O(29)	1.401(8)	O(29)-C(30)	1.339(9)
C(30)-C(31)	1.386(9)	C(30)-C(36)	1.407(10)
C(31)-C(32)	1.369(9)	C(32)-C(38)	1.398(9)
C(33)-C(34)	1.326(10)	C(34)-C(35)	1.382(10)
C(36)-C(37)	1.360(12)	C(37)-C(38)	1.362(10)
N(1)-C(39)	1.371(9)	N(1)-C(43)	1.368(8)
N(1)-C(50)	1.463(8)	C(39)-C(40)	1.382(13)
C(40)-C(41)	1.355(15)	C(41)-C(42)	1.437(17)
C(42)-C(43)	1.362(11)	C(43)-C(44)	1.431(9)
C(44)-C(45)	1.419(11)	C(44)-N(2)	1.343(8)
C(45)-C(46)	1.416(13)	C(46)-C(47)	1.276(17)
C(47)-C(48)	1.341(12)	C(48)-N(2)	1.345(8)
N(2)-C(49)	1.480(7)	C(49)-C(50)	1.475(7)
O(51)-C(52)	1.181(8)	C(52)-C(53)	1.502(13)
C(52)-C(54)	1.468(15)	P(1)-F(11)	1.536(6)
P(1)-F(12)	1.545(5)	P(1)-F(13)	1.535(6)
P(1)-F(14)	1.552(5)	P(1)-F(15)	1.543(8)
P(1)-F(16)	1.512(8)	P(2)-F(21)	1.545(6)
P(2)-F(22)	1.473(11)	P(2)-F(23)	1.531(7)
P(2)-F(24)	1.493(6)	P(2)-F(25)	1.548(11)
P(2)-F(26)	1.507(9)		

TABLE 6.8. Bond Angles (deg.)

C(2)-O(1)-C(32)	118.0(5)	O(1)-C(2)-C(3)	106.8(5)
C(2)-C(3)-O(4)	111.2(5)	C(3)-O(4)-C(5)	114.8(5)
O(4)-C(5)-C(6)	109.7(5)	C(5)-C(6)-O(7)	109.4(6)
C(6)-O(7)-C(8)	112.7(5)	O(7)-C(8)-C(9)	108.9(6)
C(8)-C(9)-O(10)	110.3(5)	C(9)-O(10)-C(11)	112.1(5)
O(10)-C(11)-C(12)	110.0(5)	C(11)-C(12)-O(13)	109.4(5)
C(12)-O(13)-C(14)	116.9(5)	O(13)-C(14)-C(15)	113.8(5)
O(13)-C(14)-C(35)	125.2(5)	C(15)-C(14)-C(35)	121.0(6)
C(14)-C(15)-C(16)	119.1(6)	C(15)-C(16)-O(17)	123.1(6)
C(15)-C(16)-C(33)	120.1(6)	O(17)-C(16)-C(33)	116.8(6)
C(16)-O(17)-C(18)	117.9(5)	O(17)-C(18)-C(19)	108.5(6)
C(18)-C(19)-O(20)	108.7(6)	C(19)-O(20)-C(21)	109.6(5)
O(20)-C(21)-C(22)	109.7(6)	C(21)-C(22)-O(23)	111.6(7)
C(22)-O(23)-C(24)	111.8(6)	O(23)-C(24)-C(25)	112.6(7)
C(24)-C(25)-O(26)	113.7(8)	C(25)-O(26)-C(27)	116.3(7)
O(26)-C(27)-C(28)	108.1(7)	C(27)-C(28)-O(29)	110.0(6)
C(28)-O(29)-C(30)	118.1(5)	O(29)-C(30)-C(31)	125.7(6)
O(29)-C(30)-C(36)	116.5(6)	C(31)-C(30)-C(36)	117.8(7)
C(30)-C(31)-C(32)	120.4(6)	O(1)-C(32)-C(31)	114.5(6)
O(1)-C(32)-C(38)	123.5(6)	C(31)-C(32)-C(38)	122.0(6)
C(16)-C(33)-C(34)	119.6(7)	C(33)-C(34)-C(35)	122.8(7)
C(14)-C(35)-C(34)	117.2(6)	C(30)-C(36)-C(37)	119.9(7)
C(36)-C(37)-C(38)	123.3(7)	C(32)-C(38)-C(37)	116.5(7)
C(39)-N(1)-C(43)	125.1(6)	C(39)-N(1)-C(50)	117.7(5)
C(43)-N(1)-C(50)	117.2(5)	N(1)-C(39)-C(40)	117.2(7)
C(39)-C(40)-C(41)	120.1(10)	C(40)-C(41)-C(42)	121.1(10)
C(41)-C(42)-C(43)	118.8(8)	N(1)-C(43)-C(42)	117.7(7)
N(1)-C(43)-C(44)	118.8(6)	C(42)-C(43)-C(44)	123.5(7)
C(43)-C(44)-C(45)	123.7(7)	C(43)-C(44)-N(2)	119.3(5)
C(45)-C(44)-N(2)	116.9(6)	C(44)-C(45)-C(46)	118.5(9)
C(45)-C(46)-C(47)	119.6(9)	C(46)-C(47)-C(48)	122.6(8)
C(47)-C(48)-N(2)	119.9(8)	C(44)-N(2)-C(48)	122.1(6)
C(44)-N(2)-C(49)	118.3(5)	C(48)-N(2)-C(49)	119.5(6)
N(2)-C(49)-C(50)	108.1(4)	N(1)-C(50)-C(49)	108.7(5)
O(51)-C(52)-C(53)	117.8(8)	O(51)-C(52)-C(54)	125.2(8)
C(53)-C(52)-C(54)	117.0(8)	F(11)-P(1)-F(12)	176.6(3)
F(11)-P(1)-F(13)	90.7(4)	F(12)-P(1)-F(13)	90.7(4)
F(11)-P(1)-F(14)	89.2(3)	F(12)-P(1)-F(14)	89.3(3)
F(13)-P(1)-F(14)	179.3(4)	F(11)-P(1)-F(15)	92.4(4)
F(12)-P(1)-F(15)	90.8(4)	F(13)-P(1)-F(15)	89.0(5)
F(14)-P(1)-F(15)	91.8(4)	F(11)-P(1)-F(16)	90.4(4)
F(12)-P(1)-F(16)	86.4(4)	F(13)-P(1)-F(16)	92.4(5)
F(14)-P(1)-F(16)	86.9(4)	F(15)-P(1)-F(16)	176.9(4)
F(21)-P(2)-F(22)	94.4(5)	F(21)-P(2)-F(23)	97.1(4)
F(22)-P(2)-F(23)	91.0(5)	F(21)-P(2)-F(24)	176.5(5)
F(22)-P(2)-F(24)	88.3(5)	F(23)-P(2)-F(24)	95.1(4)
F(21)-P(2)-F(25)	89.5(4)	F(22)-P(2)-F(25)	174.0(5)
F(23)-P(2)-F(25)	94.6(4)	F(24)-P(2)-F(25)	88.0(4)
F(21)-P(2)-F(26)	93.9(4)	F(22)-P(2)-F(26)	86.7(5)
F(23)-P(2)-F(26)	172.2(5)	F(24)-P(2)-F(26)	82.5(4)
F(25)-P(2)-F(26)	87.6(5)		

TABLE 6.9. Anisotropic temperature factors ($Å^2 \times 10^3$)

atom	U_{11}	U_{22}	U_{33}	U_{23}	U_{13}	U_{12}
O(1)	78(3)	81(3)	79(3)	-2(2)	-30(2)	-5(2)
O(2)	94(5)	60(4)	105(5)	-26(4)	-37(4)	3(3)
C(3)	120(6)	56(4)	88(5)	-2(3)	-39(4)	-11(4)
O(4)	92(3)	54(2)	106(3)	-11(2)	-8(2)	-13(2)
C(5)	115(6)	76(4)	99(5)	8(4)	-19(4)	-34(4)
C(6)	93(5)	93(5)	105(5)	-2(4)	-8(4)	-33(4)
O(7)	69(3)	70(3)	80(3)	-7(2)	-5(2)	-7(2)
C(8)	68(4)	96(5)	85(5)	-5(4)	2(3)	-11(4)
C(9)	86(5)	94(5)	69(4)	-13(4)	6(4)	-0(4)
O(10)	90(3)	73(3)	69(3)	-29(2)	7(2)	-13(2)
C(11)	124(6)	61(4)	60(4)	-20(3)	-1(4)	-8(4)
C(12)	112(6)	58(4)	57(4)	-16(3)	-14(4)	-15(4)
O(13)	93(3)	72(3)	60(2)	-5(2)	-16(2)	-14(2)
C(14)	89(4)	45(3)	63(4)	-9(3)	-16(3)	-10(3)
C(15)	78(4)	57(3)	63(4)	-17(3)	-18(3)	-13(3)
C(16)	91(5)	57(3)	66(4)	-15(3)	-17(3)	-9(3)
O(17)	109(4)	99(3)	75(3)	-14(3)	-15(3)	-23(3)
C(18)	120(6)	71(4)	90(5)	-6(4)	-18(4)	-26(4)
C(19)	173(9)	93(5)	79(5)	6(4)	-22(5)	-54(5)
O(20)	196(5)	95(3)	59(3)	-12(2)	-1(3)	-57(3)
C(21)	195(9)	105(6)	62(4)	-0(4)	4(5)	-71(6)
C(22)	202(10)	154(9)	68(5)	-6(5)	4(6)	-81(9)
O(23)	152(5)	97(3)	70(3)	-9(3)	0(3)	-54(3)
C(24)	198(9)	122(7)	76(5)	-1(5)	-21(5)	-75(7)
C(25)	162(8)	131(7)	65(5)	-2(5)	-29(5)	-61(6)
O(26)	207(6)	94(3)	69(3)	1(3)	-35(3)	-65(4)
C(27)	119(6)	90(5)	86(5)	-16(4)	-16(4)	-35(4)
C(28)	92(5)	63(4)	93(5)	-13(3)	-11(4)	-25(4)
O(29)	75(3)	97(3)	100(4)	-4(3)	-7(3)	-12(3)
C(30)	61(4)	67(4)	102(6)	-23(4)	-15(4)	-3(3)
C(31)	62(4)	53(3)	78(4)	-20(3)	-15(3)	-9(3)
C(32)	76(4)	51(3)	96(5)	-28(3)	-22(3)	-1(3)
C(33)	75(5)	115(6)	95(5)	-7(4)	-12(4)	-16(4)
C(34)	79(5)	114(6)	109(6)	2(5)	-31(4)	-10(4)
C(35)	94(5)	74(4)	80(4)	-4(3)	-39(4)	-8(4)
C(36)	74(5)	107(6)	138(7)	-22(5)	9(4)	-20(4)
C(37)	67(5)	114(6)	135(7)	-26(5)	-23(4)	-8(4)
C(38)	64(4)	99(5)	112(5)	-35(4)	-29(4)	5(3)
N(1)	77(3)	42(2)	77(3)	-15(2)	-24(3)	-4(2)
C(39)	143(7)	49(4)	107(5)	-18(4)	-53(5)	-8(4)
C(40)	177(9)	62(4)	204(10)	-31(5)	-131(8)	5(5)
C(41)	124(8)	90(6)	416(18)	-104(9)	-151(10)	25(5)
C(42)	78(5)	99(6)	242(11)	-71(7)	-14(6)	-21(4)
C(43)	60(4)	56(4)	114(5)	-41(3)	-3(3)	-8(3)
C(44)	98(5)	70(4)	97(5)	-44(4)	22(4)	-40(4)
C(45)	155(8)	131(7)	170(8)	-96(6)	95(7)	-92(6)
C(46)	333(15)	153(9)	111(7)	-77(6)	126(9)	-162(10)
C(47)	338(15)	110(6)	58(5)	-29(4)	42(6)	-126(8)
C(48)	208(9)	68(4)	58(4)	-7(3)	-19(5)	-66(5)
N(2)	116(4)	58(3)	58(3)	-20(2)	1(3)	-40(3)
C(49)	78(4)	58(3)	53(3)	-15(3)	-2(3)	-15(3)
C(50)	71(4)	63(4)	51(3)	-11(3)	-1(3)	-17(3)
O(51)	119(4)	119(4)	79(3)	-16(3)	-9(3)	-21(3)
C(52)	84(5)	112(5)	76(4)	-16(4)	-36(4)	8(4)
C(53)	115(8)	172(9)	178(10)	-37(8)	45(7)	-29(7)
C(54)	186(11)	120(7)	203(11)	-57(7)	-51(8)	-23(7)

P(1)	94(1)	74(1)	74(1)	-1(1)	-10(1)	-3(1)
P(11)	155(5)	260(7)	110(4)	87(4)	-16(3)	-12(5)
P(12)	178(5)	142(4)	126(4)	45(3)	28(4)	-2(4)
P(13)	84(4)	236(7)	291(8)	112(6)	-33(4)	2(4)
P(14)	89(3)	234(6)	143(4)	45(4)	-31(3)	-36(3)
P(15)	325(10)	134(5)	224(7)	-76(5)	42(7)	-81(6)
P(16)	276(8)	171(6)	211(7)	-101(5)	-56(6)	-45(5)
P(2)	73(1)	130(2)	109(2)	-13(1)	-14(1)	-35(1)
P(21)	105(4)	290(8)	202(6)	98(6)	-61(4)	-63(5)
P(22)	208(7)	430(13)	274(9)	-264(10)	33(6)	-111(8)
P(23)	150(5)	184(5)	178(5)	39(4)	28(4)	-34(4)
P(24)	101(4)	232(6)	277(8)	-110(6)	-90(4)	27(4)
P(25)	151(6)	296(9)	345(10)	-212(8)	24(6)	-31(6)
P(26)	155(5)	262(8)	297(9)	94(7)	-11(5)	-123(6)

The anisotropic temperature factor exponent takes the form:

$$-2\pi^2(h^2a^{*2}U_{11} + \ldots + 2\,hka^*b^*U_{12}\cos\gamma^* + \ldots)$$

TABLE 6.10. Coordinates ($\times 10^4$) and temperature factors ($Å^2 \times 10^3$)

atom	x	y	z	U
H(2a)	8390	-2799	8166	98
H(2b)	8229	-1194	8391	98
H(3a)	6937	-2636	9042	98
H(3b)	6157	-2682	8496	98
H(5a)	4338	-1901	9122	111
H(5b)	4801	-1254	9604	111
H(6a)	2689	-176	9311	111
H(6b)	3373	67	8649	111
H(8a)	2819	2321	8687	101
H(8b)	1979	2019	9302	101
H(9a)	3198	2899	9807	100
H(9b)	2495	3860	9298	100
H(11a)	4287	4959	9304	97
H(11b)	4821	3920	9818	97
H(12a)	6813	3352	9177	89
H(12b)	6571	4683	9373	89
H(15)	6590	5406	7435	74
H(18a)	6821	5814	6445	115
H(18b)	7037	7023	6645	115
H(19a)	8479	7159	5702	146
H(19b)	6962	7417	5615	146
H(21a)	7099	6792	4720	152
H(21b)	8625	6739	4666	152
H(22a)	9111	4692	4502	173
H(22b)	9296	5547	3996	173
H(24a)	8370	3139	4161	161
H(24b)	7359	4046	3747	161
H(25a)	6735	2309	4011	138
H(25b)	5695	3396	4306	138
H(27a)	5349	1296	4925	117
H(27b)	6775	594	4663	117
H(28a)	6199	-201	5668	96
H(28b)	6163	1092	5977	96
H(31)	6640	-463	6677	77
H(33)	10604	4859	7224	111
H(34)	10664	4137	8226	120
H(35)	9714	4090	9891	99
H(36)	10340	-409	5829	120
H(37)	11221	-1185	6736	124
H(38)	9917	-1729	7610	104
H(39)	6552	770	9049	112
H(40)	8738	388	9336	163
H(41)	10424	876	8637	204
H(42)	9973	1929	7633	151
H(45)	9555	2005	6652	155
H(46)	8735	2912	5701	202
H(47)	6598	3894	5679	191
H(48)	5062	3745	6506	129
H(49a)	4518	2924	7488	74
H(49b)	5381	3447	7959	74
H(50a)	5766	942	7737	71
H(50b)	5117	1557	8331	71

6.4 REFERENCES

1. See chapter 5.
2. H.M. Colquhoun, E.P. Gooding, J.M. Maud, J.F. Stoddart, D.J. Williams and J.B. Wolstenholme, J. Chem. Soc., Chem. Commun., 1983, 1140.

   H.M. Colquhoun, E.P. Gooding, J.M. Maud, J.F. Stoddart, D.J. Williams, J.B. Wolstenholme, J.Chem. Soc. Perkin Trans. 2, 1985, 607.

   See chapter 3.

   See chapter 4.
3. G.M. Sheldrick, SHELXTL, An integrated system for solving, refining, and displaying crystal structures from diffraction data, University of Göttingen, Federal Republic of Germany, 1981.
4. M.A. Bush, and M.R. Truter, J.Chem. Soc., Perkin Trans. 2, 1972, 345.

   I. R. Hanson, D. L. Hughes and M. R. Truter, J. Chem. Soc., Perkin Trans. 2, 1976, 972.

   J. D. Owen, Acta. Cryst., 1984, C40, 951.
5. I. L. Karle, J. Am. Chem. Soc., 1975, 97, 4379.

   V.Z. Pletnev, N. M. Galititsky, V. T. Ivanov, and Yu. A. Ovehinnikov, Bioorg. Chem., 1977, 3, 1427.

   M. Dobler, Helv. Chem. Acta., 1972, 55, 1371.

   Y. Nawata, T .Sakamaki, Y. Litaka, Acta. Cryst., 1974, B30, 1047.
6. I. Goldberg, The Chemistry of Functional Groups. Supplement E: The Chemistry of Ethers, Crown Ethers, Hydroxyl Groups and their Sulphur Analogues. 1980, Part 1, 175. Editor S. Patel, Chichester: John Wiley.
7. J. E. Derry, and T. A. Hamor, Nature, 1969, 221, 464.

P.D. Sullivan, and M.L. Williams, J. Am. Chem. Soc., 1972, 98, 1711.

T. Sundaresan, and S.C. Wallwork, Acta. Cryst., 1972, B28, 3065.

8. R. Foster, 'Organic Charge-Transfer Complexes,' Academic Press, London, 1969.

9. A. Makriyannis, and S. Fesik, J. Am. Chem. Soc., 1982, 104, 6462.

L. I. Kruse and J.K. Cha, J.Chem. Soc., Chem. Commun., 1982, 1329.

J. D. Mersh, J. K. M. Saunders and S. A. Martin, J. Chem Soc., Chem Commun., 1983, 306.

10. H. Shahriari-Zavareh, and J.F. Stoddart, unpublished results.

CHAPTER 7

The crystal structures of 1,4,7,10,13,20,23,26,29,32-decaoxa[13.13]paracyclophane (bisparaphenylene-34-crown-10) and its complex with diquat.

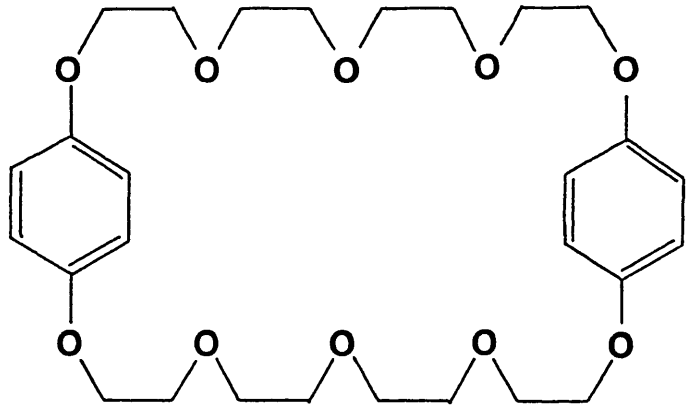
7.1 INTRODUCTION

Our rationale that dipole-pole electrostatic interactions play a dominant role over charge transfer in complexes between diquat and the catechol based receptors 1 - 7 has been vindicated by our observation of the mode of binding in the [8.diquat] complex. The separation between the resorcinol oxygens is too wide to allow the formation of two linear dipole-pole O...N...O interactions. However the optimal binding occurs when one nearly linear O...N..O interaction is formed in preference to an increase in π overlap between the π-electron-deficient diquat dication and the π-electron-rich resorcinol units. The formation of only one dipole-pole interaction leads to a decrease in the complex stability in solution compared to that for diquat complexes with receptors 1 - 7.

However, with receptor 8, solution studies, for the first time, gave evidence for complexation of the paraquat dication. We believe that complexation can be attributed to the increased separation between the aryl oxygens in 8 (ca. 4.7 Å) cf. that in the catechol receptors (ca. 2.6 Å). This separation could allow the paraquat dication to form at least one dipole-pole O...N...O interaction with 8 whilst still allowing some π overlap to occur. However, we were unable to obtain suitable crystals of [8.paraquat] to verify these proposals. Therefore we reasoned that an increase in the aryl oxygen separation, so that it matched more closely the N...N separation (ca. 7.0 Å) in paraquat, could lead to enhanced complex stability.

Hence the quinol receptor 9 was synthesised and has been complexed

with paraquat as well as diquat.



9

This chapter reports the X-ray structure analyses of 9 and [9.diquat.H_2O][PF_6]$_2$ which has been carried out to investigate the cavity size of the free receptor and its mode of binding towards diquat. The structure of the complex formed between paraquat and 9 will be discussed in chapter 8. The stability constant of the 1:1 complex formed in solution will also be discussed.

7.2 EXPERIMENTAL

Colourless crystals of 9 were obtained by recrystallisation from MeOH. A crystal of dimensions 0.20 x 0.87 x 0.87 mm was used for unit cell and intensity measurements.

Crystal data: $C_{28}H_{40}O_{10}$, M = 537, monoclinic, a = 10.890(2), b = 21.450(6), c = 12.361(4) Å, β = 106.31(2)°, U = 2771 Å^3, space group

$\underline{P}2_1/\underline{c}$, $\underline{Z}$ = 4 (the structure contains 2 independent centrosymmetric molecules in the asymmetric unit), $\underline{D}_c$ = 1.29 g cm^{-3}, $\underline{F}(000)$ = 1152, $\mu(Cu\text{-}\underline{K}_\alpha)$ = 7.67 cm^{-1}.

Refined unit-cell parameters were obtained by centering 15 reflections on a Nicolet R3m diffractometer. 2849 unique reflections ($\theta < 50^o$) were measured with Cu-$\underline{K}_\alpha$ radiation (graphite monochromator) using the omega-scan routine. Of these 2638 had $|\underline{F}_o| > 3\sigma(|\underline{F}_o|)$ and were considered to be observed. The net count of two reflections, the 2 4 -5 and the 2 3 4, measured as references every 100 reflections did not alter significantly during the data collection indicating that no deterioration of the crystal had occurred. The data were brought to a uniform arbitrary scale by the use of these reflections and Lorentz and polarisation corrections were applied.

The structure was solved by direct methods. An initial starting set comprising 3 origin defining reflections together with a further 5 automatically selected terms was used. The initial phase expansion (32 permutations) was with 200 $\underline{E}$'s > 1.5 using 1406 TPR. This was subsequently expanded to 426 probable phases with $\underline{E}$'s > 1.5 using 3317 TPR. The figures of merit for the best phase solution were NQEST = -0.470, RA(1) = 0.023, RA(2) = 0.081. This solution after 3 cycles of $\Delta\underline{E}$-map recycling gave an $\underline{R}_E$ = 0.227 and plausible positions for all the non-hydrogen atoms in structure. The non-hydrogen atoms were refined anisotropically. The methylene and phenyl hydrogens were placed at calculated positions (C-H = 0.96 Å), assigned isotropic thermal parameters, $\underline{U}(H) = 1.2\ \underline{U}_{eq}(C)$, and allowed to ride on their parent carbon atoms.

Refinement using $\underline{F}$ magnitudes was by block-cascade full-matrix least squares (344 variable parameters) and converged to $\underline{R}$ = 0.052, $\underline{R}_w$ = 0.060, $[w^{-1} = \sigma^2(\underline{F}) + 0.0013\underline{F}^2]$. An empirical extinction parameter which refined to 0.0058(9) was also used in the last cycles of the refinement. The largest parameter shift/e.s.d. was 0.153, the mean shift/e.s.d. was 0.031. The residual electron density in the final difference map was within -0.17 and 0.23 $e\text{Å}^{-3}$.

Red crystals of $[\underset{\sim}{9}.\text{diquat}.H_2O][PF_6]_2$ were obtained from a solution of $[\underset{\sim}{9}.\text{diquat}][PF_6]_2$ in acetone by vapour diffusion with n-pentane. A crystal of dimensions 0.25 x 0.30 x 0.30 mm was used for unit cell and intensity measurements.

Crystal data: $C_{28}H_{40}O_{10}.C_{12}H_{12}N_2.H_2O.P_2F_{12}$, $\underline{M}$ = 1029, triclinic, $\underline{a}$ = 10.786(5), $\underline{b}$ = 11.659(6), $\underline{c}$ = 20.098(14) Å, α = 96.90(5), β = 98.83(5), γ = 104.23(4)°, $\underline{U}$ = 2387 Å^3, space group $\underline{P\bar{1}}$, $\underline{Z}$ = 2, $\underline{D}_c$ = 1.44 g cm^{-3}, $\underline{F}(000)$ = 1068, $\mu(\text{Cu-}\underline{K}_\alpha)$ = 17.54 cm^{-1}.

Refined unit-cell parameters were obtained by centering 18 reflections on a Nicolet R3m diffractometer. 4911 unique reflections ($\theta < 50°$) were measured with Cu-$\underline{K}_\alpha$ radiation (graphite monochromator) using the omega-scan routine. Of these 4095 had $|\underline{F}_o| > 3\sigma(|\underline{F}_o|)$ and were considered to be observed. The net count of two reflections, the 0 1 4 and the 1 -3 -1 , measured as references every 50 reflections did not alter significantly during the data collection indicating that no deterioration of the crystal had occurred. The data were brought to

a uniform arbitrary scale by the use of these reflections and Lorentz and polarisation corrections were applied.

The structure was solved by direct methods. An initial starting set comprising three origin defining reflections, one $\Sigma 1$ reflection, two reflections which were weak links in the convergence mapping and six automatically selected terms was used. The initial phase expansion (256 permutations) was with 197 $\underline{E}$'s > 2.1 using 695 TPR. This was subsequently expanded to 412 probable phases with $\underline{E}$'s > 1.84 using 1158 TPR. The figures of merit for the best phase solution were NQEST = -0.202, RA(1) = 0.016, RA(2) = 0.078, these were ranked on RA(2) instead of NQEST as the number of negative quartets was low. This solution gave plausible positions for 66 of the non-hydrogen atom positions in the structure. The remaining non-hydrogen atoms were located from subsequent $\Delta\underline{F}$-maps, which also revealed the presence of an entrapped water molecule. Two discrete positions were observed for C(12) and these were refined with 60 and 40% occupancies respectively. The non-hydrogen atoms were refined anisotropically. The methylene and phenyl hydrogens were placed at calculated positions (C-H = 0.96 Å), assigned isotropic thermal parameters, $\underline{U}(H) = 1.2\ \underline{U}_{eq}(C)$ and allowed to ride on their parent carbon atoms. The hydroxyl protons were located from a $\Delta\underline{F}$-map and refined with a O-H distance constraint of 0.96 Å.

Refinement using $\underline{F}$ magnitudes was by block-cascade full-matrix least squares (620 variable parameters) and converged to $\underline{R}$ = 0.075, $\underline{R}_w$ = 0.088, $[w^{-1} = \sigma^2(\underline{F}) + 0.0015\underline{F}^2]$. The largest parameter shift/e.s.d. was 0.054, the mean shift/e.s.d.was 0.009. The residual

electron density in the final difference map was within -0.37 and 0.56 $e\mathring{A}^{-3}$.

All computations were carried out on an Eclipse S140 computer using the SHELXTL[2] program system.

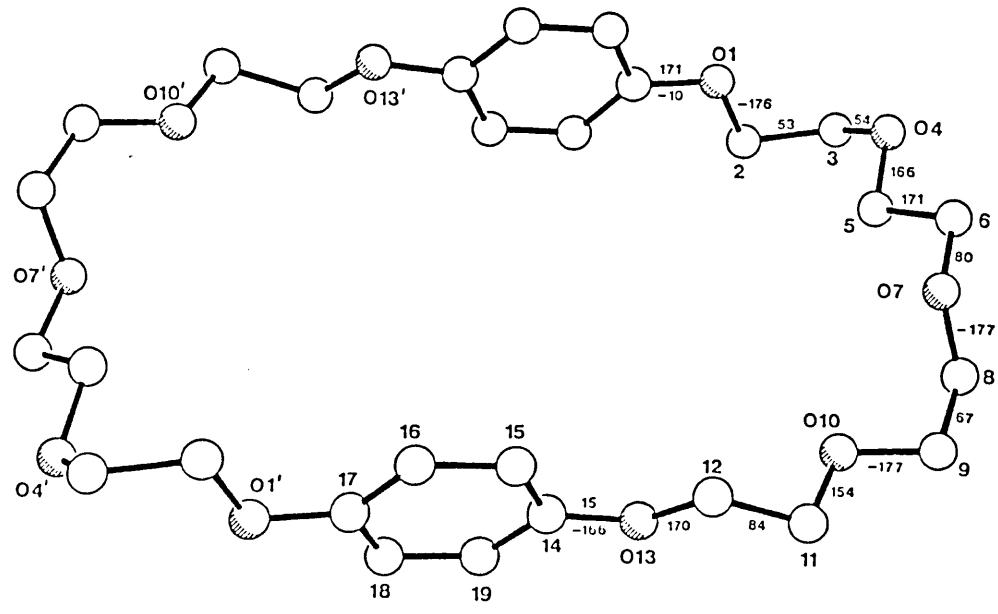
7.3 DISCUSSION

The final fractional atomic coordinates, anisotropic thermal parameters, bond lengths and bond angles for the non-hydrogen atoms of 9 and [9.diquat.H_2O][PF_6]$_2$ are shown in Tables 7.1 - 7.4 and 7.6 - 7.9 respectively. The position and isotropic temperature factors of the hydrogen atoms are listed in Tables 7.5 and 7.10 respectively.

The torsional angles associated with the polyether chains for the two independent conformations of 9 (9a and 9b) and [9.diquat] are shown beside the revelant C-C and C-O bonds in the skeletal drawings of the structures reproduced in figures 7.1 and 7.4 which also provide details of the crystallographic numbering schemes.

In the solid state 9 exists in two crystallographically independent conformations 9a and 9b. Both possess a crystallographic centre of symmetry and display, like 8[1] unusually open conformations (see figure 7.2). The free cavity size of 9a is ~ 4.6 x 11.1 $\mathring{A}$ and the separation between the parallel quinol units is 7.10 $\mathring{A}$. The cavity size of 9b is ~ 4.7 x 10.6 $\mathring{A}$, the separation between the quinol units is 7.29 $\mathring{A}$. These open geometries are very different to

(a)



(b)

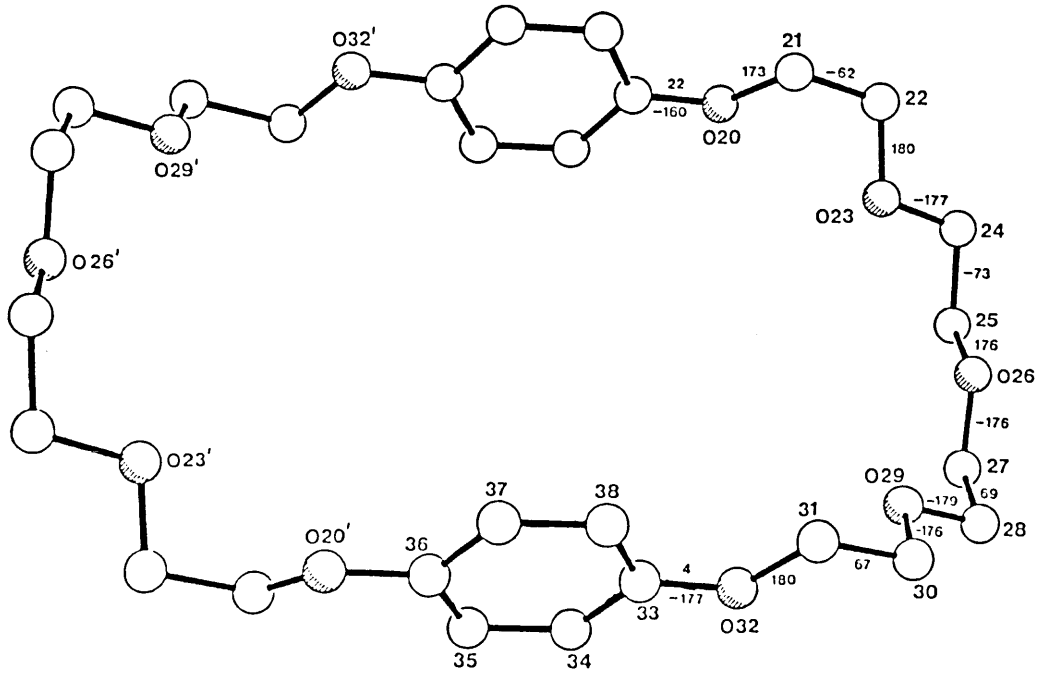


Figure 7.1. The skeletal representations of the solid-state structures of the two independent conformations 9a (a) and 9b (b), found for 9.

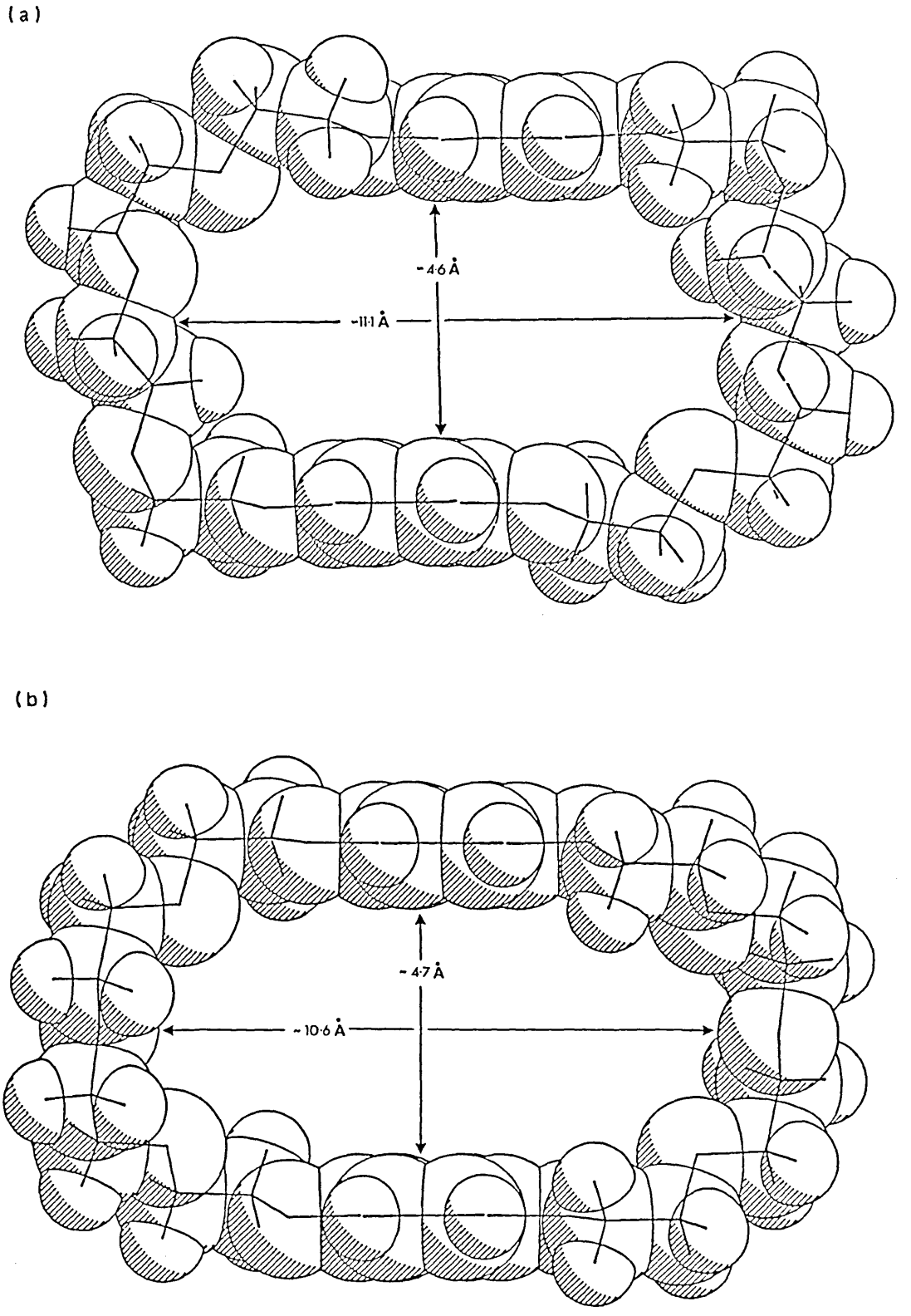
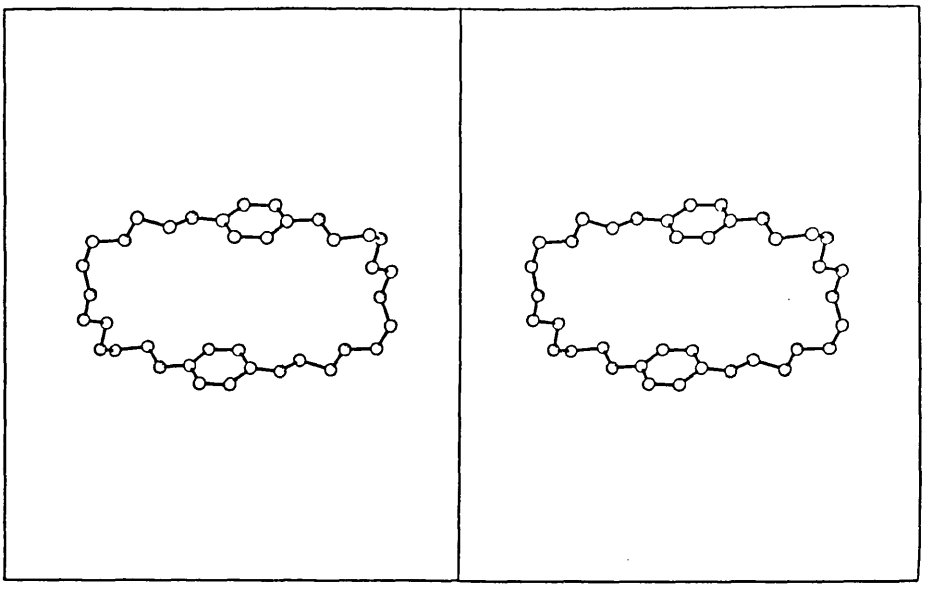


Figure 7.2. The space-filling representations of the solid-state structures of the two independent conformations 9a (a) and 9b (b), found for 9.

(a)



(B)

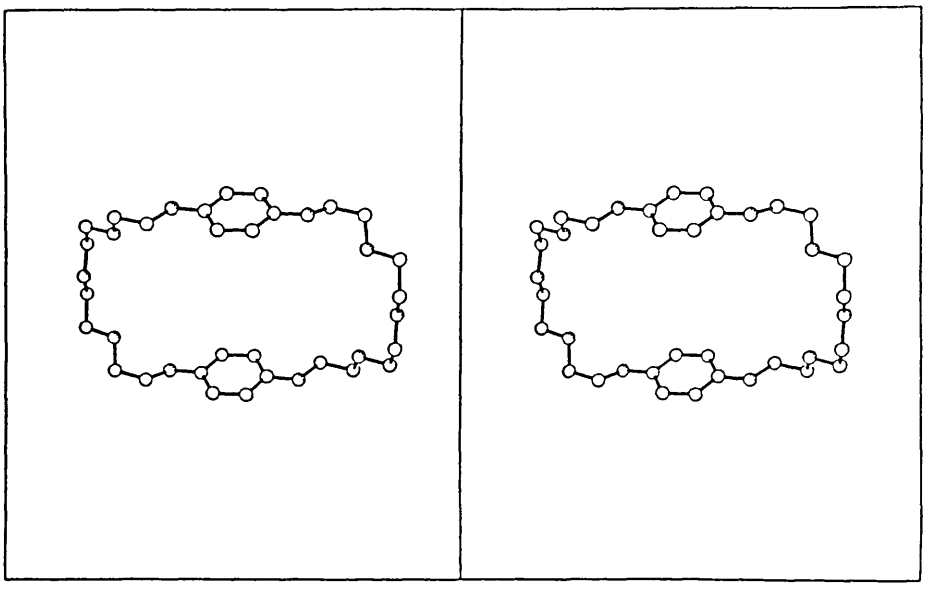


Figure 7.3. The stereo-pair representations of the solid-state structures of of the two independent conformations 9a (a) and 9b (b), found for 9.

that adopted by the analogous tetramethoxy derivative $(MeO)_4$-bisparaphenylene-34-crown-10[3], in which the two aromatic rings are nearly coplanar, with one of their methoxy groups directed towards the centre of the receptor cavity.

In both 9a and 9b the separation of the quinol units is nearly ideal for the insertion of the bipyridinium moiety into their centres. The two receptors have different conformations, the main difference being that 9b has the classic 'all gauche' torsion angle arrangement, whilst in 9a the C(3)-O(4), C(6)-O(7) bond torsional angles depart from this. The phenoxymethylene units in the receptors 9a and 9b are close to being planar, this condition has been previously observed in many of the other catechol and resorcinol derived receptors[1,4].

The crystal packing of 9 reveals that there are no contacts of less than normal van der Waals distances between macrocycles.

The crystal structure of [9.diquat.H_2O] reveals that the host conformation is nearly identical to that of the free receptor 9b. The only differences are in the magnitudes of the C(9)-O(10) and O(13)-C(14) bond torsional angles, which deviate significantly from the expected trans deposition ($\sim 180^{o}$). However, this distortion may be just a consequence of the disorder in C(12) and the high anisotropic thermal parameters of some of the other atoms in this region.

Thermal motion in the structure is high, being particulary pronounced in the PF_6 anions and in portions of the polyether chains particularly around C(12). This resulted in the slightly high R-

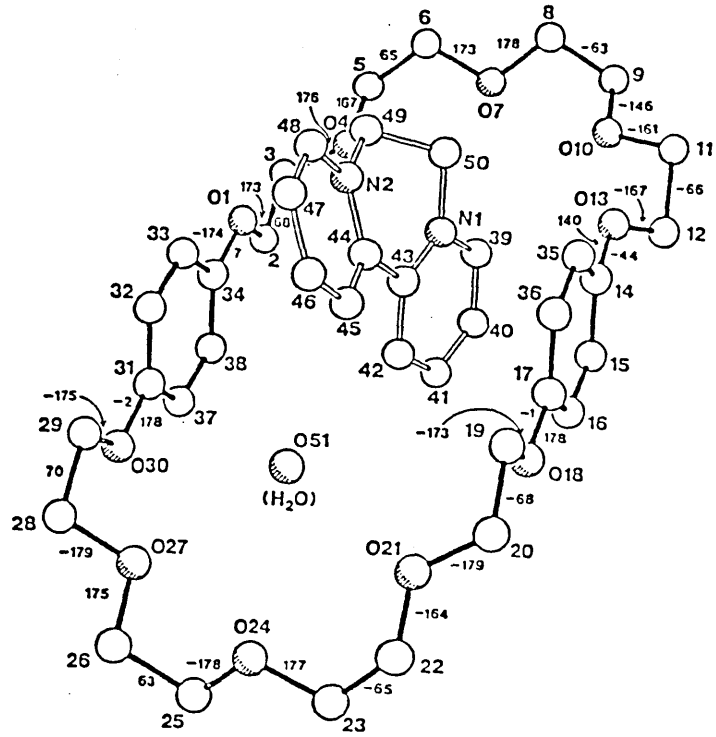


Figure 7.4. The skeletal representation of the solid-state structure of [9.diquat.H_2O]. The torsional angles taking into account the alternative position for C(12), are 143, 61, 160 and -137°, respectively for the region C(9) to C(15).

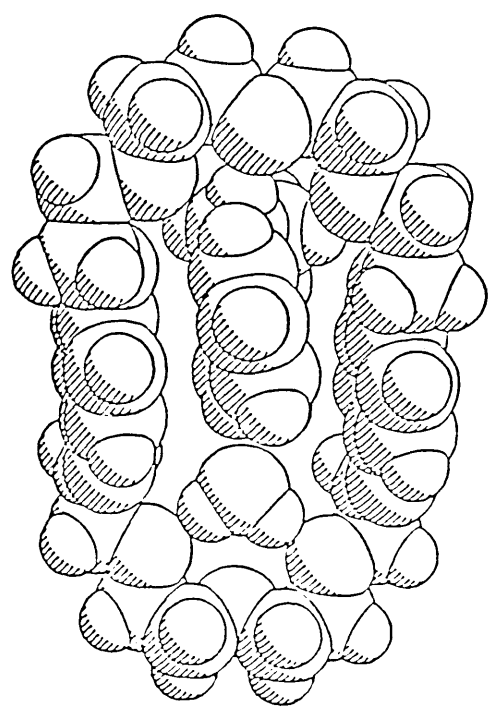


Figure 7.5. The space-filling representation of the solid-state structure of [9.diquat.H_2O].

factor obtained.

The receptor is essentially oval shaped with the diquat dication passing approximately through the centre of the host which loops one of its polyether chains (O(1) to O(13)) over a CH_2CH_2NCH portion of the diquat containing N(2). The other polyether chain is strongly hydrogen bonded to the water molecule which resides in its cavity [see table 7.11].

The dihedral angle between the pyridine rings is $23.6(6)^{o}$. This is the largest value yet observed for the diquat dihedral angle, but it is in general agreement with previous observed values[1,4,5].

The diquat dication interacts with the receptor via (i) three C-H...O hydrogen bonds [see table 7.11]; (ii) a linear electrostatic interaction between one of the bipyridinium nitrogens and one oxygen from each quinol unit [O(1)...N(1) 3.69, O(13)...N(1) 3.20 Å, O(1)...N(1)...O(13) 170^{o}], which seems to provide an axis for the diquat to pivot about; (iii) charge transfer between the C(42) to C(45) portion of the dication (figure 7.7) and the two nearly parallel (1.3^{o} between their mean planes and ~ 7 Å separation) quinol units of the receptor. The distance of 3.3 Å between the mean planes of one of the quinol units and the nearest atom of the overlapping region of the diquat (C(44)) is ideal for charge transfer[6].

The question remains to be asked. Does this complexing geometry represent the optimum for 9 with diquat or has it been influenced by

TABLE 7.11. Selected host-guest contact distances, and relevant hydrogen contact distances and angles where appropriate, in order of increasing $X^a...O$ distance for [9.diquat.H_2O].

$X^a...O$	$R(X^a...O)$ (Å)	$R(H...O)$ (Å)	$\psi(^o)^b$	$\theta(^o)^c$
O(51)-O(21)	2.89	1.93[d]	19[d]	179[d]
O(51)-O(27)	2.94	2.03[e]	36[e]	158[e]
N(1) -O(13)	3.20			
O(51)-O(24)	3.22			
C(39)-O(10)	3.25			
C(50)-O(13)	3.28			
C(50)-O(10)	3.29			
C(39)-O(13)	3.33			
C(49)-O(1)	3.33	2.47[f]	55[f]	149[f]
C(50)-O(7)	3.35	2.40[g]	71[g]	167[g]
C(50)-O(4)	3.37			
C(39)-O(4)	3.37			

[a] Carbon or Nitrogen atom of the diquat dication or Oxygen of the water molecule.
[b] Angles between COC planes and HO vectors.
[c] C-H...O angles.
[d] H(51b)
[e] H(51a)
[f] H(49a)
[g] H(50b)

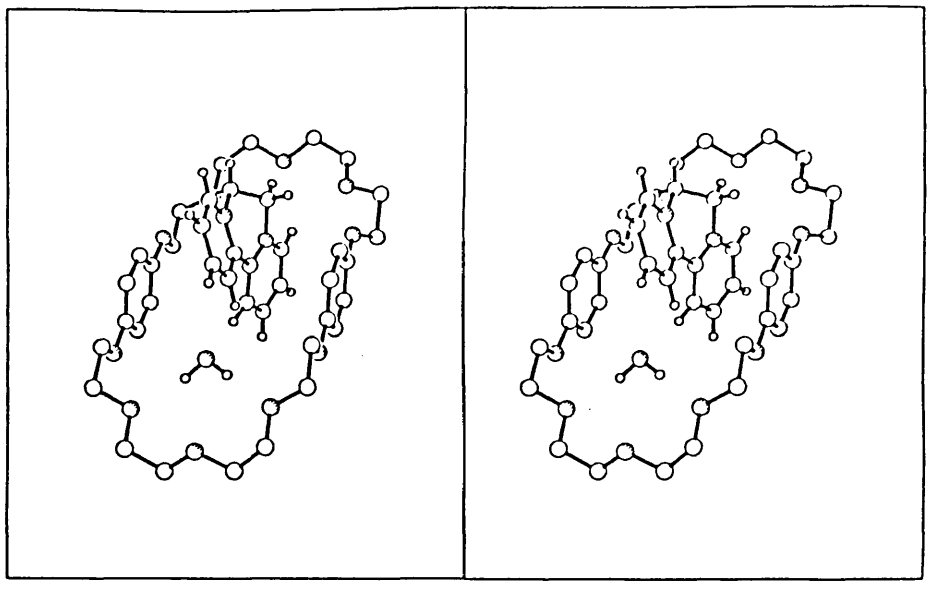


Figure 7.6. The stereo-pair representation of the solid-state structure of [9.diquat].

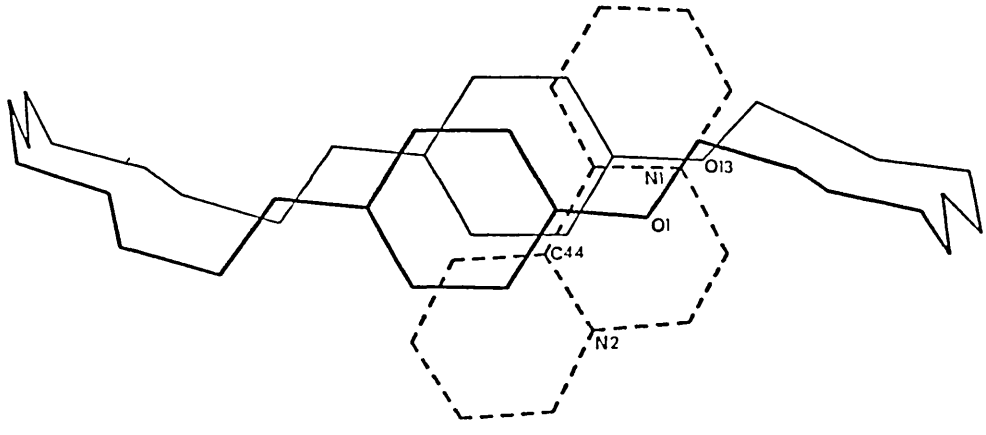


Figure 7.7. Side-on view (view normal to mean plane of diquat dication) of the skeletal representation of the solid-state structure of [9.diquat].

the presence of the H_2O molecule. Thus did the diquat dication achieve optimum complex binding prior to the entrapment of the water molecule, or did the initial water molecule entrapment prohibit increased charge transfer interactions between the diquat dication and the receptor? This question could be answered by recrystallising the complex under anhydrous conditions. The separation between the water molecule and diquat is 3.14 Å which is close to the van der Waals contact distance implying that the diquat is as close to the water molecule as possible. Due to the good overlap of the quinol units (see figure 7.7), it can be seen that if the diquat were to pivot further around the O...N...O axis, improved overlap of the other pyridine ring containing N(2), with the two quinol units could be achieved, but this would considerably reduce the overlap with the other pyridine ring. In addition a rotation about this axis would result in the polyether chain ceasing to loop over a CH_2CH_2NCH portion of the diquat moiety. The orientation of the 'looping polyether chain' is remarkably similar to that of the polyether chain which loops the CH_2CH_2NCH portion of the diquat dication in [8.diquat]. In fact a 'looping polyether chain' is a common feature of all the polyether complexes of diquat. The polyether chain oxygens are involved in hydrogen bonds and electrostatic dipole-pole interactions with the diquat dication. It is possible that these forces in association with the O...N...O electrostatic interactions predominate over charge transfer and that the initial optimising of hydrogen bonding and electrostatic interactions leads to the complex binding observed. If this is so, then the water molecule can be entrapped within the other polyether chain without affecting the host-diquat interactions.

The crystal packing of [9.diquat.H_2O][PF_6]$_2$ reveals two potential C-H...F hydrogen bonds between the diquat moiety and the PF_6 anion: C(49)...F(14) 3.15, H(49b)...F(14) 2.34 Å, C-H...F angle at H(49b) 141°; C(48)...F(26) 3.306, F(26)...H(48) 2.45 Å, C-H...F angle at H(48) 149°. The 1:1:1 complexes are linked in pairs in the c-axis direction across a centre of symmetry by two hydrogen bonds between polyether oxygen (O(7)) and a diquat atom (C(40')) {and between O(7')...C(40)} [O(7)-C(40) 3.30, O(7)-H(40) 2.38 Å, O-H-C angle at H(40) 160°]. There is also another short contact, across one of the other centres of symmetry, between O(24) and a symmetry related diquat atom, C(47), of 3.14 Å. This interaction is possible as C(47) lies outside the host cavity and does not appear to be involved in any charge transfer interactions.

Solution studies[7] reveal that complexation of diquat by 9 (ΔG^o = -3.60 Kcal mol^{-1}) is weaker than by the corresponding DB30C10 receptor[1,5]. This is not surprising due to the lack of interaction between one of the polyether chains and the diquat dication.

We have again discovered a receptor which has a preformed cavity for diquat, even though on complexation one of the polyether chains isn't involved in binding interactions with the dication.

TABLE 7.1. Coordinates ($\times 10^4$) and temperature factors ($Å^2 \times 10^3$).

tom	x	y	z	U
O(1)	-3825(2)	3600(1)	5422(1)	68(1)*
C(2)	-4858(3)	3875(1)	4577(2)	69(1)*
C(3)	-5668(3)	3357(1)	3923(2)	69(1)*
O(4)	-4996(2)	2911(1)	3482(1)	67(1)*
C(5)	-4262(3)	3180(1)	2818(2)	68(1)*
C(6)	-3862(3)	2664(1)	2170(3)	77(1)*
[illegible]	[illegible]	[illegible]	[illegible]	[illegible]
O(8)	-3534(2)	3199(1)	586(2)	69(1)*
C(9)	-2493(2)	3426(1)	137(2)	64(1)*
O(10)	-1779(2)	3895(1)	856(1)	61(1)*
[illegible]	[illegible]	[illegible]	[illegible]	[illegible]
C(12)	289(2)	4362(1)	1478(2)	56(1)*
[illegible]	[illegible]	[illegible]	[illegible]	[illegible]
O(14)	1012(2)	5301(1)	2478(2)	47(1)*
O(15)	2069(2)	5020(1)	3190(2)	61(1)*
O(16)	3009(2)	5371(1)	3910(2)	66(1)*
C(17)	2912(2)	6008(1)	3927(2)	52(1)*
C(18)	1842(2)	6294(1)	3242(2)	56(1)*
C(19)	903(2)	5939(1)	2528(2)	56(1)*
O(20)	1624(2)	3774(1)	5722(1)	66(1)*
O(21)	500(2)	4002(1)	4947(2)	57(1)*
C(22)	-101(2)	3471(1)	4203(2)	60(1)*
O(23)	[illegible]	[illegible]	6608(1)	52(1)*
C(24)	234(2)	2750(1)	2881(2)	53(1)*
C(25)	1188(2)	2523(1)	2331(2)	54(1)*
O(26)	1315(1)	2953(1)	1500(1)	53(1)*
C(27)	2285(2)	2779(1)	1005(2)	53(1)*
C(28)	2433(2)	3276(1)	202(2)	52(1)*
O(29)	2954(1)	3814(1)	806(1)	50(1)*
C(30)	3107(2)	4307(1)	97(2)	55(1)*
[illegible]	[illegible]	[illegible]	809(2)	54(1)*
O(32)	5026(1)	4645(1)	1370(1)	59(1)*
C(33)	5817(2)	5053(1)	2096(2)	47(1)*
C(34)	7048(2)	4857(1)	2563(2)	52(1)*
O(35)	7926(2)	5284(1)	3402(2)	54(1)*
O(36)	7567(2)	5812(1)	3577(2)	49(1)*
C(37)	6334(2)	6009(1)	3105(2)	61(1)*
C(38)	5449(2)	5635(1)	2371(2)	56(1)*

* Equivalent isotropic U defined as one third of the trace of the orthogonalised U_{ij} tensor

TABLE 7.2. Bond lengths (Å)

O(1)-C(2)	1.429(3)	O(1)-C(17a)	1.374(3)
C(2)-C(3)	1.505(4)	C(3)-O(4)	1.404(3)
O(4)-C(5)	1.420(4)	C(5)-C(6)	1.499(4)
C(6)-O(7)	1.415(4)	O(7)-C(8)	1.417(3)
C(8)-C(9)	1.477(4)	C(9)-O(10)	1.421(3)
O(10)-C(11)	1.413(3)	C(11)-C(12)	1.481(3)
C(12)-O(13)	1.425(3)	O(13)-C(14)	1.371(2)
C(14)-C(15)	1.377(3)	C(14)-C(19)	1.376(3)
C(15)-C(16)	1.377(3)	C(16)-C(17)	1.371(3)
C(17)-C(18)	1.377(3)	C(17)-O(1a)	1.374(3)
C(18)-C(19)	1.378(3)	O(20)-C(21)	1.413(3)
O(20)-C(36a)	1.373(3)	C(21)-C(22)	1.495(3)
C(22)-O(23)	1.406(3)	O(23)-C(24)	1.423(3)
C(24)-C(25)	1.475(4)	C(25)-O(26)	1.417(3)
O(26)-C(27)	1.412(3)	C(27)-C(28)	1.495(3)
C(28)-O(29)	1.405(3)	O(29)-C(30)	1.413(3)
C(30)-C(31)	1.487(3)	C(31)-O(32)	1.423(3)
O(32)-C(33)	1.371(2)	C(33)-C(34)	1.369(3)
C(33)-C(38)	1.383(3)	C(34)-C(35)	1.383(3)
C(35)-C(36)	1.371(3)	C(36)-C(37)	1.372(3)
C(36)-O(20a)	1.373(3)	C(37)-C(38)	1.379(3)

TABLE 7.3. Bond Angles (deg.)

C(2)-O(1)-C(17a)	117.9(2)	O(1)-C(2)-C(3)	108.1(2)
C(2)-C(3)-O(4)	114.9(2)	C(3)-O(4)-C(5)	112.7(2)
O(4)-C(5)-C(6)	107.7(2)	C(5)-C(6)-O(7)	111.3(2)
C(6)-O(7)-C(8)	114.5(2)	O(7)-C(8)-C(9)	108.2(2)
C(8)-C(9)-O(10)	110.0(2)	C(9)-O(10)-C(11)	113.3(2)
O(10)-C(11)-C(12)	111.1(2)	C(11)-C(12)-O(13)	111.5(2)
C(12)-O(13)-C(14)	116.6(2)	O(13)-C(14)-C(15)	124.8(2)
O(13)-C(14)-C(19)	116.9(2)	C(15)-C(14)-C(19)	118.3(2)
C(14)-C(15)-C(16)	120.6(2)	C(15)-C(16)-C(17)	120.6(2)
C(16)-C(17)-C(18)	119.3(2)	C(16)-C(17)-O(1a)	124.8(2)
C(18)-C(17)-O(1a)	115.9(2)	C(17)-C(18)-C(19)	119.7(2)
C(14)-C(19)-C(18)	121.4(2)	C(21)-O(20)-C(36a)	118.9(2)
O(20)-C(21)-C(22)	107.4(2)	C(21)-C(22)-O(23)	109.3(2)
C(22)-O(23)-C(24)	112.3(2)	O(23)-C(24)-C(25)	110.1(2)
C(24)-C(25)-O(26)	110.1(2)	C(25)-O(26)-C(27)	112.4(2)
O(26)-C(27)-C(28)	109.4(2)	C(27)-C(28)-O(29)	109.6(2)
C(28)-O(29)-C(30)	112.7(2)	O(29)-C(30)-C(31)	108.9(2)
C(30)-C(31)-O(32)	107.6(2)	C(31)-O(32)-C(33)	118.8(2)
O(32)-C(33)-C(34)	116.2(2)	O(32)-C(33)-C(38)	124.4(2)
C(34)-C(33)-C(38)	119.4(2)	C(33)-C(34)-C(35)	120.8(2)
C(34)-C(35)-C(36)	120.1(2)	C(35)-C(36)-C(37)	119.0(2)
C(35)-C(36)-O(20a)	124.4(2)	C(37)-C(36)-O(20a)	116.6(2)
C(36)-C(37)-C(38)	121.4(2)	C(33)-C(38)-C(37)	119.3(2)

TABLE 7.4. Anisotropic temperature factors ($Å^2 \times 10^3$)

atom	U_{11}	U_{22}	U_{33}	U_{23}	U_{13}	U_{12}
O(1)	74(1)	49(1)	65(1)	7(1)	-7(1)	-1(1)
C(2)	71(2)	61(2)	67(2)	5(1)	8(1)	6(1)
C(3)	67(2)	67(2)	67(2)	-1(1)	9(1)	-2(1)
C(4)	69(1)	61(1)	68(1)	4(1)	15(1)	-5(1)
C(5)	69(2)	58(2)	75(2)	1(1)	17(1)	-10(1)
C(6)	69(2)	53(2)	114(2)	-2(2)	32(2)	-0(1)
O(7)	56(1)	66(1)	85(1)	7(1)	19(1)	1(1)
C(8)	57(2)	60(2)	78(2)	-15(1)	2(1)	-2(1)
C(9)	71(2)	60(2)	55(1)	-14(1)	9(1)	-3(1)
O(10)	64(1)	60(1)	63(1)	-20(1)	25(1)	-14(1)
C(11)	74(2)	48(1)	56(1)	-1(1)	28(1)	2(1)
C(12)	61(2)	43(2)	65(2)	0(1)	18(1)	-3(1)
O(13)	61(1)	45(1)	63(1)	-5(1)	13(1)	6(1)
C(14)	51(1)	47(2)	47(1)	2(1)	18(1)	3(1)
C(15)	65(2)	47(1)	74(2)	6(1)	13(1)	4(1)
C(16)	62(2)	45(2)	77(2)	10(1)	-0(1)	6(1)
C(17)	60(1)	46(1)	48(1)	5(1)	11(1)	0(1)
C(18)	69(2)	41(1)	54(1)	1(1)	12(1)	7(1)
C(19)	63(2)	48(2)	53(1)	4(1)	8(1)	16(1)
O(20)	83(1)	39(1)	59(1)	-4(1)	-8(1)	4(1)
C(21)	62(2)	52(1)	56(1)	3(1)	16(1)	3(1)
C(22)	57(1)	65(2)	56(1)	-1(1)	13(1)	-4(1)
O(23)	56(1)	49(1)	49(1)	-7(1)	10(1)	-10(1)
C(24)	61(2)	45(1)	47(1)	2(1)	5(1)	-15(1)
C(25)	67(2)	40(1)	51(1)	0(1)	9(1)	-8(1)
O(26)	60(1)	44(1)	55(1)	9(1)	16(1)	3(1)
C(27)	57(1)	41(1)	57(1)	-8(1)	9(1)	-5(1)
C(28)	59(1)	49(2)	46(1)	-10(1)	12(1)	-8(1)
C(29)	63(1)	42(1)	43(1)	-1(1)	14(1)	-11(1)
C(30)	59(1)	50(1)	55(1)	7(1)	14(1)	-6(1)
C(31)	59(2)	46(1)	57(1)	6(1)	15(1)	0(1)
O(32)	55(1)	40(1)	78(1)	-8(1)	12(1)	-2(1)
C(33)	60(2)	36(1)	50(1)	2(1)	22(1)	-1(1)
C(34)	58(1)	37(1)	64(2)	-4(1)	21(1)	4(1)
C(35)	53(1)	45(1)	60(1)	1(1)	10(1)	6(1)
C(36)	62(1)	34(1)	47(1)	1(1)	11(1)	-1(1)
C(37)	77(2)	40(1)	65(2)	-4(1)	17(1)	14(1)
C(38)	56(1)	44(1)	66(2)	-3(1)	13(1)	6(1)

The anisotropic temperature factor exponent takes the form:

$$-2\pi^2(h^2a^{*2}U_{11} + \ldots + 2\,hka^*b^*U_{12}\cos\gamma^* + \ldots)$$

TABLE 7.5. Coordinates ($\times 10^4$) and temperature factors ($\AA^2 \times 10^3$)

Atom	x	y	z	U
H(2a)	-5363	4129	4927	79
H(2b)	-4526	4127	4081	79
H(3a)	-4302	3540	3404	78
H(3b)	-4079	3148	4413	78
H(5a)	-4770	3479	2305	76
H(5b)	-3520	3382	3295	76
H(6a)	-4604	2505	1623	89
H(6b)	-3473	2338	2684	89
H(8a)	-4078	2921	52	73
H(8b)	-4028	3545	723	73
H(9a)	-2853	3596	-602	75
H(9b)	-1937	3085	95	75
H(11a)	-383	3779	172	64
H(11b)	-1010	4442	-35	64
H(12a)	1094	4344	1303	64
H(12b)	331	4110	2129	64
H(15)	2150	4574	3187	66
H(16)	3739	5169	4404	71
H(18)	1750	6739	3263	63
H(19)	157	6140	2055	61
H(21a)	-79	4157	5344	63
H(21b)	710	4331	4504	63
H(22a)	-883	3608	3679	64
H(22b)	-280	3138	4655	64
H(24a)	11	2419	3313	60
H(24b)	-516	2886	2314	60
H(25a)	917	2127	1984	59
H(25b)	1999	2476	2888	59
H(27a)	3078	2730	1583	60
H(27b)	2060	2393	606	60
H(28a)	1610	3379	-304	62
H(28b)	2992	3130	-222	62
H(30a)	3620	4168	-374	64
H(30b)	2284	4438	-366	64
H(31a)	3308	4941	1352	63
H(31b)	3774	5192	344	63
H(34)	7305	4452	2378	59
H(35)	8787	5092	3621	63
H(37)	6082	6415	3290	65
H(38)	4587	5778	2056	61

TABLE 7.6. Coordinates ($\times 10^4$) and temperature factors ($\AA^2 \times 10^3$).

Atom	x	y	z	U
O(1)	2843(4)	5574(3)	7379(2)	82(2)*
C(2)	3965(6)	6306(5)	7843(3)	84(3)*
C(3)	3519(7)	6880(5)	8435(3)	94(3)*
O(4)	2980(4)	6024(3)	8826(2)	82(2)*
C(5)	2645(8)	6600(6)	9416(3)	105(3)*
C(6)	1828(7)	5737(6)	9737(3)	98(3)*
O(7)	2494(4)	4968(3)	10001(2)	76(2)*
C(8)	1735(7)	4193(7)	10392(3)	107(3)*
C(9)	2421(9)	3345(6)	10636(3)	126(4)*
O(10)	2582(7)	2587(4)	10081(2)	168(4)*
C(11)	2515(11)	1424(6)	10196(4)	148(5)*
C(12)	3208(14)	827(10)	9634(5)	116(6)*
C(12')	1807(17)	502(13)	9517(7)	89(7)*
O(13)	2489(5)	756(4)	9071(2)	118(2)*
C(14)	2562(6)	114(5)	8473(3)	75(2)*
C(15)	3740(5)	135(5)	8289(3)	76(2)*
C(16)	3786(5)	-457(4)	7668(3)	72(2)*
C(17)	2667(6)	-1090(5)	7220(3)	70(2)*
O(18)	2834(4)	-1669(4)	6618(2)	87(2)*
C(19)	1722(5)	-2368(5)	6145(3)	82(3)*
C(20)	2151(6)	-3015(5)	5576(3)	82(3)*
O(21)	2768(4)	-2214(3)	5178(2)	74(2)*
C(22)	3157(6)	-2833(5)	4627(3)	87(3)*
C(23)	4094(6)	-1976(5)	4348(3)	85(3)*
O(24)	3493(3)	-1160(3)	4056(2)	68(1)*
C(25)	4373(5)	-265(5)	3810(3)	78(3)*
C(26)	3682(6)	572(5)	3532(3)	75(2)*
O(27)	3220(3)	1164(3)	4062(2)	67(1)*
C(28)	2650(6)	2049(5)	3833(3)	78(2)*
C(29)	2199(6)	2653(5)	4417(3)	78(3)*
O(30)	3604(4)	3445(3)	4890(2)	86(2)*
C(31)	3129(6)	3904(4)	5500(3)	68(2)*
C(32)	1939(5)	3872(4)	5674(3)	64(2)*
C(33)	1886(5)	4452(4)	6305(3)	64(2)*
C(34)	3004(5)	5063(4)	6764(3)	61(2)*
C(35)	1441(6)	-504(5)	8032(3)	83(3)*
C(36)	1478(6)	-1126(5)	7398(3)	81(3)*
C(37)	4242(5)	4527(5)	5950(3)	71(2)*
C(38)	4188(5)	5097(5)	6580(3)	70(2)*
N(1)	2928(4)	3092(3)	8350(2)	60(2)*
C(39)	3988(6)	3507(5)	8853(3)	79(3)*
C(40)	5184(6)	3554(5)	8700(3)	91(3)*
C(41)	5309(5)	3219(5)	8049(3)	85(3)*
C(42)	4210(5)	2809(4)	7539(3)	73(2)*
C(43)	3017(4)	2719(4)	7709(2)	51(2)*
C(44)	1804(5)	2228(4)	7198(2)	53(2)*
C(45)	1719(5)	1462(4)	6615(2)	63(2)*
C(46)	568(6)	1040(5)	6161(3)	74(3)*
C(47)	-489(6)	1398(5)	6293(3)	81(3)*
C(48)	-399(5)	2156(4)	6885(3)	67(2)*
N(2)	739(4)	2564(3)	7322(2)	54(2)*
C(49)	849(5)	3415(4)	7955(2)	60(2)*
C(50)	1637(5)	3036(5)	8520(2)	64(2)*
O(51)	2350(4)	146(3)	5234(2)	81(2)*
F(1)	-2109(2)	1248(1)	8616(1)	79(1)*
F(11)	-1121(4)	1048(3)	8130(2)	126(2)*

TABLE 7.6. cont/d.

F(12)	-1248(5)	1059(6)	9237(3)	201(3)*
F(13)	-3015(5)	1426(4)	7973(2)	150(2)*
F(14)	-1384(5)	2625(4)	8779(2)	156(2)*
F(15)	-3106(4)	1501(5)	9064(2)	161(3)*
F(16)	-2856(4)	-111(4)	8431(2)	141(2)*
F(2)	8358(2)	5390(1)	7317(1)	74(1)*
F(21)	9254(7)	5475(6)	7944(2)	218(4)*
F(22)	7367(4)	5251(4)	6635(2)	148(2)*
F(23)	7252(4)	5592(4)	7704(2)	151(3)*
F(24)	9373(5)	5054(6)	6929(3)	192(4)*
F(25)	8800(5)	6733(4)	7313(4)	195(3)*
F(26)	7825(6)	3994(4)	7269(3)	187(3)*

* Equivalent isotropic U defined as one third of the trace of the orthogonalised U_{ij} tensor

TABLE 7.7. Bond lengths (Å)

O(1)-C(2)	1.420(6)	O(1)-C(34)	1.362(6)
C(2)-C(3)	1.496(9)	C(3)-O(4)	1.412(7)
O(4)-C(5)	1.430(8)	C(5)-C(6)	1.450(9)
C(6)-O(7)	1.413(9)	O(7)-C(8)	1.433(8)
C(8)-C(9)	1.459(12)	C(9)-O(10)	1.397(9)
O(10)-C(11)	1.389(9)	C(11)-C(12)	1.626(17)
C(11)-C(12')	1.589(14)	C(12)-O(13)	1.252(12)
C(12')-O(13)	1.263(18)	O(13)-C(14)	1.361(7)
C(14)-C(15)	1.373(9)	C(14)-C(35)	1.362(7)
C(15)-C(16)	1.365(8)	C(16)-C(17)	1.370(7)
C(17)-O(18)	1.373(7)	C(17)-C(36)	1.376(9)
O(18)-C(19)	1.410(6)	C(19)-C(20)	1.490(9)
C(20)-O(21)	1.411(7)	O(21)-C(22)	1.424(7)
C(22)-C(23)	1.465(8)	C(23)-O(24)	1.412(8)
O(24)-C(25)	1.418(7)	C(25)-C(26)	1.477(9)
C(26)-O(27)	1.419(7)	O(27)-C(28)	1.413(7)
C(28)-C(29)	1.501(9)	C(29)-O(30)	1.404(6)
O(30)-C(31)	1.379(7)	C(31)-C(32)	1.375(9)
C(31)-C(37)	1.366(7)	C(32)-C(33)	1.379(8)
C(33)-C(34)	1.375(7)	C(34)-C(38)	1.376(8)
C(35)-C(36)	1.399(8)	C(37)-C(38)	1.374(8)
N(1)-C(39)	1.349(6)	N(1)-C(43)	1.335(6)
N(1)-C(50)	1.472(7)	C(39)-C(40)	1.361(10)
C(40)-C(41)	1.356(9)	C(41)-C(42)	1.384(7)
C(42)-C(43)	1.364(8)	C(43)-C(44)	1.474(6)
C(44)-C(45)	1.361(6)	C(44)-N(2)	1.349(7)
C(45)-C(46)	1.364(7)	C(46)-C(47)	1.357(10)
C(47)-C(48)	1.370(7)	C(48)-N(2)	1.336(6)
N(2)-C(49)	1.486(6)	C(49)-C(50)	1.488(7)
P(1)-F(11)	1.591(5)	P(1)-F(12)	1.510(6)
P(1)-F(13)	1.563(5)	P(1)-F(14)	1.572(4)
P(1)-F(15)	1.561(5)	P(1)-F(16)	1.561(4)
P(2)-F(21)	1.504(5)	P(2)-F(22)	1.568(5)
P(2)-F(23)	1.568(5)	P(2)-F(24)	1.536(6)
P(2)-F(25)	1.522(5)	P(2)-F(26)	1.573(5)

TABLE 7.9. Anisotropic temperature factors ($Å^2 \times 10^3$)

atom	U_{11}	U_{22}	U_{33}	U_{23}	U_{13}	U_{12}
O(1)	90(3)	98(3)	61(2)	15(2)	20(2)	29(2)
C(2)	111(5)	69(4)	74(4)	10(3)	20(3)	25(3)
C(3)	139(5)	64(4)	82(4)	12(3)	19(4)	31(4)
O(4)	126(3)	72(2)	58(2)	12(2)	22(2)	44(2)
C(5)	175(7)	90(5)	68(4)	7(4)	61(4)	65(5)
C(6)	128(5)	108(5)	74(4)	11(4)	28(4)	62(4)
O(7)	96(3)	82(3)	53(2)	5(2)	14(2)	29(2)
C(8)	131(6)	117(6)	60(4)	-2(4)	35(4)	7(5)
C(9)	236(9)	79(5)	65(4)	4(3)	47(5)	38(5)
O(10)	372(9)	78(3)	72(3)	17(2)	87(4)	64(4)
C(11)	297(11)	86(5)	78(5)	25(4)	59(6)	63(6)
C(12)	184(12)	95(8)	84(7)	36(6)	23(8)	58(8)
C(12')	143(13)	73(10)	67(9)	11(7)	52(10)	40(9)
O(13)	177(5)	92(3)	99(3)	4(3)	51(3)	52(3)
C(14)	103(4)	60(3)	72(3)	16(3)	29(3)	28(3)
C(15)	88(4)	62(3)	79(4)	15(3)	18(3)	17(3)
C(16)	74(4)	57(3)	84(4)	14(3)	21(3)	9(3)
C(17)	91(4)	60(3)	69(4)	19(3)	34(3)	25(3)
O(18)	89(3)	101(3)	72(2)	7(2)	28(2)	21(2)
C(19)	91(4)	77(4)	81(4)	22(3)	21(3)	19(3)
C(20)	106(4)	70(4)	75(4)	16(3)	22(3)	28(3)
O(21)	108(3)	59(2)	70(2)	22(2)	30(2)	36(2)
C(22)	144(5)	71(4)	69(4)	14(3)	35(4)	61(4)
C(23)	118(5)	93(4)	71(4)	23(3)	34(3)	65(4)
O(24)	84(2)	63(2)	69(2)	17(2)	19(2)	35(2)
C(25)	87(4)	67(4)	90(4)	11(3)	36(3)	31(3)
C(26)	109(4)	66(3)	66(3)	16(3)	35(3)	37(3)
O(27)	97(2)	61(2)	55(2)	12(2)	21(2)	38(2)
C(28)	103(4)	71(4)	70(4)	13(3)	16(3)	41(3)
C(29)	100(4)	70(4)	75(4)	7(3)	17(3)	41(3)
O(30)	89(3)	80(3)	91(3)	-1(2)	28(2)	31(2)
C(31)	88(4)	55(3)	74(4)	8(3)	31(3)	35(3)
C(32)	72(4)	54(3)	72(4)	18(3)	17(3)	25(3)
C(33)	77(4)	59(3)	72(4)	26(3)	31(3)	30(3)
C(34)	81(4)	61(3)	54(3)	18(3)	20(3)	32(3)
C(35)	88(4)	80(4)	94(4)	21(3)	40(3)	32(3)
C(36)	83(4)	81(4)	86(4)	23(3)	28(3)	25(3)
C(37)	72(4)	69(4)	76(4)	10(3)	19(3)	27(3)
C(38)	73(3)	70(3)	71(3)	18(3)	11(3)	26(3)
N(1)	70(3)	54(2)	52(3)	13(2)	4(2)	16(2)
C(39)	85(4)	73(4)	62(4)	10(3)	-12(4)	10(3)
C(40)	74(4)	81(4)	107(5)	35(4)	-12(4)	9(3)
C(41)	64(3)	77(4)	123(5)	44(3)	15(3)	25(3)
C(42)	78(4)	64(3)	88(4)	27(3)	24(3)	30(3)
C(43)	65(3)	47(3)	48(3)	15(2)	13(2)	22(2)
C(44)	68(3)	52(3)	47(3)	13(2)	15(2)	25(2)
C(45)	85(4)	58(3)	51(3)	5(2)	17(3)	29(3)
C(46)	107(5)	58(3)	51(3)	-4(3)	9(3)	23(3)
C(47)	82(4)	92(4)	56(3)	3(3)	-7(3)	18(3)
C(48)	67(3)	72(4)	60(3)	7(3)	9(3)	20(3)
N(2)	65(3)	55(2)	41(2)	7(2)	8(2)	18(2)
C(49)	70(3)	63(3)	55(3)	9(3)	17(3)	31(3)
C(50)	78(3)	67(3)	50(3)	7(2)	17(3)	24(3)
O(51)	112(3)	76(2)	72(2)	17(2)	31(2)	45(2)
P(1)	87(1)	80(1)	70(1)	19(1)	17(1)	20(1)
F(11)	118(3)	106(3)	156(4)	-5(2)	59(3)	26(2)

TABLE 7.10. Coordinates ($\times 10^4$) and temperature factors ($Å^2 \times 10^3$)

Atom	x	y	z	U
H(2a)	4519	5823	7999	94
H(2b)	4435	6912	7623	94
H(3a)	2871	7264	8267	108
H(3b)	4250	7468	8720	108
H(5a)	3429	7010	9737	126
H(5b)	2186	7169	9281	126
H(6a)	1076	5283	9404	116
H(6b)	1556	6160	10103	116
H(8a)	1592	4485	10776	124
H(8b)	911	3759	10111	124
H(9a)	1924	2874	10913	151
H(9b)	3260	3778	10901	151
H(11a)	2929	1425	10661	177
H(11b)	1612	953	10134	177
H(11c)	3367	1326	10386	177
H(11d)	2025	1251	10562	177
H(12a)	3335	68	9736	143
H(12b)	4103	1364	9667	143
H(12c)	941	590	9380	110
H(12d)	1718	-313	9599	110
H(15)	4534	568	8597	93
H(16)	4616	-429	7543	85
H(19a)	1196	-2936	6367	96
H(19b)	1224	-1856	5968	96
H(20a)	1405	-3584	5291	99
H(20b)	2753	-3430	5764	99
H(22a)	3553	-3426	4787	107
H(22b)	2407	-3218	4277	107
H(23a)	4415	-2405	4004	101
H(23b)	4808	-1542	4708	101
H(25a)	5072	170	4178	92
H(25b)	4720	-638	3457	92
H(26a)	2957	133	3179	93
H(26b)	4267	1155	3346	93
H(28a)	3281	2631	3672	92
H(28b)	1920	1681	3469	92
H(29a)	1687	2060	4630	93
H(29b)	1684	3161	4253	93
H(32)	1150	3448	5359	78
H(33)	1053	4429	6425	73
H(35)	615	-513	8158	97
H(36)	687	-1570	7092	94
H(37)	5073	4566	5824	82
H(38)	4979	5520	6893	83
H(39)	3900	3765	9311	94
H(40)	5945	3826	9055	108
H(41)	6156	3266	7943	100
H(42)	4286	2592	7074	83
H(45)	2471	1217	6524	79
H(46)	504	495	5752	84
H(47)	-1298	1190	5972	93
H(48)	-1150	2393	6986	79
H(49a)	1274	4215	7902	72
H(49b)	-1	3387	8051	72
H(50a)	1217	2231	8567	73
H(50b)	1728	3565	8940	73
H(51a)	2861(49)	540(49)	9932(19)	97
H(51b)	2502(45)	-432(18)	5220(24)	97

7.4 REFERENCES.

1. See chapter 6.
2. G.M. Sheldrick, SHELXTL, An integrated system for solving, refining, and displaying crystal structures from diffraction data, University of Göttingen, Federal Republic of Germany, 1981.
3. J.D. Owen, Acta. Cryst., 1984, C40, 951.
4. See Chapter 5.

   See Chapter 4.

   See Chapter 3.

   See Chapter 2.

   H.M. Colquhoun, E.P. Gooding, J.M. Maud, J.F. Stoddart, D.J. Williams and J.B. Wolstenholme, J. Chem. Soc., Chem. Commun., 1983, 1140.

   H.M. Colquhoun, E.P. Gooding, J.M. Maud, J.F. Stoddart, D.J. Williams, J.B. Wolstenholme, J.Chem. Soc. Perkin Trans. 2, 1985, 607.
5. J. E. Derry, and T. A. Hamor, Nature, 1969, 221, 464.

   P.D. Sullivan, and M.L. Williams, J. Am. Chem. Soc., 1972, 98, 1711.

   T. Sundaresan, and S.C. Wallwork, Acta. Cryst., 1972, B28, 3065.
6. R. Foster, 'Organic Charge-Transfer Complexes,' Academic Press, London, 1969.
7. H. Shahriari-Zavareh, and J.F. Stoddart, unpublished results.

CHAPTER 8

The crystal structure of the complex of 1,4,7,10,13,20,23,26,29,32-decaoxa[13.13]paracyclophane (bisparaphenylene-34-crown-10) with paraquat.

8.1 INTRODUCTION

Molecular 1:1 complexes with paraquat have been claimed for both receptor 8[1] in acetone and a speleand[2] type chiral marcocyclic host containing two tartaric acid groups and two diphenylmethane fragments[3] in aqueous solution. Common features of these two receptors are a preorganised cavity and the presence of phenyl groups orientated more or less perpendicular to the average plane of the ring. The quinol-based receptor 9 has also been demonstrated to possess these features[4].

Our research has led to the evaluation of 9 as a molecular receptor for paraquat for reasons discussed earlier[4]. This chapter reports the X-ray structural analysis of [9.paraquat] which has been carried out to investigate the mode of binding of 9 towards paraquat. The stability constant of the 1:1 complex formed in solution will also be discussed.

8.2 EXPERIMENTAL

Red crystals of [9.paraquat][PF_6]$_2$(C_3H_6O)$_2$ were obtained from a acetone solution by vapour diffusion with n-pentane. A crystal of dimensions 0.17 x 0.30 x 0.50 mm was used for unit cell and intensity measurements.

Crystal data: $C_{28}H_{40}O_{10}.C_{12}H_{14}N_2.P_2F_{12}(C_3H_6O)_2$, M = 1129, triclinic, a = 10.204(2), b = 11.562(2), c = 13.835(5) Å, α = 105.59(2), β = 98.70(2), γ = 115.47(1)°, U = 1350 Å^3, space group $P\bar{1}$, Z = 1 (the

[$\underset{\sim}{9}$.paraquat] complex possesses a crystallographic centre of symmetry), $\underline{D}_c$ = 1.39 g cm^{-3}, $\underline{F}(000)$ = 590, $\mu(Cu\text{-}\underline{K}_\alpha)$ = 16.10 cm^{-1}.

Refined unit-cell parameters were obtained by centering 18 reflections on a Nicolet R3m diffractometer. 2679 unique reflections ($\theta < 50^o$) were measured with Cu-$\underline{K}_\alpha$ radiation (graphite monochromator) using the omega-scan routine. Of these 2369 had $|\underline{F}_o| > 3\sigma(|\underline{F}_o|)$ and were considered to be observed. The net count of two reflections, the -3 2 -1 and the 0 2 1, measured as references every 50 reflections did not alter significantly during the data collection indicating that no deterioration of the crystal had occurred. The data were brought to a uniform arbitrary scale by the use of these reflections and Lorentz and polarisation corrections were applied.

The structure was solved by direct methods. An initial starting set comprising three origin defining reflections, one $\Sigma 1$ reflection, three reflections which were weak links in the convergence mapping together with 5 automatically selected terms was used. The initial phase expansion (256 permutations) was with 196 $\underline{E}$'s > 1.80 using 851 TPR. This was subsequently expanded to 406 probable phases with $\underline{E}$'s > 1.52 using 1678 TPR. The figures of merit for the best phase solution were NQEST = -0.699, RA(1) = 0.004, RA(2) = 0.031. This solution gave plausible positions for all the expected non-hydrogen atoms in the structure. The subsequent $\Delta\underline{F}$-map revealed the presence of an additional acetone molecule. The non-hydrogen atoms were refined anisotropically. The methylene and phenyl hydrogens were placed at calculated positions (C-H = 0.96 Å), assigned isotropic thermal

parameters, $\underline{U}(H) = 1.2\ \underline{U}_{eq}(C)$ and allowed to ride on their parent carbon atoms. The methyl protons on the paraquat and acetone molecules were located from a $\Delta\underline{F}$-map and these groups refined as rigid bodies.

Refinement using $\underline{F}$ magnitudes was by block-cascade full-matrix least squares (344 variable parameters) and converged to $\underline{R} = 0.080$, $\underline{R}_w = 0.095$, $[w^{-1} = \sigma^2(F) + 0.0013F^2]$. The largest parameter shift/e.s.d. was 0.098, the mean shift/e.s.d. was 0.013. The residual electron density in the final difference map was within -0.29 and 0.69 eA^{-3}.

All computations were carried out on an Eclipse S140 computer using the SHELXTL[5] program system.

8.3 DISCUSSION

The final fractional atomic coordinates, anisotropic thermal parameters, bond lengths and bond angles for the non-hydrogens atoms are shown in Tables 8.1 - 8.4. The positions and isotropic temperature factors of the hydrogen atoms are listed in Table 8.5.

The torsional angles associated with the polyether chains of the [9.paraquat] are shown beside the relevant C-C and C-O bonds in the skeletal drawing of the structure reproduced in figure 8.1. This figure also provides details of the crystallographic numbering scheme.

The conformation of receptor 9 on complexation of paraquat remains virtually unchanged from that in its uncomplexed form 9b[4].

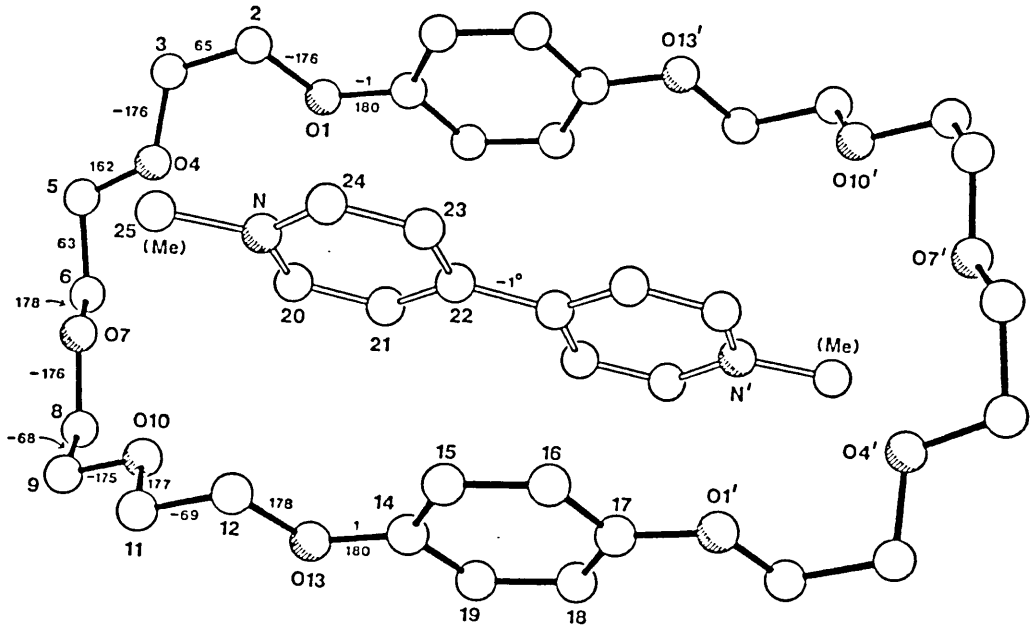


Figure 8.1. The skeletal representation of the solid-state structure of [9.paraquat].

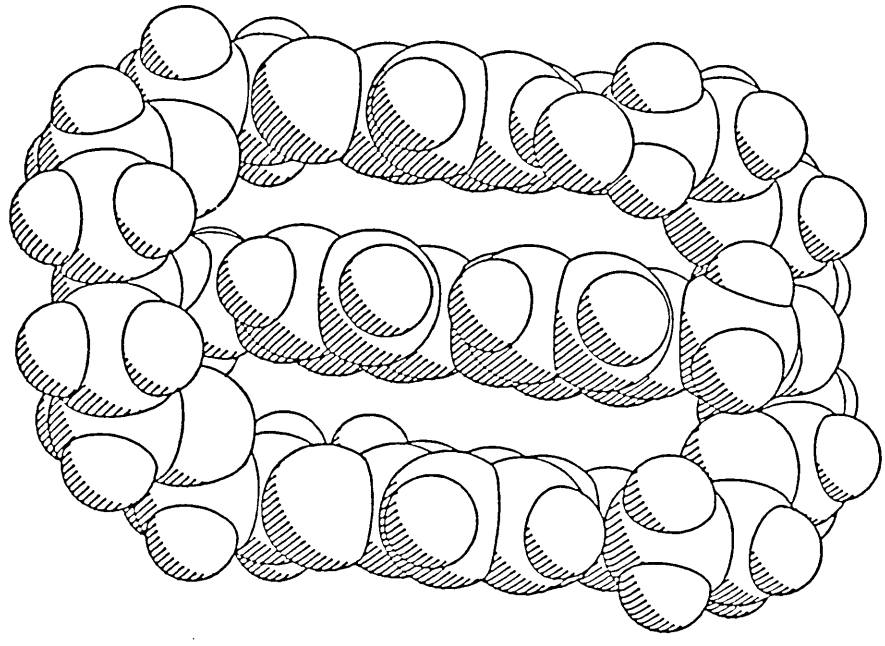


Figure 8.2. The space-filling representation of the solid-state structure of [9.paraquat].

The paraquat dication is planar. This is the most common conformation observed from X-ray structure analyses[6,7], though torsional angles of 20 and 50° between the two pyridine rings have been observed[8].

The interaction between the oval shaped receptor 9 and paraquat seems to be mainly charge transfer. The paraquat dication is sandwiched between the two parallel quinol units (separation 7.4 Å), though it is not parallel to them, being tilted by 7.7°. The distance of 3.5 Å between the mean plane of one of the quinol units and the nearest overlapping atom of the paraquat, C(21'), is just within charge transfer interaction range[9]. This separation between the paraquat dication and the quinol units is similar to the separation observed between paraquat with hydroquinone[6] and quinol[7] (3.38 and 3.30 Å respectively) in charge transfer layer structures.

The paraquat dication has its central axis (C(25)...C(25') tilted ~ 28° with respect to the O...O axis of the quinol units (see figure 8.4). This compares with an angle of 60° to the O...O axis in its complexes with hydroquinone[6] and quinol[7]. This tilting of the paraquat could be due to the cavity length of the receptor (~ 10.6 Å) which is too short to accomodate a horizontally aligned dication (van der Waals radius length ~ 12.6 Å). The use of a host with an enlarged polyether chain might allow the central axis of the dication to align itself with the O...O axis of the quinol units and hence achieve increased overlap for charge transfer interactions.

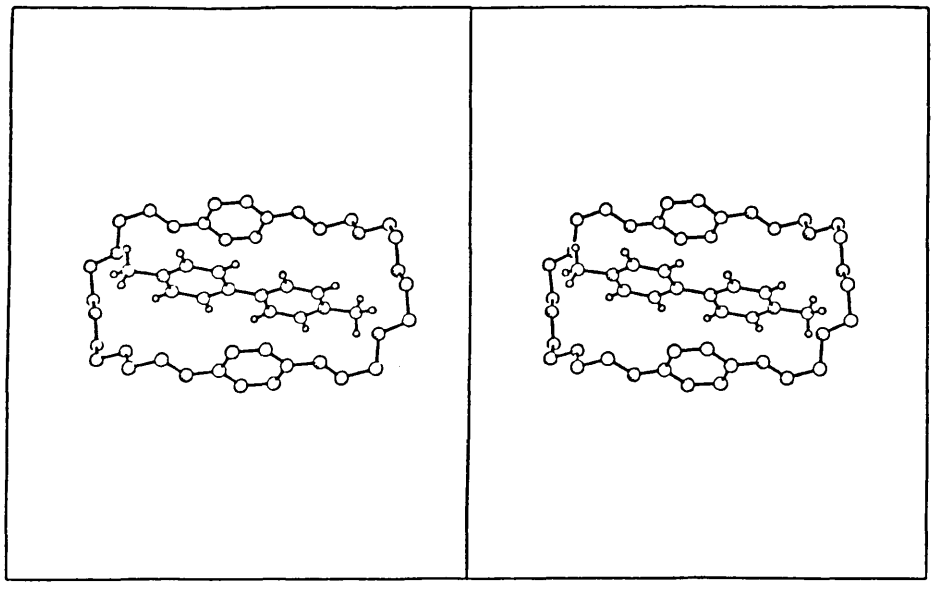


Figure 8.3. The stereo-pair representation of the solid-state structure of [9.paraquat].

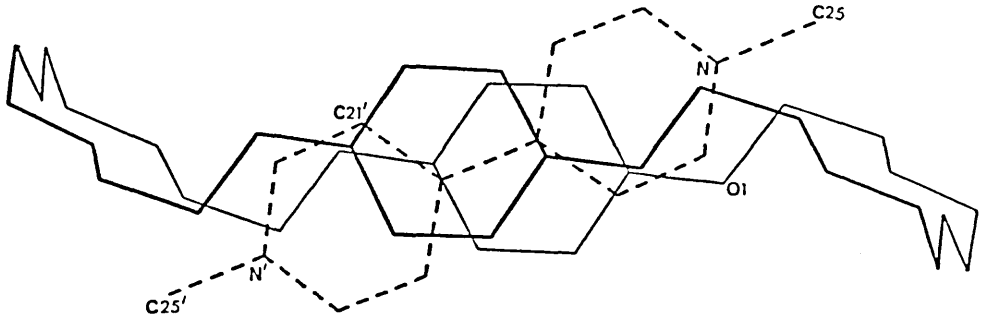


Figure 8.4. Side-on view (view normal to mean plane of paraquat dication) of the skeletal representation of the solid-state structure of [9.paraquat]

The mode of binding in this complex contrasts significantly with that in [9.diquat]^{4}. In the present structure there is no linear alignment of the nitrogens of paraquat with the aryl oxygens of the receptor. The shortest contact between any of the receptor oxygens to the paraquat nitrogens is 3.53 Å which infers that there is probably little stabilisation of the complex by O...N electrostatic interactions. There are eight contacts of less than 3.4 Å between the paraquat carbon atoms and the hosts oxygens [see table 8.6]. Four of these contacts involve the ortho paraquat atom, C(20). Current theory suggests[10] that the some of positive charge may be concentrated towards the ortho positions and therefore these contacts could provide electrostatic stabilisation of the complex. There are no hydrogen bond interactions between the host and paraquat.

The crystal packing reveals that the shortest contact between the [9.paraquat] and a PF_6 anion is 3.10 Å between C(24) and a symmetry related F(5). The shortest contact between [9.paraquat] and a acetone molecule is 3.21 Å between O(26) and the diquat atom C(24). This interaction is possible as the C(24) lies outside the cavity of the host and does not appear to interact with it. In both these short contacts there are no hydrogen bonding interactions. There are no significant contacts between symmetry related [9.paraquat] complexes of less than normal van der Waals distances.

Evidence from solution studies[11] of the treatment of the UV charge transfer absorption bands indicate the presence of a 1:1 complex in solution. The complex stability (ΔG^{o} = -5.60 Kcal mol^{-1}) of

TABLE 8.6. Selected host-guest contact distances, and relevant hydrogen contact distances and angles where appropriate, in order of increasing $X^a...O$ distance for [9.paraquat].

$X^a...O$	$R(X^a...O)$ (Å)	$R(H...O)$ (Å)	$\psi(^o)^b$	$\theta(^o)^c$
C(25)-O(4)	3.25			
C(20)-O(10)	3.28			
C(25)-O(7)	3.33			
C(20)-O(4)	3.36			

[a] Carbon or Nitrogen atom of the diquat dication.
[b] Angles between COC planes and HO vectors.
[c] C-H...O angles.

[9.paraquat] is far greater that the value obtained for the [8.paraquat] complex[1]. The stability of the [9.paraquat] complex is similar to that of the [1.diquat][12] complex.

TABLE 8.1. Coordinates ($\times 10^4$) and temperature factors ($Å^2 \times 10^3$)

Atom	x	y	z	U
O(1)	4530(4)	5708(4)	-3327(3)	86(2)*
C(2)	2998(7)	5146(6)	-4944(5)	80(4)*
C(3)	2748(8)	4123(6)	-4979(5)	89(4)*
O(4)	2896(5)	3034(4)	-4765(3)	94(3)*
C(5)	2797(8)	2039(6)	-5638(4)	91(4)*
C(6)	3428(7)	1222(7)	-5309(5)	87(4)*
O(7)	2561(4)	493(4)	-4751(3)	70(2)*
C(8)	3097(7)	-342(7)	-4462(5)	87(4)*
C(9)	2115(8)	-1151(7)	-3949(5)	94(4)*
O(10)	2232(5)	-289(4)	-2967(3)	82(2)*
C(11)	1420(7)	-1017(7)	-2391(5)	92(4)*
C(12)	1671(7)	-46(7)	-1348(5)	81(4)*
O(13)	3215(4)	529(4)	-735(3)	90(3)*
C(14)	3719(6)	1489(6)	262(4)	66(3)*
C(15)	2860(6)	1957(6)	745(4)	69(3)*
C(16)	3467(6)	2876(6)	1759(4)	72(3)*
C(17)	4978(6)	3383(5)	2317(4)	65(3)*
C(18)	5869(6)	2947(6)	1837(4)	71(3)*
C(19)	5230(7)	2008(6)	816(5)	79(4)*
N	2055(4)	2798(4)	-2375(3)	50(2)*
C(20)	3458(6)	3029(6)	-2306(4)	71(3)*
C(21)	4637(6)	3898(6)	-1390(4)	68(3)*
C(22)	4390(5)	4547(4)	-497(3)	46(2)*
C(23)	2912(5)	4297(5)	-616(4)	62(3)*
C(24)	1787(5)	3440(5)	-1543(4)	63(3)*
C(25)	789(6)	1800(6)	-3357(4)	69(3)*
O(26)	-1247(6)	788(5)	-1696(5)	135(4)*
C(26)	-1973(7)	1248(7)	-1299(5)	86(4)*
C(27)	-3603(8)	674(8)	-1836(5)	109(5)*
C(28)	-1300(8)	2433(8)	-265(5)	120(5)*
P(1)	8525(2)	4366(2)	7270(1)	74(1)*
F(1)	8292(5)	2880(4)	7125(4)	139(3)*
F(2)	8799(6)	5843(5)	7423(5)	163(4)*
F(3)	8284(7)	4578(6)	8359(4)	185(4)*
F(4)	8594(13)	4088(8)	6182(5)	283(9)*
F(5)	10237(5)	5020(6)	7804(6)	211(5)*
F(6)	6828(6)	3774(7)	6833(6)	235(5)*

* Equivalent isotropic U defined as one third of the trace of the orthogonalised U_{ij} tensor

TABLE 8.2. Bond lengths (Å)

O(1)-C(2)	1.421(7)	O(1)-C(17a)	1.362(6)
C(2)-C(3)	1.495(9)	C(3)-O(4)	1.431(10)
O(4)-C(5)	1.381(8)	C(5)-C(6)	1.477(13)
C(6)-O(7)	1.415(8)	O(7)-C(8)	1.409(10)
C(8)-C(9)	1.466(10)	C(9)-O(10)	1.405(8)
O(10)-C(11)	1.410(9)	C(11)-C(12)	1.476(9)
C(12)-O(13)	1.427(7)	O(13)-C(14)	1.367(6)
C(14)-C(15)	1.377(10)	C(14)-C(19)	1.388(8)
C(15)-C(16)	1.360(7)	C(16)-C(17)	1.392(8)
C(17)-C(18)	1.385(10)	C(17)-O(1a)	1.362(6)
C(18)-C(19)	1.374(7)	N-C(20)	1.321(8)
N-C(24)	1.328(7)	N-C(25)	1.480(5)
C(20)-C(21)	1.370(6)	C(21)-C(22)	1.383(8)
C(22)-C(23)	1.389(8)	C(22)-C(22a)	1.457(7)
C(23)-C(24)	1.355(6)	O(26)-C(26)	1.199(11)
C(26)-C(27)	1.474(10)	C(26)-C(28)	1.495(9)
P(1)-F(1)	1.580(6)	P(1)-F(2)	1.555(6)
P(1)-F(3)	1.564(6)	P(1)-F(4)	1.471(8)
P(1)-F(5)	1.531(5)	P(1)-F(6)	1.508(6)

TABLE 8.3. Bond Angles (deg.)

C(2)-O(1)-C(17a)	118.8(5)	O(1)-C(2)-C(3)	107.2(6)
C(2)-C(3)-O(4)	106.8(6)	C(3)-O(4)-C(5)	114.1(5)
O(4)-C(5)-C(6)	110.3(5)	C(5)-C(6)-O(7)	110.7(6)
C(6)-O(7)-C(8)	112.1(6)	O(7)-C(8)-C(9)	110.7(7)
C(8)-C(9)-O(10)	110.8(5)	C(9)-O(10)-C(11)	113.6(5)
O(10)-C(11)-C(12)	110.3(5)	C(11)-C(12)-O(13)	108.0(6)
C(12)-O(13)-C(14)	118.3(5)	O(13)-C(14)-C(15)	125.8(5)
O(13)-C(14)-C(19)	115.4(6)	C(15)-C(14)-C(19)	118.8(5)
C(14)-C(15)-C(16)	120.7(5)	C(15)-C(16)-C(17)	120.4(7)
C(16)-C(17)-C(18)	119.8(5)	C(16)-C(17)-O(1a)	115.7(6)
C(18)-C(17)-O(1a)	124.5(5)	C(17)-C(18)-C(19)	118.9(6)
C(14)-C(19)-C(18)	121.5(7)	C(20)-N-C(24)	119.2(4)
C(20)-N-C(25)	120.4(4)	C(24)-N-C(25)	120.4(4)
N-C(20)-C(21)	121.5(5)	C(20)-C(21)-C(22)	120.9(6)
C(21)-C(22)-C(23)	115.4(4)	C(21)-C(22)-C(22a)	122.3(6)
C(23)-C(22)-C(22a)	122.3(6)	C(22)-C(23)-C(24)	121.5(5)
N-C(24)-C(23)	121.5(5)	O(26)-C(26)-C(27)	120.6(6)
O(26)-C(26)-C(28)	126.2(6)	C(27)-C(26)-C(28)	116.2(7)
F(1)-P(1)-F(2)	178.5(3)	F(1)-P(1)-F(3)	91.5(4)
F(2)-P(1)-F(3)	88.6(4)	F(1)-P(1)-F(4)	87.7(5)
F(2)-P(1)-F(4)	92.2(5)	F(3)-P(1)-F(4)	174.5(5)
F(1)-P(1)-F(5)	90.8(3)	F(2)-P(1)-F(5)	87.7(4)
F(3)-P(1)-F(5)	88.9(4)	F(4)-P(1)-F(5)	96.5(6)
F(1)-P(1)-F(6)	90.7(4)	F(2)-P(1)-F(6)	90.7(4)
F(3)-P(1)-F(6)	86.4(4)	F(4)-P(1)-F(6)	88.2(6)
F(5)-P(1)-F(6)	175.2(5)		

TABLE 8.4. Anisotropic temperature factors ($Å^2 \times 10^3$)

atom	U_{11}	U_{22}	U_{33}	U_{23}	U_{13}	U_{12}
O(1)	83(3)	96(3)	85(3)	26(2)	33(2)	51(2)
C(2)	91(4)	74(4)	88(4)	37(3)	29(3)	46(3)
C(3)	109(5)	79(4)	81(4)	39(4)	25(4)	44(4)
O(4)	141(4)	81(3)	75(3)	44(2)	50(3)	59(3)
C(5)	111(5)	81(4)	68(4)	24(3)	36(4)	36(4)
C(6)	85(4)	94(4)	68(4)	11(3)	28(3)	42(4)
O(7)	73(2)	83(2)	64(2)	23(2)	24(2)	49(2)
C(8)	102(5)	100(5)	69(4)	14(4)	15(4)	73(4)
C(9)	126(6)	79(4)	76(4)	18(3)	10(4)	63(4)
O(10)	113(3)	70(2)	67(2)	22(2)	21(2)	52(2)
C(11)	87(4)	85(4)	98(5)	42(4)	8(4)	41(4)
C(12)	88(4)	96(4)	80(4)	43(4)	27(3)	55(4)
O(13)	83(3)	116(3)	76(3)	18(3)	20(2)	64(3)
C(14)	69(3)	77(4)	71(4)	37(3)	28(3)	45(3)
C(15)	65(3)	95(4)	82(4)	49(3)	32(3)	55(3)
C(16)	80(4)	90(4)	80(4)	42(3)	42(3)	58(3)
C(17)	76(4)	69(3)	70(3)	32(3)	33(3)	44(3)
C(18)	65(3)	76(4)	83(4)	30(3)	28(3)	42(3)
C(19)	76(4)	97(4)	88(4)	35(3)	40(3)	57(3)
N	45(2)	52(2)	51(2)	17(2)	12(2)	24(2)
C(20)	66(4)	85(4)	59(3)	13(3)	23(3)	42(3)
C(21)	56(3)	84(4)	58(3)	9(3)	19(3)	38(3)
C(22)	51(3)	48(3)	50(3)	23(2)	25(2)	29(2)
C(23)	61(3)	72(3)	55(3)	12(3)	20(3)	41(3)
C(24)	51(3)	72(3)	64(3)	14(3)	18(3)	36(3)
C(25)	66(4)	69(4)	57(3)	15(3)	10(3)	30(3)
O(26)	134(4)	121(4)	201(6)	80(4)	89(4)	81(4)
C(26)	92(4)	95(4)	105(5)	64(4)	55(4)	50(4)
C(27)	108(5)	124(6)	88(5)	45(4)	35(4)	46(5)
C(28)	99(6)	151(7)	87(5)	45(5)	31(4)	42(5)
F(1)	81(1)	81(1)	84(1)	38(1)	33(1)	53(1)
F(1)	164(4)	104(3)	179(4)	61(3)	59(3)	85(3)
F(2)	195(5)	112(3)	228(5)	82(4)	76(4)	101(3)
F(3)	232(6)	174(5)	113(3)	47(3)	87(4)	63(4)
F(4)	587(16)	230(7)	150(5)	114(5)	214(8)	243(9)
F(5)	72(3)	165(5)	382(10)	98(6)	40(4)	58(3)
F(6)	97(4)	210(6)	298(8)	2(6)	-37(5)	77(4)

The anisotropic temperature factor exponent takes the form:

$$-2\pi^2(h^2a^{*2}U_{11} + \ldots + 2\,hka^*b^*U_{12}\cos\gamma^* + \ldots)$$

TABLE 8.5. Coordinates ($\times 10^4$) and temperature factors ($\AA^2 \times 10^3$)

atom	x	y	z	U
H(2a)	2308	4697	-3595	95
H(2b)	2837	5867	-4052	95
H(3a)	3495	4552	-5301	98
H(3b)	1745	3763	-5441	98
H(5a)	1746	1436	-6053	101
H(5b)	3360	2480	-6052	101
H(6a)	4462	1844	-4462	93
H(6b)	3407	575	-5923	93
H(8a)	3099	-961	-5083	102
H(8b)	4116	235	-3984	102
H(9a)	2415	-1802	-3847	105
H(9b)	1075	-1640	-4392	105
H(11a)	451	-1579	-2774	102
H(11b)	1766	-1642	-2298	102
H(12a)	991	-528	-1007	95
H(12b)	1490	677	-1429	95
H(15)	1824	1463	363	80
H(16)	2848	3177	2091	82
H(18)	6915	4294	2211	81
H(19)	5842	1704	478	87
H(20)	3654	2577	-2912	80
H(21)	5647	4060	-1369	75
H(23)	2674	4740	-29	67
H(24)	774	3295	-1599	69
H(25a)	1092	1558	-3971	75
H(25b)	209	2250	-3462	75
H(25c)	176	979	-3240	75
H(27a)	-4106	514	-1314	118
H(27b)	-3862	-195	-2356	118
H(27c)	-3926	1176	-2171	118
H(28a)	-1574	3093	-379	133
H(28b)	-210	2844	-48	133
H(28c)	-1684	2154	273	133

8.4 REFERENCES

1. See chapter 6.
2. J. Canceill, A. Collet, J. Gabard, F. Kotzyba-Hibert, J.M. Lehn, Helv. Chem. Acta., 1982, 65, 1894.
3. M. Dhaenens, L. Lacombe, J.M. Lehn and J.P. Vigneron, J. Chem. Soc., Chem. Commun., 1984, 1097.
4. See chapter 7.
5. G.M. Sheldrick, SHELXTL, An integrated system for solving, refining, and displaying crystal structures from diffraction data, University of Göttingen, Federal Republic of Germany, 1981.
6. M. M. Mahmoud and S. C. Wallwork, Acta. Cryst. 1976, B32, 440.
7. M. M. Mahmoud and S. C. Wallwork, Acta. Cryst. 1981, B37, 398.
8. K. Nakamura, Y. Kai, N. Yasuoka and N. Kasai, Bull. Chem. Soc. Jpn., 1981, 54, 3300.

   C. K. Prout and P. Murray-Rust, J. Chem. Soc. 1969, A, 1520.
9. R. Foster, 'Organic Charge-Transfer Complexes,' Academic Press, London, 1969.
10. J.Burdon, M.H.B. Hayes, and M.E. Pick, J. Environ. Sci. Health, 1977, B12(1), 37.
11. H. Shahriari-Zavareh, and J.F. Stoddart unpublished work.
12. H.M. Colquhoun, E.P. Gooding, J.M. Maud, J.F. Stoddart, D.J. Williams and J.B. Wolstenholme, J. Chem. Soc., Chem. Commun., 1983, 1140.

    H.M. Colquhoun, E.P. Gooding, J.M. Maud, J.F. Stoddart, D.J. Williams, J.B. Wolstenholme, J.Chem. Soc. Perkin Trans. 2, 1985, 607.

CHAPTER 9

CONCLUSIONS

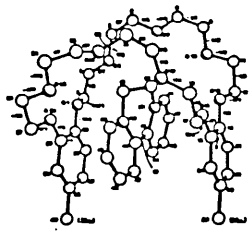
9.1 Summary

Our research in designing improved molecular receptors for the bipyridinium herbicides diquat and paraquat has been successful.

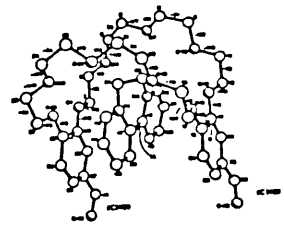
We have shown that by increasing the π-donor capability of the catechol units in receptor 2[1], an improved complex stability with diquat, compared to that of the DB30C10 complex, was achieved. The first bridged receptor 5[2] was even more successful in enhancing the complex stability with diquat. The X-ray structural analysis of 5 indicated that a reduction in the size of the apolar bridge should lead to a further enhancement of the complexation of diquat. Therefore receptor 6[3] was synthesised and has been shown to form the most stable complex, so far, with diquat in solution.

The complexation of diquat by DN30C10[4] (7) indicated that the diquat dication prefers to form linear O...N...O interactions rather than increase π-π^* overlap. This observation was further reinforced by the complexation of diquat with receptors 8[5] and 9[6], in which the formation of one O...N...O interaction predominates in contrast to any apparent increase in π-π^* overlap.

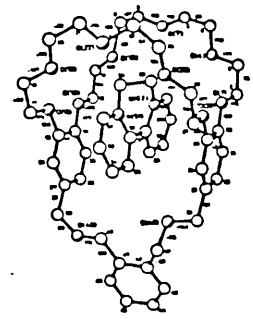
The solution evidence for the complexation of paraquat by 8 led us to believe that the 'key' to encapsulation of the paraquat dication was in achieving a near match between the separation of the aryl oxygens in a receptor with that of the nitrogens in paraquat, thus enabling at least one linear O...N...O interaction to be formed. However, we were surprised that in the X-ray structure of the



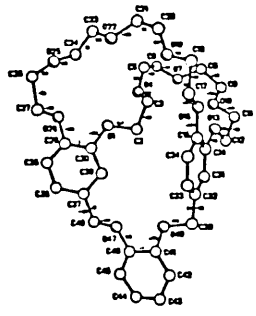
[2.diquat]



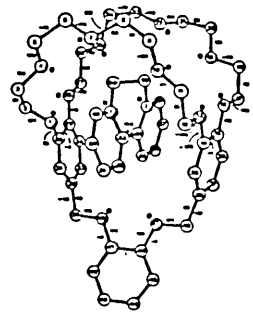
[4.diquat]



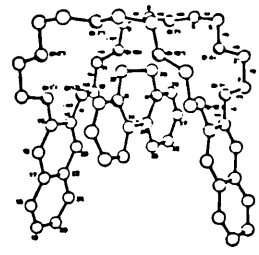
[5.diquat]



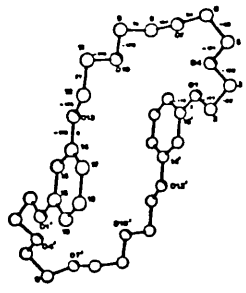
6



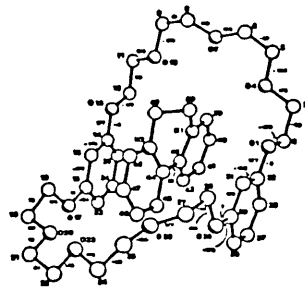
[6.diquat]



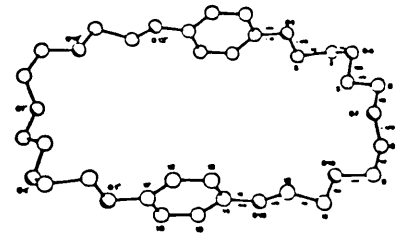
[7.diquat]



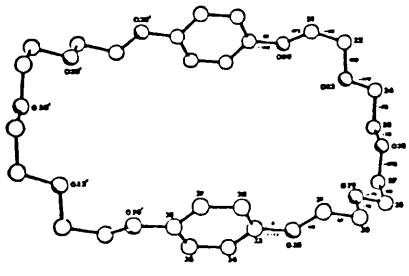
8



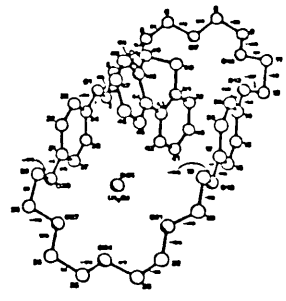
[8.diquat]



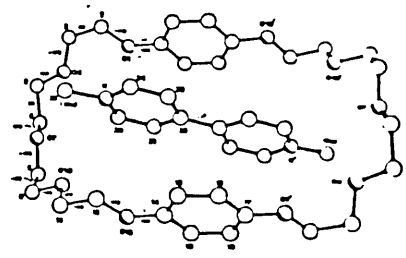
9a



9b



[9.diquat.H_2O]



[9.paraquat]

[9.paraquat] complex[7], there were no short contacts between the nitrogens of the paraquat and the quinol oxygens of the receptor, though there was still a degree of π-π^* overlap.

9.2 Charge Distribution Within the Bipyridinium Dications.

Theoretical studies[8] have indicated that the two formal positive charges associated with the diquat and paraquat dications are not located predominantly on the nitrogen atoms. The positive charges are distributed around the dications being greatest at the ortho and para positions to the nitrogens in diquat, and at the ortho position to the nitrogens in paraquat, though the nitrogens do still retain a partial positive charge. However, these theoretical calculations do not take into account changes in charge distribution within the dications which can be induced by different molecular environments.

All the diquat and paraquat complexes involving receptors 1 - 9 have short contacts (< 3.4 Å) between the ortho carbon atoms of the dication and the aryl oxygens of the receptors. These interactions may contribute to the stabilisation of these complexes.

All the diquat complexes have at least one linear O...N...O interaction. Initially we believed that this was a favourable dipole-pole electrostatic interaction between the lone pair on the aryl oxygens and a formal positive charge on the nitrogens of the diquat dication. In the light of the theoretical calculations, this interaction may now need to be termed a dipole-dipole electrostatic

interaction as we are uncertain about the amount of positive charge which resides on the nitrogen atoms.

9.3 Orientation of Charge Transfer Interactions.

A theoretical study of the relative orientations[9] of π-donors and π-acceptors in charge transfer complexes has been attempted. The charge transfer stabilisation energies were calculated for a large number of possible donor-acceptor orientations in each complex studied. The orientation of the π-donor, and the π-acceptor with the maximum charge transfer stabilisation energy was then compared with the observed X-ray structure of the complex. These comparisons revealed that in the absence of other intermolecular forces, such as hydrogen bonding, strong dipole-dipole and charge-dipole interactions, the charge transfer stabilisation energy of the complex is generally maximised. However, when these other intermolecular forces are present the charge transfer stabilisation energy is not maximised. This results in a poor agreement of the calculated donor-acceptor orientation with the observed X-ray structure. It was concluded that the other intermolecular interactions can predominate over charge transfer interactions and determine the orientation of the donor-acceptor complex. We believe that in the diquat and paraquat complexes studied, these other intermolecular forces dominate the geometry and mode of binding.

Clearly, more X-ray structures of different charge transfer complexes of both diquat and paraquat are needed before the relative strengths of the charge transfer, hydrogen bonding (C-H...O), and

electrostatic ($C^{\delta+}...O^{\delta-}$ and $N^{\delta+}...O^{\delta-}$) interactions may be ascertained and the mode of binding in diquat and paraquat complexes predicted. This approach should lead to the design of improved molecular receptors for the diquat and paraquat dications.

9.4 Conformation of the Uncomplexed Receptors.

The design of receptors with preformed cavities for encapsulation of diquat and paraquat should result in a reduction of the energy needed in reorganising the receptor prior to complexation. This with a retention of the neccessary in built binding sites should lead to enhanced complex stability.

The X-ray structure of the uncomplexed catechol-based receptor 6 revealed that it partially fills its own cavity whilst the resorcinol and quinol-based receptors are preformed. The resorcinol and quinol based receptors appear to have the optimum ring size for the formation of a preformed macrocyclic cavitity, though, interestingly the tetra-substituted $(MeO)_4$-bisparaphenylene 34-crown-10 receptor[10] is self filling. Likewise, an X-ray structure of a quinol-based 40-crown-12 macrocycle[11] has shown it too adopts a folded conformation, in this instance, more akin to that of uncomplexed DB30C10[12] than that of receptors 8 and 9.

9.5 Conclusion

Our results have demonstrated the essential and powerful role

played by X-ray crystallography in both unravelling the mode of complexation and designing improved molecular receptors for diquat and paraquat.

9.6 REFERENCES

1. See Chapter2.
2. See Chapter3.
3. See Chapter4.
4. See Chapter5.
5. See Chapter6.
6. See Chapter7.
7. See Chapter8.
8. J. Burdon, M.H.B. Hayes, and M.E. Pick, J. Environ. Sci. Health, 1977, B12(1), 37.
9. B. Mayoh, and C.K. Prout, J. Chem. Soc., Faraday 2, 1972, 1072.
10. J.D. Owen, Acta. Cryst., 1984, C40, 951.
11. A.M.Z. Slawin, and D.J. Williams, unpublished results.
12. M.A. Bush, and M.R. Truter, J. Chem. Soc., Perkin Trans. 2, 1972, 345.

PART 2

CHAPTER 10

INTRODUCTION

10.1 Enantioselective Reduction of Prochiral Aromatic Ketones.

Enantioselective reduction of prochiral aromatic ketones is currently one of the areas of research being undertaken by J.F. Stoddart and his co-workers[1]. Although NH_3BH_3, RNH_2BH_3, and R_2NHBH_3 adducts[2] exhibit excellent (>90%) chemo- and diastereo-selectivities in their reduction of RCHO and R_2CO substrates, high enantiomeric excesses (e.e.s) in the reduction of RCOR' substrates with $R^*NH_2BH_3$ adducts have been much more elusive. Thus, the rather low e.e.s (<5%), obtained[3] when BH_3 is bound to $PHCH_2C^*HMeNRR'$ and PhC^*HMeNH_2, were only slightly improved upon (to ca. 21%) by BF_3 activation[4] of the RCOR' substrates, and (to ca. 33%) by employing[3c,3d] $RC^*H(CO_2Me)NH_2$ as the chiral auxiliaries instead of R^*NH_2. More recently, $RC^*H(CH_2OH)NH_2$ auxiliaries have afforded[5] e.e.s approaching 100% and RNH_2BH_3, $RR'NHBH_3$ and $R_2R'NBH_3$ adducts modified[6] with axially chiral 2,2'-dihydroxy-6,6'-dimethylbiphenyl are almost (e.e.s < 84%) as good. However, in all these reagents, the chiral auxiliary is covalently bonded to the boron atom and hence not easily recycled.

Recently[1a] we described the first examples of chiral reagents where the reducing agent is bound non-covalently to the chiral auxiliaries. The chiral auxiliaries used were the (RRRR) and (SSSS) trans-anti-trans tetraphenyl-18-crown-6 derivatives. The complexes formed between the (RRRR) and (SSSS) 2,3,11,12 tetraphenyl-18-crown-6 derivatives and borane-ammonia were successful in performing enantioselective reductions of prochiral ketones and afforded the corresponding (S) and (R) aromatic secondary alcohols with e.e.s of 20-67%. However, the complexes formed between chiral carbohydrate 18C6

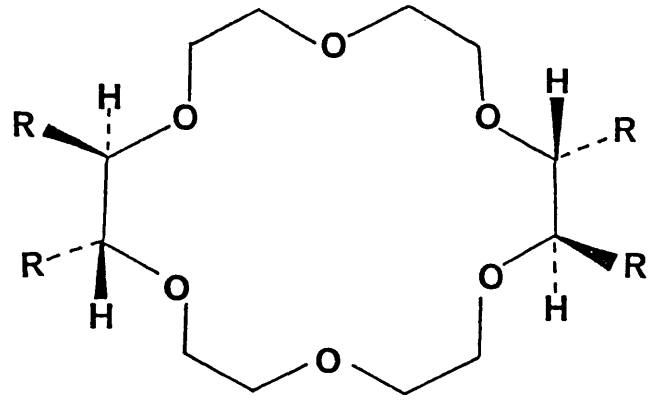
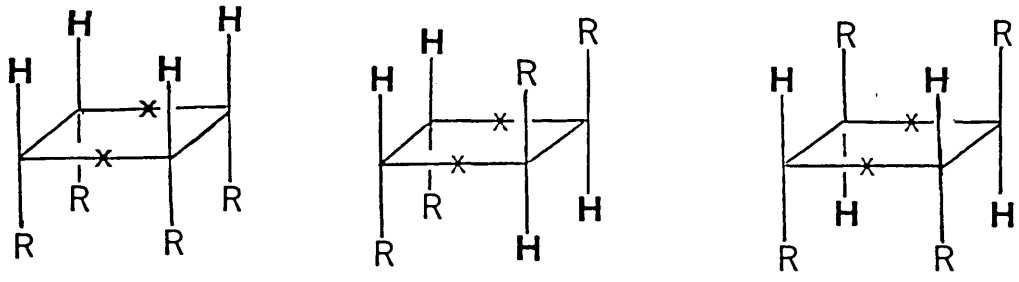


Figure 10.1. trans-anti-trans 2,3,11,12 tetra-anisyl-18-crown-6



cis-syn-cis | cis-anti-cis | trans-syn-trans



trans-anti-trans | trans-cis

X = -O-CH_2-CH_2-O-CH_2-CH_2-O-

R = p-$MeOC_6H_4$

Figure 10.2. A graphic representation of the five stereoisomers of 2,3,11,12 tetra-anisyl-18-crown-6.

derivatives and borane-ammonia[1c] only produced enantiomeric excesses of between 5-10%.

The observation that the chiral trans-anti-trans tetraphenyl 18C6 derivatives when complexed with borane-ammonia produced encouraging enantioselective excesses led to the synthesis of other chiral 18C6 hosts containing bulkier aromatic constituents which could act as chiral auxiliaries. It was decided to use as a bulkier substituent the para-methoxy-phenyl (anisyl) group. Four stereoisomers of 2,3,11,12 tetra-anisyl 18-crown-6 were synthesised and complexed with borane-ammonia. The synthesis of the trans-cis stereoisomer was not attempted as it involves a different synthetic methodology. Only the chiral trans-anti-trans derivative was expected to show any enantioselectivity.

10.2 18C6 Macrocycles.

There is a large amount of X-ray[7] structural data available on complexes formed between 18C6 and its derivatives both with neutral and cationic species. The most common conformation adopted by the complexed 18C6 is termed the 'all-gauche' conformation. In this conformation the C-C bond torsional angles are alternatively plus and minus gauche (g) while the C-O bond torsional angles are antiperiplanar (a). This sequence of torsional angles can be described in terms of the O-C-C-O subunits as $ag^{+}a\ ag^{-}a\ ag^{+}a\ ag^{-}a\ ag^{+}a\ ag^{-}a$. The 18-membered ring also has pseudo D_{3d} symmetry.

Several complexes of both 18C6 and its derivatives with borane-ammonia have been studied by X-ray crystallography[1,8]. These complexes are formed by hydrogen bonding between the NH_3 group and the polyether oxygens of the crown ethers. When 18C6 adopts the 'all-gauche' conformation, hydrogen bonding usually occurs via the upper triangle of polyether oxygens in the so-called perching arrangement[9]. The stoicheiometry of the host-guest complexes are either 1:1 or 1:2 depending upon the substituents on the crown ether ring.

There are only eight reported X-ray structures of 2,3,11,12 substituted 18C6 macrocycles[1a,1b,10].

In its uncomplexed form the 18C6 molecule fills its own cavity[11]. This is achieved by assuming a conformation such that some of the methylene protons are orientated towards the centre of the macrocycle cavity. In the 'all-gauche' conformation the methylene protons are orientated away from the macrocycle cavity.

10.3 Aim of Research

The solid-state structures of the tetra-anisyl 2,3,11,12 derivatives and their complexes with borane-ammonia have been determined so as to (i) investigate the conformational changes that the hosts undergo on complexation, (ii) establish the stoicheiometry of the complexes formed, (iii) correlate stoicheiometry with disposition of the bulkly substituents on the macrocycles.

10.4 REFERENCES

1a. B.L. Allwood, H. Shahriari-Zavareh, J.F. Stoddart, and D.J. Williams, J. Chem. Soc., Chem. Commun., 1984, 1461.

b. D.R. Alston, J.F. Stoddart, J.B. Wolstenholme, B.L. Allwood, and D.J. Williams, Tetrahedron, 1985, 41, 2923.

c. B.L. Allwood, H. Shahriari-Zavareh, J.F. Stoddart, and D.J. Williams, J. Incl. Phenom., 1985, 3, 355.

2a. G.C. Andrews, Tetrahedron lett., 1980, 21, 693.

G.C. Andrews, and T.C. Crawford, IBID., 1980, 21, 693.

3a. J.C. Fiaud, and H.B. Kagan, Bull. Soc. Chim. Fr., 1969, 2742.

b. R.F. Borch and S.R. Levitan, J. Org. Chem., 1972, 37, 2347.

c. M.F. Grundon, D.G. McCleery, and J.W. Wilson, Tetrahedron Lett., 1976, 295.

d. M.F. Grundon, D.G. McCleery, and J.W. Wilson, J. Chem. Soc., Perkin Trans. I, 1981, 231.

4. W.M. Jones, J. Am. Chem. Soc., 1960, 82, 2528.

5. A. Hirao, S. Itsuno, S. Nakahama, and N. Yamazaki, J. Chem. Soc., Chem. Commun., 1981, 315.

S. Itsuno, K. Ito, A. Hirao, and S. Nakahama, IBID., 1983, 469.

6. H. Suda, S.Kanoh, N.Umeda, T. Kakajo, and M. Motoi, Tetrahedron Lett., 1983, 24, 1513.

7. E. Weber, and F. Vögtle, Topics in Current Chemistry, 1981, 98, 1.

D.J. Cram, and K.N. Trueblood, IBID, 1981, 98, 43.

F. Vögtle, H. Seiger, and W.M. Muller, IBID, 1981, 98, 107.

M. Dobler, ' Ionophores and Their Structures,' Wiley-Interscience, 1981.

8. H.M. Colquhoun, G. Jones, J.M. Maud, J.F. Stoddart, and D.J. Williams J. Chem. Soc., Dalton Trans., 1984, 63.

9. K.N. Trueblood, C.B. Knobler, D.S. Lawence, R.V. Stevens, J. Am. Chem. Soc., 1982, 104, 1355.

10. J.J. Daly, P.Schonholzer, J.P. Behr, and J.M. Lehn, Helv. Chim. Acta., 1981, 64, 1444.

J.P. Behr, P. Dumas, and D. Moras, J. Am. Chem. Soc., 1982, 104, 4540.

J.P. Behr, J.M. Lehn, A.C. Dock, and D. Moras, Nature, 1982, 295, 526.

G. Weber, G.M. Sheldrick, T. Burgemeister, F. Dietl, A. Mannschreck, and A. Merz, Tetrahedron 1984, 40, 855.

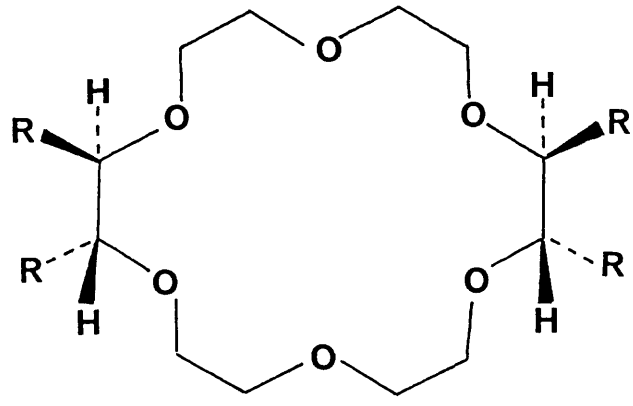
11. J.D. Dunitz, and P. Seiler, Acta. Cryst., 1974, B30, 2739.

CHAPTER 11

The crystal structures of *trans*-*syn*-*trans* 2,3,11,12 tetra-anisyl-18-crown-6 and its complex with borane-ammonia.

11.1 INTRODUCTION

This chapter reports the X-ray structure analyses of trans-syn-trans 2,3,11,12 tetra-anisyl-18-crown-6 (10) and its complex with borane-ammonia.



R = p-$MeOC_6H_4$

10

11.2 EXPERIMENTAL

Clear crystals of 10.X† were obtained by recrystallisation from a 2-methoxy ethanol solution. A crystal of dimensions 0.35 x 0.18 x 0.10 mm was used for unit cell and intensity measurements.

Crystal data: $C_{40}H_{48}O_{10}.X^{\dagger}$, M = 701‡, triclinic, a = 7.121(2), b = 12.489(3), c = 13.770(4) Å, α = 113.64(2), β = 92.58(3), γ = 105.26(2)°, U = 1066 Å^3, space group $P\bar{1}$, Z = 1, D_c = 1.09‡ g cm^{-3}, F(000) = 374‡, μ(Cu-K_α) = 6.01‡ cm^{-1}.

† X denotes unidentified solvent fragment assigned mass of carbon atom.

‡ contribution from unidentified solvent fragment.

Refined unit-cell parameters were obtained by centering 18

reflections on a Nicolet R3m diffractometer. 2860 unique reflections ($\theta \leq 58^{o}$) were measured with Cu-$\underline{K}_{\alpha}$ radiation (graphite monochromator) using the omega-scan routine. Of these 2505 had $|\underline{F}_{o}| > 3\sigma(|\underline{F}_{o}|)$ and were considered to be observed. The net count of two reflections, the 0 3 -1 and the -1 4 -2, measured as references every 50 reflections did not alter significantly during the data collection indicating that no deterioration of the crystal had occurred. The data were brought to a uniform arbitrary scale by the use of these reflections and Lorentz and polarisation corrections were applied.

Although the intensity statistics indicated that the space group was centrosymmetric the structure did not immediately solve in $\underline{P}\bar{1}$. The structure was eventually solved by direct methods in the space group $\underline{P}1$. A starting set comprising 2 origin defining reflections together with a further 6 automatically selected terms was used. The initial phase refinement (39 permutations) was with 200 $\underline{E}$'s > 1.34 using 1235 TPR. This was subsequently expanded to 427 probable phases with $\underline{E}$'s > 1.34 using 2439 TPR. The figures of merit for the best phase solution were NQEST = -0.418, RA(1) = 0.005, RA(2) = 0.040. An $\underline{E}$-map computed using this phase solution gave plausible positions for all non-hydrogen atoms of the host. Inspection of the coordinates revealed the presence of a centre of symmetry in the molecule. The coordinates of the host were shifted so that the inversion centre of the host was on a crystallographic centre of symmetry. One half of the atomic positions were retained and all subsequent refinement was in the space group $\underline{P}\bar{1}$. A subsequent $\Delta\underline{F}$-map revealed the presence of an unknown partial occupancy solvent fragment which was refined

isotropically with 25% occupancy. The remaining non-hydrogen atoms were refined anisotropically. The hydrogens, with the exception of those of the methyl groups which were refined as rigid bodies, were placed at calculated positions (C-H = 0.96 Å), assigned isotropic thermal parameters, $U(H) = 1.2\ U_{eq}(C)$, and allowed to ride on their parent carbon atoms. Several low angle reflections had $|F_o| << |F_c|$ indicating possible extinction. Refinement using a refinable empirical extinction parameter was attempted, but unfortunately proved unsuccessful, 14 reflections were therefore omitted manually.

Refinement using F magnitudes was by block-cascade full-matrix least squares (204 variable parameters) and converged to $R = 0.073$, $R_w = 0.079$, a fixed weight was used [$w^{-1} = \sigma^2(F) + 0.0005F^2$]. The largest parameter shift/e.s.d. was 0.088, the mean shift/e.s.d. was 0.007. The residual electron density in the final difference map was within -0.25 and 0.39 $e Å^{-3}$.

Clear crystals of $\underset{\sim\sim}{10}.(BH_3NH_3)_2$ were grown from a methanol/n-hexane solution. A crystal of dimensions 0.10 x 0.40 x 0.50 mm was used for unit cell and intensity measurements.

Crystal data: $C_{40}H_{48}O_{10}.B_2N_2H_{12}$, $M = 751$, triclinic, $a = 8.742(2)$, $b = 13.727(4)$, $c = 18.616(5)$ Å, $\alpha = 92.01(3)$, $\beta = 97.76(2)$, $\gamma = 102.98(2)^o$, $U = 2151$ $Å^3$, space group $P\bar{1}$, $Z = 2$, $D_c = 1.16$ g cm^{-3}, $F(000) = 808$, $\mu(Cu\text{-}K_\alpha) = 6.27$ cm^{-1}.

Refined unit-cell parameters were obtained by centering 18

reflections on a Nicolet R3m diffractometer. 4437 unique reflections ($\theta < 50^{o}$) were measured with Cu-$\underline{K}_{\alpha}$ radiation (graphite monochromator) using the omega-scan routine. Of these 3914 had $|\underline{F}_{o}| > 3\sigma(|\underline{F}_{o}|)$ and were considered to be observed. The net count of two reflections, the 2 -2 1 and the 1 -2 -2, measured as references every 50 reflections did not alter significantly during the data collection indicating that no deterioration of the crystal had occurred. The data were brought to a uniform arbitrary scale by the use of these reflections and Lorentz and polarisation corrections were applied.

The structure was solved by direct methods. A starting set comprising 3 origin defining reflections together with a further 5 automatically selected terms was used. The initial phase refinement (32 permutations) was with 200 $\underline{E}$'s > 1.74 using 612 TPR. This was subsequently expanded to 428 probable phases with $\underline{E}$'s > 1.74 using 1168 TPR. The figures of merit for the best phase solution were NQEST = -0.344, RA(1) = 0.015, RA(2) = 0.064. An $\underline{E}$-map computed using this phase solution gave plausible positions for 48 non-hydrogen atoms of the two independent centrosymmetric complexes. The remaining non-hydrogen atoms were found in a succession of $\Delta\underline{F}$-maps. The non-hydrogen atoms were refined anisotropically. One of the methoxy groups, O(19)-C(19+), had high anisotropic thermal parameters indicating probable disorder, but no alternative sites could be located for the group. As the methoxy group was distorting the phenyl ring the whole anisyl group, C(16)-C(21), was refined as a rigid body. The carbon hydrogens, with the exception of those of the methyl groups which were refined as rigid bodies, were placed at calculated positions (C-H = 0.96 Å),

assigned isotropic thermal parameters, $\underline{U}(H) = 1.2\ \underline{U}_{eq}(C)$, and allowed to ride on their parent carbon atoms. The hydrogens of the NH_3 and BH_3 groups were clearly located in $\Delta\underline{F}$-maps and the groups refined as rigid bodies (B-H = 1.08, N-H = 0.96 Å).

Refinement using $\underline{F}$ magnitudes was by block-cascade full-matrix least squares (493 variable parameters) and converged to $\underline{R} = 0.089$, $\underline{R}_w = 0.111$, $[w^{-1} = \sigma^2(\underline{F}) + 0.0009\underline{F}^2]$. The largest parameter shift/e.s.d. was 0.286, the mean shift/e.s.d. was 0.018. The residual electron density in the final difference map was within -0.84 and 1.04 $eÅ^{-3}$.

All computations were carried out on an Eclipse S140 computer using the SHELXTL[1] program system.

11.3 DISCUSSION

The final fractional atomic coordinates, anisotropic thermal parameters, bond lengths and bond angles for the non-hydrogen atoms in $\underset{\sim\sim}{10}.X$ and $\underset{\sim\sim}{10}.(BH_3NH_3)_2$ are shown in Tables 11.1 - 11.4 and 11.6 - 11.9 respectively. The positions and isotropic temperature factors for the hydrogen atoms in $\underset{\sim\sim}{10}.X$ and $\underset{\sim\sim}{10}.(BH_3NH_3)_2$ are shown in Tables 11.5 and 11.10 respectively.

The torsional angles associated with the 18-membered macrocyles in $\underset{\sim\sim}{10}$ and $\underset{\sim\sim}{10}.(BH_3NH_3)_2$ are shown beside the relevant C-C and C-O bonds in the skeletal drawings of the structures reproduced in figures 11.1 and 11.3 which also provide details of the crystallographic numbering schemes.

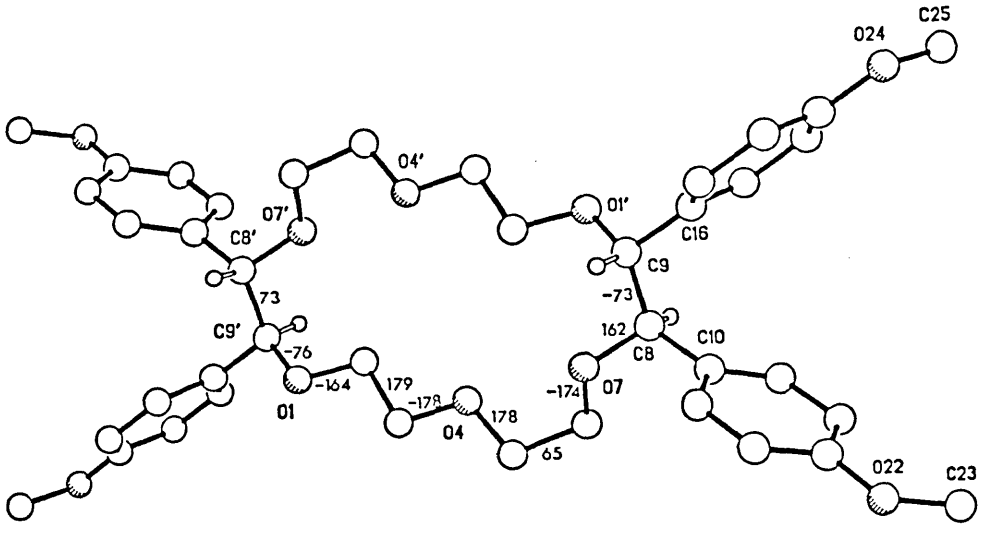


Figure 11.1. The skeletal representation of the solid-state structure of 10.

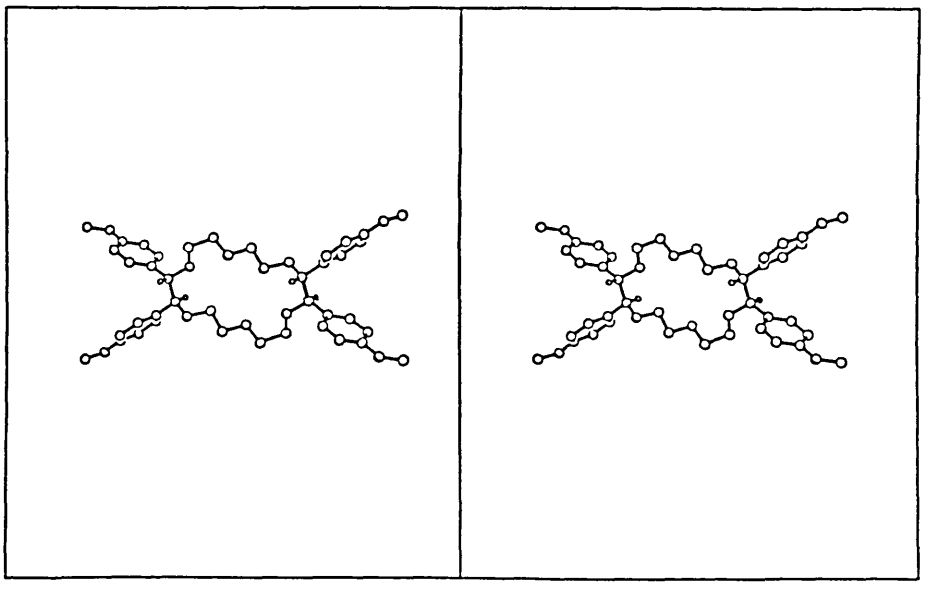


Figure 11.2. The stereo-pair representation of the solid-state structure of 10.

The conformation of the centrosymmetric 18-membered ring of the trans-syn-trans stereoisomer of tetra-anisyl-18C6 can be described in terms of the three sequential independent O-C-C-O subunits as aaa ag^+a ag^-g^+ starting from O(1). This conformation is the same as observed for uncomplexed 18C6[3], though it differs from that of the uncomplexed trans-syn-trans tetraphenyl-18-crown-6 macrocycle[2] which has a sequence of aaa ag^+g^- aag^+ for the independent O-C-C-O subunits.

The three O...O trans-annular distances for receptor 10 are O(1)...O(1') 6.95, O(4)...O(4') 4.12 and O(7)...O(7') 6.69 Å.

The observed lengths of the C-O bonds (average 1.415 Å) and bond angles (O-C-C 108.6°) in the 18-membered macrocycle are similar to those observed in uncomplexed 18C6[2]. Two of the ring C-C bond lengths (C(2)-C(3) and C(5)-C(6)) are similar to those in uncomplexed 18C6, whilst the bridgehead C(8)-C(9) bond length, 1.541 Å, is comparable with that for a single aliphatic C-C bond. The C-O-C angles (average 115.1°) are slightly greater than those observed in uncomplexed 18C6.

The adjacent pseudo equatorial anisyl subsituents have a synclinal relationship to each other while the adjacent pseudo axial methene protons are antiperiplanar.

The crystal packing reveals that there are no contacts of less than normal van der Waals distances between symmetry related receptors. The unidentified disordered solvent fragments X(1) and X(2)

are separated by 1.84 Å across a centre of symmetry. The shortest contact between the receptor and the disordered solvent fragments is 4.0 Å between X(1) and C(25).

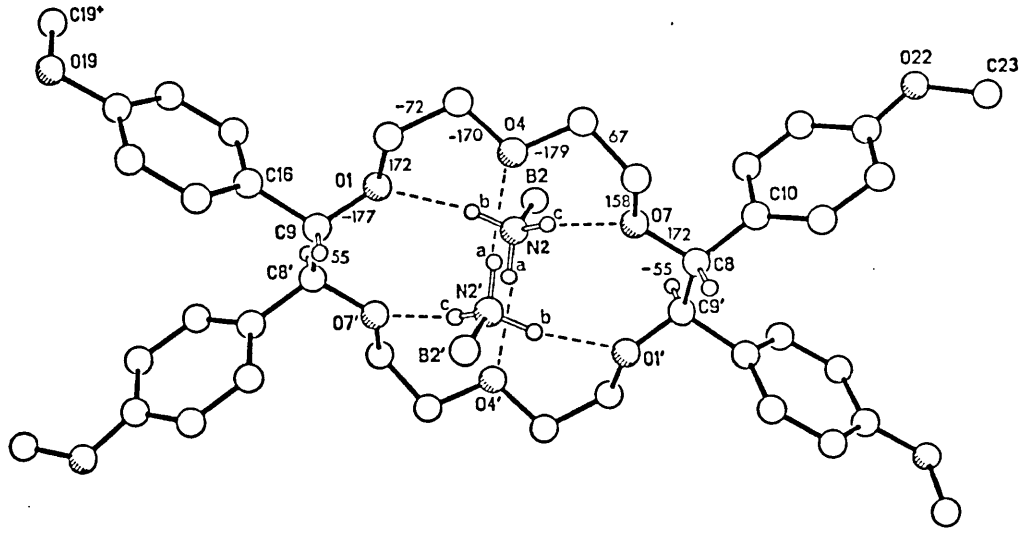
The somewhat high final R-factor can be attributed to the disorder in the unidentified solvent fragment.

Inspection of the torsional angles shows (figure 11.3) that the conformations of the 18-membered macrocycles of two crystallographically independent centrosymmetric 1:2 complexes of 10 with borane-ammonia (10a and 10b) do not differ significantly.

On complexation with two molecules of borane ammonia the 18-membered macrocycle of 10 adopts the classic 'all gauche' conformation. The oxygen atoms of the crown ether alternate 0.18 Å above and below the mean plane of the six polyether oxygens in complex 10a and 0.19 Å in complex 10b.

Each of the borane-ammonia molecules is bound to the host via three hydrogen bonds to the corresponding upper triangle of crown ether oxygens in a perching arrangement. Details of the hydrogen bonding are shown in table 11.11. Observation of the stereo-pair representation of 10b (figure 11.4) shows that each trio of oxygens is orientated towards the appropriate hydrogen bonding NH_3 group. One of the hydrogen bonds is significantly longer than the other two. This is due to a tilt of the N-B vector to the normal of the mean planes of the polyether oxygens, 10.9 and 10.0° in complexes 10a and 10b respectively. These tilt angles compare with values of 7, 23,

(a)



(b)

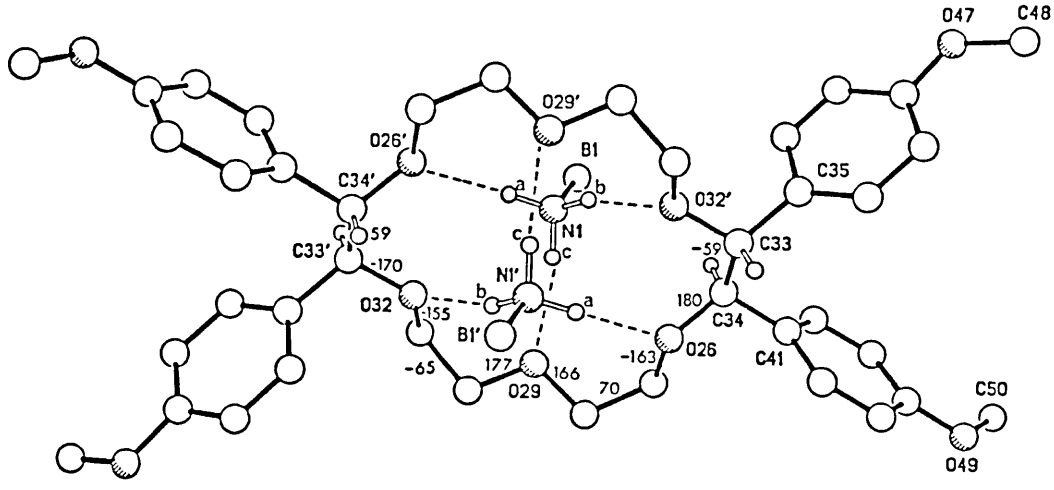


Figure 11.3. The skeletal representations of the solid-state structures of the two independent complexes 10a (a) and 10b (b) found in 10.$(BH_3NH_3)_2$.

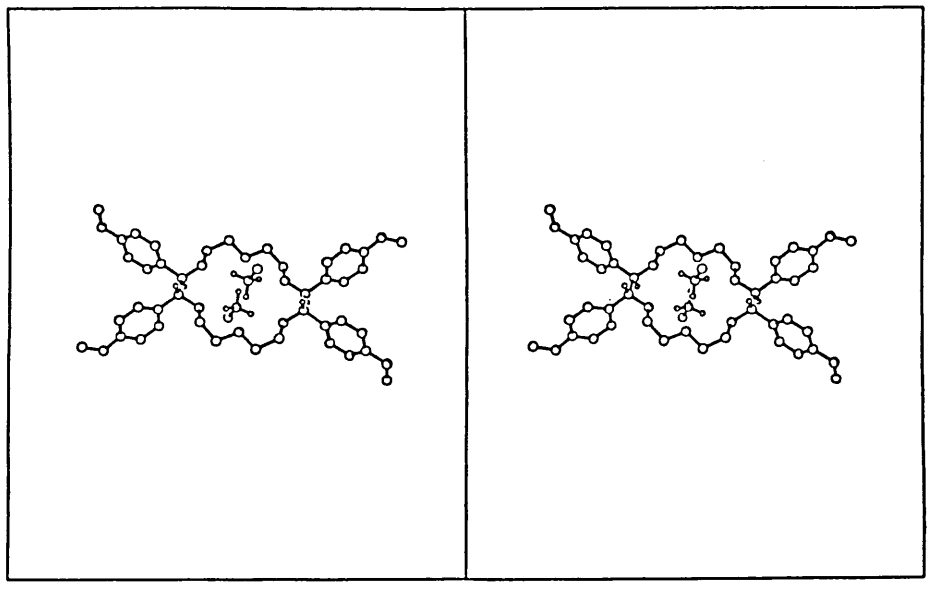


Figure 11.4. The stereo-pair representation of the solid-state structure of 10b.

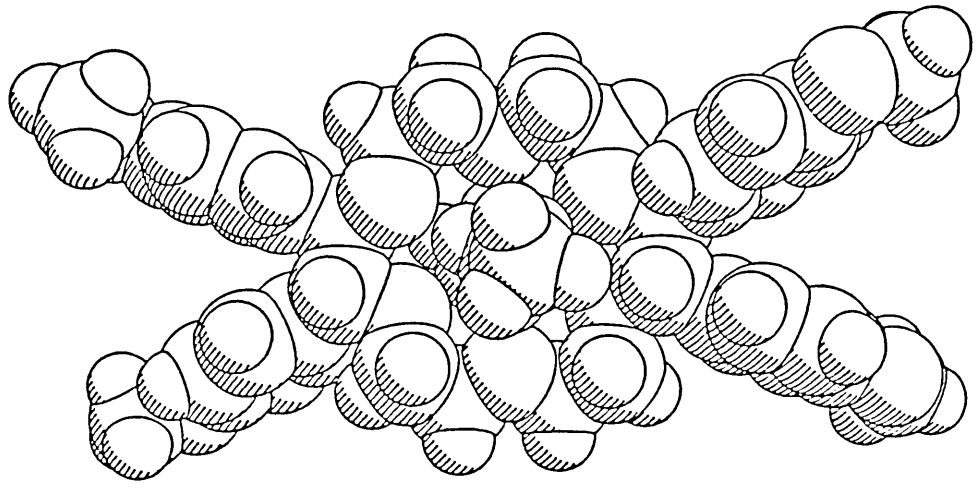


Figure 11.5. The space-filling representation (view normal to the mean plane of the six polyether oxygens) of one of the homotopic faces of 10b.

TABLE 11.11. The nitrogen-polyether oxygens contact distances, and relevant hydrogen bond distances and angles where appropriate, in order of increasing N...O distance for 10a.

N...O	R(N...O) (Å)	R(H...O) (Å)	$\psi(^{o})^{a}$	$\theta(^{o})^{b}$
N(2)-O(4')	3.02	2.08[d]	4.2[d]	167[d]
N(2)-O(7)	3.06	2.11[c]	3[c]	169[c]
N(2)-O(4)	3.29			
N(2)-O(7')	3.33			
N(2)-O(1)	3.36	2.49[e]	16[e]	154[e]
N(2)-O(1')	3.37			

[a]Angles between COC planes and HO vectors.
[b]N-H...O angles.
[c]H(1na)
[d]H(1nc)
[e]H(1nb)

TABLE 11.12. The nitrogen-polyether oxygens contact distances, and relevant hydrogen bond distances and angles where appropriate, in order of increasing N...O distance for 10b.

N...O	R(N...O) (Å)	R(H...O) (Å)	$\psi(^{o})^{a}$	$\theta(^{o})^{b}$
N(1)-O(29)	3.04	2.11[c]	0[c]	163[c]
N(1)-O(32')	3.08	2.14[d]	6[d]	166[d]
N(1)-O(29')	3.24			
N(1)-O(32)	3.26			
N(1)-O(26')	3.29	2.36[e]	23[e]	163[e]
N(1)-O(26)	3.49			

[a]Angles between COC planes and HO vectors.
[b]N-H...O angles.
[c]H(1nc)
[d]H(1nb)
[e]H(1na)

24 25° in 1:2 complexes between borane-ammonia and other 18C6 substituted macrocycles[4]. The tilt angles of the N-B vector to the appropriate upper triangle of polyether oxygens are 11.0 and 10.2° for complexes 10a and 10b respectively.

The distances of the borane-ammonia nitrogen atoms to the mean planes of the six ether oxygens in complexes 10a and 10b are 1.64 and 1.66 Å respectively and the distances of these nitrogens to the mean plane of the upper triangle of polyether oxygens are 1.46 and 1.47 Å respectively. The guest-guest, through the ring N...N, distances in complexes 10a and 10b are 3.30 and 3.32 Å respectively. These compare with distances of 3.3, 3.6 and 3.5 Å in 1:2 complexes of borane-ammonia with substituted 18C6 macrocycles[4].

The C-O bond lengths (average 1.426 Å) and the bond angles (average C-O-C 112.6°; average O-C-C 108.5°) of the macrocyclic rings in both complexes are similar to those found in 18C6 complexes[5]. However, the bridgehead C-C bond lengths (1.533(7) and 1.517(6) Å in complexes 10a and 10b respectively) are longer than the other ring C-C bonds (average 1.484 Å). As already mentioned, this lengthening of the bridgehead bond was also observed for uncomplexed 10.

The adjacent pseudo equatorial anisyl substituents on the polyether ring are again in a synclinal relationship to each other while the pseudo axial protons are antiperiplanar.

The borane-ammonia hydrogens are in a nearly staggered

relationship with respect to each other with the smallest H-N-B-H torsional angles being 37 and 44° for complexes 10a and 10b respectively.

There are no contacts of less than normal van der Waals distances between the 1:2 complexes.

The high final value of the R-factor is due to the unresolved disorder in one of the anisyl groups (C(16) to C(21)).

These analyses have shown that the 2,3,11,12 trans-syn-trans substitutions on the 18C6 macrocycle have very little effect on the conformation of the uncomplexed 18-membered macrocycle of receptor 10. Likewise, there is little conformational change on complexation with borane-ammonia. However, 10 binds two molecules of borane-ammonia whereas 18C6 binds only one guest molecule in the solid state[6].

TABLE 11.1. Coordinates ($\times 10^4$) and temperature factors ($\AA^2 \times 10^3$)

atom	x	y	z	U
O(1)	4201(3)	1860(2)	-381(2)	61(1)*
C(2)	2266(5)	1403(3)	-221(3)	63(2)*
C(3)	1961(5)	2269(3)	846(3)	58(1)*
O(4)	6(3)	1763(2)	944(2)	62(1)*
C(5)	-576(5)	2481(3)	1903(3)	63(2)*
C(6)	-2691(5)	1851(3)	1869(3)	64(2)*
O(7)	-2812(3)	719(2)	1901(2)	58(1)*
C(8)	-4771(4)	-54(3)	1760(3)	54(1)*
C(9)	-4566(4)	-1344(3)	1446(2)	54(1)*
C(10)	-5659(4)	420(3)	2761(3)	52(1)*
C(11)	-4606(5)	741(4)	3761(3)	72(2)*
C(12)	-5343(6)	1166(4)	4684(3)	78(2)*
C(13)	-7190(5)	1287(4)	4658(3)	69(2)*
C(14)	-8290(5)	999(3)	3688(3)	72(2)*
C(15)	-7497(5)	577(3)	2739(3)	62(2)*
C(16)	-6351(4)	-2242(3)	1532(2)	53(1)*
C(17)	-8175(5)	-2562(3)	940(3)	66(2)*
C(18)	-9820(5)	-3413(3)	995(3)	67(2)*
C(19)	-9635(5)	-3953(3)	1674(3)	63(2)*
C(20)	-7816(6)	-3664(3)	2270(3)	71(2)*
C(21)	-6194(5)	-2813(3)	2208(3)	61(2)*
O(22)	-7824(4)	1701(3)	5628(2)	100(2)*
C(23)	-9721(7)	1804(5)	5669(4)	108(3)*
O(24)	-11138(4)	-4779(2)	1816(3)	90(1)*
C(25)	-13048(6)	-5063(4)	1267(5)	116(3)*
X(1)	5071(27)	4894(18)	3964(15)	156(6)
X(2)	3394(61)	5308(46)	5048(38)	248(17)

* Equivalent isotropic U defined as one third of the trace of the orthogonalised U_{ij} tensor

TABLE 11.2. Bond lengths (Å)

O(1)-C(2)	1.410(4)	O(1)-C(9a)	1.415(4)
C(2)-C(3)	1.501(5)	C(3)-O(4)	1.406(4)
O(4)-C(5)	1.419(4)	C(5)-C(6)	1.493(5)
C(6)-O(7)	1.411(5)	O(7)-C(8)	1.426(4)
C(8)-C(9)	1.541(5)	C(8)-C(10)	1.507(5)
C(9)-C(16)	1.502(5)	C(9)-O(1a)	1.415(4)
C(10)-C(11)	1.387(5)	C(10)-C(15)	1.374(5)
C(11)-C(12)	1.356(5)	C(12)-C(13)	1.363(6)
C(13)-C(14)	1.378(6)	C(13)-O(22)	1.371(5)
C(14)-C(15)	1.405(5)	C(16)-C(17)	1.371(5)
C(16)-C(21)	1.397(6)	C(17)-C(18)	1.387(5)
C(18)-C(19)	1.375(7)	C(19)-C(20)	1.379(5)
C(19)-O(24)	1.359(5)	C(20)-C(21)	1.381(5)
O(22)-C(23)	1.392(6)	O(24)-C(25)	1.409(6)

TABLE 11.3. Bond Angles (deg.)

C(2)-O(1)-C(9a)	116.2(2)	O(1)-C(2)-C(3)	109.3(2)
C(2)-C(3)-O(4)	106.1(2)	C(3)-O(4)-C(5)	114.3(2)
O(4)-C(5)-C(6)	107.8(2)	C(5)-C(6)-O(7)	108.0(3)
C(6)-O(7)-C(8)	114.9(3)	O(7)-C(8)-C(9)	104.9(3)
O(7)-C(8)-C(10)	110.7(2)	C(9)-C(8)-C(10)	114.5(3)
C(8)-C(9)-C(16)	113.7(3)	C(8)-C(9)-O(1a)	111.6(3)
C(16)-C(9)-O(1a)	107.4(2)	C(8)-C(10)-C(11)	120.3(3)
C(8)-C(10)-C(15)	122.7(3)	C(11)-C(10)-C(15)	117.0(3)
C(10)-C(11)-C(12)	122.5(4)	C(11)-C(12)-C(13)	120.4(4)
C(12)-C(13)-C(14)	119.5(4)	C(12)-C(13)-O(22)	116.2(3)
C(14)-C(13)-O(22)	124.2(4)	C(13)-C(14)-C(15)	119.5(4)
C(10)-C(15)-C(14)	121.0(3)	C(9)-C(16)-C(17)	122.2(4)
C(9)-C(16)-C(21)	120.5(3)	C(17)-C(16)-C(21)	117.2(3)
C(16)-C(17)-C(18)	122.5(4)	C(17)-C(18)-C(19)	119.2(3)
C(18)-C(19)-C(20)	119.7(3)	C(18)-C(19)-O(24)	124.8(3)
C(20)-C(19)-O(24)	115.5(4)	C(19)-C(20)-C(21)	120.4(4)
C(16)-C(21)-C(20)	120.9(3)	C(13)-O(22)-C(23)	120.0(4)
C(19)-O(24)-C(25)	117.9(4)		

TABLE 11.4. Anisotropic temperature factors ($Å^2 \times 10^3$)

atom	U_{11}	U_{22}	U_{33}	U_{23}	U_{13}	U_{12}
O(1)	49(1)	69(1)	52(1)	20(1)	15(1)	8(1)
C(2)	53(2)	56(2)	69(2)	19(2)	20(2)	8(2)
C(3)	51(2)	58(2)	62(2)	26(2)	18(2)	9(1)
O(4)	56(1)	54(1)	63(1)	18(1)	26(1)	10(1)
C(5)	71(2)	52(2)	67(2)	24(2)	26(2)	18(2)
C(6)	67(2)	58(2)	76(2)	31(2)	31(2)	24(2)
O(7)	52(1)	53(1)	70(1)	28(1)	18(1)	12(1)
C(8)	44(2)	63(2)	56(2)	29(2)	8(1)	10(1)
C(9)	49(2)	59(2)	51(2)	24(2)	11(1)	10(1)
C(10)	44(2)	52(2)	56(2)	23(1)	9(1)	8(1)
C(11)	60(2)	95(3)	60(2)	29(2)	10(2)	28(2)
C(12)	67(2)	109(3)	53(2)	27(2)	11(2)	30(2)
C(13)	70(2)	76(2)	53(2)	22(2)	15(2)	18(2)
C(14)	50(2)	77(2)	86(3)	29(2)	21(2)	23(2)
C(15)	54(2)	65(2)	65(2)	29(2)	9(2)	12(2)
C(16)	53(2)	52(2)	50(2)	20(1)	15(1)	14(1)
C(17)	57(2)	78(2)	69(2)	43(2)	7(2)	12(2)
C(18)	53(2)	65(2)	73(2)	29(2)	6(2)	7(2)
C(19)	65(2)	46(2)	70(2)	20(2)	23(2)	8(2)
C(20)	83(3)	63(2)	78(2)	41(2)	23(2)	20(2)
C(21)	62(2)	61(2)	59(2)	27(2)	10(2)	18(2)
O(22)	82(2)	140(3)	66(2)	25(2)	24(1)	43(2)
C(23)	92(3)	133(4)	94(3)	32(3)	40(3)	49(3)
O(24)	77(2)	68(2)	119(2)	47(2)	28(2)	1(1)
C(25)	74(3)	78(3)	172(5)	41(3)	44(3)	1(2)

The anisotropic temperature factor exponent takes the form:

$$-2\pi^2(h^2a^{*2}U_{11} + \ldots + 2\,hka^*b^*U_{12}\cos\gamma^* + \ldots)$$

TABLE 11.5. Coordinates ($\times 10^4$) and temperature factors ($Å^2 \times 10^3$)

atom	x	y	z	U
H(2a)	1331	1332	-785	79
H(2b)	2081	610	-228	79
H(3a)	2145	3067	864	69
H(3b)	2871	2336	1418	69
H(5a)	226	2550	2517	74
H(5b)	-432	3285	1945	74
H(6a)	-3473	1709	1218	77
H(6b)	-3163	2351	2478	77
H(8)	-5675	-74	1210	62
H(9)	-3467	-1213	1955	64
H(11)	-3307	655	3800	82
H(12)	-4561	1381	5360	89
H(14)	-9588	1086	3660	82
H(15)	-8250	395	2066	73
H(17)	-8319	-2182	469	74
H(18)	-11072	-3623	563	77
H(20)	-7677	-4057	2730	82
H(21)	-4941	-2611	2635	70
H(23a)	-10152	1968	6350	127
H(23b)	-10505	1002	5149	127
H(23c)	-9870	2408	5433	127
H(25a)	-13823	-5604	1536	123
H(25b)	-13268	-5463	495	123
H(25c)	-13426	-4327	1498	123

TABLE 11.6. Coordinates ($\times 10^4$) and temperature factors ($Å^2 \times 10^3$)

atom	x	y	z	U
O(1)	6468(4)	3278(3)	9999(2)	89(2)*
C(2)	8105(7)	3631(5)	10286(3)	97(3)*
C(3)	8277(7)	4264(5)	10966(3)	104(3)*
O(4)	7901(4)	5185(3)	10776(2)	93(2)*
C(5)	8285(7)	5915(5)	11364(4)	112(3)*
C(6)	7830(7)	6828(5)	11127(4)	111(3)*
O(7)	6137(4)	6637(3)	10965(2)	92(2)*
C(8)	5526(6)	7519(4)	10990(3)	79(2)*
C(9)	6255(6)	2783(4)	9295(3)	74(2)*
C(10)	5829(5)	8020(3)	11743(2)	62(2)*
C(11)	6483(6)	9014(4)	11892(3)	77(2)*
C(12)	6698(6)	9470(4)	12590(3)	75(2)*
C(13)	6265(6)	8896(4)	13146(2)	66(2)*
C(14)	5658(6)	7882(4)	13010(3)	73(2)*
C(15)	5431(6)	7455(4)	12319(3)	73(2)*
C(16)	6964(4)	1842(2)	9300(2)	74(2)*
C(17)	7885(4)	1740(2)	8758(2)	75(2)*
C(18)	8511(4)	895(2)	8706(2)	90(3)*
C(19)	8216(4)	152(2)	9194(2)	128(4)*
O(19)	8866(4)	-726(2)	9139(2)	205(4)*
C(19')	8395(4)	-1382(2)	9704(2)	376(13)*
C(20)	7295(4)	254(2)	9736(2)	149(4)*
C(21)	6669(4)	1099(2)	9789(2)	108(3)*
O(22)	6464(5)	9249(3)	13847(2)	97(2)*
C(23)	6882(8)	10283(4)	14015(3)	104(3)*
O(26)	4479(4)	2913(2)	4380(2)	63(1)*
C(27)	4946(6)	2321(4)	4957(3)	75(2)*
C(28)	6502(6)	2872(4)	5376(3)	73(2)*
O(29)	6273(3)	3702(2)	5776(2)	59(1)*
C(30)	7576(6)	4126(3)	6321(3)	71(2)*
C(31)	7248(6)	5029(3)	6688(3)	72(2)*
O(32)	7190(4)	5768(2)	6167(1)	62(1)*
C(33)	2430(5)	3233(3)	3508(2)	56(2)*
C(34)	2819(5)	2565(3)	4105(2)	56(2)*
C(35)	694(5)	2927(3)	3173(2)	59(2)*
C(36)	227(6)	2458(4)	2500(2)	79(2)*
C(37)	-1400(7)	2197(4)	2201(3)	87(2)*
C(38)	-2486(6)	2417(4)	2606(3)	82(2)*
C(39)	-2048(6)	2877(4)	3284(3)	83(2)*
C(40)	-480(6)	3125(4)	3571(3)	75(2)*
C(41)	2397(5)	1471(3)	3844(2)	56(2)*
C(42)	1242(6)	785(4)	4118(3)	68(2)*
C(43)	841(6)	-222(4)	3867(3)	73(2)*
C(44)	1571(6)	-548(3)	3346(3)	67(2)*
C(45)	2766(6)	127(4)	3081(3)	75(2)*
C(46)	3162(6)	1113(4)	3321(3)	68(2)*
O(47)	-4116(4)	2195(4)	2364(2)	119(2)*
C(48)	-4673(8)	1760(6)	1667(3)	140(4)*
O(49)	1257(4)	-1509(2)	3056(2)	93(2)*
C(50)	-57(7)	-2206(4)	3256(4)	104(3)*
N(1)	3529(5)	4731(3)	5490(2)	70(2)*
B(1)	2055(10)	4278(7)	5877(6)	129(4)*
N(2)	4005(5)	4531(4)	10649(2)	96(2)*
B(2)	2986(12)	4221(8)	11275(5)	130(5)*

* Equivalent isotropic U defined as one third of the trace of the orthogonalised U_{ij} tensor

TABLE 11.7. Bond lengths (Å)

O(1)-C(2)	1.426(6)	O(1)-C(9)	1.424(6)
C(2)-C(3)	1.480(8)	C(3)-O(4)	1.420(8)
O(4)-C(5)	1.409(7)	C(5)-C(6)	1.463(10)
C(6)-O(7)	1.432(6)	O(7)-C(8)	1.430(8)
C(8)-C(10)	1.504(7)	C(8)-C(9a)	1.533(7)
C(9)-C(16)	1.553(6)	C(9)-C(8a)	1.533(7)
C(10)-C(11)	1.359(6)	C(10)-C(15)	1.381(7)
C(11)-C(12)	1.393(7)	C(12)-C(13)	1.365(7)
C(13)-C(14)	1.375(6)	C(13)-O(22)	1.350(6)
C(14)-C(15)	1.365(7)	C(16)-C(17)	1.395
C(16)-C(21)	1.395	C(17)-C(18)	1.395
C(18)-C(19)	1.395	C(19)-O(19)	1.450
C(19)-C(20)	1.395	O(19)-C(19')	1.450
C(20)-C(21)	1.395	O(22)-C(23)	1.397(7)
O(26)-C(27)	1.440(6)	O(26)-C(34)	1.438(5)
C(27)-C(28)	1.497(6)	C(28)-O(29)	1.406(6)
O(29)-C(30)	1.419(5)	C(30)-C(31)	1.497(7)
C(31)-O(32)	1.434(5)	O(32)-C(33a)	1.428(5)
C(33)-C(34)	1.517(6)	C(33)-C(35)	1.519(6)
C(33)-O(32a)	1.428(5)	C(34)-C(41)	1.510(6)
C(35)-C(36)	1.354(6)	C(35)-C(40)	1.412(7)
C(36)-C(37)	1.415(7)	C(37)-C(38)	1.368(9)
C(38)-C(39)	1.358(7)	C(38)-O(47)	1.396(6)
C(39)-C(40)	1.364(7)	C(41)-C(42)	1.383(6)
C(41)-C(46)	1.388(7)	C(42)-C(43)	1.394(7)
C(43)-C(44)	1.347(8)	C(44)-C(45)	1.389(7)
C(44)-O(49)	1.362(6)	C(45)-C(46)	1.362(7)
O(47)-C(48)	1.386(7)	O(49)-C(50)	1.422(7)
N(1)-B(1)	1.578(10)	N(2)-B(2)	1.576(11)

TABLE 11.8. Bond Angles (deg.)

C(2)-O(1)-C(9)	111.9(4)	O(1)-C(2)-C(3)	110.1(5)
C(2)-C(3)-O(4)	107.8(5)	C(3)-O(4)-C(5)	112.8(4)
O(4)-C(5)-C(6)	109.2(5)	C(5)-C(6)-O(7)	109.2(5)
C(6)-O(7)-C(8)	113.9(4)	O(7)-C(8)-C(10)	111.9(4)
O(7)-C(8)-C(9a)	107.9(4)	C(10)-C(8)-C(9a)	111.1(4)
O(1)-C(9)-C(16)	112.3(4)	O(1)-C(9)-C(8a)	108.4(4)
C(16)-C(9)-C(8a)	109.8(4)	C(8)-C(10)-C(11)	123.1(4)
C(8)-C(10)-C(15)	119.3(4)	C(11)-C(10)-C(15)	117.5(4)
C(10)-C(11)-C(12)	122.2(4)	C(11)-C(12)-C(13)	118.9(4)
C(12)-C(13)-C(14)	119.6(4)	C(12)-C(13)-O(22)	124.2(4)
C(14)-C(13)-O(22)	116.1(4)	C(13)-C(14)-C(15)	120.4(4)
C(10)-C(15)-C(14)	121.2(4)	C(9)-C(16)-C(17)	116.3(2)
C(9)-C(16)-C(21)	123.6(2)	C(17)-C(16)-C(21)	120.0
C(16)-C(17)-C(18)	120.0	C(17)-C(18)-C(19)	120.0
C(18)-C(19)-O(19)	120.0	C(18)-C(19)-C(20)	120.0
O(19)-C(19)-C(20)	120.0	C(19)-O(19)-C(19')	109.5
C(19)-C(20)-C(21)	120.0	C(16)-C(21)-C(20)	120.0
C(13)-O(22)-C(23)	119.3(4)	C(27)-O(26)-C(34)	110.8(3)
O(26)-C(27)-C(28)	109.3(4)	C(27)-C(28)-O(29)	109.2(4)
C(28)-O(29)-C(30)	113.0(4)	O(29)-C(30)-C(31)	108.8(4)
C(30)-C(31)-O(32)	108.3(4)	C(31)-O(32)-C(33a)	112.9(3)
C(34)-C(33)-C(35)	111.7(3)	C(34)-C(33)-O(32a)	104.6(3)
C(35)-C(33)-O(32a)	110.8(4)	O(26)-C(34)-C(33)	107.2(3)
O(26)-C(34)-C(41)	112.1(4)	C(33)-C(34)-C(41)	112.3(3)
C(33)-C(35)-C(36)	122.0(4)	C(33)-C(35)-C(40)	119.6(4)
C(36)-C(35)-C(40)	118.4(4)	C(35)-C(36)-C(37)	120.5(5)
C(36)-C(37)-C(38)	118.7(4)	C(37)-C(38)-C(39)	121.9(5)
C(37)-C(38)-O(47)	123.5(5)	C(39)-C(38)-O(47)	114.6(5)
C(38)-C(39)-C(40)	119.1(5)	C(35)-C(40)-C(39)	121.3(5)
C(34)-C(41)-C(42)	121.4(4)	C(34)-C(41)-C(46)	121.2(4)
C(42)-C(41)-C(46)	117.3(4)	C(41)-C(42)-C(43)	121.2(5)
C(42)-C(43)-C(44)	120.5(4)	C(43)-C(44)-C(45)	118.9(4)
C(43)-C(44)-O(49)	125.2(4)	C(45)-C(44)-O(49)	115.9(5)
C(44)-C(45)-C(46)	121.1(5)	C(41)-C(46)-C(45)	121.0(4)
C(38)-O(47)-C(48)	118.9(5)	C(44)-O(49)-C(50)	117.9(5)

TABLE 11.9. Anisotropic temperature factors ($Å^2 \times 10^3$)

atom	U_{11}	U_{22}	U_{33}	U_{23}	U_{13}	U_{12}
O(1)	60(2)	123(3)	67(2)	-23(2)	-0(2)	-5(2)
C(2)	67(4)	111(4)	95(4)	-30(3)	-19(3)	6(3)
C(3)	76(4)	129(5)	88(4)	-27(4)	-12(3)	7(4)
O(4)	75(2)	117(3)	75(2)	-33(2)	-9(2)	10(2)
C(5)	63(4)	150(5)	108(4)	-62(4)	-17(3)	21(4)
C(6)	54(3)	138(5)	120(5)	-66(4)	4(3)	-4(3)
O(7)	52(2)	112(3)	97(3)	-41(2)	3(2)	1(2)
C(8)	61(3)	94(4)	72(3)	-8(3)	12(3)	-3(3)
C(9)	59(3)	90(4)	59(3)	-6(2)	9(2)	-11(3)
C(10)	51(3)	74(3)	55(3)	-3(2)	7(2)	4(2)
C(11)	84(4)	75(3)	59(3)	8(2)	4(3)	-5(3)
C(12)	86(4)	61(3)	73(3)	5(3)	5(3)	12(3)
C(13)	75(3)	70(3)	52(3)	-5(2)	-1(2)	22(3)
C(14)	93(4)	67(3)	56(3)	4(2)	8(3)	14(3)
C(15)	67(3)	66(3)	81(4)	-2(3)	11(3)	7(3)
C(16)	59(3)	86(4)	61(3)	-1(3)	0(3)	-13(3)
C(17)	71(4)	58(3)	87(4)	15(3)	-7(3)	8(3)
C(18)	82(4)	84(4)	90(4)	24(3)	-10(3)	-2(3)
C(19)	79(5)	142(7)	123(6)	-18(5)	-49(4)	-19(5)
O(19)	206(6)	61(3)	280(7)	51(3)	-161(6)	-2(3)
C(19')	275(18)	264(17)	504(26)	-31(17)	-235(19)	67(14)
C(20)	170(8)	53(4)	164(7)	56(4)	-104(6)	-29(4)
C(21)	99(5)	134(6)	54(3)	24(4)	2(3)	-46(4)
O(22)	137(4)	84(3)	68(2)	-11(2)	10(2)	28(2)
C(23)	116(5)	97(4)	99(4)	-32(4)	-12(4)	47(4)
O(26)	56(2)	70(2)	57(2)	0(2)	-1(1)	10(2)
C(27)	83(4)	67(3)	72(3)	-10(3)	-14(3)	28(3)
C(28)	69(3)	80(3)	72(3)	-9(3)	-6(3)	34(3)
O(29)	47(2)	63(2)	62(2)	-3(1)	-9(1)	13(1)
C(30)	63(3)	68(3)	71(3)	5(2)	-11(3)	8(3)
C(31)	78(4)	65(3)	62(3)	6(3)	-9(3)	2(3)
O(32)	68(2)	57(2)	51(2)	3(1)	-5(1)	4(1)
C(33)	51(3)	57(3)	53(3)	-3(2)	7(2)	-0(2)
C(34)	42(3)	67(3)	54(3)	-0(2)	4(2)	7(2)
C(35)	55(3)	57(3)	59(3)	5(2)	1(2)	1(2)
C(36)	66(3)	105(4)	49(3)	-1(3)	2(2)	-13(3)
C(37)	80(4)	115(4)	45(3)	8(3)	4(3)	-17(3)
C(38)	57(3)	102(4)	68(3)	27(3)	-7(3)	-11(3)
C(39)	68(4)	93(4)	83(4)	-1(3)	5(3)	13(3)
C(40)	53(3)	82(3)	83(3)	-13(3)	2(3)	7(3)
C(41)	48(3)	63(3)	56(3)	-2(2)	5(2)	11(2)
C(42)	65(3)	68(3)	73(3)	3(3)	18(3)	14(3)
C(43)	67(3)	67(3)	79(3)	10(3)	13(3)	1(3)
C(44)	65(3)	58(3)	78(3)	-8(2)	7(3)	15(2)
C(45)	64(3)	72(3)	87(3)	-18(3)	21(3)	9(3)
C(46)	57(3)	71(3)	70(3)	-10(3)	19(3)	-2(2)
O(47)	57(2)	179(4)	101(3)	22(3)	-2(2)	-7(2)
C(48)	89(5)	192(8)	93(5)	30(5)	-33(4)	-36(5)
O(49)	82(3)	67(2)	124(3)	-9(2)	16(2)	9(2)
C(50)	71(4)	64(3)	168(6)	2(4)	3(4)	6(3)
N(1)	65(3)	75(3)	70(2)	11(2)	12(2)	15(2)
B(1)	97(6)	129(7)	166(8)	5(6)	79(6)	5(5)
N(2)	61(3)	133(4)	85(3)	-23(3)	8(2)	13(3)
B(2)	128(7)	179(9)	102(6)	15(6)	55(5)	51(6)

The anisotropic temperature factor exponent takes the form:

$$-2\pi^2(h^2a^{*2}U_{11} + \ldots + 2\,hka^*b^*U_{12}\cos\gamma^* + \ldots)$$

TABLE 11.10. Coordinates ($\times 10^4$) and temperature factors ($\AA^2 \times 10^3$)

atom	x	y	z	U
H(2a)	8567	3069	10386	122
H(2b)	8642	4020	9937	122
H(3a)	9348	4385	11211	118
H(3b)	7563	3934	11278	118
H(5a)	7723	5667	11754	144
H(5b)	9406	6060	11529	144
H(6a)	8290	7029	10700	138
H(6b)	8205	7352	11507	138
H(8)	6060	8000	10691	95
H(9)	6808	3237	8984	89
H(11)	6807	9416	11503	88
H(12)	7145	10177	12680	91
H(14)	5393	7473	13403	90
H(15)	4985	6748	12232	83
H(17)	8088(4)	2252(2)	8422(2)	84
H(18)	9145(4)	826(2)	8332(2)	112
H(19a)	8826(4)	-1963(2)	9668(2)	513
H(19b)	7258(4)	-1584(2)	9647(2)	513
H(19c)	8789(4)	-1032(2)	10171(2)	513
H(20)	7091(4)	-258(2)	10072(2)	167
H(21)	6035(4)	1169(2)	10162(2)	129
H(23a)	6946	10440	14526	123
H(23b)	6080	10564	13752	123
H(23c)	7888	10559	13863	123
H(27a)	4156	2205	5275	87
H(27b)	5052	1690	4755	87
H(28a)	7240	3097	5046	90
H(28b)	6913	2434	5702	90
H(30a)	7710	3643	6671	88
H(30b)	8524	4318	6103	88
H(31a)	8078	5291	7086	86
H(31b)	6250	4850	6868	86
H(33)	3030	3177	3119	73
H(34)	2192	2608	4485	68
H(36)	1003	2301	2225	102
H(37)	-1733	1872	1722	102
H(39)	-2832	3026	3558	102
H(40)	-167	3439	4053	89
H(42)	706	1006	4488	84
H(43)	38	-686	4066	92
H(45)	3322	-105	2724	86
H(46)	3982	1567	3125	83
H(48a)	-5774	1765	1647	150
H(48b)	-4566	1080	1624	150
H(48c)	-4257	2117	1275	150
H(50a)	-217	-2883	3059	127
H(50b)	-946	-1939	3071	127
H(50c)	39	-2197	3776	127
H(1na)	4062	5416	5629	79
H(1nb)	3190	4655	4974	79
H(1nc)	4243	4305	5618	79
H(1ba)	1511	3493	5751	151
H(1bb)	1415	4721	5537	151
H(1nc)	2020	4471	6441	151
H(2na)	3253	4590	10236	105
H(2nb)	4515	4003	10544	105
H(2nc)	4788	5152	10753	105
H(2ba)	2531	4831	11476	153
H(2bb)	3572	3904	11726	153
H(2bc)	2016	3651	10987	153

11.4 REFERENCES

1. G.M. Sheldrick, SHELXTL, An integrated system for solving, refining, and displaying crystal structures from diffractometer data, University of Göttingen, Federal Republic of Germany, 1981.
2. G. Weber, G.M. Sheldrick, T. Burgemeister, F. Dietl, A. Mannschreck, and A. Merz, Tetrahedron 1984, 40, 855.
3. J.D. Dunitz, and P. Seiler, Acta. Cryst., 1974, B30, 2739.

4a. B.L. Allwood, H. Shahriari-Zavareh, J.F. Stoddart, and D.J. Williams, J. Chem. Soc., Chem. Commun., 1984, 1461.

b. D.R. Alston, J.F. Stoddart, J.B. Wolstenholme, B.L. Allwood, and D.J. Williams, Tetrahedron, 1985, 41, 2923.

c. B.L. Allwood, H. Shahriari-Zavareh, J.F. Stoddart, and D.J. Williams, J. Incl. Phenom., 1985, 3, 355.

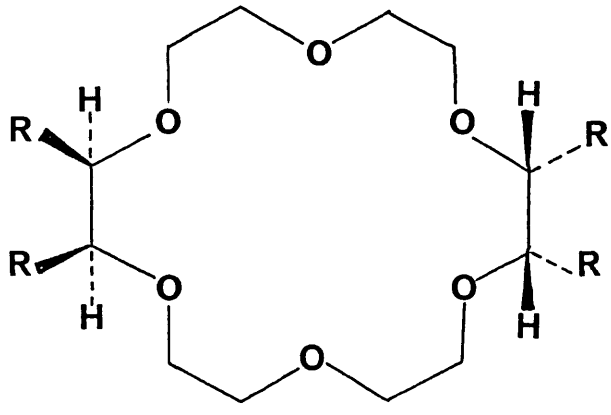
5. I. Goldberg, The Chemistry of Functional Groups. Supplement E: The Chemistry of Ethers, Crown Ethers, Hydroxy Groups and their Sulphur Analogues, 1980, Part 1, 175. Editor S. Patel, Chichester: John Wiley.
6. H.M. Colquhoun, G. Jones, J.M. Maud, J.F. Stoddart, and D.J. Williams, J. Chem. Soc., Dalton Trans., 1984, 63.

CHAPTER 12

The crystal structures of cis-anti-cis 2,3,11,12 tetra-anisyl-18-crown-6 and its complex with borane-ammonia.

12.1 INTRODUCTION

This chapter reports the X-ray structure analyses of the cis-anti-cis 2,3,11,12 tetra-anisyl-18-crown-6 (11) and its complex with borane-ammonia.



R = p-$MeOC_6H_4$

11

12.2 EXPERIMENTAL

Clear crystals of 11 were grown from a dichloromethane/n-pentane solution. A crystal of dimensions 0.13 x 0.28 x 0.45 mm was used for unit cell and intensity measurements.

Crystal data: $C_{40}H_{48}O_{10}$, M = 689, monoclinic, a = 8.238(2), b = 20.616(7), c = 10.883(2) Å, $\beta = 99.99(2)^{o}$, U = 1820 $Å^3$, space group $P2_1/a$, Z = 2, D_c = 1.26 g cm^{-3}, F(000) = 736, μ(Cu-K_α) = 6.95 cm^{-1}.

Refined unit-cell parameters were obtained by centering 15 reflections on a Nicolet R3m diffractometer. 1869 unique reflections ($\theta < 50^{o}$) were measured with Cu-K_α radiation (graphite monochromator) using the omega-scan routine. Of these 1636 had $|F_o| > 3\sigma(|F_o|)$ and

were considered to be observed. The net count of two reflections, the -1 -1 3 and the -1 -1 2, measured as references every 50 reflections did not alter significantly during the data collection indicating that no deterioration of the crystal had occurred. The data were brought to a uniform arbitrary scale by the use of these reflections and Lorentz and polarisation corrections were applied.

The structure was solved by direct methods. A starting set comprising 3 origin defining reflections together with 5 automatically selected terms was used. The initial phase refinement (32 permutations) was with 200 $\underline{E}$'s > 1.24 using 1794 TPR. This was subsequently expanded to 423 probable phases with $\underline{E}$'s > 1.24 using 4712 TPR. The figures of merit for the best phase solution were NQEST = -0.508, RA(1) = 0.065, RA(2) = 0.093. An $\underline{E}$-map computed for this phase solution gave plausible positions for all the non-hydrogen atoms in the structure. The non-hydrogen atoms were refined anisotropically. The hydrogens, with the exception of those of the methyl groups which were refined as rigid bodies, were placed at calculated positions (C-H = 0.96 Å), assigned isotropic thermal parameters, $\underline{U}(H) = 1.2\ \underline{U}_{eq}(C)$, and allowed to ride on their parent carbon atoms.

Refinement using $\underline{F}$ magnitudes was by block-cascade full-matrix least squares (233 variable parameters) and converged to $\underline{R} = 0.040$, $\underline{R}_w = 0.046$, $[w^{-1} = \sigma^2(\underline{F}) + 0.0011\underline{F}^2]$. The largest parameter shift/e.s.d. was 0.204, the mean shift/e.s.d. was 0.030. The residual electron density in the final difference map was within -0.14 and 0.15 $e\text{Å}^{-3}$.

Clear crystals of $\underset{\sim\sim}{11}.(BH_3NH_3)_2$ were grown from a dichloromethane/n-pentane solution. A crystal of dimensions 0.03 x 0.27 x 0.63 mm was used for unit cell and intensity measurements.

Crystal data: $C_{40}H_{48}O_{10}.B_2N_2H_{12}$, M = 751, monoclinic, a = 8.224(2), b = 8.848(3), c = 28.47(1) Å, β = 90.56(3)°, U = 2072 Å^3, space group $P2_1/c$, Z = 2, D_c = 1.21 g cm^{-3}, $F(000)$ = 808, $\mu(Cu\text{-}K_\alpha)$ = 6.51 cm^{-1}.

Refined unit-cell parameters were obtained by centering 16 reflections on a Nicolet R3m diffractometer. 2124 unique reflections ($\theta < 50°$) were measured with Cu-K_α radiation (graphite monochromator) using the omega-scan routine. Of these 1730 had $|F_o| > 3\sigma(|F_o|)$ and were considered to be observed. The net count of two reflections, the -2 0 2 and the -2 0 4, measured as references every 50 reflections did not alter significantly during the data collection indicating that no deterioration of the crystal had occurred. The data were brought to a uniform arbitrary scale by the use of these reflections and Lorentz and polarisation corrections were applied.

The structure was solved by direct methods. A starting set comprising 3 origin defining reflections together with a further 5 automatically selected terms was used. The initial phase refinement (32 permutations) was with 200 E's > 1.36 using 1465 TPR. This was subsequently expanded to 424 probable phases with E's > 1.36 using 3932 TPR. The figures of merit for the best phase solution were NQEST = -0.378, RA(1) = 0.028, RA(2) = 0.090. An E-map computed for this

phase solution gave plausible positions for all the non-hydrogen atoms in the 1:2 complex. The non-hydrogen atoms were refined anisotropically. The carbon hydrogens, with the exception of those of the methyl groups which were refined as rigid bodies, were placed at calculated positions (C-H = 0.96 Å), assigned isotropic thermal parameters, $\underline{U}(H) = 1.2\ \underline{U}_{eq}(C)$, and allowed to ride on their parent carbon atoms. The hydrogens of the NH_3 and BH_3 groups were clearly located in a $\Delta\underline{F}$-map and were refined as rigid bodies (B-H = 1.08, N-H = 0.96 Å).

Refinement using $\underline{F}$ magnitudes was by block-cascade full-matrix least squares (258 variable parameters) and converged to $\underline{R} = 0.051$, $\underline{R}_w = 0.053$, $[w^{-1} = \sigma^2(\underline{F}) + 0.0008\underline{F}^2]$. The largest parameter shift/e.s.d. was 0.084, the mean shift/e.s.d. was 0.016. The residual electron density in the final difference map was within -0.18 and 0.19 $e\text{Å}^{-3}$.

All computations were carried out on an Eclipse S140 computer using the SHELXTL[1] program system.

12.3 DISCUSSION

The final fractional atomic coordinates, anisotropic thermal parameters, bond lengths and bond angles for the non-hydrogen atoms in 11 and 11.$(BH_3NH_3)_2$ are shown in Tables 12.1 - 12.4 and 12.6 - 12.9 respectively. The positions and isotropic temperature factors for the hydrogen atoms in 11 and 11.$(BH_3NH_3)_2$ are shown in Tables 12.5 and 12.10 respectively.

The torsional angles associated with the 18-membered macrocyles in 11 and 11.$(BH_3NH_3)_2$ are shown beside the relevant C-C and C-O bonds in the skeletal drawings of the structures reproduced in figures 12.1 and 12.2 which also provide details of the crystallographic numbering schemes.

The uncomplexed macrocycle 11 has the same unusual conformation (see figure 12.1) as observed for the uncomplexed cis-anti-cis tetraphenyl 18C6 receptor[2]. The most striking features are (i) an anti torsional angle at the bridgehead O-C-C-O groups, (ii) an antiperiplanar relationship between the adjacent pseudo axial substituents at the C-C bridgehead bond, even though 11 is the cis-anti-cis stereoisomer, (iii) two of the axial substituents are orientated over the macrocyclic cavity partially obscuring both of its faces.

The sequence of the torsional angles of the O-C-C-O subunits starting from O(1) are g^+g^-a ag^+a aaa.

The three trans-annular O...O distances for receptor 11 are O(1)...O(1') 7.70, O(4)...O(4') 6.08, O(7)...O(7') 4.53 Å.

The lengths of the C-O bonds (average 1.419 Å and the bond angles (average C-O-C 112.6°; average O-C-C 109.2°) are similar to those observed in uncomplexed 18C6[3]. However, the bridgehead C-C bond length 1.535(3) Å is significantly longer than the other macrocyclic C-C bond lengths (average 1.505 Å).

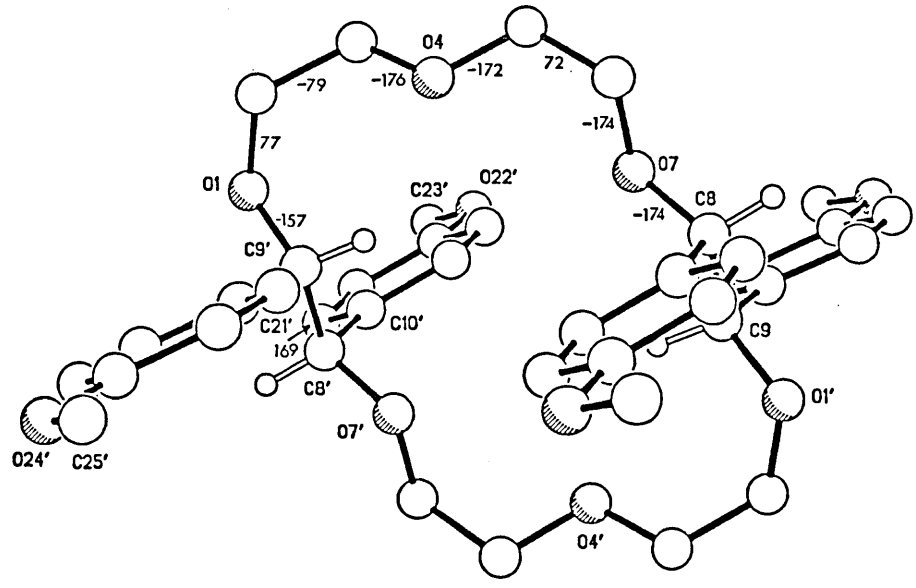


Figure 12.1. The skeletal representation of the solid-state structure of 11.

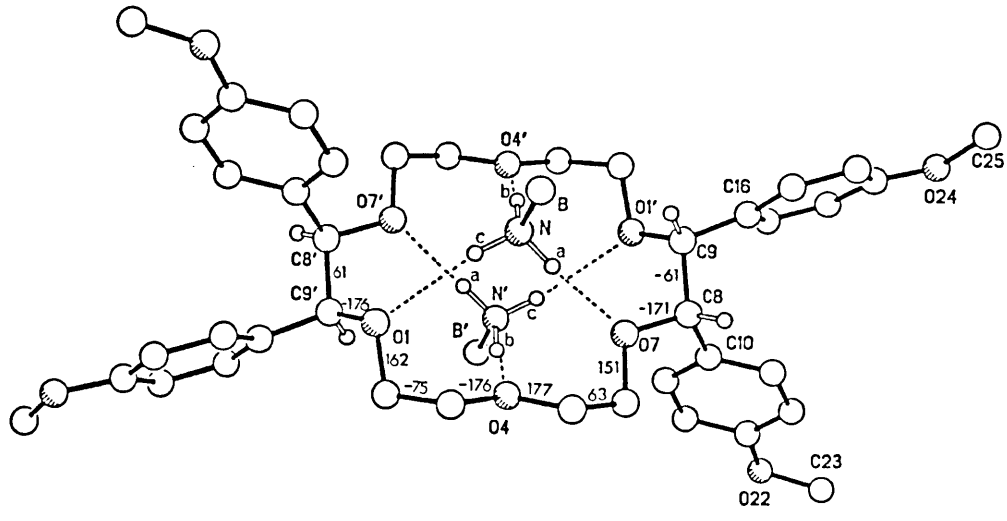


Figure 12.2. The skeletal representation of the solid-state structure of 11.$(BH_3NH_3)_2$.

There are no contacts of less than normal van der Waals distances between symmetry related macrocycles.

On complexation with two molecules of borane-ammonia the 18-membered macrocycle of 11 adopts the classic 'all gauche' polyether conformation (see figure 12.2). This is achieved by rotation about four bonds of the uncomplexed receptor. The brigehead C-C bonds torsion angles change from anti to gauche and the O(1)-C(2) bond torsion angle changes from gauche to anti. The two anisyl substituents which were partially obscuring the macrocyclic cavity are now orientated away from the macrocyclic cavity. This results in both faces of the macrocycle now being free for hydrogen bonding interactions with borane-ammonia.

The polyether oxygens alternate by ~ 1.4 Å above and below their mean plane.

Each of the borane-ammonia molecules are bound to the host via three hydrogen bonds to the upper triangle of polyether oxygens in a perching arrangement. Details of hydrogen bonding are shown in table 12.11. One of the hydrogen bond distances (H1Na...O(1)) is significantly longer than the other two. This is due to a tilt of 7.7^{o} for the borane-ammonia B-N vector to the normal of the mean plane of the polyether oxygens. The angle between this vector and the three upper oxygens is 8.0^{o}.

The distances of both the borane-ammonia nitrogens to the mean

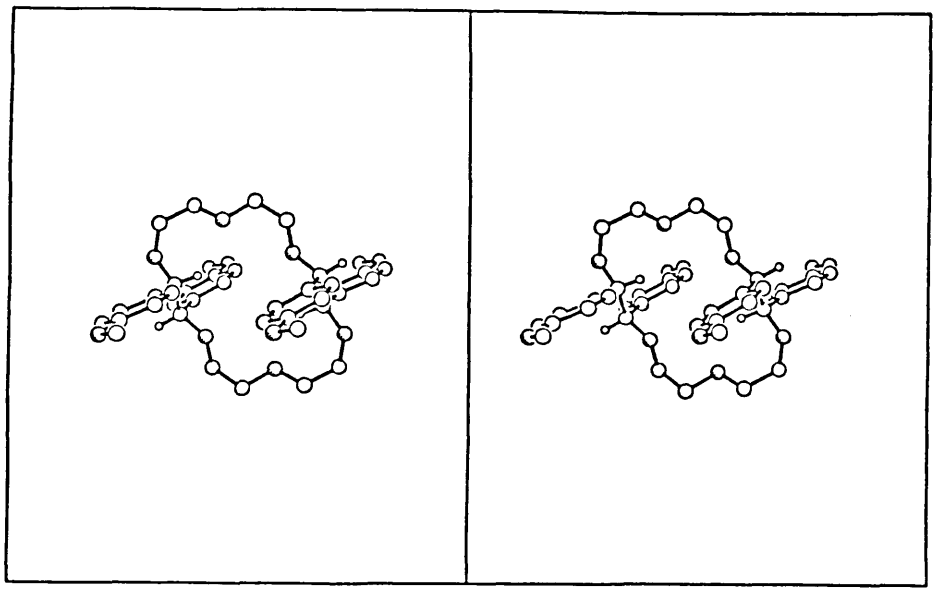


Figure 12.3. The stereo-pair representation of the solid-state structure of 11.

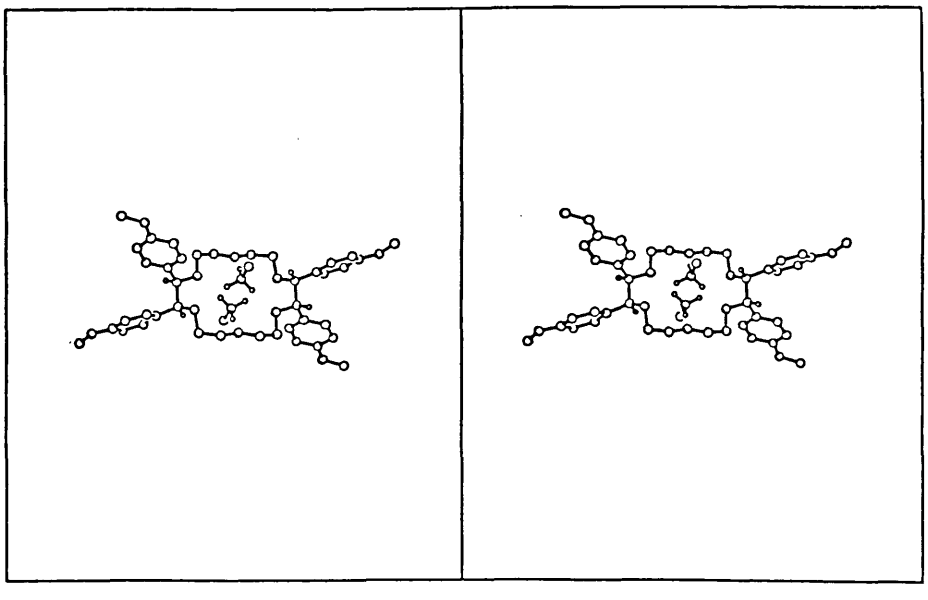


Figure 12.4. The stereo-pair representation of the solid-state structure of 11.$(BH_3NH_3)_2$.

TABLE 12.11. The nitrogen-polyether oxygens contact distances, and relevant hydrogen bond distances and angles where appropriate, in order of increasing N...O distance.

N...O	R(N...O) (Å)	R(H...O) (Å)	$\psi(^{o})$[a]	$\theta(^{o})$[b]
N(1)-O(7)	3.04	2.09[c]	23[c]	172[c]
N(1)-O(4')	3.13	2.21[d]	9[d]	161[d]
N(1)-O(7')	3.17			
N(1)-O(4)	3.20			
N(1)-O(1)	3.34	2.40[e]	19[e]	168[e]
N(1)-O(1')	3.55			

[a] Angles between COC planes and HO vectors.
[b] N-H...O angles.
[c] H(1na)
[d] H(1nb)
[e] H(1nc)

plane of the six polyether oxygens are 1.61 Å and their distance to the corresponding upper triangle of hydrogen bonding polyether oxygens is 1.47 Å. These distances are comparable to those observed in $\underset{\sim\sim}{10}.(BH_3NH_3)_2$[4]. The N...N through the ring distance is 3.21 Å. This is the shortest N...N distance we have observed for 1:2 borane-ammonia complexes[5].

One of the adjacent anisyl groups is equatorial whilst the other is axial to the 18-membered macrocycle. They both have a synclinical relationship about the C-C bridgehead bond.

The lengths of the C-O bonds (average 1.428 Å) and the bond angles (average C-O-C 112.5°; average O-C-C 108.8°) are similar to those observed in complexed 18C6 macrocycles[6]. However, the bridgehead C-C bond length 1.523(4) Å is significantly longer than the other macrocyclic C-C bond lengths (average 1.482 Å). This lengthening has been observed in macrocycle $\underset{\sim\sim}{10}$[4].

The hydrogen atoms of borane-ammonia are in a nearly staggered relationship with respect to each other, the smallest H-N-B-H torsional angle being 51°.

The shortest non-hydrogen contact between symmetry related complexes is 3.12 Å between the methoxy oxygen O(24) and a macrocyclic carbon C(12). There are no other intermolecular contacts of less than normal van der Waals distances.

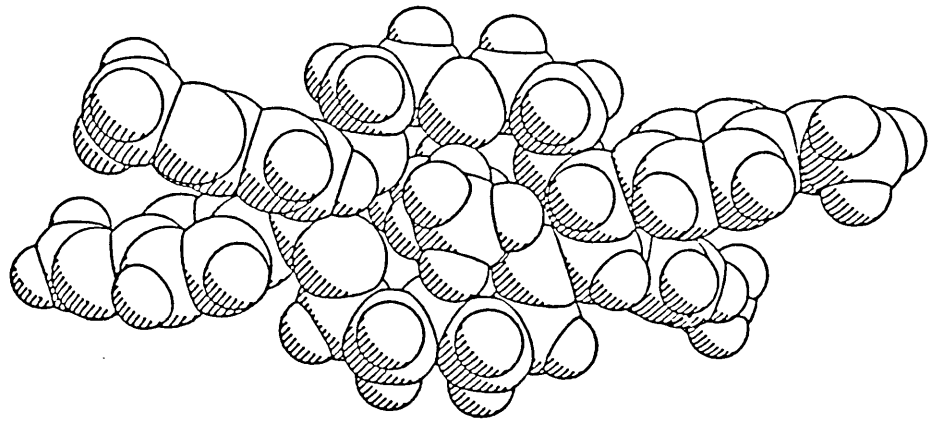


Figure 12.5. The space-filling representation (view normal to the mean plane of the six polyether oxygens) of one of the homotopic faces of $\underset{\sim}{11}.(BH_3NH_3)_2$.

The conformation of the macrocycle in the complex $\underset{\sim\sim}{11}.(BH_3NH_3)_2$ is similar to that of the cis-anti-cis tetraphenyl 18C6 complex with Na and two water molecules[2].

These analyses have shown that although this uncomplexed receptor adopts an unusual geometry, upon complexation with two molecules of borane-ammonia it prefers to adopt the 'all gauche' conformation. Thus the presence of cis-anti-cis substituents appears to have very little effect on the conformation of the 18-membered ring. However, it does result in the binding of two molecules of borane-ammonia whereas in the solid-state, 18C6 only binds one.

TABLE 12.1. Coordinates ($\times 10^4$) and temperature factors ($\AA^2 \times 10^3$)

atom	x	y	z	U
O(1)	8307(2)	-1713(1)	9158(2)	53(1)*
C(2)	6596(3)	-1566(1)	8915(3)	58(1)*
C(3)	6164(3)	-952(1)	8178(2)	58(1)*
O(4)	6479(2)	-401(1)	8955(2)	50(1)*
C(5)	5979(3)	176(1)	8290(2)	57(1)*
C(6)	6560(3)	751(1)	9095(3)	53(1)*
O(7)	8286(2)	813(1)	9195(1)	47(1)*
C(8)	8991(3)	1306(1)	10036(2)	45(1)*
C(9)	10801(3)	1323(1)	9863(2)	46(1)*
C(10)	8815(3)	1159(1)	11366(2)	43(1)*
C(11)	8075(3)	1594(1)	12057(2)	46(1)*
C(12)	7915(3)	1463(1)	13290(2)	50(1)*
C(13)	8495(3)	885(1)	13822(2)	47(1)*
C(14)	9231(3)	445(1)	13142(2)	53(1)*
C(15)	9392(3)	581(1)	11930(2)	51(1)*
C(16)	11041(3)	1570(1)	8602(2)	45(1)*
C(17)	10567(3)	2191(1)	8185(2)	53(1)*
C(18)	10807(3)	2403(1)	7033(2)	58(1)*
C(19)	11527(3)	2005(1)	6258(2)	52(1)*
C(20)	12029(3)	1393(1)	6655(3)	57(1)*
C(21)	11788(3)	1185(1)	7823(2)	53(1)*
O(22)	8382(2)	705(1)	15015(2)	68(1)*
C(23)	7642(4)	1145(2)	15750(3)	73(1)*
O(24)	11658(3)	2258(1)	5122(2)	73(1)*
C(25)	12326(4)	1848(2)	4271(3)	76(1)*

* Equivalent isotropic U defined as one third of the trace of the orthogonalised U_{ij} tensor

TABLE 12.2. Bond lengths (Å)

O(1)-C(2)	1.421(3)	O(1)-C(9a)	1.432(3)
C(2)-C(3)	1.506(4)	C(3)-O(4)	1.414(3)
O(4)-C(5)	1.415(3)	C(5)-C(6)	1.503(4)
C(6)-O(7)	1.412(3)	O(7)-C(8)	1.422(3)
C(8)-C(9)	1.535(3)	C(8)-C(10)	1.511(3)
C(9)-C(16)	1.508(3)	C(9)-O(1a)	1.432(3)
C(10)-C(11)	1.378(3)	C(10)-C(15)	1.386(3)
C(11)-C(12)	1.398(3)	C(12)-C(13)	1.373(3)
C(13)-C(14)	1.377(4)	C(13)-O(22)	1.369(3)
C(14)-C(15)	1.378(4)	C(16)-C(17)	1.391(3)
C(16)-C(21)	1.381(4)	C(17)-C(18)	1.375(4)
C(18)-C(19)	1.382(4)	C(19)-C(20)	1.374(4)
C(19)-O(24)	1.364(3)	C(20)-C(21)	1.388(4)
O(22)-C(23)	1.416(4)	O(24)-C(25)	1.433(4)

TABLE 12.3. Bond Angles (deg.)

C(2)-O(1)-C(9a)	112.5(2)	O(1)-C(2)-C(3)	114.5(2)
C(2)-C(3)-O(4)	110.8(2)	C(3)-O(4)-C(5)	111.3(2)
O(4)-C(5)-C(6)	109.2(2)	C(5)-C(6)-O(7)	109.3(2)
C(6)-O(7)-C(8)	114.1(2)	O(7)-C(8)-C(9)	103.6(2)
O(7)-C(8)-C(10)	112.2(2)	C(9)-C(8)-C(10)	112.3(2)
C(8)-C(9)-C(16)	113.8(2)	C(8)-C(9)-O(1a)	107.8(2)
C(16)-C(9)-O(1a)	110.9(2)	C(8)-C(10)-C(11)	121.2(2)
C(8)-C(10)-C(15)	120.9(2)	C(11)-C(10)-C(15)	117.9(2)
C(10)-C(11)-C(12)	121.5(2)	C(11)-C(12)-C(13)	119.3(2)
C(12)-C(13)-C(14)	119.9(2)	C(12)-C(13)-O(22)	124.0(2)
C(14)-C(13)-O(22)	116.1(2)	C(13)-C(14)-C(15)	120.4(2)
C(10)-C(15)-C(14)	121.0(2)	C(9)-C(16)-C(17)	122.2(2)
C(9)-C(16)-C(21)	120.5(2)	C(17)-C(16)-C(21)	117.3(2)
C(16)-C(17)-C(18)	120.9(2)	C(17)-C(18)-C(19)	120.7(2)
C(18)-C(19)-C(20)	119.5(2)	C(18)-C(19)-O(24)	115.8(2)
C(20)-C(19)-O(24)	124.7(2)	C(19)-C(20)-C(21)	119.2(3)
C(16)-C(21)-C(20)	122.3(2)	C(13)-O(22)-C(23)	117.9(2)
C(19)-O(24)-C(25)	117.4(2)		

TABLE 12.4. Anisotropic temperature factors ($Å^2 \times 10^3$)

atom	U_{11}	U_{22}	U_{33}	U_{23}	U_{13}	U_{12}
O(1)	49(1)	53(1)	56(1)	-10(1)	9(1)	-2(1)
C(2)	52(2)	52(2)	71(2)	-11(1)	13(1)	-11(1)
C(3)	58(2)	57(2)	56(2)	-10(1)	3(1)	-7(1)
O(4)	55(1)	45(1)	51(1)	-0(1)	8(1)	3(1)
C(5)	52(2)	55(2)	60(2)	4(1)	1(1)	0(1)
C(6)	48(2)	51(2)	61(2)	9(1)	11(1)	5(1)
O(7)	43(1)	51(1)	48(1)	-6(1)	12(1)	-3(1)
C(8)	51(2)	37(1)	48(1)	-0(1)	15(1)	2(1)
C(9)	48(2)	39(1)	51(2)	-3(1)	13(1)	1(1)
C(10)	49(1)	36(1)	46(1)	1(1)	14(1)	-2(1)
C(11)	50(1)	37(1)	50(1)	1(1)	12(1)	1(1)
C(12)	56(2)	47(2)	49(2)	-9(1)	15(1)	-1(1)
C(13)	53(2)	48(2)	39(1)	2(1)	4(1)	-7(1)
C(14)	67(2)	40(1)	51(2)	5(1)	6(1)	3(1)
C(15)	60(2)	43(1)	52(2)	-2(1)	15(1)	4(1)
C(16)	45(1)	42(2)	52(2)	-4(1)	17(1)	-5(1)
C(17)	61(2)	42(2)	61(2)	-5(1)	24(1)	1(1)
C(18)	72(2)	44(2)	61(2)	6(1)	25(1)	1(1)
C(19)	59(2)	54(2)	48(2)	-4(1)	22(1)	-12(1)
C(20)	66(2)	50(2)	63(2)	-9(1)	30(1)	-3(1)
C(21)	56(2)	43(1)	66(2)	-2(1)	22(1)	2(1)
O(22)	97(1)	65(1)	44(1)	6(1)	18(1)	5(1)
C(23)	85(2)	88(2)	49(2)	2(2)	21(2)	0(2)
O(24)	103(2)	66(1)	58(1)	-3(1)	36(1)	-9(1)
C(25)	95(2)	82(2)	59(2)	-14(2)	35(2)	-18(2)

The anisotropic temperature factor exponent takes the form:

$$-2\pi^2(h^2a^{*2}U_{11} + \ldots + 2\,hka^*b^*U_{12}\cos\gamma^* + \ldots)$$

TABLE 12.5. Coordinates ($\times 10^4$) and temperature factors ($Å^2 \times 10^3$)

atom	x	y	z	U
H(2a)	6029	-1920	8455	70
H(2b)	6224	-1522	9699	70
H(3a)	5017	-962	7810	69
H(3b)	6820	-927	7532	69
H(5a)	6453	190	7544	67
H(5b)	4799	185	8071	67
H(6a)	6291	690	9911	65
H(6b)	6032	1137	8727	65
H(8)	8453	1717	9865	53
H(9)	11212	886	9908	56
H(11)	7667	1995	11674	57
H(12)	7395	1773	13753	54
H(14)	9651	43	13512	65
H(15)	9897	273	11451	62
H(17)	10067	2474	8712	61
H(18)	10468	2833	6763	70
H(20)	12550	1114	6133	69
H(21)	12145	757	8097	65
H(23a)	6475	1132	15451	82
H(23b)	8027	1583	15727	82
H(23c)	7870	987	16593	82
H(25a)	11983	2044	3469	84
H(25b)	11875	1418	4268	84
H(25c)	13508	1825	4449	84

TABLE 12.6. Coordinates ($\times 10^4$) and temperature factors ($Å^2 \times 10^3$)

atom	x	y	z	U
O(1)	7256(3)	-774(3)	5821(1)	52(1)*
C(2)	8795(4)	-128(4)	5700(1)	64(2)*
C(3)	8562(4)	1471(4)	5560(1)	60(1)*
O(4)	7856(3)	1535(2)	5102(1)	49(1)*
C(5)	7704(4)	3047(4)	4937(1)	53(1)*
C(6)	7058(4)	3042(4)	4450(1)	54(1)*
O(7)	5452(3)	2397(3)	4453(1)	49(1)*
C(8)	4433(4)	2964(4)	4086(1)	45(1)*
C(9)	2723(4)	2391(4)	4183(1)	47(1)*
C(10)	5089(4)	2601(4)	3600(1)	45(1)*
C(11)	4932(4)	3644(4)	3246(1)	48(1)*
C(12)	5545(4)	3387(4)	2800(1)	50(1)*
C(13)	6337(4)	2065(4)	2710(1)	52(1)*
C(14)	6504(4)	993(4)	3061(1)	58(1)*
C(15)	5871(4)	1264(4)	3498(1)	51(1)*
C(16)	1525(4)	3091(4)	3843(1)	44(1)*
C(17)	762(4)	4414(4)	3959(1)	46(1)*
C(18)	-212(4)	5204(4)	3647(1)	50(1)*
C(19)	-424(4)	4629(4)	3199(1)	48(1)*
C(20)	262(4)	3264(4)	3080(1)	53(1)*
C(21)	1229(4)	2494(4)	3396(1)	51(1)*
O(22)	7039(3)	1706(3)	2289(1)	74(1)*
C(23)	6999(6)	2811(5)	1932(1)	84(2)*
O(24)	-1299(3)	5337(3)	2850(1)	62(1)*
C(25)	-2138(5)	6672(4)	2972(2)	75(2)*
N	4105(3)	1116(3)	5360(1)	52(1)*
B	3296(6)	2400(5)	5672(2)	68(2)*

* Equivalent isotropic U defined as one third of the trace of the orthogonalised U_{ij} tensor

TABLE 12.7. Bond lengths (Å)

O(1)-C(2)	1.433(4)	O(1)-C(9a)	1.431(4)
C(2)-C(3)	1.483(5)	C(3)-O(4)	1.423(4)
O(4)-C(5)	1.422(4)	C(5)-C(6)	1.480(5)
C(6)-O(7)	1.439(4)	O(7)-C(8)	1.424(4)
C(8)-C(9)	1.523(4)	C(8)-C(10)	1.524(5)
C(9)-C(9a)	1.504(5)	C(9)-O(9a)	1.431(4)
C(10)-C(11)	1.371(5)	C(10)-C(15)	1.379(5)
C(11)-C(12)	1.391(5)	C(12)-C(13)	1.365(5)
C(13)-C(14)	1.384(5)	C(13)-O(22)	1.373(4)
C(14)-C(15)	1.373(5)	C(16)-C(17)	1.370(5)
C(16)-C(21)	1.398(5)	C(17)-C(18)	1.380(5)
C(18)-C(19)	1.383(5)	C(19)-C(20)	1.377(5)
C(19)-O(24)	1.373(4)	C(20)-C(21)	1.376(5)
O(22)-C(23)	1.411(5)	O(24)-C(25)	1.413(5)
N-B	1.593(6)		

TABLE 12.8. Bond Angles (deg.)

C(2)-O(1)-C(9a)	112.7(2)	O(1)-C(2)-C(3)	109.5(3)
C(2)-C(3)-O(4)	109.6(3)	C(3)-O(4)-C(5)	111.9(2)
O(4)-C(5)-C(6)	109.6(3)	C(5)-C(6)-O(7)	108.5(3)
C(6)-O(7)-C(8)	113.0(2)	O(7)-C(8)-C(9)	109.8(3)
O(7)-C(8)-C(10)	112.3(3)	C(9)-C(8)-C(10)	115.5(3)
C(8)-C(9)-C(16)	110.3(3)	C(8)-C(9)-O(1a)	108.7(3)
C(16)-C(9)-O(1a)	114.5(3)	C(8)-C(10)-C(11)	119.5(3)
C(8)-C(10)-C(15)	122.9(3)	C(11)-C(10)-C(15)	117.6(3)
C(10)-C(11)-C(12)	121.9(3)	C(11)-C(12)-C(13)	119.3(3)
C(12)-C(13)-C(14)	119.7(3)	C(12)-C(13)-O(22)	124.6(3)
C(14)-C(13)-O(22)	115.7(3)	C(13)-C(14)-C(15)	119.9(3)
C(10)-C(15)-C(14)	121.5(3)	C(9)-C(16)-C(17)	119.7(3)
C(9)-C(16)-C(21)	122.4(3)	C(17)-C(16)-C(21)	117.8(3)
C(16)-C(17)-C(18)	122.9(3)	C(17)-C(18)-C(19)	118.3(3)
C(18)-C(19)-C(20)	120.1(3)	C(18)-C(19)-O(24)	124.1(3)
C(20)-C(19)-O(24)	115.8(3)	C(19)-C(20)-C(21)	120.6(3)
C(16)-C(21)-C(20)	120.2(3)	C(13)-O(22)-C(23)	117.5(3)
C(19)-O(24)-C(25)	117.3(3)		

TABLE 12.9. Anisotropic temperature factors ($Å^2 \times 10^3$)

atom	U_{11}	U_{22}	U_{33}	U_{23}	U_{13}	U_{12}
O(1)	44(1)	47(1)	64(2)	10(1)	4(1)	-3(1)
C(2)	[illegible]	[illegible]	[illegible]	[illegible]	[illegible]	-7(2)
C(3)	57(2)	65(3)	59(2)	12(2)	-8(2)	-14(2)
O(4)	54(1)	44(1)	48(1)	6(1)	-4(1)	-8(1)
C(5)	54(2)	46(2)	59(3)	3(2)	0(2)	-8(2)
C(6)	48(2)	54(2)	58(3)	10(2)	-2(2)	-10(2)
O(7)	46(1)	53(1)	49(1)	9(1)	1(1)	-7(1)
C(8)	48(2)	44(2)	45(2)	6(2)	2(2)	3(2)
C(9)	48(2)	43(2)	50(2)	6(2)	12(2)	4(2)
C(10)	44(2)	41(2)	44(2)	4(2)	3(2)	-1(2)
C(11)	54(2)	40(2)	51(2)	6(2)	10(2)	4(2)
C(12)	58(2)	49(2)	43(2)	11(2)	3(2)	-1(2)
C(13)	56(2)	52(3)	48(2)	-7(2)	3(2)	-5(2)
C(14)	67(3)	44(2)	64(3)	-4(2)	6(2)	9(2)
C(15)	64(2)	41(2)	48(2)	6(2)	8(2)	2(2)
C(16)	46(2)	42(2)	45(2)	2(2)	11(2)	1(2)
C(17)	54(2)	48(2)	38(2)	-1(2)	7(2)	-1(2)
C(18)	58(2)	46(2)	46(2)	-2(2)	14(2)	6(2)
C(19)	40(2)	50(2)	53(2)	8(2)	8(2)	6(2)
C(20)	54(2)	60(2)	45(2)	-6(2)	4(2)	7(2)
C(21)	55(2)	48(2)	50(2)	-10(2)	7(2)	12(2)
O(22)	96(2)	73(2)	54(2)	-7(1)	19(1)	6(2)
C(23)	105(3)	103(4)	46(3)	-2(2)	23(2)	1(3)
O(24)	60(2)	70(2)	57(2)	13(1)	2(1)	18(1)
C(25)	75(3)	75(3)	73(3)	19(2)	4(2)	22(2)
N	58(2)	51(2)	47(2)	-1(1)	12(1)	2(2)
B	77(3)	62(3)	65(3)	-10(3)	10(3)	6(3)

The anisotropic temperature factor exponent takes the form:

$$-2\pi^2(h^2a^{*2}U_{11} + \ldots + 2\,hka^*b^*U_{12}\cos\gamma^* + \ldots)$$

TABLE 12.10. Coordinates ($\times 10^4$) and temperature factors ($Å^2 \times 10^3$)

atom	x	y	z	U
H(2a)	9512	-174	5968	77
H(2b)	9258	-688	5446	77
H(3a)	9598	1972	5557	76
H(3b)	7861	1967	5779	76
H(5a)	6978	3595	5137	66
H(5b)	8753	3522	4942	66
H(6a)	7754	2454	4253	67
H(6b)	7002	4059	4334	67
H(8)	4402	4049	4086	59
H(9)	2364	2692	4489	60
H(11)	4380	4577	3309	58
H(12)	5414	4130	2557	59
H(14)	7070	67	2999	70
H(15)	5967	503	3737	65
H(17)	915	4809	4270	57
H(18)	-726	6131	3739	63
H(20)	58	2845	2774	64
H(21)	1704	1545	3308	63
H(23a)	7540	3727	2024	105
H(23b)	5922	3045	1820	105
H(23c)	7598	2331	1686	105
H(25a)	-1403	7471	3057	89
H(25b)	-2909	6525	3219	89
H(25c)	-2704	6937	2687	89
H(1na)	4581	1592	5091	65
H(1nb)	3297	402	5258	65
H(1nc)	4935	601	5537	65
H(1ba)	2517	3088	5452	61
H(1bb)	4271	3086	5813	60
H(1bc)	2596	1936	5957	60

12.4 REFERENCES

1. G.M. Sheldrick, SHELXTL, An integrated system for solving, refining, and displaying crystal structures from diffractometer data, University of Göttingen, Federal Republic of Germany, 1981.
2. G. Weber, G.M. Sheldrick, T. Burgemeister, F. Dietl, A. Mannschreck, and A. Merz, Tetrahedron 1984, 40, 855.
3. J.D. Dunitz, and P. Seiler, Acta. Cryst., 1974, B30, 2739.
4. See Chapter 11.
5. B.L. Allwood, H. Shahriari-Zavareh, J.F. Stoddart, and D.J. Williams, J. Chem. Soc., Chem. Commun., 1984, 1461.

   D.R. Alston, J.F. Stoddart, J.B. Wolstenholme, B.L. Allwood, and D.J. Williams, Tetrahedron, 1985, 41, 2923.

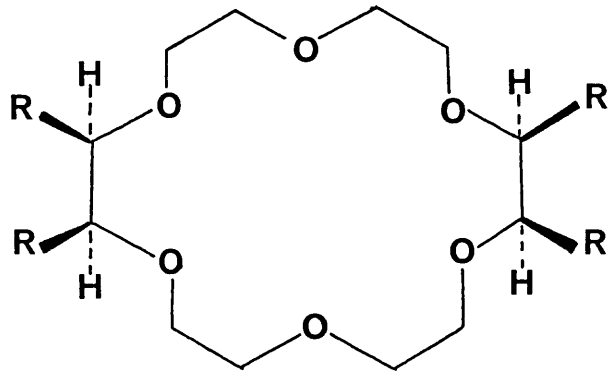
   B.L. Allwood, H. Shahriari-Zavareh, J.F. Stoddart, and D.J. Williams, J. Incl. Phenom., 1985, 3, 355.
6. I. Goldberg, The Chemistry of Functional Groups. Supplement E: The Chemistry of Ethers, Crown Ethers, Hydroxy Groups and their Sulphur Analogues, 1980, Part 1, 175, Editor S. Patel, Chichester: John Wiley.

CHAPTER 13

The crystal structures of *cis*-*syn*-*cis* 2,3,11,12 tetra-anisyl-18-crown-6 and its complex with borane-ammonia.

13.1 INTRODUCTION

This chapter reports the X-ray structure analyses of cis-syn-cis 2,3,11,12 tetra-anisyl-18-crown-6 (12) and its complex with borane-ammonia.



R = p-$MeOC_6H_4$

12

13.2 EXPERIMENTAL

Clear crystals of 12 were grown from a dichloromethane/n-pentane solution. A crystal of dimensions 0.13 x 0.43 x 0.50 mm was used for unit cell and intensity measurements.

Crystal data: $C_{40}H_{48}O_{10}$, M = 689, triclinic, a = 10.960(2), b = 13.194(2), c = 13.785(4) Å, α = 85.76(2), β = 81.87(2), γ = 73.14(1)°, U = 1889 $Å^3$, space group $P\bar{1}$, Z = 2, D_c = 1.22 g cm^{-3}, F(000) = 736, μ(Cu-K_α) = 6.70 cm^{-1}.

Refined unit-cell parameters were obtained by centering 12 reflections on a Nicolet R3m diffractometer. 3878 unique reflections ($\theta \leq 50°$) were measured with Cu-K_α radiation (graphite monochromator)

using the omega-scan routine. Of these 3294 had $|\underline{F}_o| > 3\sigma(|\underline{F}_o|)$ and were considered to be observed. The net count of two reflections, the -3 -3 -1 and the -2 2 1, measured as references every 50 reflections did not alter significantly during the data collection indicating that no deterioration of the crystal had occurred. The data were brought to a uniform arbitrary scale by the use of these reflections and Lorentz and polarisation corrections were applied.

The structure was solved by direct methods. A starting set comprising 3 origin defining reflections together with 8 automatically selected terms was used. The initial phase refinement (256 permutations) was with 200 $\underline{E}$'s > 2.0 using 815 TPR. This was subsequently expanded to 411 probable phases with $\underline{E}$'s > 1.70 using 1534 TPR. The figures of merit for the best phase solution were NQEST = -0.458, RA(1) = 0.027, RA(2) = 0.051. Three cycles of $\Delta\underline{E}$-map recycling for this solution gave an $\underline{R}_E$ = 0.26 for all the non-hydrogen atoms in the structure. The non-hydrogen atoms were refined anisotropically. All the methoxy groups of the macrocycle have high anisotropic thermal parameters indicating possible disorder. Two alternative sites were located for C(46) and refined with occupancies of 40 and 60%. There was also evidence for disorder in the O(47) methoxy group, though discrete alternative orientations could not be resolved. This group was refined using distance constraints for the C(34)-O(47) and O(47)-C(48) bonds of 1.45 Å. The protons on the methyl carbon C(48) were not located. The remaining hydrogens, with the exception of those of the methyl groups which were refined as rigid bodies, were placed at calculated positions (C-H = 0.96 Å), assigned

isotropic thermal parameters, $\underline{U}(H) = 1.2\ \underline{U}_{eq}(C)$, and allowed to ride on their parent carbon atoms.

Refinement using $\underline{F}$ magnitudes was by block-cascade full-matrix least squares (473 variable parameters) and converged to $\underline{R} = 0.096$, $\underline{R}_w = 0.116$, $[w^{-1} = \sigma^2(\underline{F}) + 0.0018\underline{F}^2]$. The largest parameter shift/e.s.d. was 0.385, the mean shift/e.s.d. was 0.060. The residual electron density in the final difference map was within -0.40 and 0.80 $e\text{Å}^{-3}$.

Clear crystals of $\underline{12}.BH_3NH_3$ were grown from a dichloromethane/n-pentane solution. A clear crystal of dimensions 0.33 x 0.48 x 0.83 mm was used for unit cell and intensity measurements.

Crystal data: $C_{40}H_{48}O_{10}.BNH_6$, $\underline{M} = 720$, monolinic, $\underline{a} = 11.078(4)$, $\underline{b} = 18.010(2)$, $\underline{c} = 20.639(9)$ Å, $\beta = 101.07(3)^o$, $\underline{U} = 4041$ Å^3, space group $\underline{P2_1/n}$, $\underline{Z} = 4$, $\underline{D}_c = 1.19$ g cm^{-3}, $\underline{F}(000) = 1549$, $\mu(Cu\text{-}\underline{K}_\alpha) = 6.49$ cm^{-1}.

Refined unit-cell parameters were obtained by centering 16 reflections on a Nicolet R3m diffractometer. 4123 unique reflections ($\theta < 50^o$) were measured with Cu-$\underline{K}_\alpha$ radiation (graphite monochromator) using the omega-scan routine. Of these 3503 had $|\underline{F}_o| > 3\sigma(|\underline{F}_o|)$ and were considered to be observed. The net count of two reflections, the 1 0 3 and the 0 0 8, measured as references every 50 reflections did not alter significantly during the data collection indicating that no deterioration of the crystal had occurred. The data were brought to a uniform arbitrary scale by the use of these reflections and Lorentz and polarisation corrections were applied.

The structure was solved by direct methods. A starting set comprising 3 origin defining reflections together with a further 5 automatically selected terms was used. The initial phase refinement (32 permutations) was with 200 $\underline{E}$'s > 1.9 using 1170 TPR. This was subsequently expanded to 425 probable phases with $\underline{E}$'s > 1.72 using 2375 TPR. The figures of merit for the best phase solution were NQEST = -0.310, RA(1) = 0.032, RA(2) = 0.073. An $\underline{E}$-map computed for this phase solution gave plausible positions for 45 of the 52 non-hydrogen atoms in the structure. The remaining non-hydrogen atoms were located in a subsequent $\Delta\underline{F}$-map. The non-hydrogen atoms were refined anisotropically. The carbon hydrogens, with the exception of those of the methyl groups which were refined as rigid bodies, were placed at calculated positions (C-H = 0.96 Å), assigned isotropic thermal parameters, $\underline{U}(H) = 1.2\ \underline{U}_{eq}(C)$, and allowed to ride on their parent carbon atoms. The hydrogens of the NH_3 and BH_3 groups were clearly located in a $\Delta\underline{F}$-map and the groups refined as rigid bodies (B-H = 1.08, N-H = 0.96 Å).

Refinement using $\underline{F}$ magnitudes was by block-cascade full-matrix least squares (488 variable parameters) and converged to $\underline{R}$ = 0.045, $\underline{R}_w$ = 0.052, $[w^{-1} = \sigma^2(\underline{F}) + 0.0007\underline{F}^2]$. The largest parameter shift/e.s.d. was 0.094, the mean shift/e.s.d. was 0.031. The residual electron density in the final difference map was within -0.14 and 0.20 $eÅ^{-3}$.

All computations were carried out on an Eclipse S140 computer using the SHELXTL[1] program system.

13.3 DISCUSSION

The final fractional atomic coordinates, anisotropic thermal parameters, bond lengths and bond angles for the non-hydrogen atoms in **12** and **12**.BH_3NH_3 are shown in Tables 13.1 - 13.4 and 13.6 - 13.9 respectively. The positions and isotropic temperature factors for the hydrogen atoms in **12** and **12**.BH_3NH_3 are shown in Tables 13.5 and 13.10 respectively.

The torsional angles associated with the 18-membered macrocyles in **12** and **12**.BH_3NH_3 are shown beside the relevant C-C and C-O bonds in the skeletal drawings of the structures reproduced in figures 13.1 and 13.4 which also provide details of the crystallographic numbering schemes.

The conformation of the 18-membered ring of the *trans*-*syn*-*trans* stereoisomer of tetra-anisyl-18C6 can be described, in terms of the six sequential independent O-C-C-O subunits starting from O(1), as aaa g^+g^-a ag^+a aaa g^-g^+a ag^+a. Though the torsional angles about the C(15)-O(16), O(13)-C(14), and C(5)-C(6) bonds (see figure 13.1) have large deviations from the expected *gauche* values[2].

It can be seen from the space-filling representation of **12** (figure 13.3) that the axial substituents partially obscure one face of the polyether macrocycle.

The three trans-annular O...O distances for receptor **12** are

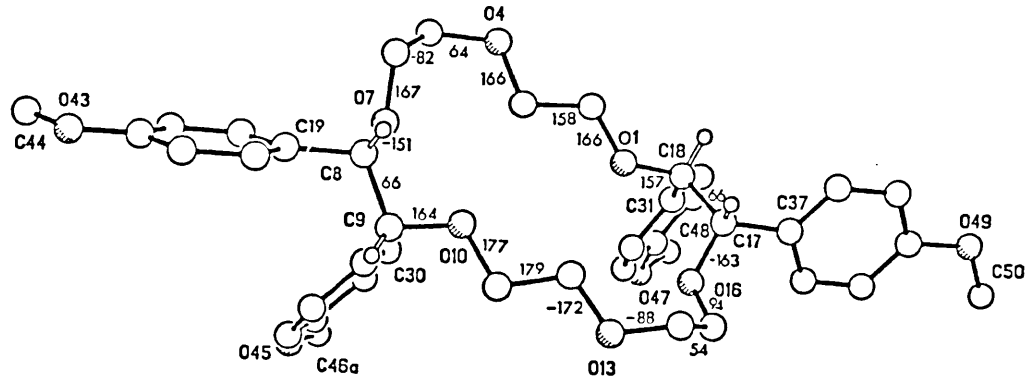


Figure 13.1. The skeletal representation of the solid-state structure of 12.

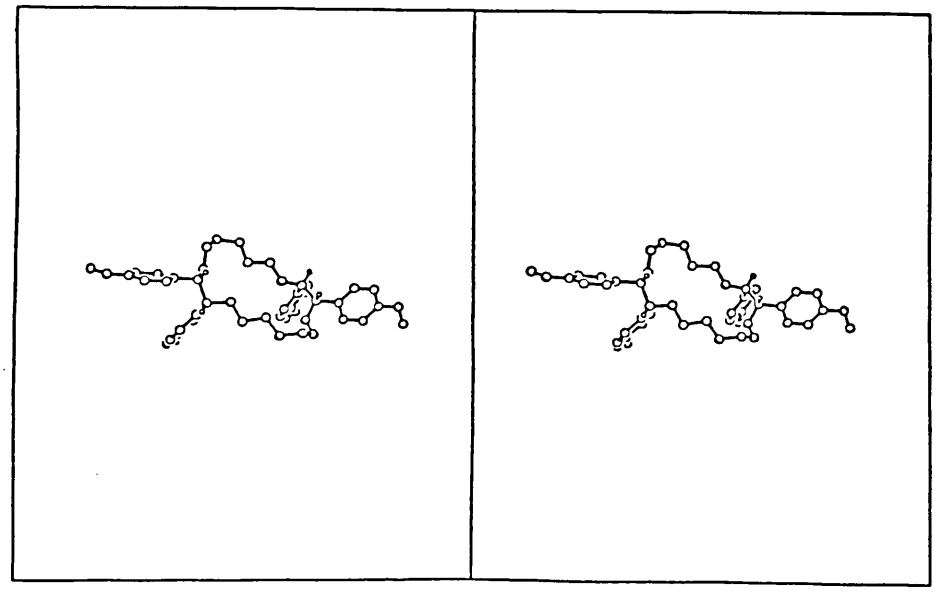


Figure 13.2. The stereo-pair representation of the solid-state structure of 12.

O(1)...O(10) 4.13, O(4)...O(13) 6.67 and O(7)...O(16) 7.06 Å.

The C-O bonds lengths (average 1.403 Å) in the 18-membered macrocycle are similar to those observed in uncomplexed 18C6[3]. Four of the ring C-C bond lengths are similar to those in uncomplexed 18C6 whilst the C-C bridgehead bond lengths 1.533 and 1.541 Å are comparable with that for a single aliphatic C-C bond[4]. The C-O-C bond angles range from 112.7 to 120.1° (average 116.1°). The O-C-C bond angles range from 105.5 to 120.8° (average 111.7°). Both the C-O-C and O-C-C bond angles show a much greater spread of values than those observed in uncomplexed 18C6.

There are several short contacts between symmetry related macrocycles, C(46a)...C(46b) 2.67, C(48)...C(46b) 2.86, C(46a)...O(13) 3.19 Å. However, all these contacts involve the disordered methoxy atoms [C(46a), C(46b) and C(48)] and may represent contacts between different conformations of the anisyl groups that may not truely be related by the crystallographic symmetry. There are no other intermolecular contacts of less than normal van der Waals distances.

The high final R-factor can be attributed to the unresolved disorder in the methoxy group, O(47)-C(48).

On complexation with one molecule of borane-ammonia the 18-membered macrocycle of 12 adopts a pseudo 'all gauche' conformation. This transformation is achieved by rotations about five bonds of the uncomplexed receptor: one of the bridgehead C-C bond torsion angles

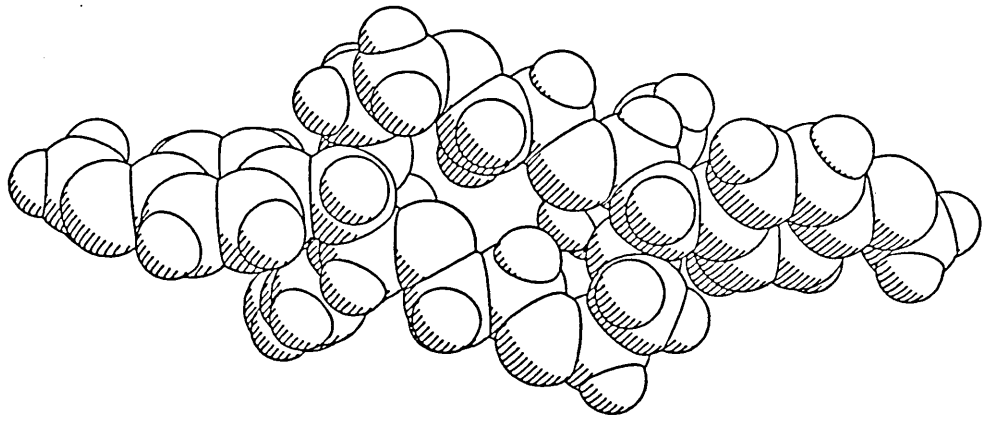


Figure 13.3. The space-filling representation (view normal to the mean plane of the six polyether oxygens) of one of the distereotopic faces of 12.

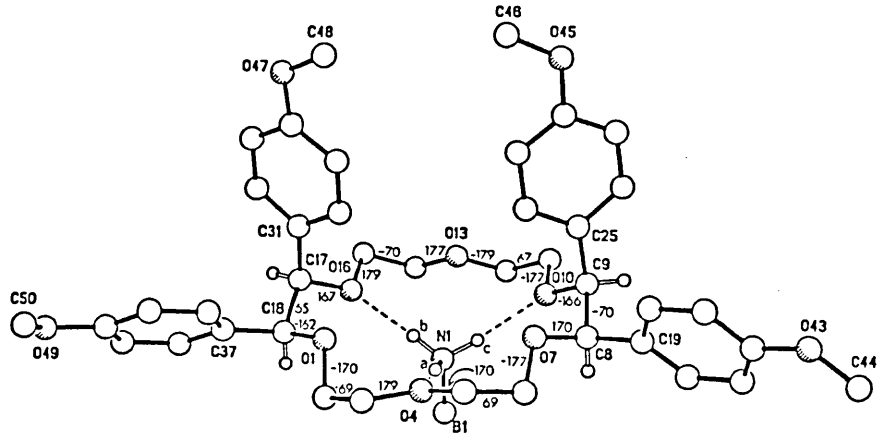


Figure 13.4. The skeletal representation of the solid-state structure of $12.BH_3NH_3$.

changes sign; three C-O bond torsion angles [O(4)-C(5), C(14)-O(13), C(15)-O(16)] change from gauche to anti; the C(11)-C(12) bond torsional angle changes from anti to gauche.

However, the polyether oxygens do not alternate symmetrically above and below their mean plane. The deviation of the oxygens from the mean plane are O(1) -0.21, O(4) 0.34, O(7) -0.34, O(10) 0.17, O(13) -0.06, and O(16) 0.07 Å. Even so, the borane-ammonia molecule is bound to the upper triangle of polyether oxygens via hydrogen bonding in a perching type arrangement.

The distance of the borane-ammonia nitrogen to the mean plane of the polyether oxygens is 1.23 Å and its distance to the upper triangle of polyether oxygens is 1.03 Å. This compares with distances of the nitrogen to the mean plane of the polyether oxygens in other 1:1 complexes with 18C6 macrocycles[5] of 1.30, 1.27 and 1.24 Å. In The 1:1 complex between borane-ammonia and a bismannosido-18C6 macrocycle[5b], the distance of the nitrogen to the mean plane of the polyether oxygens is unusually long 1.59 Å. This was attributed to the non 'all gauche' conformation of the 18-membered macrocycle. The borane-ammonia molecule approaches nearly parallel (4.8°) to the normal of the mean plane of the polyether oxygens. This tilt angle compares with values of 1, 11, 4.5 and 13° in 1:1 complexes of borane-ammonia with other 18C6 macrocycles[5].

The hydrogen atoms of the borane-ammonia are in a nearly staggered relationship with respect to each other, with the smallest H-N-B-H torsional angle being 55.2°.

TABLE 13.11. The nitrogen-polyether oxygens contact distances, and relevant hydrogen bond distances and angles where appropriate, in order of increasing N...O distance.

N...O	R(N...O) (Å)	R(H...O) (Å)	$\psi(^{o})$[a]	$\theta(^{o})$[b]
N(1)-O(4)	2.90	1.94[c]	7[c]	179[c]
N(1)-O(10)	2.95	1.99[d]	12[d]	175[d]
N(1)-O(16)	2.97	2.02[e]	16[e]	177[e]
N(1)-O(13)	3.10			
N(1)-O(1)	3.19			
N(1)-O(7)	3.31			

[a] Angles between COC planes and HO vectors.
[b] N-H...O angles.
[c] H(1na)
[d] H(1nc)
[e] H(1nb)

The C-O bond lengths (average 1.421 Å) and the bond angles (average C-O-C 113.2°; average O-C-C 108.7°) of the macrocyclic ring in the complex are similar to those found in 18C6 complexes[2]. However, the bridgehead C-C bond length 1.533(3) Å is longer than the other ring C-C bonds (average 1.487 Å). This lengthening of the bridgehead C-C bond has also been observed for receptors 10 and 11[6].

There are no contacts of less than normal van der Waals distances between symmetry related complexes.

Inspection of the two space-filling representations of the complex (figure 13.5) reveals that the two axial anisyl substituents obscure one of the faces of the macrocycle thus preventing the approach of a borane-ammonia molecule to it. This provides an explanation for the 1:1 host guest stoicheiometry of the complex.

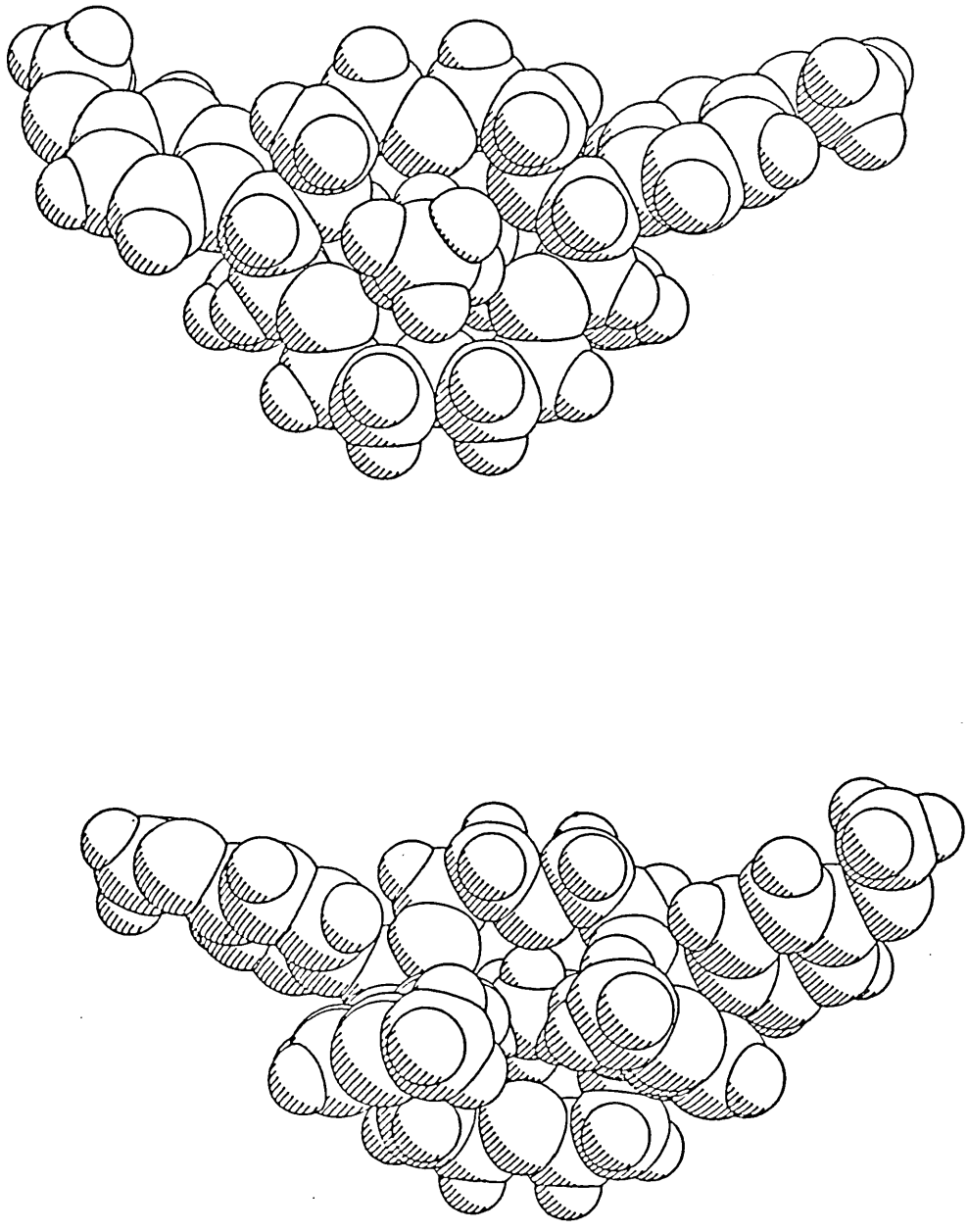


Figure 13.5. The space-filling representations (view normal to the mean plane of the six polyether oxygens) of the distereotopic faces of 12.BH_3NH_3.

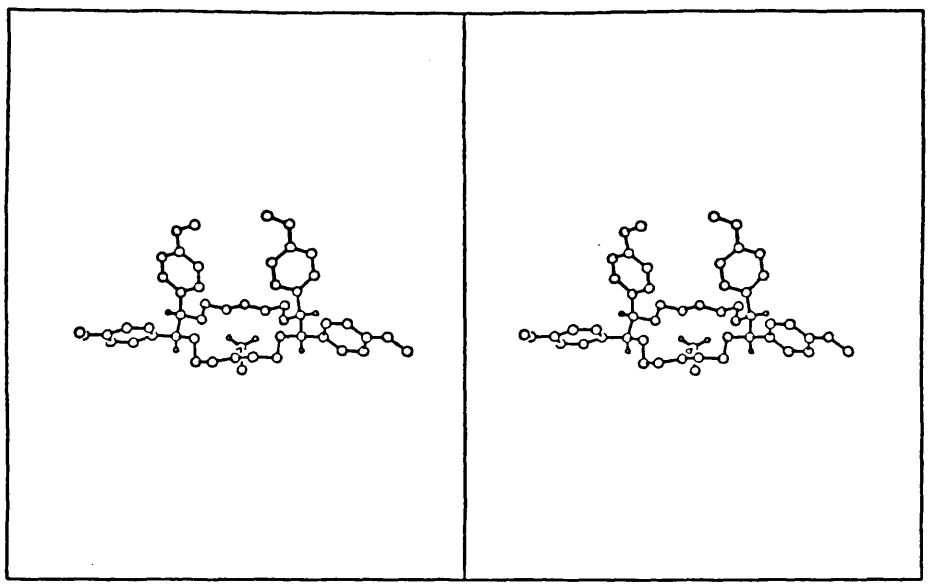


Figure 13.6. The stereo-pair representation of the solid-state structure of 12.BH_3NH_3.

TABLE 13.1. Coordinates ($\times 10^4$) and temperature factors ($Å^2 \times 10^3$)

atom	x	y	z	U
O(1)	6156(3)	1440(3)	-3627(2)	79(1)*
C(2)	7119(5)	484(4)	-3578(4)	86(2)*
C(3)	7421(5)	217(4)	-2574(4)	73(2)*
O(4)	7984(4)	-837(3)	-2443(3)	110(2)*
C(5)	8594(6)	-1191(4)	-1599(4)	96(3)*
C(6)	7777(6)	-1015(4)	-666(4)	90(3)*
O(7)	7591(4)	38(3)	-385(3)	82(2)*
C(8)	6602(5)	370(4)	397(4)	79(2)*
C(9)	6059(5)	1569(4)	266(4)	78(2)*
O(10)	5474(4)	1721(3)	-612(3)	93(2)*
C(11)	4627(6)	2728(4)	-759(4)	88(3)*
C(12)	4165(7)	2778(5)	-1697(4)	117(3)*
O(13)	3306(4)	3731(3)	-1888(3)	115(2)*
C(14)	2708(7)	3793(8)	-2715(4)	156(4)*
C(15)	3258(6)	4066(7)	-3602(5)	127(4)*
O(16)	4544(3)	3469(3)	-3943(3)	89(2)*
C(17)	4625(5)	2626(4)	-4551(4)	77(2)*
C(18)	6017(4)	1876(4)	-4593(4)	68(2)*
C(19)	7018(5)	48(4)	1407(4)	71(2)*
C(20)	6132(5)	14(4)	2203(4)	79(2)*
C(21)	6482(5)	-269(4)	3115(4)	82(3)*
C(22)	7735(6)	-560(4)	3258(4)	80(2)*
C(23)	8656(5)	-515(5)	2479(4)	86(3)*
C(24)	8297(5)	-217(5)	1553(4)	83(3)*
C(25)	7067(5)	2158(4)	235(4)	72(2)*
C(26)	7103(5)	2713(4)	1055(4)	81(2)*
C(27)	8036(5)	3213(4)	1060(4)	86(3)*
C(28)	8932(6)	3184(4)	269(5)	90(3)*
C(29)	8895(6)	2663(4)	-563(5)	94(3)*
C(30)	7968(7)	2167(4)	-556(4)	95(3)*
C(31)	7030(5)	2377(4)	-4994(3)	64(2)*
C(32)	7353(5)	3085(4)	-4463(4)	85(2)*
C(33)	8265(7)	3555(5)	-4820(6)	101(3)*
C(34)	8887(5)	3349(5)	-5758(6)	112(3)*
C(35)	8596(7)	2645(6)	-6299(5)	105(3)*
C(36)	7671(5)	2175(4)	-5914(4)	77(2)*
C(37)	4327(4)	3005(4)	-5586(4)	70(2)*
C(38)	4504(5)	3938(4)	-5996(4)	74(2)*
C(39)	4262(5)	4267(4)	-6942(4)	73(2)*
C(40)	3799(5)	3653(4)	-7478(4)	72(2)*
C(41)	3633(6)	2717(4)	-7087(5)	90(3)*
C(42)	3860(5)	2407(4)	-6128(4)	84(3)*
O(43)	7974(5)	-840(4)	4207(3)	114(2)*
C(44)	9261(8)	-1165(9)	4377(6)	182(5)*
O(45)	9889(5)	3654(4)	305(4)	126(3)*
C(46a)	10703(12)	3733(9)	-513(11)	142(7)*
C(46b)	10064(23)	4244(15)	1066(14)	149(11)*
O(47)	9784(7)	3982(6)	-5979(7)	226(5)*
C(48)	10484(15)	3825(14)	-6941(9)	288(11)*
O(49)	3505(4)	3919(3)	-8421(3)	100(2)*
C(50)	3645(8)	4892(5)	-8840(5)	124(4)*

* Equivalent isotropic U defined as one third of the trace of the orthogonalised U_{ij} tensor

TABLE 13.2. Bond lengths (Å)

O(1)-C(2)	1.396(6)	O(1)-C(18)	1.439(6)
C(2)-C(3)	1.474(8)	C(3)-O(4)	1.364(6)
O(4)-C(5)	1.419(7)	C(5)-C(6)	1.445(8)
C(6)-O(7)	1.406(7)	O(7)-C(8)	1.400(6)
C(8)-C(9)	1.533(7)	C(8)-C(19)	1.532(7)
C(9)-O(10)	1.429(7)	C(9)-C(25)	1.519(9)
O(10)-C(11)	1.409(6)	C(11)-C(12)	1.447(9)
C(12)-O(13)	1.376(7)	O(13)-C(14)	1.382(8)
C(14)-C(15)	1.367(9)	C(15)-O(16)	1.424(7)
O(16)-C(17)	1.392(7)	C(17)-C(18)	1.554(6)
C(17)-C(37)	1.541(8)	C(18)-C(31)	1.482(8)
C(19)-C(20)	1.367(7)	C(19)-C(24)	1.385(8)
C(20)-C(21)	1.373(8)	C(21)-C(22)	1.356(8)
C(22)-C(23)	1.378(8)	C(22)-O(43)	1.385(7)
C(23)-C(24)	1.397(8)	C(25)-C(26)	1.383(8)
C(25)-C(30)	1.366(8)	C(26)-C(27)	1.370(9)
C(27)-C(28)	1.354(8)	C(28)-C(29)	1.371(10)
C(28)-O(45)	1.373(9)	C(29)-C(30)	1.356(11)
C(31)-C(32)	1.360(9)	C(31)-C(36)	1.356(7)
C(32)-C(33)	1.350(10)	C(33)-C(34)	1.372(10)
C(34)-C(35)	1.347(11)	C(34)-O(47)	1.459(11)
C(35)-C(36)	1.371(10)	C(37)-C(38)	1.386(7)
C(37)-C(42)	1.353(9)	C(38)-C(39)	1.396(7)
C(39)-C(40)	1.360(9)	C(40)-C(41)	1.378(8)
C(40)-O(49)	1.391(7)	C(41)-C(42)	1.403(9)
O(43)-C(44)	1.401(10)	O(45)-C(46a)	1.355(15)
O(45)-C(46b)	1.396(23)	O(47)-C(48)	1.426(15)
O(49)-C(50)	1.427(8)		

TABLE 13.3. Bond Angles (deg.)

C(2)-O(1)-C(18)	115.9(3)	O(1)-C(2)-C(3)	112.9(4)
C(2)-C(3)-O(4)	113.4(4)	C(3)-O(4)-C(5)	120.1(5)
O(4)-C(5)-C(6)	116.6(5)	C(5)-C(6)-O(7)	107.7(5)
C(6)-O(7)-C(8)	112.7(4)	O(7)-C(8)-C(9)	105.5(4)
O(7)-C(8)-C(19)	114.1(4)	C(9)-C(8)-C(19)	113.9(5)
C(8)-C(9)-O(10)	106.8(4)	C(8)-C(9)-C(25)	113.2(4)
O(10)-C(9)-C(25)	111.7(4)	C(9)-O(10)-C(11)	117.1(4)
O(10)-C(11)-C(12)	110.8(5)	C(11)-C(12)-O(13)	114.4(5)
C(12)-O(13)-C(14)	117.5(6)	O(13)-C(14)-C(15)	120.8(7)
C(14)-C(15)-O(16)	117.5(6)	C(15)-O(16)-C(17)	113.6(5)
O(16)-C(17)-C(18)	106.7(5)	O(16)-C(17)-C(37)	111.8(4)
C(18)-C(17)-C(37)	110.7(4)	O(1)-C(18)-C(17)	107.2(4)
O(1)-C(18)-C(31)	113.7(4)	C(17)-C(18)-C(31)	114.0(4)
C(8)-C(19)-C(20)	121.0(5)	C(8)-C(19)-C(24)	121.7(5)
C(20)-C(19)-C(24)	117.4(5)	C(19)-C(20)-C(21)	121.9(5)
C(20)-C(21)-C(22)	121.1(5)	C(21)-C(22)-C(23)	118.7(5)
C(21)-C(22)-O(43)	116.0(5)	C(23)-C(22)-O(43)	125.3(6)
C(22)-C(23)-C(24)	120.1(5)	C(19)-C(24)-C(23)	120.7(5)
C(9)-C(25)-C(26)	119.0(5)	C(9)-C(25)-C(30)	124.1(5)
C(26)-C(25)-C(30)	116.9(6)	C(25)-C(26)-C(27)	120.1(5)
C(26)-C(27)-C(28)	121.2(6)	C(27)-C(28)-C(29)	119.8(6)
C(27)-C(28)-O(45)	120.1(6)	C(29)-C(28)-O(45)	120.1(6)
C(28)-C(29)-C(30)	118.4(6)	C(25)-C(30)-C(29)	123.7(6)
C(18)-C(31)-C(32)	121.7(4)	C(18)-C(31)-C(36)	122.2(5)
C(32)-C(31)-C(36)	116.0(5)	C(31)-C(32)-C(33)	122.5(6)
C(32)-C(33)-C(34)	120.4(7)	C(33)-C(34)-C(35)	118.5(6)
C(33)-C(34)-O(47)	109.8(7)	C(35)-C(34)-O(47)	131.7(7)
C(34)-C(35)-C(36)	119.7(6)	C(31)-C(36)-C(35)	122.9(6)
C(17)-C(37)-C(38)	123.4(5)	C(17)-C(37)-C(42)	118.9(5)
C(38)-C(37)-C(42)	117.7(5)	C(37)-C(38)-C(39)	123.3(5)
C(38)-C(39)-C(40)	118.1(5)	C(39)-C(40)-C(41)	119.3(5)
C(39)-C(40)-O(49)	122.7(5)	C(41)-C(40)-O(49)	118.0(6)
C(40)-C(41)-C(42)	121.7(6)	C(37)-C(42)-C(41)	119.6(6)
C(22)-O(43)-C(44)	117.5(5)	C(28)-O(45)-C(46a)	120.6(8)
C(28)-O(45)-C(46b)	128.4(11)	C(46a)-O(45)-C(46b)	110.2(12)
C(34)-O(47)-C(48)	114.3(11)	C(40)-O(49)-C(50)	119.3(5)

TABLE 13.4. Anisotropic temperature factors ($Å^2 \times 10^3$)

atom	U_{11}	U_{22}	U_{33}	U_{23}	U_{13}	U_{12}
O(1)	76(2)	75(2)	70(2)	11(2)	-8(2)	2(2)
C(2)	86(4)	78(4)	77(4)	0(3)	-11(3)	6(3)
C(3)	74(3)	56(3)	82(4)	10(3)	-12(3)	-6(3)
O(4)	135(4)	83(3)	93(3)	-2(2)	-43(3)	9(2)
C(5)	120(5)	63(3)	96(4)	-2(3)	-46(4)	6(3)
C(6)	120(5)	63(4)	80(4)	0(3)	-20(3)	-9(3)
O(7)	95(3)	72(2)	78(2)	-8(2)	-23(2)	-13(2)
C(8)	80(4)	76(4)	79(4)	-4(3)	-20(3)	-16(3)
C(9)	86(4)	78(4)	69(3)	-5(3)	-33(3)	-11(3)
O(10)	113(3)	74(2)	83(3)	-10(2)	-47(2)	6(2)
C(11)	98(4)	71(4)	81(4)	-2(3)	-26(3)	2(3)
C(12)	137(6)	99(5)	88(4)	-10(3)	-54(4)	28(4)
O(13)	137(4)	99(3)	72(2)	-3(2)	-30(2)	32(3)
C(14)	93(5)	239(9)	65(4)	4(5)	-11(3)	65(5)
C(15)	74(4)	181(7)	86(4)	-7(4)	-19(3)	30(4)
O(16)	80(2)	95(3)	69(2)	0(2)	-6(2)	10(2)
C(17)	69(3)	76(4)	83(4)	22(3)	-16(3)	-17(3)
C(18)	66(3)	70(3)	63(3)	11(2)	-8(2)	-11(3)
C(19)	74(4)	63(3)	81(4)	2(3)	-35(3)	-16(3)
C(20)	60(3)	96(4)	85(4)	14(3)	-10(3)	-29(3)
C(21)	69(4)	88(4)	90(4)	17(3)	-11(3)	-26(3)
C(22)	88(4)	65(3)	80(4)	1(3)	-25(3)	-7(3)
C(23)	62(3)	103(4)	84(4)	-18(3)	-23(3)	-4(3)
C(24)	65(4)	104(4)	76(4)	-10(3)	-15(3)	-13(3)
C(25)	84(4)	60(3)	61(3)	0(3)	-13(3)	-2(3)
C(26)	79(4)	85(4)	73(4)	-2(3)	-17(3)	-11(3)
C(27)	94(4)	86(4)	76(4)	4(3)	-17(3)	-19(3)
C(28)	86(4)	56(3)	123(5)	17(3)	-13(4)	-16(3)
C(29)	109(5)	71(4)	88(4)	-1(3)	13(3)	-17(3)
C(30)	136(5)	75(4)	67(4)	-4(3)	-7(4)	-24(4)
C(31)	66(3)	62(3)	55(3)	-1(2)	-11(2)	-1(2)
C(32)	78(4)	84(4)	83(4)	-7(3)	-12(3)	-10(3)
C(33)	92(5)	91(5)	135(6)	15(4)	-39(4)	-39(4)
C(34)	48(3)	118(5)	177(7)	66(5)	-14(4)	-42(3)
C(35)	91(5)	113(6)	96(5)	17(4)	-11(4)	-10(4)
C(36)	77(4)	76(4)	75(4)	5(3)	-18(3)	-14(3)
C(37)	61(3)	64(3)	85(4)	7(3)	-14(3)	-17(2)
C(38)	91(4)	64(3)	71(4)	-1(3)	-21(3)	-23(3)
C(39)	93(4)	61(3)	66(3)	2(3)	-12(3)	-21(3)
C(40)	65(3)	69(4)	76(4)	-6(3)	-20(3)	-5(3)
C(41)	98(4)	68(4)	121(5)	-4(3)	-43(4)	-34(3)
C(42)	83(4)	70(3)	109(4)	18(3)	-32(3)	-29(3)
O(43)	133(4)	112(3)	81(3)	8(2)	-38(3)	0(3)
C(44)	122(6)	256(11)	110(6)	-28(6)	-59(5)	61(7)
O(45)	132(4)	98(3)	151(4)	12(3)	-17(3)	-41(3)
C(46a)	107(9)	89(8)	206(14)	5(8)	46(9)	-24(7)
C(46b)	231(23)	94(12)	131(15)	8(11)	-80(15)	-38(14)
O(47)	155(6)	237(8)	251(9)	112(8)	-24(6)	-16(6)
C(48)	190(13)	246(16)	363(22)	-12(15)	-32(14)	38(11)
O(49)	122(3)	102(3)	76(3)	-3(2)	-34(2)	-23(2)
C(50)	179(7)	95(5)	80(4)	10(4)	-35(5)	-2(5)

The anisotropic temperature factor exponent takes the form:

$$-2\pi^2(h^2a^{*2}U_{11} + \ldots + 2\,hka^*b^*U_{12}\cos\gamma^* + \ldots)$$

TABLE 13.5. Coordinates ($\times 10^4$) and temperature factors ($Å^2 \times 10^3$)

atom	x	y	z	U
H(2a)	6837	-71	-3818	110
H(2b)	7885	536	-3985	110
H(3a)	6636	432	-2128	92
H(3b)	7997	600	-2429	92
H(5a)	8999	-1939	-1670	120
H(5b)	9238	-833	-1584	120
H(6a)	8185	-1491	-185	115
H(6b)	6965	-1129	-727	115
H(8)	5952	19	379	96
H(9)	5440	1862	822	95
H(11a)	3908	2866	-248	113
H(11b)	5072	3254	-740	113
H(12a)	3747	2233	-1714	157
H(12b)	4893	2648	-2201	157
H(14a)	1880	4304	-2575	207
H(14b)	2598	3107	-2799	207
H(15a)	2731	4000	-4082	169
H(15b)	3248	4792	-3557	169
H(17)	3998	2272	-4295	101
H(18)	6144	1316	-5054	88
H(20)	5239	189	2120	98
H(21)	5829	-261	3660	102
H(23)	9544	-690	2573	104
H(24)	8944	-195	1011	101
H(26)	6474	2748	1623	96
H(27)	8055	3592	1636	109
H(29)	9512	2645	-1135	119
H(30)	7944	1806	-1141	111
H(32)	6918	3252	-3809	101
H(33)	8474	4041	-4417	124
H(35)	9033	2475	-6952	124
H(36)	7469	1681	-6311	95
H(38)	4809	4379	-5610	88
H(39)	4415	4910	-7206	91
H(41)	3354	2267	-7482	107
H(42)	3683	1775	-5858	107
H(44a)	9513	-1848	4068	209
H(44b)	9256	-1253	5072	209
H(44c)	9860	-782	4126	209
H(46a)	11124	3121	-916	167
H(46b)	11299	3870	-125	167
H(46c)	10399	4334	-922	167
H(46d)	9865	3789	1587	169
H(46e)	9316	4830	1007	169
H(46f)	10751	4505	1208	169
H(50a)	3372	5490	-8405	139
H(50b)	3248	5074	-9425	139
H(50c)	4564	4697	-9006	139

TABLE 13.6. Coordinates ($\times 10^4$) and temperature factors ($Å^2 \times 10^3$)

atom	x	y	z	U
O(1)	12137(1)	7929(1)	-248(1)	73(1)*
C(2)	13071(2)	7746(2)	307(1)	87(1)*
C(3)	12982(2)	6947(2)	469(1)	87(1)*
O(4)	11896(2)	6830(1)	712(1)	86(1)*
C(5)	11692(3)	6093(2)	874(2)	94(1)*
C(6)	10655(3)	6069(2)	1238(1)	95(1)*
O(7)	9539(2)	6254(1)	805(1)	75(1)*
C(8)	8516(2)	6278(1)	1130(1)	69(1)*
C(9)	7412(2)	6616(1)	660(1)	69(1)*
O(10)	7697(1)	7386(1)	604(1)	72(1)*
C(11)	6658(2)	7822(1)	318(1)	78(1)*
C(12)	7060(2)	8601(1)	239(1)	73(1)*
O(13)	7815(1)	8626(1)	-237(1)	63(1)*
C(14)	8253(2)	9350(1)	-324(1)	66(1)*
C(15)	9093(2)	9324(1)	-807(1)	70(1)*
O(16)	10204(1)	8949(1)	-511(1)	68(1)*
C(17)	11064(2)	8882(1)	-939(1)	65(1)*
C(18)	12288(2)	8646(1)	-506(1)	70(1)*
C(19)	8217(2)	5528(1)	1389(1)	65(1)*
C(20)	8230(3)	4881(1)	1024(1)	81(1)*
C(21)	7928(3)	4208(2)	1261(1)	81(1)*
C(22)	7585(2)	4158(2)	1865(1)	70(1)*
C(23)	7590(3)	4788(1)	2238(1)	76(1)*
C(24)	7912(2)	5460(1)	1999(1)	73(1)*
C(25)	7059(2)	6250(1)	-4(1)	68(1)*
C(26)	7771(3)	6302(2)	-480(1)	85(1)*
C(27)	7413(3)	5962(2)	-1098(1)	93(1)*
C(28)	6341(3)	5566(2)	-1231(1)	94(1)*
C(29)	5616(3)	5523(2)	-774(2)	104(1)*
C(30)	5967(3)	5860(2)	-169(1)	87(1)*
C(31)	10631(2)	8375(1)	-1517(1)	60(1)*
C(32)	10702(3)	8597(2)	-2145(1)	81(1)*
C(33)	10382(3)	8131(2)	-2677(1)	98(1)*
C(34)	9981(3)	7432(2)	-2593(1)	84(1)*
C(35)	9856(2)	7201(2)	-1975(2)	83(1)*
C(36)	10187(2)	7675(2)	-1439(1)	72(1)*
C(37)	13338(2)	8666(1)	-884(1)	65(1)*
C(38)	13954(2)	9319(1)	-957(1)	76(1)*
C(39)	14907(3)	9334(2)	-1301(1)	80(1)*
C(40)	15289(2)	8702(2)	-1565(1)	71(1)*
C(41)	14693(2)	8051(2)	-1494(1)	78(1)*
C(42)	13723(2)	8041(2)	-1162(1)	79(1)*
O(43)	7295(2)	3465(1)	2053(1)	92(1)*
C(44)	6990(4)	3379(2)	2675(2)	119(2)*
O(45)	5922(2)	5191(1)	-1819(1)	129(1)*
C(46)	6575(4)	5261(2)	-2323(2)	150(2)*
O(47)	9724(2)	7003(1)	-3149(1)	124(1)*
C(48)	9318(4)	6276(2)	-3073(2)	156(2)*
O(49)	16261(2)	8771(1)	-1886(1)	90(1)*
C(50)	16854(3)	8109(2)	-2026(2)	105(2)*
N(1)	10163(2)	8039(1)	689(1)	66(1)*
B(1)	10541(3)	8557(2)	1317(2)	84(1)*

* Equivalent isotropic U defined as one third of the trace of the orthogonalised U_{ij} tensor

TABLE 13.8. Bond Angles (deg.)

C(2)-O(1)-C(18)	113.1(2)	O(1)-C(2)-C(3)	109.6(2)
C(2)-C(3)-O(4)	108.9(2)	C(3)-O(4)-C(5)	114.6(2)
O(4)-C(5)-C(6)	108.9(2)	C(5)-C(6)-O(7)	109.9(2)
C(6)-O(7)-C(8)	112.8(2)	O(7)-C(8)-C(9)	108.9(2)
O(7)-C(8)-C(19)	112.8(2)	C(9)-C(8)-C(19)	112.0(2)
C(8)-C(9)-O(10)	105.9(2)	C(8)-C(9)-C(25)	116.1(2)
O(10)-C(9)-C(25)	111.9(2)	C(9)-O(10)-C(11)	113.1(2)
O(10)-C(11)-C(12)	109.1(2)	C(11)-C(12)-O(13)	109.6(2)
C(12)-O(13)-C(14)	112.4(2)	O(13)-C(14)-C(15)	109.3(2)
C(14)-C(15)-O(16)	109.0(2)	C(15)-O(16)-C(17)	113.4(2)
O(16)-C(17)-C(18)	106.5(2)	O(16)-C(17)-C(31)	113.2(2)
C(18)-C(17)-C(31)	113.9(2)	O(1)-C(18)-C(17)	108.4(2)
O(1)-C(18)-C(37)	111.9(2)	C(17)-C(18)-C(37)	111.9(2)
C(8)-C(19)-C(20)	122.0(2)	C(8)-C(19)-C(24)	120.9(2)
C(20)-C(19)-C(24)	117.0(2)	C(19)-C(20)-C(21)	121.2(3)
C(20)-C(21)-C(22)	120.7(3)	C(21)-C(22)-C(23)	118.9(3)
C(21)-C(22)-O(43)	116.1(2)	C(23)-C(22)-O(43)	125.0(3)
C(22)-C(23)-C(24)	119.8(3)	C(19)-C(24)-C(23)	122.3(2)
C(9)-C(25)-C(26)	122.5(2)	C(9)-C(25)-C(30)	120.5(3)
C(26)-C(25)-C(30)	116.9(2)	C(25)-C(26)-C(27)	121.3(3)
C(26)-C(27)-C(28)	119.5(3)	C(27)-C(28)-C(29)	120.0(3)
C(27)-C(28)-O(45)	124.0(3)	C(29)-C(28)-O(45)	116.0(3)
C(28)-C(29)-C(30)	120.4(3)	C(25)-C(30)-C(29)	121.9(3)
C(17)-C(31)-C(32)	120.4(2)	C(17)-C(31)-C(36)	121.9(2)
C(32)-C(31)-C(36)	117.7(2)	C(31)-C(32)-C(33)	121.7(3)
C(32)-C(33)-C(34)	120.2(3)	C(33)-C(34)-C(35)	119.6(3)
C(33)-C(34)-O(47)	115.9(3)	C(35)-C(34)-O(47)	124.5(3)
C(34)-C(35)-C(36)	119.7(3)	C(31)-C(36)-C(35)	120.9(3)
C(18)-C(37)-C(38)	121.3(2)	C(18)-C(37)-C(42)	121.7(2)
C(38)-C(37)-C(42)	116.9(3)	C(37)-C(38)-C(39)	121.1(2)
C(38)-C(39)-C(40)	121.1(3)	C(39)-C(40)-C(41)	118.5(3)
C(39)-C(40)-O(49)	116.7(2)	C(41)-C(40)-O(49)	124.8(2)
C(40)-C(41)-C(42)	120.2(3)	C(37)-C(42)-C(41)	122.2(3)
C(22)-O(43)-C(44)	118.3(2)	C(28)-O(45)-C(46)	118.6(3)
C(34)-O(47)-C(48)	117.0(3)	C(40)-O(49)-C(50)	117.4(2)

TABLE 13.9. Anisotropic temperature factors ($Å^2 \times 10^3$)

atom	U_{11}	U_{22}	U_{33}	U_{23}	U_{13}	U_{12}
O(1)	51(1)	94(1)	70(1)	9(1)	2(1)	-0(1)
C(2)	49(2)	131(3)	76(2)	10(2)	-1(1)	5(2)
C(3)	63(2)	114(3)	79(2)	14(2)	6(2)	25(2)
O(4)	64(1)	90(1)	108(1)	15(1)	22(1)	21(1)
C(5)	75(2)	94(2)	109(2)	16(2)	8(2)	22(2)
C(6)	78(2)	109(2)	93(2)	28(2)	3(2)	18(2)
O(7)	63(1)	87(1)	71(1)	14(1)	4(1)	10(1)
C(8)	71(2)	74(2)	60(2)	2(1)	9(1)	4(1)
C(9)	61(2)	68(2)	76(2)	13(1)	12(1)	-2(1)
O(10)	54(1)	70(1)	88(1)	12(1)	5(1)	8(1)
C(11)	57(2)	85(2)	91(2)	17(2)	14(2)	12(2)
C(12)	64(2)	79(2)	78(2)	7(1)	16(1)	21(1)
O(13)	59(1)	64(1)	69(1)	-1(1)	18(1)	6(1)
C(14)	59(2)	64(2)	75(2)	0(1)	9(1)	9(1)
C(15)	59(2)	72(2)	77(2)	7(1)	8(1)	9(1)
O(16)	53(1)	86(1)	64(1)	2(1)	11(1)	11(1)
C(17)	57(2)	72(2)	67(2)	-1(1)	14(1)	-2(1)
C(18)	55(2)	82(2)	71(2)	-7(1)	6(1)	-4(1)
C(19)	73(2)	65(2)	55(1)	1(1)	5(1)	7(1)
C(20)	110(2)	81(2)	54(2)	-0(1)	18(2)	8(2)
C(21)	108(2)	68(2)	66(2)	-5(1)	12(2)	3(2)
C(22)	70(2)	68(2)	71(2)	3(1)	12(1)	2(1)
C(23)	86(2)	80(2)	67(2)	1(1)	27(2)	5(2)
C(24)	86(2)	67(2)	66(2)	-6(1)	17(1)	8(1)
C(25)	64(2)	70(2)	68(2)	16(1)	6(1)	-1(1)
C(26)	83(2)	99(2)	71(2)	7(2)	10(2)	-19(2)
C(27)	104(2)	104(2)	71(2)	18(2)	18(2)	-7(2)
C(28)	107(2)	83(2)	77(2)	8(2)	-16(2)	-3(2)
C(29)	87(2)	108(2)	106(2)	9(2)	-6(2)	-22(2)
C(30)	71(2)	97(2)	90(2)	9(2)	7(2)	-12(2)
C(31)	48(2)	71(2)	62(2)	2(1)	11(1)	-3(1)
C(32)	82(2)	95(2)	67(2)	-0(2)	17(2)	-14(2)
C(33)	108(2)	121(3)	65(2)	-7(2)	19(2)	-17(2)
C(34)	71(2)	100(2)	73(2)	-28(2)	-4(1)	8(2)
C(35)	65(2)	72(2)	104(2)	-6(2)	-1(2)	-3(1)
C(36)	62(2)	78(2)	74(2)	4(2)	7(1)	-6(2)
C(37)	49(2)	70(2)	75(2)	-5(1)	8(1)	-5(1)
C(38)	60(2)	70(2)	98(2)	-4(2)	12(2)	1(1)
C(39)	66(2)	70(2)	103(2)	12(2)	12(2)	-10(1)
C(40)	52(2)	90(2)	70(2)	13(1)	6(1)	-2(1)
C(41)	64(2)	83(2)	89(2)	-13(2)	22(2)	-1(2)
C(42)	65(2)	76(2)	99(2)	-12(2)	23(2)	-13(1)
O(43)	110(2)	72(1)	98(2)	9(1)	28(1)	-7(1)
C(44)	138(3)	101(3)	134(3)	18(2)	66(3)	-16(2)
O(45)	149(2)	126(2)	97(2)	-6(1)	-13(1)	-12(2)
C(46)	215(5)	141(3)	83(2)	10(2)	7(3)	4(3)
O(47)	126(2)	125(2)	107(2)	-48(1)	-10(1)	11(1)
C(48)	166(4)	110(3)	157(4)	-46(3)	-57(3)	38(3)
O(49)	64(1)	117(2)	93(1)	17(1)	26(1)	1(1)
C(50)	75(2)	149(3)	98(2)	1(2)	31(2)	13(2)
N(1)	54(1)	73(1)	68(1)	1(1)	7(1)	7(1)
B(1)	86(3)	95(3)	66(2)	-7(2)	3(2)	1(2)

The anisotropic temperature factor exponent takes the form:

$$-2\pi^2(h^2a^{*2}U_{11} + \ldots + 2\,hka^*b^*U_{12}\cos\gamma^* + \ldots)$$

TABLE 13.10. Coordinates ($\times 10^4$) and temperature factors ($Å^2 \times 10^3$)

atom	x	y	z	U
H(2a)	13865	7846	205	105
H(2b)	12963	8042	680	105
H(3a)	13680	6807	799	103
H(3b)	12965	6653	79	103
H(5a)	11489	5801	478	111
H(5b)	12421	5896	1148	111
H(6a)	10806	6419	1596	114
H(6b)	10591	5577	1409	114
H(8)	8728	6588	1515	85
H(9)	6690	6537	845	83
H(11a)	6295	7621	-106	96
H(11b)	6063	7814	601	96
H(12a)	7513	8780	654	85
H(12b)	6351	8910	99	85
H(14a)	7571	9672	-488	82
H(14b)	8691	9536	91	82
H(15a)	9281	9821	-926	85
H(15b)	8703	9059	-1196	85
H(17)	11162	9350	-1148	79
H(18)	12507	8994	-151	87
H(20)	8453	4905	597	94
H(21)	7956	3767	1002	98
H(23)	7370	4762	2665	89
H(24)	7925	5896	2269	86
H(26)	8527	6577	-387	105
H(27)	7919	6006	-1426	110
H(29)	4854	5254	-872	120
H(30)	5440	5823	148	102
H(32)	10983	9091	-2213	97
H(33)	10444	8302	-3110	114
H(35)	9543	6713	-1915	98
H(36)	10102	7511	-1007	86
H(38)	13715	9769	-765	89
H(39)	15305	9799	-1355	98
H(41)	14950	7598	-1675	93
H(42)	13304	7579	-1126	95
H(44a)	6904	2852	2730	140
H(44b)	6254	3626	2741	140
H(44c)	7679	3557	2993	140
H(46a)	6211	4950	-2686	171
H(46b)	7388	5084	-2141	171
H(46c)	6623	5763	-2475	171
H(48a)	9249	6058	-3503	179
H(48b)	8559	6209	-2921	179
H(48c)	9974	6040	-2772	179
H(50a)	17530	8269	-2222	120
H(50b)	16327	7787	-2328	120
H(50c)	17164	7845	-1624	120
H(1na)	10750	7644	700	75
H(1nb)	10140	8332	298	75
H(1nc)	9364	7832	687	75
H(1ba)	9852	8978	1334	101
H(1bb)	11410	8820	1300	101
H(1bc)	10637	8212	1753	101

13.4 REFERENCES

1. G.M. Sheldrick, SHELXTL, An integrated system for solving, refining, and displaying crystal structures from diffractometer data, University of Göttingen, Federal Republic of Germany, 1981.
2. I. Goldberg, The Chemistry of Functional Groups. Supplement E: The Chemistry of Ethers, Crown Ethers, Hydroxy Groups and their Sulphur Analogues, 1980, Part 1, 175. Editor S. Patel, Chichester: John Wiley.
3. J.D. Dunitz, and P. Seiler, Acta. Cryst., 1974, B30, 2739.
4. I. Goldberg, Acta. Cryst., 1975, B31, 754.

5a. B.L. Allwood, H. Shahriari-Zavareh, J.F. Stoddart, and D.J. Williams, J. Chem. Soc., Chem. Commun., 1984, 1461.

b. B.L. Allwood, H. Shahriari-Zavareh, J.F. Stoddart, and D.J. Williams, J. Incl. Phenom., 1985, 3, 355.

c. H.M. Colquhoun, G. Jones, J.M. Maud, J.F. Stoddart, and D.J. Williams, J. Chem. Soc., Dalton Trans., 1984, 63.

6. See Chapter 11.

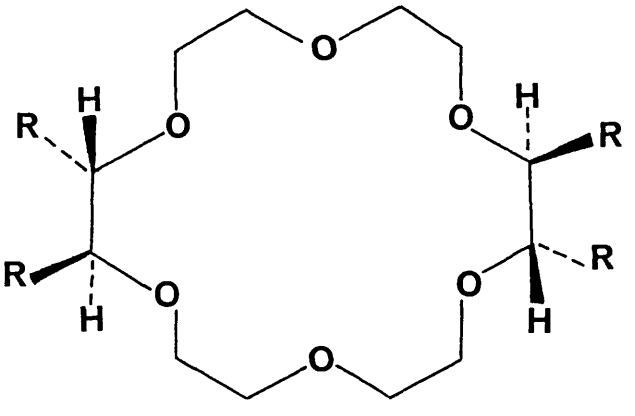
See Chapter 12.

CHAPTER 14

The crystal structures of trans-anti-trans 2,3,11,12 tetra-anisyl-18-crown-6 and its complex with borane-ammonia.

14.1 INTRODUCTION

This chapter reports the X-ray structure analyses of chiral RRRR trans-anti-trans 2,3,11,12 tetra-anisyl-18-crown-6 (13) and its complex with borane-ammonia.



R = p-$M_eOC_6H_4$

13

14.2 EXPERIMENTAL

Clear crystals of 13 were grown from a methanol/n-pentane solution. A crystal of dimensions 0.40 x 0.40 x 0.40 mm was used for unit cell and intensity measurements.

Crystal data: $C_{40}H_{48}O_{10}$, M = 689, monoclinic, a = 8.494(1), b = 11.419(1), c = 19.351(3) Å, $\beta = 91.43(1)^{o}$, U = 1876 $Å^3$, space group $P2_1$, Z = 2, D_c = 1.22 g cm^{-3}, F(000) = 736, μ(Cu-K_α) = 6.74cm^{-1}.

Refined unit-cell parameters were obtained by centering 18 reflections on a Nicolet R3m diffractometer. 2685 unique reflections ($\theta \leq 58^{o}$) were measured with Cu-K_α radiation (graphite monochromator) using the omega-scan routine. Of these 2311 had $|F_o| > 3\sigma(|F_o|)$ and

were considered to be observed. The net count of two reflections, the -1 -1 2 and the -2 0 1, measured as references every 50 reflections did not alter significantly during the data collection indicating that no deterioration of the crystal had occurred. The data were brought to a uniform arbitrary scale by the use of these reflections and Lorentz and polarisation corrections were applied.

The structure was solved, with difficulty, by direct methods. A starting set comprising 3 origin defining reflections, one reflection which was a weak link in the convergence map, the four principal contributors to the list of negative quartets and 12 automatically selected terms was used. The initial phase refinement (9582 permutations) was with 195 $\underline{E}$'s > 1.70 using 1139 TPR. This was subsequently expanded to 396 probable phases with $\underline{E}$'s > 1.70 using 2504 TPR. The figures of merit for the fourth best phase solution were NQEST = -0.155, RA(1) = 0.058, RA(2) = 0.147. Three cycles of $\Delta\underline{E}$-map recycling for this solution gave an $\underline{R}_E$ = 0.20 for all the non-hydrogen atoms in the structure. The non-hydrogen atoms were refined anisotropically. The carbon hydrogens, except those of the methyl groups which were refined as rigid bodies, were placed at calculated positions (C-H = 0.96 Å), assigned isotropic thermal parameters, $\underline{U}$(H) = 1.2 $\underline{U}_{eq}$(C), and allowed to ride on their parent carbon atoms.

Refinement using $\underline{F}$ magnitudes was by block-cascade full-matrix least squares (464 variable parameters) and converged to $\underline{R}$ = 0.054, $\underline{R}_w$ = 0.059, [$w^{-1} = \sigma^2(\underline{F}) + 0.0015\underline{F}^2$]. The largest parameter shift/e.s.d. was 0.150, the mean shift/e.s.d. was 0.036. The residual electron

density in the final difference map was within -0.19 and 0.24 $e\mathring{A}^{-3}$.

Clear crystals of $\underset{\sim\sim}{13}.BH_3NH_3(CH_3OH)_{0.75}$ were grown from a dichloromethane/n-pentane solution. A crystal of dimensions 0.28 x 0.43 x 0.43 mm was used for unit cell and intensity measurements.

Crystal data: $C_{40}H_{48}O_{10}.BNH_6(CH_3OH)_{0.75}$, $\underline{M}$ = 744, triclinic, $\underline{a}$ = 7.995(2), $\underline{b}$ = 11.035(2), $\underline{c}$ = 13.371(4) $\mathring{A}$, α = 68.34(2), β = 74.62(2), γ = 82.84(2), $\underline{U}$ = 1057 $\mathring{A}^3$, space group $\underline{P}1$, $\underline{Z}$ = 1, $\underline{D}_c$ = 1.17 g cm^{-3}, $\underline{F}(000)$ = 403, $\mu(Cu\text{-}\underline{K}_\alpha)$ = 6.54 cm^{-1}.

Refined unit-cell parameters were obtained by centering 18 reflections on a Nicolet R3m diffractometer. 2810 unique reflections ($\theta \leq 58^o$) were measured with Cu-$\underline{K}_\alpha$ radiation (graphite monochromator) using the omega-scan routine. Of these 2765 had $|\underline{F}_o| > 3\sigma(|\underline{F}_o|)$ and were considered to be observed. The net count of two reflections, the -1 -2 -3 and the 0 -2 -2, measured as references every 50 reflections did not alter significantly during the data collection indicating that no deterioration of the crystal had occurred. The data were brought to a uniform arbitrary scale by the use of these reflections and Lorentz and polarisation corrections were applied.

The structure was solved by direct methods. A starting set comprising 2 origin defining reflections together with a further 10 automatically selected terms was used. The initial phase refinement (267 permutations) was with 200 $\underline{E}$'s > 1.60 using 1101 TPR. This was subsequently expanded to 414 probable phases with $\underline{E}$'s > 1.48 using

1710 TPR. The figures of merit for the second best phase solution were NQEST = -0.231, RA(1) = 0.016, RA(2) = 0.060. Three cycles of $\Delta\underline{E}$-map recycling for this solution gave an $\underline{R}_E$ = 0.22 for all the non-hydrogen atoms in the 1:1 complex. A subsequent $\Delta\underline{F}$-map revealed the presence of a 75% occupancy methanol molecule. The non-hydrogen atoms were refined anisotropically. The carbon hydrogens, except those of the methyl which were refined as rigid bodies, were placed at calculated positions (C-H = 0.96 Å), assigned isotropic thermal parameters, $\underline{U}(H) = 1.2\ \underline{U}_{eq}(C)$, and allowed to ride on their parent carbon atoms. The hydrogens of the NH_3 and BH_3 groups were clearly located in a $\Delta\underline{F}$-map and the groups refined as rigid bodies (B-H = 1.08, N-H = 0.96 Å). The hydroxy proton on methanol molecule was not located.

Refinement using $\underline{F}$ magnitudes was by block-cascade full-matrix least squares (509 variable parameters) and converged to $\underline{R}$ = 0.044, $\underline{R}_w$ = 0.053, $[w^{-1} = \sigma^2(\underline{F}) + 0.0016\underline{F}^2]$. The largest parameter shift/e.s.d. was 0.369, the mean shift/e.s.d. was 0.036. The residual electron density in the final difference map was within -0.15 and 0.19 $eÅ^{-3}$.

All computations were carried out on an Eclipse S140 computer using the SHELXTL[1] program system.

13.3 DISCUSSION

The final fractional atomic coordinates, anisotropic thermal parameters, bond lengths and bond angles for the non-hydrogen atoms in

13 and 13.BH_3NH_3.$(CH_3OH)_{0.75}$ are shown in Tables 14.1 - 14.4 and 14.6 - 14.9 respectively. The positions and isotropic temperature factors for the hydrogen atoms in 13 and 13.BH_3NH_3.$(CH_3OH)_{0.75}$ are shown in Tables 14.5 and 14.10 respectively.

The torsional angles associated with the 18-membered macrocyles in 13 and 13.BH_3NH_3 are shown beside the relevant C-C and C-O bonds in the skeletal drawings of the structures reproduced in figures 14.1 and 14.3 which also provide details of the crystallographic numbering schemes.

The chiral macrocycle 13 has more open rectangular shape than the other uncomplexed tetra-anisyl-18-crown-6 receptors 10 - 12^2. The sequence of O-C-C-O subunit torsional angles starting from O(1) can be described as ag^-g^+ ag^+a ag^+a ag^-g^+ ag^+a ag^+a.

The three trans-annular O...O distances for receptor 13 are O(1)-O(10) 6.20, O(4)...O(13) 6.28 and O(7)...O(16) 4.43 Å.

The adjacent pseudo equatorial anisyl substituents have a synclinal relationship about their C-C bridgehead bond.

The C-O bonds lengths (average 1.423 Å) in the 18-membered macrocycle are similar to those observed in uncomplexed 18C6[3]. Four of the ring C-C bond lengths (average 1.495 Å) are similar to those in uncomplexed 18C6 whilst the C-C bridgehead bond lengths 1.520(7) and 1.524(7) Å are longer than expected. The bond angles (average C-O-C 116.1°; average C-C-O 108.6°) are similar to those in uncomplexed

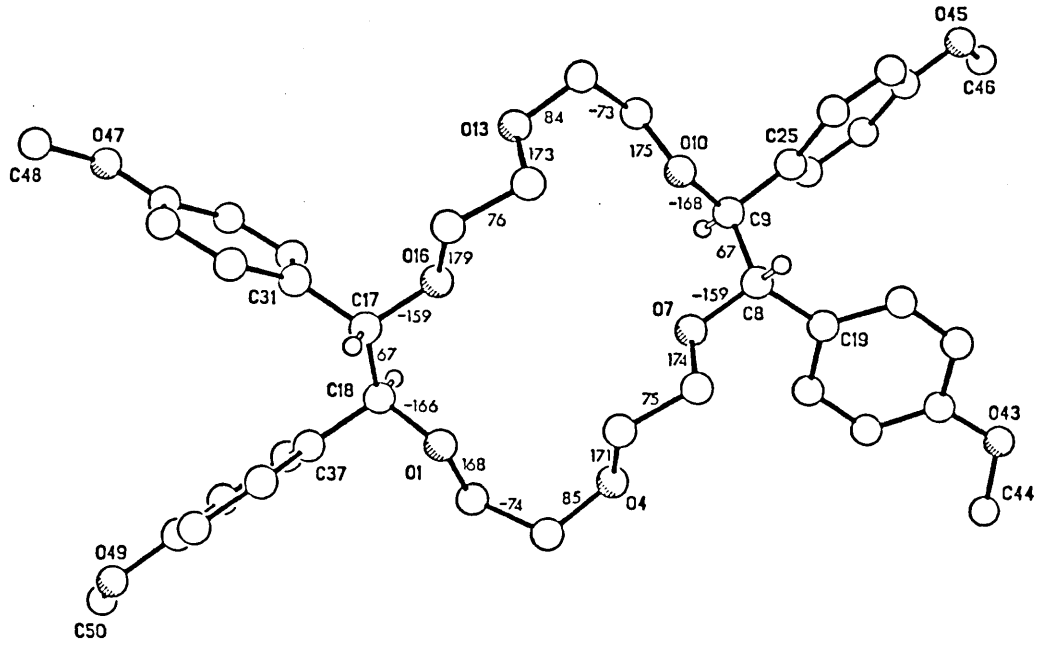


Figure 14.1. The skeletal representation of the solid-state structure of 13.

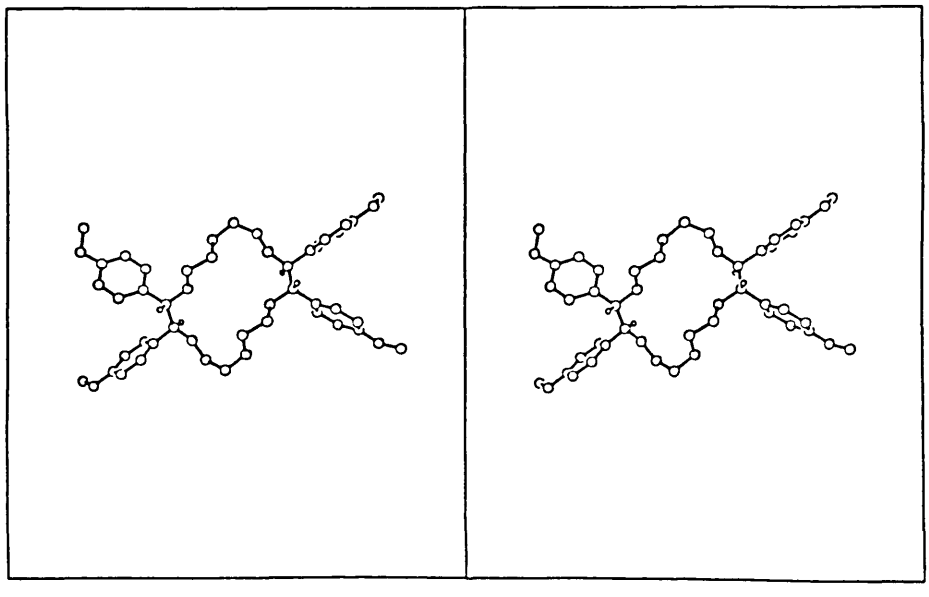


Figure 14.2. The stereo-pair representation of the solid-state structure of 13.

18C6.

There are several short contacts between symmetry related macrocycles: C(50)...O(16) 3.16, C(47)...C(39) 3.31, O(47)...C(38) 3.38, C(50)...O(7) 3.39, and C(44)...O(13) 3.39 Å. Not surprisingly all these short contacts involve the methoxy groups of the macrocycle. There are no other intermolecular contacts of less than normal van der Waals distances.

On complexation with one molecule of borane-ammonia the 18-membered ring adopts a pseudo 'all gauche' conformation. This transformation is achieved by rotations about three of the bonds in the uncomplexed receptor. One of the bridgehead C-C bond torsion angles changes sign and two C-O bond torsion angles [about C(3)-O(4) and C(13)-O(13)] change from gauche to anti. However, several torsional angles [about C(2)-C(3), C(6)-O(7) and O(7)-C(8)] whilst retaining an essentially gauche or anti geometry, have magnitudes that differ significantly from the ideal values[4]. A consequence of this is that instead of the polyether oxygens alternating symmetrically above and below their mean plane, five of the polyether oxygens are essentially coplanar (with a max. deviation of 0.03 Å), and the sixth, O(16), lies 0.6 Å out of this plane towards the borane-ammonia molecule.

The borane-ammonia guest is again bound to the host via three hydrogen bonds to polyether oxygens. However, the geometry of this binding is not the classic perching arrangement. Not surprisingly the

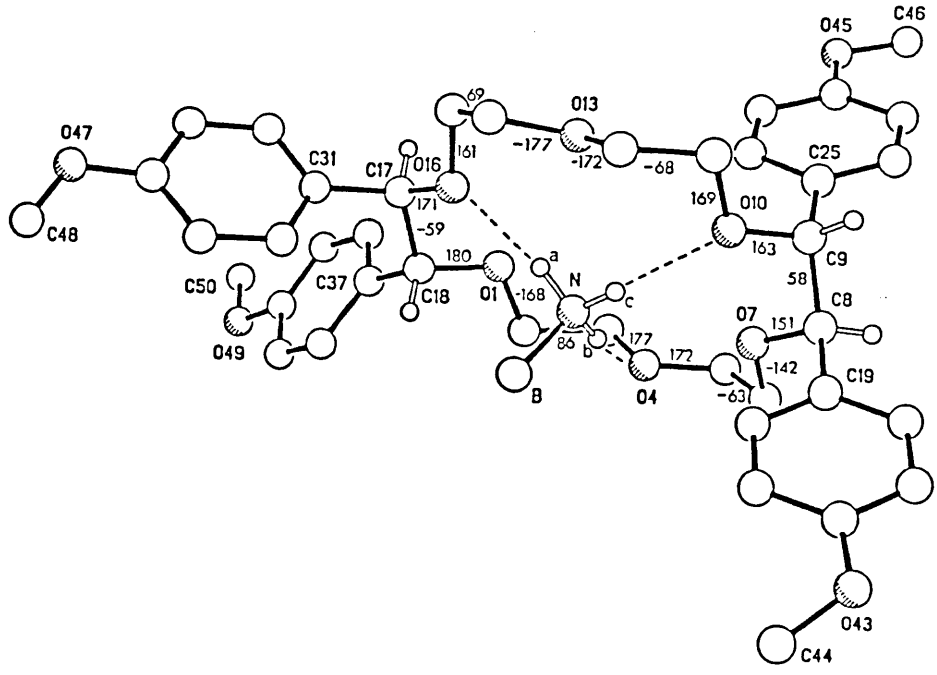


Figure 14.3. The skeletal representation of the solid-state structure of 13.BH_3NH_3.

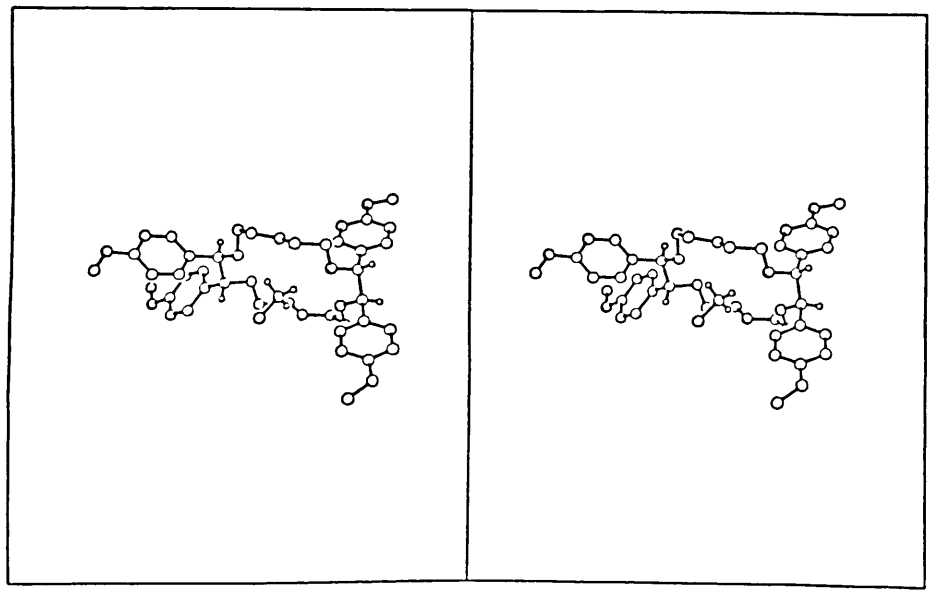


Figure 14.4. The stereo-pair representation of the solid-state structure of 13.BH_3NH_3.

out of plane oxygen, O(16), is involved in the shortest hydrogen bond contact [see table 14.11].

The distance of the nitrogen to the mean plane of all the polyether oxygen is 1.27 Å, and its distance to the mean plane of the hydrogen bonding oxygens is 1.15 Å. This compares with distances of 1.23 Å of the nitrogen to the mean plane of the polyether oxygens in the 1:1 complexes with receptor 13. The tilt angle of the borane-ammonia molecule to the normal of the mean plane of the six polyether oxygens is 11.1°, while the tilt angle to the 5 in-plane oxygens is 7.2°. The tilt angle to the normal of the mean plane of the six polyether oxygens compares with values of 4.8 and 13° in the 1:1 borane-ammonia complexes with 12 and trans-anti-trans tetraphenyl-18-crown-6[5] respectively. It is noteworthy that the borane-ammonia is tilted away from the pseudo axial anisyl substituent which resides on the hydrogen bonding face of the macrocycle (see figure 14.5).

On complexation one pair of adjacent anisyl substituents change from a pseudo diequatorial synclinal relationship to a pseudo diaxial antiperiplanar relationship. The other adjacent pair retain their pseudo diequatorial synclinal relationship.

The hydrogen atoms of the borane-ammonia are in a nearly staggered relationship with respect to each other, with the smallest H-N-B-H torsional angle being -54.3°.

The C-O bond lengths (average 1.415 Å) and the bond angles (average C-O-C 114.6°; average O-C-C 108.6°) of the macrocyclic ring

TABLE 14.11. The nitrogen-polyether oxygens contact distances, and relevant hydrogen bond distances and angles where appropriate, in order of increasing N...O distance.

N...O	R(N...O) (Å)	R(H...O) (Å)	$\psi(^{o})$[a]	$\theta(^{o})$[b]
N(1)-O(16)	2.93	1.99[c]	11[c]	165[c]
N(1)-O(4)	3.05	2.11[d]	33[d]	165[d]
N(1)-O(7)	3.01			
N(1)-O(13)	3.01			
N(1)-O(10)	3.13	2.20[e]	19[e]	165[e]
N(1)-O(1)	3.25			

[a] Angles between COC planes and HO vectors.
[b] N-H...O angles.
[c] H(1na)
[d] H(1nb)
[e] H(1nc)

in the complex are similar to those found in 18C6 complexes[4]. However, the bridgehead C-C bond lengths [1.528(5) and 1.526(5) Å] are again longer than the other ring C-C bonds (average 1.490 Å). This lengthening of the bridgehead C-C bond has also been observed for receptors 10, 11 and 12[2].

There is one short intermolecular contact between symmetry related 1:1 complexes, C(44)...O(1) 3.37 Å. Not surprisingly, this short contacts, involves a methoxy carbon of the anisyl group. There are no other intermolecular contacts of less than normal van der Waals distances.

Inspection of the two space-filling representations of the complex (figure 14.5) reveals that one of the pseudo axial substituents obscures one of the faces of the macrocycle thus preventing the approach of a borane-ammonia molecule to it. This provides an explanation for the 1:1 host guest stoicheometry of the complex.

The mode of binding and the gross conformation of the host in 13.BH_3NH_3 complex is very similar to that of the host in the complex between trans-anti-trans tetraphenyl 18-crown-6 and borane ammonia[5].

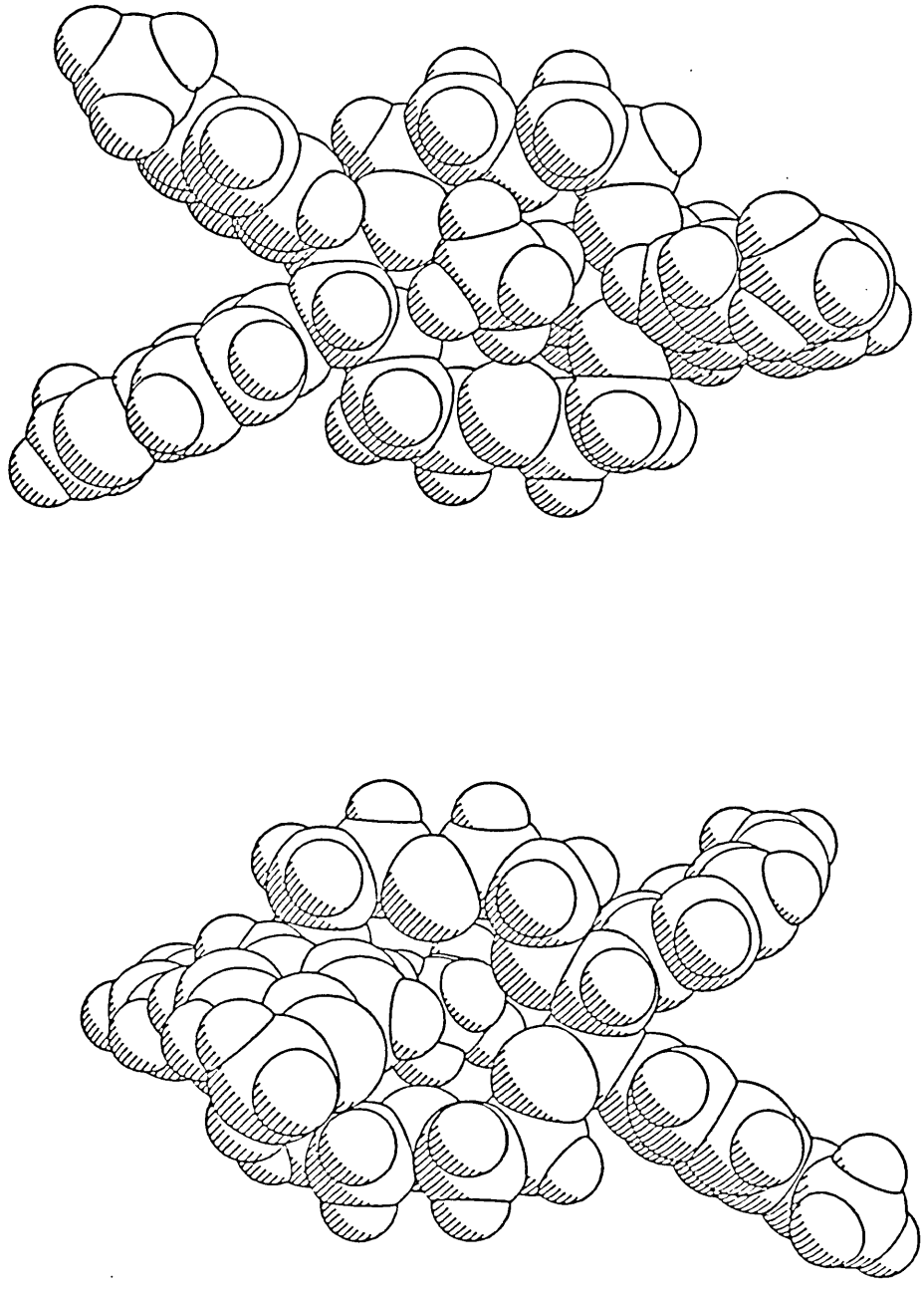


Figure 14.5. The space-filling representations (view normal to the mean plane of the six polyether oxygens) of the macrocyclic faces of $\underset{\sim\sim}{13}.8BH_3NH_3$.

TABLE 14.1. Coordinates ($\times 10^4$) and temperature factors ($Å^2 \times 10^3$)

atom	x	y	z	U
O(1)	7143(4)	4334(3)	3604(2)	59(1)*
C(2)	7692(7)	3422(6)	4051(3)	69(2)*
C(3)	8960(7)	2767(6)	3700(3)	77(2)*
O(4)	8419(5)	2019(4)	3160(2)	70(1)*
C(5)	8214(7)	2604(5)	2510(3)	64(2)*
C(6)	7890(6)	1700(5)	1967(3)	58(2)*
O(7)	6339(4)	1276(3)	2021(2)	53(1)*
C(8)	5860(5)	501(5)	1486(2)	49(2)*
C(9)	4070(6)	505(5)	1467(3)	51(2)*
O(10)	3647(4)	1641(3)	1244(2)	60(1)*
C(11)	2038(6)	1938(5)	1313(3)	62(2)*
C(12)	1818(6)	3191(5)	1107(3)	60(2)*
O(13)	2435(4)	4007(3)	1596(2)	60(1)*
C(14)	4072(6)	4248(5)	1539(3)	58(2)*
C(15)	4516(7)	5221(5)	2027(3)	61(2)*
O(16)	4607(4)	4732(3)	2706(2)	56(1)*
C(17)	5059(6)	5572(5)	3228(2)	52(2)*
C(18)	5708(6)	4860(5)	3838(3)	51(2)*
C(19)	6623(5)	-690(5)	1567(3)	51(2)*
C(20)	6796(6)	-1429(5)	994(3)	62(2)*
C(21)	7539(6)	-2481(6)	1076(3)	69(2)*
C(22)	8138(6)	-2857(5)	1708(3)	62(2)*
C(23)	7970(6)	-2155(5)	2276(3)	61(2)*
C(24)	7212(6)	-1077(5)	2200(3)	54(2)*
C(25)	3315(5)	-447(5)	1038(2)	50(2)*
C(26)	3231(6)	-353(5)	320(3)	62(2)*
C(27)	2577(6)	-1237(5)	-78(3)	60(2)*
C(28)	2026(6)	-2242(5)	233(3)	58(2)*
C(29)	2064(6)	-2349(6)	943(3)	64(2)*
C(30)	2716(6)	-1432(5)	1337(3)	58(2)*
C(31)	3681(5)	6345(5)	3426(3)	49(2)*
C(32)	2401(6)	5861(5)	3759(3)	63(2)*
C(33)	1186(7)	6568(5)	3967(3)	73(2)*
C(34)	1225(6)	7753(5)	3847(3)	62(2)*
C(35)	2469(7)	8238(5)	3518(3)	67(2)*
C(36)	3701(6)	7515(5)	3320(3)	58(2)*
C(37)	6009(5)	5570(4)	4483(2)	47(2)*
C(38)	6972(5)	6556(5)	4479(3)	53(2)*
C(39)	7267(6)	7206(5)	5069(3)	56(2)*
C(40)	6577(6)	6872(5)	5673(2)	52(2)*
C(41)	5622(6)	5929(5)	5699(3)	58(2)*
C(42)	5335(7)	5274(5)	5102(3)	58(2)*
O(43)	8884(5)	-3912(4)	1714(2)	77(2)*
C(44)	9731(8)	-4235(7)	2331(4)	84(3)*
O(45)	1404(5)	-3082(4)	-207(2)	73(1)*
C(46)	1036(7)	-4189(6)	71(3)	77(2)*
O(47)	-63(5)	8380(4)	4066(3)	90(2)*
C(48)	-87(8)	9598(7)	3972(5)	104(3)*
O(49)	6960(4)	7582(4)	6234(2)	69(1)*
C(50)	6515(10)	7181(6)	6904(3)	92(3)*

* Equivalent isotropic U defined as one third of the trace of the orthogonalised U_{ij} tensor

TABLE 14.2. Bond lengths (Å)

O(1)-C(2)	1.425(7)	O(1)-C(18)	1.443(6)
C(2)-C(3)	1.490(9)	C(3)-O(4)	1.417(7)
O(4)-C(5)	1.432(7)	C(5)-C(6)	1.494(8)
C(6)-O(7)	1.410(6)	O(7)-C(8)	1.415(6)
C(8)-C(9)	1.520(7)	C(8)-C(19)	1.512(7)
C(9)-O(10)	1.411(6)	C(9)-C(25)	1.501(7)
O(10)-C(11)	1.418(6)	C(11)-C(12)	1.496(8)
C(12)-O(13)	1.419(7)	O(13)-C(14)	1.424(6)
C(14)-C(15)	1.500(8)	C(15)-O(16)	1.428(6)
O(16)-C(17)	1.438(6)	C(17)-C(18)	1.524(7)
C(17)-C(31)	1.522(7)	C(18)-C(37)	1.505(7)
C(19)-C(20)	1.403(8)	C(19)-C(24)	1.384(7)
C(20)-C(21)	1.365(8)	C(21)-C(22)	1.381(8)
C(22)-C(23)	1.372(8)	C(22)-O(43)	1.361(7)
C(23)-C(24)	1.395(8)	C(25)-C(26)	1.394(7)
C(25)-C(30)	1.369(8)	C(26)-C(27)	1.378(8)
C(27)-C(28)	1.382(8)	C(28)-C(29)	1.378(7)
C(28)-O(45)	1.379(7)	C(29)-C(30)	1.402(8)
C(31)-C(32)	1.392(7)	C(31)-C(36)	1.352(8)
C(32)-C(33)	1.378(8)	C(33)-C(34)	1.374(8)
C(34)-C(35)	1.365(8)	C(34)-O(47)	1.383(7)
C(35)-C(36)	1.395(8)	C(37)-C(38)	1.391(7)
C(37)-C(42)	1.382(7)	C(38)-C(39)	1.379(7)
C(39)-C(40)	1.375(7)	C(40)-C(41)	1.350(8)
C(40)-O(49)	1.386(6)	C(41)-C(42)	1.393(7)
O(43)-C(44)	1.427(8)	O(45)-C(46)	1.411(8)
O(47)-C(48)	1.402(9)	O(49)-C(50)	1.435(7)

TABLE 14.3. Bond Angles (deg.)

C(2)-O(1)-C(18)	112.3(4)	O(1)-C(2)-C(3)	108.6(5)
C(2)-C(3)-O(4)	114.5(5)	C(3)-O(4)-C(5)	113.3(4)
O(4)-C(5)-C(6)	108.1(5)	C(5)-C(6)-O(7)	110.0(4)
C(6)-O(7)-C(8)	114.4(4)	O(7)-C(8)-C(9)	106.5(4)
O(7)-C(8)-C(19)	111.9(4)	C(9)-C(8)-C(19)	115.5(4)
C(8)-C(9)-O(10)	104.9(4)	C(8)-C(9)-C(25)	115.1(4)
O(10)-C(9)-C(25)	113.3(4)	C(9)-O(10)-C(11)	115.4(4)
O(10)-C(11)-C(12)	108.5(4)	C(11)-C(12)-O(13)	114.1(4)
C(12)-O(13)-C(14)	114.9(4)	O(13)-C(14)-C(15)	109.0(4)
C(14)-C(15)-O(16)	107.3(4)	C(15)-O(16)-C(17)	113.2(4)
O(16)-C(17)-C(18)	105.9(4)	O(16)-C(17)-C(31)	111.7(4)
C(18)-C(17)-C(31)	112.3(4)	O(1)-C(18)-C(17)	105.7(4)
O(1)-C(18)-C(37)	111.0(4)	C(17)-C(18)-C(37)	113.9(4)
C(8)-C(19)-C(20)	120.8(4)	C(8)-C(19)-C(24)	121.5(5)
C(20)-C(19)-C(24)	117.7(5)	C(19)-C(20)-C(21)	119.7(5)
C(20)-C(21)-C(22)	122.4(6)	C(21)-C(22)-C(23)	119.0(5)
C(21)-C(22)-O(43)	116.4(5)	C(23)-C(22)-O(43)	124.6(5)
C(22)-C(23)-C(24)	119.2(5)	C(19)-C(24)-C(23)	122.1(5)
C(9)-C(25)-C(26)	120.4(5)	C(9)-C(25)-C(30)	121.3(4)
C(26)-C(25)-C(30)	118.3(5)	C(25)-C(26)-C(27)	120.7(5)
C(26)-C(27)-C(28)	120.1(5)	C(27)-C(28)-C(29)	120.5(5)
C(27)-C(28)-O(45)	116.0(4)	C(29)-C(28)-O(45)	123.5(5)
C(28)-C(29)-C(30)	118.4(5)	C(25)-C(30)-C(29)	121.9(5)
C(17)-C(31)-C(32)	120.1(5)	C(17)-C(31)-C(36)	121.5(4)
C(32)-C(31)-C(36)	118.4(5)	C(31)-C(32)-C(33)	120.2(5)
C(32)-C(33)-C(34)	120.4(5)	C(33)-C(34)-C(35)	120.1(5)
C(33)-C(34)-O(47)	115.9(5)	C(35)-C(34)-O(47)	124.0(5)
C(34)-C(35)-C(36)	118.9(5)	C(31)-C(36)-C(35)	122.1(5)
C(18)-C(37)-C(38)	121.3(4)	C(18)-C(37)-C(42)	121.4(5)
C(38)-C(37)-C(42)	117.3(5)	C(37)-C(38)-C(39)	121.7(5)
C(38)-C(39)-C(40)	118.8(5)	C(39)-C(40)-C(41)	121.5(5)
C(39)-C(40)-O(49)	114.0(5)	C(41)-C(40)-O(49)	124.5(4)
C(40)-C(41)-C(42)	119.3(5)	C(37)-C(42)-C(41)	121.3(5)
C(22)-O(43)-C(44)	117.5(5)	C(28)-O(45)-C(46)	118.3(4)
C(34)-O(47)-C(48)	118.9(5)	C(40)-O(49)-C(50)	117.3(5)

TABLE 14.4. Anisotropic temperature factors ($Å^2 \times 10^3$)

atom	U_{11}	U_{22}	U_{33}	U_{23}	U_{13}	U_{12}
O(1)	64(2)	56(2)	56(2)	-6(2)	6(2)	13(2)
C(2)	81(4)	71(4)	53(3)	-4(3)	-8(3)	18(3)
C(3)	74(4)	78(4)	79(4)	-22(4)	-27(3)	25(3)
O(4)	92(3)	53(2)	63(2)	-14(2)	-10(2)	8(2)
C(5)	70(3)	56(3)	67(4)	-7(3)	8(3)	-2(3)
C(6)	59(3)	58(3)	57(3)	-17(3)	12(2)	-2(3)
O(7)	48(2)	57(2)	55(2)	-23(2)	11(1)	-0(2)
C(8)	58(3)	49(3)	41(3)	-8(2)	5(2)	4(2)
C(9)	61(3)	47(3)	45(3)	-2(2)	11(2)	2(2)
O(10)	53(2)	54(2)	72(2)	-0(2)	8(2)	5(2)
C(11)	53(3)	62(4)	71(4)	2(3)	-6(2)	1(3)
C(12)	55(3)	69(4)	56(3)	-10(3)	-14(2)	7(3)
O(13)	54(2)	66(2)	61(2)	-19(2)	-0(2)	6(2)
C(14)	57(3)	65(4)	51(3)	-9(3)	2(2)	1(3)
C(15)	77(4)	55(3)	50(3)	3(3)	1(3)	-3(3)
O(16)	77(2)	48(2)	44(2)	-2(2)	-1(2)	-4(2)
C(17)	58(3)	48(3)	48(3)	-10(3)	8(2)	-3(2)
C(18)	51(3)	51(3)	50(3)	-6(3)	5(2)	3(2)
C(19)	43(3)	56(3)	55(3)	-8(3)	12(2)	5(2)
C(20)	62(3)	66(4)	59(3)	-14(3)	9(3)	11(3)
C(21)	67(3)	71(4)	70(4)	-32(3)	4(3)	13(3)
C(22)	57(3)	52(3)	77(4)	-7(3)	17(3)	6(3)
C(23)	68(3)	59(3)	57(3)	4(3)	15(3)	2(3)
C(24)	61(3)	54(3)	48(3)	-6(3)	9(2)	3(3)
C(25)	51(3)	56(3)	42(3)	-6(2)	7(2)	6(2)
C(26)	72(4)	63(3)	53(3)	10(3)	9(3)	-8(3)
C(27)	80(4)	63(4)	37(3)	-1(3)	2(2)	-5(3)
C(28)	57(3)	63(3)	53(3)	-1(3)	0(2)	2(3)
C(29)	72(4)	72(4)	50(3)	13(3)	7(3)	-11(3)
C(30)	64(3)	68(4)	41(3)	-1(3)	6(2)	-10(3)
C(31)	51(3)	56(3)	41(3)	-1(2)	1(2)	-2(2)
C(32)	58(3)	51(3)	81(4)	21(3)	10(3)	1(3)
C(33)	65(3)	65(4)	89(4)	13(3)	22(3)	2(3)
C(34)	51(3)	54(3)	80(4)	5(3)	10(3)	4(3)
C(35)	76(4)	43(3)	82(4)	-1(3)	15(3)	-6(3)
C(36)	58(3)	53(3)	63(3)	-2(3)	14(2)	-6(3)
C(37)	43(3)	52(3)	46(3)	-2(2)	3(2)	3(2)
C(38)	51(3)	65(3)	44(3)	-3(3)	14(2)	-1(3)
C(39)	58(3)	60(3)	51(3)	-10(3)	7(2)	-10(3)
C(40)	59(3)	54(3)	43(3)	-3(3)	11(2)	12(3)
C(41)	77(4)	53(3)	44(3)	5(3)	20(2)	-3(3)
C(42)	67(4)	55(3)	52(3)	-2(3)	12(2)	-11(3)
O(43)	84(3)	58(2)	89(3)	-5(2)	18(2)	14(2)
C(44)	89(5)	73(4)	92(5)	11(4)	23(4)	27(4)
O(45)	98(3)	62(2)	58(2)	-9(2)	-2(2)	-13(2)
C(46)	89(4)	66(4)	77(4)	-5(3)	-1(3)	-7(4)
O(47)	77(3)	69(3)	126(4)	9(3)	35(3)	14(2)
C(48)	84(5)	74(5)	155(8)	-0(5)	23(5)	21(4)
O(49)	88(3)	73(3)	47(2)	-15(2)	9(2)	7(2)
C(50)	164(7)	74(4)	37(3)	-11(3)	17(4)	17(4)

The anisotropic temperature factor exponent takes the form:

$$-2\pi^2(h^2a^{*2}U_{11} + \ldots + 2\,hka^*b^*U_{12}\cos\gamma^* + \ldots)$$

TABLE 14.5. Coordinates ($\times 10^4$) and temperature factors ($Å^2 \times 10^3$)

atom	x	y	z	U
H(2a)	8101	3755	4475	81
H(2b)	6840	2901	4151	81
H(3a)	9512	2299	4039	87
H(3b)	9671	3326	3508	87
H(5a)	7343	3139	2529	86
H(5b)	9154	3028	2405	86
H(6a)	8618	1063	2028	72
H(6b)	8016	2042	1519	72
H(8)	6214	751	1042	59
H(9)	3677	331	1916	62
H(11a)	1398	1445	1019	72
H(11b)	1741	1835	1784	72
H(12a)	710	3337	1045	69
H(12b)	2333	3313	677	69
H(14a)	4670	3560	1655	71
H(14b)	4286	4481	1074	71
H(15a)	3731	5826	2005	71
H(15b)	5518	5542	1908	71
H(17)	5841	6103	3063	65
H(18)	4942	4291	3972	58
H(20)	6390	-1196	547	76
H(21)	7649	-2977	679	77
H(23)	8367	-2404	2721	74
H(24)	7098	-587	2598	61
H(26)	3630	336	100	70
H(27)	2505	-1155	-571	76
H(29)	1654	-3034	1162	73
H(30)	2742	-1496	1832	65
H(32)	2369	5034	3845	71
H(33)	305	6230	4196	87
H(35)	2490	9063	3421	81
H(36)	4595	7859	3104	65
H(38)	7437	6793	4055	66
H(39)	7947	7877	5059	67
H(41)	5146	5710	6126	70
H(42)	4654	4604	5120	65
H(44a)	10247	-4928	2171	91
H(44b)	9035	-4436	2696	91
H(44c)	10505	-3687	2501	91
H(46a)	746	-4786	-258	85
H(46b)	268	-4156	425	85
H(46c)	2050	-4368	274	85
H(48a)	-1068	9900	4131	116
H(48b)	33	9804	3495	116
H(48c)	766	9925	4243	116
H(50a)	6782	7754	7251	103
H(50b)	7047	6459	7010	103
H(50c)	5397	7053	6895	103

TABLE 14.6. Coordinates ($\times 10^4$) and temperature factors ($Å^2 \times 10^3$)

atom	x	y	z	U
O(1)	2626(3)	13276(2)	1462(2)	72(1)*
C(2)	4167(6)	13544(4)	1641(4)	90(2)*
C(3)	4149(6)	12951(3)	2956(3)	84(2)*
O(4)	4771(3)	11632(2)	3108(2)	76(1)*
C(5)	4856(6)	11036(3)	4234(3)	86(2)*
C(6)	5284(4)	9620(4)	4492(3)	79(1)*
O(7)	3955(3)	9031(2)	4352(2)	69(1)*
C(8)	3476(4)	7762(3)	5114(3)	65(1)*
C(9)	1556(4)	7662(3)	5184(3)	69(1)*
O(10)	1392(3)	7988(2)	4106(2)	70(1)*
C(11)	-172(5)	7486(3)	4031(3)	84(2)*
C(12)	-284(5)	8010(4)	2860(4)	88(2)*
O(13)	-493(3)	9384(2)	2516(2)	77(1)*
C(14)	-861(6)	9939(4)	1455(4)	94(2)*
C(15)	-972(5)	11393(4)	1123(4)	91(2)*
O(16)	690(3)	11860(2)	929(2)	77(1)*
C(17)	885(4)	13215(3)	237(3)	68(1)*
C(18)	2643(4)	13569(3)	330(3)	67(1)*
C(19)	4612(4)	6698(3)	4778(3)	63(1)*
C(20)	5176(5)	6785(3)	3696(3)	74(1)*
C(21)	6215(5)	5823(3)	3392(3)	74(1)*
C(22)	6675(4)	4726(3)	4201(3)	69(1)*
C(23)	6104(5)	4606(3)	5294(3)	78(1)*
C(24)	5072(5)	5591(3)	5576(3)	74(1)*
C(25)	458(4)	8605(3)	5697(3)	71(1)*
C(26)	25(5)	8311(3)	6828(3)	80(1)*
C(27)	-865(6)	9181(4)	7320(3)	90(2)*
C(28)	-1350(5)	10399(4)	6647(3)	92(2)*
C(29)	-967(5)	10700(3)	5515(3)	83(2)*
C(30)	-69(5)	9830(3)	5035(3)	77(1)*
C(31)	748(4)	13496(3)	-882(3)	66(1)*
C(32)	-485(4)	14384(3)	-1337(3)	72(1)*
C(33)	-628(5)	14634(3)	-2394(3)	75(1)*
C(34)	477(4)	14008(3)	-3044(3)	69(1)*
C(35)	1735(5)	13127(4)	-2615(3)	79(1)*
C(36)	1923(5)	12870(3)	-1540(3)	76(1)*
C(37)	3064(4)	14974(3)	-370(3)	67(1)*
C(38)	4519(5)	15264(3)	-1280(3)	74(1)*
C(39)	4919(5)	16536(4)	-1928(3)	82(1)*
C(40)	3921(5)	17553(3)	-1712(3)	79(1)*
C(41)	2496(6)	17294(4)	-832(3)	89(2)*
C(42)	2087(5)	16012(4)	-170(3)	84(1)*
O(43)	7724(4)	3724(3)	3973(2)	91(1)*
C(44)	8693(7)	3941(5)	2898(4)	106(2)*
O(45)	-2251(4)	11345(3)	7022(3)	110(1)*
C(46)	-2553(9)	11133(6)	8163(5)	123(3)*
O(47)	256(4)	14335(3)	-4090(2)	87(1)*
C(48)	1364(7)	13745(5)	-4795(4)	104(2)*
O(49)	4445(4)	18764(3)	-2420(3)	103(1)*
C(50)	3489(9)	19870(4)	-2221(5)	122(3)*
N(1)	3271(3)	10153(3)	2031(2)	66(1)*
B(1)	4460(7)	9852(6)	1000(4)	91(2)*
C(51)	7815(8)	7625(7)	424(5)	142(3)*
C(52)	6852(12)	6945(8)	160(7)	123(4)*

* Equivalent isotropic U defined as one third of the trace of the orthogonalised U_{ij} tensor

TABLE 14.7. Bond lengths (Å)

O(1)-C(2)	1.401(6)	O(1)-C(18)	1.424(4)
C(2)-C(3)	1.507(6)	C(3)-O(4)	1.423(4)
O(4)-C(5)	1.420(5)	C(5)-C(6)	1.496(5)
C(6)-O(7)	1.398(5)	O(7)-C(8)	1.421(3)
C(8)-C(9)	1.529(5)	C(8)-C(19)	1.521(4)
C(9)-O(10)	1.402(5)	C(9)-C(25)	1.519(5)
O(10)-C(11)	1.418(5)	C(11)-C(12)	1.479(7)
C(12)-O(13)	1.414(4)	O(13)-C(14)	1.417(5)
C(14)-C(15)	1.496(6)	C(15)-O(16)	1.410(5)
O(16)-C(17)	1.427(4)	C(17)-C(18)	1.526(5)
C(17)-C(31)	1.507(5)	C(18)-C(37)	1.512(4)
C(19)-C(20)	1.367(5)	C(19)-C(24)	1.384(4)
C(20)-C(21)	1.390(5)	C(21)-C(22)	1.390(4)
C(22)-C(23)	1.358(5)	C(22)-O(43)	1.379(4)
C(23)-C(24)	1.392(5)	C(25)-C(26)	1.379(5)
C(25)-C(30)	1.399(4)	C(26)-C(27)	1.381(6)
C(27)-C(28)	1.389(5)	C(28)-C(29)	1.379(6)
C(28)-O(45)	1.367(6)	C(29)-C(30)	1.374(6)
C(31)-C(32)	1.394(5)	C(31)-C(36)	1.374(5)
C(32)-C(33)	1.369(5)	C(33)-C(34)	1.377(5)
C(34)-C(35)	1.391(5)	C(34)-O(47)	1.364(5)
C(35)-C(36)	1.379(6)	C(37)-C(38)	1.411(4)
C(37)-C(42)	1.373(5)	C(38)-C(39)	1.375(5)
C(39)-C(40)	1.369(6)	C(40)-C(41)	1.373(5)
C(40)-O(49)	1.361(4)	C(41)-C(42)	1.389(5)
O(43)-C(44)	1.387(5)	O(45)-C(46)	1.412(7)
O(47)-C(48)	1.402(6)	O(49)-C(50)	1.429(6)
N(1)-B(1)	1.574(6)	O(51)-C(52)	1.328(14)

TABLE 14.8. Bond Angles (deg.)

C(2)-O(1)-C(18)	114.6(2)	O(1)-C(2)-C(3)	110.1(3)
C(2)-C(3)-O(4)	109.4(4)	C(3)-O(4)-C(5)	112.1(3)
O(4)-C(5)-C(6)	110.0(4)	C(5)-C(6)-O(7)	109.0(3)
C(6)-O(7)-C(8)	117.9(3)	O(7)-C(8)-C(9)	106.0(2)
O(7)-C(8)-C(19)	112.2(2)	C(9)-C(8)-C(19)	113.1(3)
C(8)-C(9)-O(10)	107.4(2)	C(8)-C(9)-C(25)	110.6(3)
O(10)-C(9)-C(25)	113.1(3)	C(9)-O(10)-C(11)	115.9(2)
O(10)-C(11)-C(12)	109.0(3)	C(11)-C(12)-O(13)	109.2(4)
C(12)-O(13)-C(14)	112.3(4)	O(13)-C(14)-C(15)	109.3(4)
C(14)-C(15)-O(16)	109.3(3)	C(15)-O(16)-C(17)	114.6(3)
O(16)-C(17)-C(18)	106.3(3)	O(16)-C(17)-C(31)	111.0(3)
C(18)-C(17)-C(31)	112.4(2)	O(1)-C(18)-C(17)	107.7(2)
O(1)-C(18)-C(37)	112.4(3)	C(17)-C(18)-C(37)	112.1(3)
C(8)-C(19)-C(20)	122.0(3)	C(8)-C(19)-C(24)	120.3(3)
C(20)-C(19)-C(24)	117.7(3)	C(19)-C(20)-C(21)	121.9(3)
C(20)-C(21)-C(22)	119.3(3)	C(21)-C(22)-C(23)	119.9(3)
C(21)-C(22)-O(43)	123.3(3)	C(23)-C(22)-O(43)	116.9(3)
C(22)-C(23)-C(24)	120.2(3)	C(19)-C(24)-C(23)	121.0(3)
C(9)-C(25)-C(26)	121.0(3)	C(9)-C(25)-C(30)	121.1(3)
C(26)-C(25)-C(30)	117.9(3)	C(25)-C(26)-C(27)	122.7(3)
C(26)-C(27)-C(28)	118.6(4)	C(27)-C(28)-C(29)	119.6(4)
C(27)-C(28)-O(45)	124.8(4)	C(29)-C(28)-O(45)	115.6(3)
C(28)-C(29)-C(30)	121.2(3)	C(25)-C(30)-C(29)	120.1(3)
C(17)-C(31)-C(32)	121.7(3)	C(17)-C(31)-C(36)	121.3(3)
C(32)-C(31)-C(36)	117.0(3)	C(31)-C(32)-C(33)	122.0(3)
C(32)-C(33)-C(34)	120.1(3)	C(33)-C(34)-C(35)	119.3(3)
C(33)-C(34)-O(47)	115.9(3)	C(35)-C(34)-O(47)	124.9(3)
C(34)-C(35)-C(36)	119.5(3)	C(31)-C(36)-C(35)	122.2(3)
C(18)-C(37)-C(38)	119.8(3)	C(18)-C(37)-C(42)	123.2(3)
C(38)-C(37)-C(42)	117.0(3)	C(37)-C(38)-C(39)	120.6(3)
C(38)-C(39)-C(40)	121.1(3)	C(39)-C(40)-C(41)	119.2(3)
C(39)-C(40)-O(49)	115.4(3)	C(41)-C(40)-O(49)	125.4(3)
C(40)-C(41)-C(42)	120.0(4)	C(37)-C(42)-C(41)	122.0(3)
C(22)-O(43)-C(44)	118.7(3)	C(28)-O(45)-C(46)	118.0(4)
C(34)-O(47)-C(48)	118.4(3)	C(40)-O(49)-C(50)	119.2(3)

TABLE 14.9. Anisotropic temperature factors ($Å^2 \times 10^3$)

atom	U_{11}	U_{22}	U_{33}	U_{23}	U_{13}	U_{12}
C(1)	74(1)	68(1)	64(1)	-10(1)	-15(1)	-5(1)
C(2)	101(2)	66(2)	91(2)	-1(2)	-36(2)	-19(2)
C(3)	107(2)	59(2)	89(2)	-19(2)	-40(2)	-2(2)
C(4)	94(1)	58(1)	72(1)	-14(1)	-24(1)	-4(1)
C(5)	121(3)	60(2)	77(2)	-12(2)	-37(2)	-14(2)
C(6)	66(2)	72(2)	86(2)	-5(2)	-26(2)	-4(1)
O(7)	76(1)	48(1)	73(1)	-8(1)	-22(1)	-2(1)
C(8)	76(2)	49(1)	57(2)	-8(1)	-13(1)	2(1)
C(9)	80(2)	45(1)	64(2)	-6(1)	-9(1)	1(1)
O(10)	67(1)	60(1)	73(1)	-17(1)	-11(1)	-3(1)
C(11)	76(2)	56(2)	102(3)	-1(2)	-27(2)	-11(2)
C(12)	97(2)	63(2)	117(3)	-21(2)	-39(2)	-9(2)
O(13)	78(1)	62(1)	80(1)	-9(1)	-22(1)	-10(1)
C(14)	98(3)	93(3)	90(2)	-6(2)	-39(2)	-24(2)
C(15)	78(2)	89(2)	88(2)	1(2)	-35(2)	-11(2)
O(16)	69(1)	69(1)	74(1)	5(1)	-24(1)	-9(1)
C(17)	72(2)	57(2)	60(2)	-6(1)	-13(1)	2(1)
C(18)	71(2)	58(2)	57(2)	-10(1)	-10(1)	6(1)
C(19)	67(2)	49(1)	63(2)	-11(1)	-14(1)	4(1)
C(20)	84(2)	56(2)	65(2)	-9(1)	-14(1)	6(1)
C(21)	95(2)	64(2)	61(2)	-15(1)	-7(1)	1(2)
C(22)	66(2)	58(2)	79(2)	-23(1)	-16(1)	6(1)
C(23)	91(2)	61(2)	75(2)	-19(2)	-21(2)	17(2)
C(24)	95(2)	62(2)	63(2)	-17(1)	-15(1)	15(2)
C(25)	69(2)	53(2)	73(2)	-10(1)	-7(1)	1(1)
C(26)	90(2)	60(2)	72(2)	-9(2)	-13(2)	6(2)
C(27)	102(3)	77(2)	71(2)	-20(2)	-3(2)	5(2)
C(28)	81(2)	70(2)	86(2)	-29(2)	-5(2)	6(2)
C(29)	99(2)	54(2)	89(2)	-15(2)	-15(2)	14(2)
C(30)	86(2)	58(2)	70(2)	-9(1)	-12(2)	3(2)
C(31)	73(2)	54(2)	60(2)	-12(1)	-12(1)	5(1)
C(32)	73(2)	65(2)	62(2)	-14(1)	-10(1)	12(1)
C(33)	84(2)	63(2)	67(2)	-12(1)	-20(2)	11(2)
C(34)	82(2)	49(1)	60(2)	-10(1)	-12(1)	-1(1)
C(35)	89(2)	67(2)	71(2)	-23(2)	-13(2)	13(2)
C(36)	91(2)	59(2)	72(2)	-20(1)	-24(2)	19(2)
C(37)	76(2)	59(2)	57(2)	-14(1)	-13(1)	1(1)
C(38)	79(2)	62(2)	68(2)	-18(1)	-5(1)	5(1)
C(39)	90(2)	67(2)	70(2)	-13(2)	-3(2)	-2(2)
C(40)	94(2)	58(2)	74(2)	-9(2)	-21(2)	0(2)
C(41)	104(3)	62(2)	91(2)	-24(2)	-19(2)	20(2)
C(42)	90(2)	67(2)	75(2)	-18(2)	-5(2)	11(2)
O(43)	103(2)	71(1)	88(2)	-32(1)	-13(1)	26(1)
C(44)	114(3)	104(3)	93(3)	-46(2)	-15(2)	30(2)
O(45)	125(2)	87(2)	102(2)	-43(2)	2(2)	16(2)
C(46)	149(4)	105(3)	107(3)	-54(3)	5(3)	1(3)
O(47)	115(2)	77(2)	65(1)	-21(1)	-27(1)	7(1)
C(48)	140(4)	104(3)	77(2)	-42(2)	-31(2)	6(3)
O(49)	123(2)	56(1)	101(2)	-3(1)	-15(2)	-2(1)
C(50)	131(4)	54(2)	160(5)	-17(2)	-35(3)	11(2)
N(1)	65(1)	63(1)	63(1)	-16(1)	-13(1)	1(1)
O(1)	92(3)	102(3)	76(2)	-36(2)	-18(2)	19(2)
O(51)	140(4)	156(5)	142(4)	-76(4)	-29(3)	15(3)
O(52)	157(5)	108(4)	132(5)	-65(4)	-47(4)	4(4)

The anisotropic temperature factor exponent takes the form:

$$-2\pi^2(h^2a^{*2}U_{11} + \ldots + 2\,hka^*b^*U_{12}\cos\gamma^* + \ldots)$$

TABLE 14.10. Coordinates ($\times 10^4$) and temperature factors ($Å^2 \times 10^3$)

atom	x	y	z	U
H(2a)	5135	13181	1229	112
H(2b)	4277	14471	1397	112
H(3a)	2995	12979	3287	97
H(3b)	4882	13435	3029	97
H(5a)	5735	11439	4365	109
H(5b)	3753	11149	4701	109
H(6a)	5395	9230	5243	95
H(6b)	6358	9501	4000	95
H(8)	3646	7634	5821	78
H(9)	1139	6811	5658	80
H(11a)	-182	6550	4297	100
H(11b)	-1143	7011	4471	100
H(12a)	-1260	7651	2787	101
H(12b)	761	7780	2407	101
H(14a)	49	9693	926	112
H(14b)	-1945	9626	1480	112
H(15a)	-1753	11632	1706	109
H(15b)	-1391	11766	459	108
H(17)	-23	13739	577	77
H(18)	3551	13662	19	78
H(20)	4837	7537	2132	95
H(21)	6614	5915	2624	87
H(23)	6422	3843	5848	98
H(24)	4665	5483	6344	83
H(26)	359	7469	7292	96
H(27)	-1146	8947	8110	97
H(29)	-1337	11532	5054	93
H(30)	199	10062	4245	89
H(32)	-1259	14835	-899	84
H(33)	-1498	15247	-2682	84
H(35)	2538	12703	-3066	91
H(36)	2663	12234	-1241	91
H(38)	5237	14566	-1447	87
H(39)	5914	16714	-2544	93
H(41)	1781	17999	-676	106
H(42)	1091	15846	445	94
H(44a)	9525	3227	2941	120
H(44b)	9291	4745	2617	120
H(44c)	7988	3963	2412	120
H(46a)	-3219	11857	8316	140
H(46b)	-1491	11022	8398	140
H(46c)	-3209	10355	8555	140
H(48a)	1068	14036	-5499	123
H(48b)	1256	12816	-4455	123
H(48c)	2538	13966	-4901	123
H(50a)	4070	20664	-2696	141
H(50b)	3223	19831	-1466	141
H(50c)	2434	19847	-2427	141
H(1na)	2367	10759	1786	71
H(1nb)	3929	10526	2345	71
H(1nc)	2769	9361	2580	71
H(1ba)	5455	9114	1218	101
H(1bb)	5059	10765	459	101
H(1bc)	3691	9557	581	101
H(52a)	5773	6804	710	164
H(52b)	7417	6120	178	164
H(52c)	6633	7409	-559	164

14.4 REFERENCES

1. G.M. Sheldrick, SHELXTL, An integrated system for solving, refining, and displaying crystal structures from diffractometer data, University of Göttingen, Federal Republic of Germany, 1981.

2. See Chapter 11.

   See Chapter 12.

   See Chapter 13.

3. J.D. Dunitz, and P. Seiler, Acta. Cryst., 1974, B30, 2739.

4. I. Goldberg, The Chemistry of Functional Groups. Supplement E: The Chemistry of Ethers, Crown Ethers, Hydroxy Groups and their Sulphur Analogues, 1980, Part 1, 175. Editor S. Patel, Chichester: John Wiley.

5. B.L. Allwood, H. Shahriari-Zavareh, J.F. Stoddart, and D.J. Williams, J. Chem. Soc., Chem. Commun., 1984, 1461.

CHAPTER 15

CONCLUSIONS

15.1 Summary

In all the uncomplexed tetra-anisyl receptors 10 - 13 the equatorial substituents are, as one would expect, orientated away from the macrocyclic cavity. However, in 11 (cis-anti-cis) the axial substituents obscure both faces of the macrocyclic cavity, whilst in 12 (cis-syn-cis) they partially obscure only one face. 11 also has unusual C-C bridgehead bond torsion angles. These are anti and the relationship of the substituents about these bonds is antiperiplanar.

On complexation with borane-ammonia all the 18-membered macrocycles adopt a pseudo 'all gauche' conformation. The mode of binding is via hydrogen bonding between tha NH_3 group of the borane-ammonia and the polyether oxygens.

15.2 The Receptor C-C Bridgehead Bond Length.

The C-C bridgehead bond lengths in the complexed and uncomplexed receptors 10 - 13 are systematically longer than the other ring C-C bonds lengths. This lengthening has been observed for the C-C bridgehead bond lengths in all the structures but one, tetracarboxamide-18-crown-6[1], of the other 2,3,11,12 tetrasubstituted 18-crown-6 macrocycles[2]. This lengthening has also been observed for a 2,3,11,12 octamethyl-18-crown-6 receptor[3]. However, there is not a consistent lengthening of the ring junction C-C bond in the X-ray structures of cyclohexano-18-crown-6 complexes[4].

15.3 The Stoicheiometry of the Borane-ammonia Complexes.

As with previous X-ray studies[2b,3,5] of borane-ammonia complexes with 18C6 derivatives, there is no correlation between the presence of diastereotopic and homotopic macrocyclic faces and complex stoicheiometry. Though, receptors 10 and 11, which both have homotopic faces, form 1:2 host-guest complexes whilst 12 which has diastereotopic faces, forms a 1:1 host guest complex. However, receptor 13 which can possess D_2 symmetry and hence homotopic faces, upon complexation one of its macrocyclic faces is obscured by an axial anisyl substituent thus presenting only one accessible hydrogen bonding face to the borane-ammonia molecules. This results in the formation a 1:1 complex.

15.4 Enantioselective Reduction of Prochiral Ketones.

The chiral trans-anti-trans tetra-anisyl receptor was synthesised to evaluate its potential as a chiral auxiliary in enantioselective reduction of prochiral ketones. Unfortunately the (RRRR) and (SSSS) trans-anti-trans tetra-anisyl 18-crown-6 proved less effective as a chiral auxiliary than the corresponding tetraphenyl 18C6 macrocycle[6].

15.5 Hydrogen Bond Geometry.

All of these complexes of borane-ammonia, with the exception of receptor 13, have a 'perching' type hydrogen bonding arrangement. There is no correlation between this arrangement and the directionality of the hydrogen bond vectors to the relevant C-O-C planes.

15.6 Conclusion

Although there is no correlation between complex stoicheiometry and the potential homotopic or diastereotopic faces of the receptors, we have in this instance noticed a correlation between the number of accessible hydrogen bonding faces of the complexed receptors with the host guest stoicheiometry.

15.7 REFERENCES

1. J.P. Behr, J.M. Lehn, A.C. Dock, and D. Moras, Nature, 1982, 295, 526.

2a. G. Weber, G.M. Sheldrick, T. Burgemeister, F. Dietl, A. Mannschreck, and A. Merz, Tetrahedron 1984, 40, 855.

b. B.L. Allwood, H. Shahriari-Zavareh, J.F. Stoddart, and D.J. Williams, J. Chem. Soc., Chem. Commun., 1984, 1461.

c. J.J. Daly, P.Schonholzer, J.P. Behr, and J.M. Lehn, Helv. Chim. Acta., 1981, 64, 1444.

d. J.P. Behr, P. Dumas, and D. Moras, J. Am. Chem. Soc., 1982, 104, 4540.

3. D.R. Alston, J.F. Stoddart, J.B. Wolstenholme, B.L. Allwood, and D.J. Williams, Tetrahedron, 1985, 41, 2923.

4. D.L. Hughes, and M.R. Truter, Acta. Cryst., 1983, B39, 329.

5. B.L. Allwood, H. Shahriari-Zavareh, J.F. Stoddart, and D.J. Williams, J. Incl. Phenom., 1985, 3, 355.

H.M. Colquhoun, G. Jones, J.M. Maud, J.F. Stoddart, and D.J. Williams, J. Chem. Soc., Dalton Trans., 1984, 63.

6. D.Pears, Ph.D. Thesis. University of Sheffield, 1985.

APPENDIX 1

CRYSTALLOGRAPHIC METHODS

INTRODUCTION

Both the theory and the general practice of X-ray crystal analysis are well established and have been comprehensively described in several texts[1]. Therefore, the purpose of this appendix will be to describe briefly the hardware and software used in this research and give details of when user intervention has been necessary.

Two papers have recently appeared, one describing how to collect better quality X-ray data[2] and another reviewing some of the 'cosmetic' crystallographic tricks[3].

Photographic Methods

Preliminary oscillation, zero and first level Weissenberg photographs were sometimes taken to determine the unit cell dimensions, the space group, and whether a crystal was single. Sometimes these photographs were taken after the X-ray data on a crystal had been collected on the diffractometer and problems in the structure solution had arisen.

Hardware Used

For all the data collections, the Nicolet R3m/E Crystallographic system was used. This consists of a Nicolet R3m diffractometer linked to a Data General Eclipse S140 minicomputer with its peripherals. A

more detailed description can be obtained from the Operations manual[4].

The Diffractometer

The Nicolet R3m is an on-line four-circle single crystal diffractometer. The circles can be automatically controlled by the external control console or manually. The X-ray detector is a NaI (T1) scintillation counter.

Once the crystal has been mounted onto the goniometer head and centered by using a telemicrosopic, a polaroid rotation photograph is taken. The diffractometer does not require prior knowledge of the orientation of the crystallographic axis of the crystal or its unit-cell dimensions. The following programs are used to obtain this information.

(1) Centering Program.

This program reads the coordinates of up to 25 reflections obtained from the rotation photograph. It then calculates the corresponding 2θ and χ values for each reflection (assuming $\omega = 0^{o}$), searches in ϕ for each reflection. When a diffraction intensity maximum greater than a predetermined value is detected the position of the reflection is optimised in 2θ, ω, and χ. This is then repeated for the remainder of the input coordinates and a set of refined angles (2θ, ω, χ and ϕ) for each reflection produced.

(2) Autoindexing Program.

This program reads the set of refined angles from the centering program and produces a list of axial vectors and the angles between them. The program then selects what it believes to be the three best axial solutions, calculates the unit cell volume and then indexes all the reflections in the array. This procedure is not infallible and user intervention is occasionally required.

(3) Least Squares Orientation Matrix Programme.

From the set of indices and refined angles, this program calculates the least squares orientation matrix and unit cell parameters and volume with their standard deviations.

(4) Index Transformation Program.

This program can automatically transform the unit cell from the reduced primitive cell to the most likely Bravais lattice. It then prints out new unit cell dimensions with their standard deviations.

User Intervention in Validating automatically chosen Unit Cell.

At this stage the unit cell and Bravais lattice should be manually validated especially if no preliminary photographs have been taken.

Initially the unit cell size should be checked to evaluate whether it is the right size for the proposed structure. Equivalent

reflections should be checked to ensure that they are indeed equivalent. If the unit cell size is reasoned to be incorrect, the user should go back to the autoindexing program. The vector solutions and angles should be analysed manually to see if an alternative set of axes and angles can be chosen.

An automatically chosen centered cell should be validated by scanning all the reflections in selected areas of reciprocal space including the reflections which should be absent due to the centering condition and checking that they are genuinely absent.

On occasions it has been necessary to transform the indices of a monoclinic cell which contains a large β angle to a centered monoclinic cell containing a smaller β angle. This avoids correlation effects in the least squares refinement.

Data Collection Program

For all the compounds studied, data were collected using the omega-scan measuring routine. Several of the data collection program parameters were varied for each structure.

Data were collected at variable scan speeds, with a fast (2 seconds) prelimianary scan through the peak determining the optimum speed. The minimum scan speed was set depending on the size and stability of the crystal, and the chemical problem to be solved.

The scan width and background off-set for the data collection was based on the observation of the mo saic spread of the reflections peak profiles from a preliminary data collection scan.

For each reflection the program records on magnetic tape the indices, angles, scan rate, background and peak height, reflection intensity with its standard deviation, cumulative X-ray exposure time and peak profile.

The SHELXTL System

After the collection of the data the SHELXTL[5] system was used for solving, refining and displaying the molecular structures. The system is fully descibed in the user manual. Only the most important facilities, programs and features within the system will be described.

XTAPE

This program reads the diffractometer data and creates a raw data input file. It calculates Lorentz and polarisation corrections and scales the data using the check reflections. Normally two check reflections were remeasured every 50 reflections to enable corrections to the data to be made to compensate for fluctuations of the X-ray beam intensity or changes in the stability of the crystal. They can also indicate, if the change in the intensities of the check reflections differ significantly, whether the unit cell of the crystal is changing or that the crystal is decomposing at different rates in different directions.

Direct Methods

The system provides two programs for structure determination by direct methods, RANT and SOLV. The SOLV program is a general purpose procedure, fully automatic for all space groups. The RANT instruction involves tangent refinement of random starting phase sets. The SOLV program was initially attempted for all structures and only if it eventually failed, after many different attempts, to produce a meaningful solution was the RANT routine used. Though the SOLV program occasionally succeeds using the default parameters, on numerous occasions user intervention was required in solving the phase problem.

User intervention normally begins by analysing the distribution of E-values. The minimum value is sometimes raised so that only ~ 200 of the strongest E-values are used in the initial phase refinement, though care is taken to make sure that the number of linking $\Sigma 2$ relationships is not reduced too dramatically. After this a variety of 'tricks' are used. When the structure is large, the choice of the starting set is important, and there should be experimentation with different starting reflections. Additional reflections which can be added to the starting set are weak links in the convergence mapping, principal contributors to list of negative quartets, and $\Sigma 1$ reflections. Sometimes when a recognisable structural fragment of the expected structure is obtained, an expanded structure may be produced by using ΔE-map recycling rather than by a least squares refinement followed by a conventional ΔF-map.

Structure Refinement

The blocked cascade procedure employed in SHEXTL makes a minimum of disc transfers whilst retaining relatively large (103 parameters) full matrix blocks which faciliate constrained refinements. On occasions structure refinement has not run smoothly and user intervention has been neccessary. This has mainly consisted of using rigid group and geometrical constraints, especially on disordered groups, and a damping factor for unstable refinements.

XP - The Molecular Geometry and Graphics Programme

This program provides interactive molecular geometry calculations, least-squares planes, symmetry transformations, librational analysis, and can write a plotfile containing mono- or stereo drawing as shown in this thesis. The plotfiles were all drawn on a Nicolet Zeta plotter.

REFERENCES

1. M.J. Buerger, ' Crystal Structure Analysis ' Wiley, New York, 1960.

M.F.C. Ladd, and R.A. Palmer, ' Structure Determination by X-ray Crystallography ' Plenum, New York, 1977.

G.H. Stout and L.H. Jensen ' X-ray Crystal Determination ' Macmillan, New York, 1968.

M.M. Woolfson, ' X-ray Crystallography ' Cambridge, U.K, 1970.

2. T.A. Hamor, H. Steinfink, and B.T.M. Willis, Acta. Cryst., 1985,

C41, 301.

3. P.G. Jones, Chem., Soc., Rev., 1984, 13, 157.

4. Data Collection Operations Manual, Nicolet Instruments Ltd, Warwick, U.K.

5. G.M. Sheldrick, SHELTYX, an integrated system for Solving, Refining and displaying Structures from Diffraction Data. University of Göttingen.

APPENDIX 2

PUBLICATIONS

Stereospecific Syntheses of Macrobicyclic Polyethers with Carbon Bridgeheads from Chiral Glycerol Derivatives.
B.L. Allwood, S.E. Fuller, P.C.Y.K. Ning, A.M.Z. Slawin, J.F. Stoddart, D.J. Williams, J.Chem. Soc., Chem. Commun., 1984, 1356.

Enantioselective Reductions of Aromatic Ketones with Ammonia-Borane Complexes of Chiral Tetraphenyl-18-Crown-6 Derivatives.
B.L. Allwood, H. Shahriari-Zavarem, J.F. Stoddart, D.J. Williams, J.Chem. Soc., Chem. Commun., 1984, 1461.

Crown Ether Complexes of Phosphonium Salts-The X-Ray Structure Analysis of $[(Ph_3PMe)_2.[18]Crown\text{-}6][PF_6]_2$.
B.L. Allwood, H.M. Colquhoun, J. Crosby, D.A. Pears, J.F. Stoddart, D.J. Williams, Angew. Chem. 1984, 96, 806; Angew. Chem. Int. Ed. Engl. 1984, 23, 824.

Crown Ether Complexes of Sulfonium Salts-The X-Ray Crystal Structures of $[PhCOCH_2SMe_2.[18]Crown\text{-}6]_n[PF_6]_n$ and $[(PhCOCHPhSMe_2)_2.[18]Crown\text{-}6][PF_6]_2$.
B.L. Allwood, J. Crosby, D.A. Pears, J.F. Stoddart, D.J. Williams, Angew. Chem. 1984, 96, 987; Angew. Chem. Int. Ed. Engl. 1984, 23, 977.

Ammonium Chloride Complexes with 18-Crown-6 (18C6). The X-Ray Crystal Structures of $NH_4Cl.NH_4PF_6.(18C6)_2$ and $(NH_4Cl.2H_2O.18C6)_n$.
B.L. Allwood, M.E. Fakley, D.A. Pears, J.F. Stoddart, D.J. Williams, Polyhedron, in press.

A 1:2 Complex between 1,4,7,10,13,16-Hexaoxacyclo-octadecane(18-crown-6) and Diphenylmethylsulphonium Tetraiododi-μ-iododimercurate (II) $C_{12}H_{24}O_6.[(C_6H_5)_2SCH_3]_2[Hg_2I_6]$.
B.L. Allwood, J. Crosby, D.A. Pears, J.F. Stoddart, D.J. Williams, Acta. Cryst., in press.

A 1:1 Complex Between 1,4,7,10,13,16-Hexaoxacyclooctadecane (18-Crown-6) and Mercury (II) Iodine, HgI_2.
B.L. Allwood, J. Crosby, D.A. Pears, J.F. Stoddart, D.J. Williams, Acta. Cryst., in press.

The Supramolecular Structures and Reactivities of Some Complexes of Chiral Crown Ethers with Borane-Ammonia.
B.L. Allwood, H. Shahriari-Zavarem, J.F. Stoddart, D.J. Williams, M.K. Williams, J. Incl. Phenom., 1985, 3, 355.

Synthesis of an Octamethyl-18-Crown-6 Derivative and The X-Ray Crystal Structure of its 2:1 Complex with Borane-Ammonia.
B.L. Allwood, D.R. Alston, J.F. Stoddart, D.J. Williams, J.B. Wolstenholme, Tetrahedron, 1985, 41, 2923.

The Stereospecific Synthesis of Macrobicyclic and Macropolycyclic Polyethers from Carbohydrate Precursors.
B.L. Allwood, H.M. Colquhoun, S.M. Doughty, S.E. Fuller, P.C.Y.K. Ning, A.M.Z. Slawin, J.F. Stoddart, D.J. Williams, Pure & Applied Chemistry, Organic Synthesis: An interdisciplinary Challenge, 1985, 295.

Complexation of Diquat by a Regiospecifically Synthesised Macrobicyclic Receptor Molecule.
B.L. Allwood, F.H. Kohnke, A.M.Z. Slawin, J.F. Stoddart, D.J. Williams, J. Chem. Soc., Chem. Commun., 1985, 311.

Complexation of Diquat by Disubstituted Dibenzo-30-crown-10 Derivatives.
B.L. Allwood, F.H. Kohnke, J.F. Stoddart, D.J. Williams, Tetrahedron Lett., 1985, 26, 1681.

A Macrobicyclic Receptor Molecule for the Diquat Dication.
B.L. Allwood, F.H. Kohnke, J.F. Stoddart, D.J. Williams, Angew. Chem. 1985, 97, 584; Angew. Chem. Int. Ed. Engl. 1985, 24, 581.

A Novel Hydrogen Bonded Complex Formed by the Reaction between Bromine and 1,4 Diazabicyclo[2.2.2]Octane in Dichloromethane Solution.
B.L. Allwood, P.I. Moysak, H.S. Rzepa, D.J. Williams, J.Chem. Soc., Chem. Commun., 1985, 1127.

The Formation and X-Ray Crystal Structures of Novel Spiro[aziridine]-azetidiones From Thermal Reactions Between 6-diazopencillanates and Aromatic Imines.
B.L. Allwood, J.E. Elliot, D. Ivor-John, V.J. Jephcote, M.M. Khalaf, D.J. Williams, J. Chem. Soc., Chem. Commun., submitted.

APPENDIX 3

MOLECULAR GEOMETRY PROGRAM

The following Molecular Geometry Program, written in BBC Basic, can rotate and display molecules on a graphics screen.

```
L.
  1 PRINT "WELCOME MOLECULAR GRAPHICS PROGRAME"
  2 PRINT "COPYRIGHT B.L.ALLWOOD  30/11/84"
  3 ON ERROR GOTO  1900
  5 PRINT "BILL2"
 10MODE4
 20 PROCCOUNT
 30 PROCCART
 40 PROCSCALE
 50 PROCCONN
 60 PROCROTA
 70 END
 80 DEF PROCCOUNT
 90 INPUT"INPUT NAME OF FILE  " N$
100 FILE%=OPENUP(N$)
110 N%=FNcount
120 PRINT N%
130 CLOSE£FILE%
140 ENDPROC
150 DEF FNcount
160LOCAL A%,L$,X,Y,Z,a,b,c,A,B,C
162 INPUT£FILE%,a,b,c,A,B,C
170A%=-1
180REPEAT
190INPUT£FILE%,L$,X,Y,Z
200A%=A%+1
210UNTIL EOF£FILE%
220=A%
230DEF PROCCART
240 FILE%=OPENUP(N$)
250DIM XYZ(2,N%) :DIM L$(N%)
260LOCAL a,b,c,A,B,C,cosc,sinc,X,Y,Z
270LOCAL CART1,CART2,CART3,CART4,CART5,CART6
280 PRINT" AXIAL LENGTHS A,B,C AND ANGLES ALPHA,BETA,GAMMA ARE "
290 INPUT£FILE%,a,b,c,A,B,C
292 PRINT a,b,c,A,B,C
300N%=0
310cosc=(COS(RAD(A))*COS(RAD(B))-COS(RAD(C)))/(SIN(RAD(A))*SIN(RAD(B)))
320sinc=SQR(1-(cosc)^2)
330CART1=a*SIN(RAD(B))*sinc
340CART2=-a*SIN(RAD(B))*cosc
350CART3=b*SIN(RAD(A))
360CART4=a*COS(RAD(B))
370CART5=b*COS(RAD(A))
380CART6=c
390REPEAT
400INPUT£FILE%,L$(N%),XYZ(0,N%),XYZ(1,N%),XYZ(2,N%)
410X=CART1*XYZ(0,N%)
```

```
420Y=CART2*XYZ(0,N%)+CART3*XYZ(1,N%)
430Z=CART4*XYZ(0,N%)+CART5*XYZ(1,N%) +CART6*XYZ(2,N%)
440XYZ(0,N%)=X:XYZ(1,N%)=Y:XYZ(2,N%)=Z
450 N%=N%+1
460UNTIL EOF£FILE%
470CLOSE£FILE%
480N%=N%-1
490ENDPROC
500DEF PROCSCALE
510Xmax=FNmax(0):Ymax=FNmax(1):Zmax=FNmax(2)
520Xmin=FNmin(0):Ymin=FNmin(1):Zmin=FNmin(2)
530PRINT Xmax,Ymax,Zmax,Xmin,Ymin,Zmin
540DISTMAX=SQR((Xmax-Xmin)^2+(Ymax-Ymin)^2+(Zmax-Zmin)^2)
550SCRWID=1000
560SCALE=SCRWID/DISTMAX
570FOR J%=0 TO N%
580XYZ(0,J%)=(XYZ(0,J%)-Xmin-(Xmax-Xmin)/2)
590XYZ(1,J%)=(XYZ(1,J%)-Ymin-(Ymax-Ymin)/2)
600XYZ(2,J%)=(XYZ(2,J%)-Zmin-(Zmax-Zmin)/2)
610NEXT
620ENDPROC
630DEF FNmax(D%)
640LOCAL M,B%
650 M=XYZ(D%,0)
660FOR B%=1 TO N%
670IF XYZ(D%,B%)>=M THEN M=XYZ(D%,B%)
680NEXT
690=M
700DEF FNmin(E%)
710LOCAL M,C%
720M=XYZ(E%,0)
730FOR C%=1  TO N%
740IF XYZ(E%,C%)<=M THEN M=XYZ(E%,C%)
750NEXT
760=M
770DEF PROCCONN
780DIM CONN(3,N%-1)
790FOR I%=0 TO N%-1
800Q%=0
810FOR B%=I%+1 TO N%
820DIST=SQR(FNcd(XYZ(0,B%),XYZ(0,I%))+FNcd(XYZ(1,B%),XYZ(1,I%))+FNcd(XYZ(2,B%)
,XYZ(2,I%)))
830IF DIST<=1.8 THEN CONN(Q%,I%)=B% :PRINT "B%"B%:Q%=Q%+1 :PRINT "Q%" Q%
840NEXT
850NEXT
860ENDPROC
870 DEF FNcd(F,G)=(F-G)^2
880DEF PROCROTA
890DIM UPXYZ(2,N%),orimat(2,2),ROTA(2,2),UPORIMAT(2,2)
900orimat(0,0)=1:orimat(1,1)=1:orimat(2,2)=1
910LOCAL AXIS%,THETA%,cos,sin
920 PRINT" INPUT AXIS OF ROTATION X=1,Y=2,Z=3,ORIENTATION MATRIX INPUT X=99,OR
IENTATION MATRIX PRINT X=100 "
930 INPUT AXIS%
932 IF AXIS%=99 THEN PROCMATIN
934 IF AXIS%=100 THEN PROCMATPR
950 PRINT" INPUT ANGLE OF ROTATION THETA"
960INPUT THETA%
970sin=SIN(RAD(THETA%)):PRINT sin
980cos=COS(RAD(THETA%)):PRINT cos
```

```
 990IF AXIS% =1 THEN PROCAXIS1
1000IF AXIS% =2 THEN PROCAXIS2
1010IF AXIS% =3 THEN PROCAXIS3
1050PROCROTori
1060PROCUPCOOR
1070PROCCHANGE
1080 GOTO 920
1090ENDPROC
1100DEF PROCAXIS1
1110ROTA(0,0)=1:ROTA(0,1)=0:ROTA(0,2)=0:
1120ROTA(1,0)=0:ROTA(1,1)=cos:ROTA(1,2)=-sin
1130ROTA(2,0)=0:ROTA(2,1)=sin:ROTA(2,2)=cos
1140ENDPROC
1150DEF PROCAXIS2
1160ROTA(0,0)=cos:ROTA(0,1)=0:ROTA(0,2)=sin
1170ROTA(1,0)=0:ROTA(1,1)=1:ROTA(1,2)=0
1180ROTA(2,0)=-sin:ROTA(2,1)=0:ROTA(2,2)=cos
1190ENDPROC
1200DEF PROCAXIS3
1210ROTA(0,0)=cos:ROTA(0,1)=-sin:ROTA(0,2)=0
1220ROTA(1,0)=sin:ROTA(1,1)=cos:ROTA(1,2)=0
1230ROTA(2,0)=0:ROTA(2,1)=0:ROTA(2,2)=1
1240ENDPROC
1250DEF PROCROTori
1260LOCAL A%,B%,C%
1270FOR A% =0 TO 2
1280FOR B% =0 TO 2
1290UPORIMAT(A%,B%)=0
1300FOR C% =0 TO 2
1310UPORIMAT(A%,B%)=ROTA(A%,C%)*orimat(C%,B%)+UPORIMAT(A%,B%)
1320NEXT
1330NEXT
1340NEXT
1350ENDPROC
1360DEF PROCUPCOOR
1370LOCAL A%,B%,C%
1380FOR A% =0 TO 2
1390FOR B% =0 TO N%
1400UPXYZ(A%,B%)=0
1410FOR C% =0 TO 2
1420UPXYZ(A%,B%)=UPORIMAT(A%,C%)*XYZ(C%,B%)+UPXYZ(A%,B%)
1430NEXT
1440NEXT
1450NEXT
1460PROCDRAW
1470ENDPROC
1480DEF PROCDRAW
1490LOCAL Z%,X%
1500CLS
1510VDU 29,512;512;
1520FOR Z%=0TO N%-1
1530FOR X%=0 TO 3
1540MOVE UPXYZ(1,Z%)*SCALE,-UPXYZ(0,Z%)*SCALE
1550IF CONN(X%,Z%)>0 THEN DRAW UPXYZ(1,CONN(X%,Z%))*SCALE,-UPXYZ(0,(CONN(X%,Z%
))*SCALE
1560NEXT
1570NEXT
1580ENDPROC
1590DEF PROCCHANGE
```

```
1600LOCAL X%,Y%
1610FOR X% =0 TO 2
1620FOR Y% =0 TO 2
1630orimat(X%,Y%)=UPORIMAT(X%,Y%)
1640NEXT
1650NEXT
1660ENDPROC
1670 DEF PROCMATIN
1680PRINT "INPUT 1st ROW ORIENTATION MATRIX"
1690 INPUT UPORIMAT(0,0) UPORIMAT(0,1) UPORIMAT(0,2)
1790 PRINT "INPUT 2nd ROW ORIENTATION MATRIX"
1795 INPUT UPORIMAT(1,0) UPORIMAT(1,1) UPORIMAT(1,2)
1800 PRINT "INPUT 3rd ROW ORIENTATION MATRIX"
1805 INPUT UPORIMAT(2,0) UPORIMAT(2,1) UPORIMAT(2,2)
1810  GOTO  1060
1820  END PROC
1830DEF PROCMATPR
1832 PRINT "CURRENT ORIENTATION MATRIX FOLLOWS ROW BY ROW "
1834 @%=&2050C
1860PRINT orimat(0,0) ,orimat(0,1) orimat(0,2)
1862 PRINT orimat(1,0) ,orimat(1,1) orimat(1,2)
1864 PRINT orimat(2,0) ,orimat(2,1) orimat(2,2)
1880 GOTO 920
1890END PROC
1900 REPORT
1905 @%=10
1910PRINT "ERROR ";ERR;" AT LINE NUMBER ";ERL
1920IF ERR=222 PRINT' "NO FILE ON DISC CALLED ";N$:GOTO 20
1930CLOSE£ 0
1940END
>
```

APPENDIX 4

OBSERVED and CALCULATED STRUCTURE FACTORS

The observed and calculated structure factors for the X-ray structures reported in this thesis are listed on the microfiches in the following order:

F1 [2.diquat][PF_6]$_2$$H_2O$

F2 [4.diquat][PF_6]$_2$(CH_3CN)$_{0.75}$

F3 [5.diquat][PF_6]$_2$(C_2H_3N)$_{1.5}$

F4 6.X_3.H_2O

F5 [6.diquat][PF_6]$_2$$X_2$

F6 [7.diquat][PF_6]$_2$(H_2O)$_{0.5}$

F7 8

F8 [8.diquat][PF_6]$_2$(C_3H_6O)

F9 9

F10 [9.diquat.H_2O][PF_6]$_2$

F11 [9.paraquat][PF_6]$_2$$C_3H_6O$

F12 10.X

F13 10.(BH_3NH_3)$_2$

F14 11

F15 11.(BH_3NH_3)$_2$

F16 12

F17 12.BH_3NH_3

F18 13

F19 13.BH_3NH_3(CH_3OH)$_{0.75}$